



UNIVERSIDAD NACIONAL DE COLOMBIA

Modeling Techniques for Photovoltaic Systems Under Mismatching Conditions

Luz Adriana Trejos Grisales

Universidad Nacional de Colombia
Facultad de Ingeniería y Arquitectura, Departamento de Ingeniería Eléctrica, Electrónica y
Computación
Manizales, Colombia
2018

Modeling Techniques for Photovoltaic Systems Under Mismatching Conditions

Luz Adriana Trejos Grisales

Doctoral Thesis

Supervised by:

Carlos Andrés Ramos Paja, Ph.D.

Giovanni Spagnuolo, Ph.D.

Departamento de Energía Eléctrica y Automática - Universidad Nacional de Colombia
Dipartimento di Ingegneria dell'informazione, Ingegneria Elettrica e Matematica Applicata -
Università degli Studi di Salerno

Manizales, Colombia

2018

To my family. All of you are the best of me

In loving memory of the bravest, most worker and lovely man I've ever meet, my father (1955 - 2013)

In loving memory of the person who taught me the meaning of loyalty. My baby, you're up there, you're always with me, smiling down on me (1983 - 2015)

A mi familia. Ustedes son lo mejor de mi

En amoroso recuerdo del hombre más valiente, trabajador y amoroso que he conocido, mi padre (1955 - 2013)

En amoroso recuerdo de la persona quien me enseñó el significado de lealtad. Mi amor, estas allá arriba, estas siempre conmigo, sonriendo hacia mi (1983 - 2015)

Acknowledgments

I thank to life and God and his loving energy for giving the chance of reaching this achievement and for giving me the strength to face everything I lived during the fulfillment of the doctorate. To my family because they always have been the fundamental support in every stage of my life, personally and professionally. Special thanks to my parents Martha and Alvaro for their sacrifices and guidance, for their endless love and patience, for being my role model. To my brother Richy for his unconditional support and his affection in the distance, for giving me a hand in the hard times and putting a smile on my face. To my cousins who are like my siblings and always have surrounded me with good vibes, specially Kathe, Jason and Lilly. To my sister in law Mavy who always have me in her prayers wishing the best for me. To my aunts for being my second moms especially to the loving memory of Edi (r.i.p) because she always inculcated the love for studying and the discipline to reach my objectives. To my uncle Nelson for his support through all this years of vocational training. To the little ones of the family because they have inspired me to be better everyday and because it's our duty to plant the seed of the effort and work, so one day they'll make their dreams come true and reach far. To my grandma Maria (r.i.p) for her affection and especially for the support and love given to my parents and for being always in my life. To whom have become part of my family, Pacho, Erika and Marce who always have been with me all this years being attentive to each step, thanks for your love and support. Special thanks to Karen, Ber and Bonie for their voice of encouragement. To MaE for her wise advices and affection.

I want to give special thanks to my advisor professor Carlos Ramos for his priceless teachings professionally and personally, for his unconditional support, for his patience and commitment with this project, for transmitting me the love for researching and teaching. To my co-advisor Giovanni Spagnuolo for his support and help during my internship in Salerno, for his simplicity and human quality, for all his advices and contributions in the fulfillment of this work. In the same way, special thanks to Patrizio Manganiello and to the professor Giovanni Petrone for their important support during my internship in Salerno. Thanks to Daniel Gonzalez for his unconditional support in all the stages of this work, for his fellowship and good vibes, for giving me his time and attention, for his solidarity and friendship. To Juan David Bastidas for his significant contributions and help, for his patience and comprehension. To professors Andrés Julian Saavedra and Eliana Arango for their valuable advices in the first part of the doctorate. Thank you all !!

Agradecimientos

Agradezco a la vida y a Dios y su energía amorosa por darme la oportunidad de alcanzar este logro y darme la fuerza y la voluntad para afrontar todo lo que viví durante la realización del doctorado. A mi familia porque desde siempre han sido el apoyo fundamental en todas las etapas de mi vida tanto a nivel personal como profesional. Agradezco en especial a mis padres Martha y Alvaro por sus sacrificios y orientación, por su interminable amor y paciencia, por ser mi ejemplo a seguir. A mi hermano Richy por su apoyo incondicional y su cariño en la distancia, por darme la mano en los momentos difíciles y sacarme una sonrisa. A mis primos que son como mis hermanos quienes siempre me han rodeado de buena energía, en especial Kathe, Jason y Lilly. A mi cuñada Mavy quien siempre me lleva en sus oraciones deseando lo mejor para mí. A mis tías por ser mis segundas mamás en especial al amoroso recuerdo de Edi (q.e.p.d) porque siempre me inculcó el amor al estudio y la disciplina para lograr mis objetivos. A mi tío Nelson por todo su apoyo a lo largo de todos estos años de formación profesional. A los pequeñines de la familia porque me han inspirado a ser mejor cada día y porque es nuestro deber plantar en ellos la semilla del esfuerzo y el trabajo, para que así un día alcancen sus sueños y lleguen lejos. A mi abuelita María (q.e.p.d) por su afecto y en especial por el apoyo y amor a mis padres y por estar siempre presente en mi vida. A quienes se han vuelto parte de mi familia, Pacho, Erika y Marce quienes siempre me acompañaron todos estos años y estuvieron pendientes de cada paso, gracias por su amor y apoyo. Agradecimientos especiales a Karen, Ber y Bonie por su voz de aliento. A MaE por sus sabios consejos y afecto.

Quiero agradecer especialmente a mi asesor profesor Carlos Ramos por sus invaluable enseñanzas a nivel profesional y personal, por su incondicional apoyo, por su paciencia y entrega a este proyecto, por transmitirme el amor a la investigación y a la docencia. A mi co-asesor profesor Giovanni Spagnuolo por su apoyo y ayuda durante mi estancia en Salerno, por su sencillez y calidad humana, por todos sus consejos y aportes en la realización de este trabajo. De igual forma mi agradecimiento especial a Patrizio Manganiello y al profesor Giovanni Petrone por su importante apoyo durante mi estancia en Salerno. Agradezco a Daniel Gonzalez por su apoyo incondicional en todas las etapas de este trabajo, por su compañerismo y buena energía, por regalarme su tiempo y atención, por su solidaridad y su amistad. A Juan David Bastidas por sus importantes aportes y ayuda, por su paciencia y comprensión. A los profesores Andrés Julian Saavedra y Eliana Arango por sus valiosos consejos en la parte inicial del doctorado. Gracias a todos !!

Abstract

There is a growing interest in photovoltaic (PV) systems since they represent a strong option for power supply around the world. Therefore, there is also a growing necessity for developing tools to analyze the behavior of the PV systems under realistic conditions. Hence, better planning, design and operative strategies can be developed. This thesis addresses the issues related with the modeling of PV systems operating under uniform and mismatched irradiance conditions. Moreover, this work considers the PV array connected in different configurations. In this way, the first part of the thesis presents the state-of-the-art in modeling techniques, it including circuitual representations of PV cells and modules and its behavior under different scenarios, operation characteristics of different configurations, the effects of the operation under shading conditions, available modeling techniques, among others.

The Series-Parallel (SP) is one of the most studied configuration, then some modeling techniques for SP arrays are introduced in this thesis. Such procedures allowed to understand the operation of PV arrays to detect the main aspects that need to be considered in a modeling process. The first technique is based on the ideal single diode model but considers the operation of the modules in the second quadrant by using a linear model to represent the bypass diodes. The approach allows to avoid introducing errors which may cause overestimation in the predicted power when the array is exposed to partial shading conditions. A second approach introduces a combination between the single diode model to represent the modules and a linear model to represent the bypass diodes; the mathematical relationships between the voltages and currents in the modules are typically implicit expression which requires the use of special functions as the Lambert-W function. However, the approach introduced a procedure to avoid the use of such a function, which allows to reduce the computation burden. The third approach is based on the single diode model for representing the PV modules and the Schottky model for representing the bypass diode; it proposes a procedure to calculate the maximum power point (MPP) for a given condition operation, without the need of calculating the whole power vs. voltage curve as it is typically performed. Instead, the procedure calculates some points in the neighborhood of the local maximum power points (LMPP) to define the MPP, it providing a fast calculation of the power delivered by the array for a given operating condition. Moreover, the procedure applies the mathematical treatment introduced in the second approach to avoid using the Lambert-W function. Finally, the fourth approach is based on simplified versions of the single diode model and the Schottky model; such versions are named ideal single diode model and ideal switch model, respectively. The main purpose of the approach is to introduce a procedure for modeling the shading considering its dynamic behavior which enables to achieve a more realistic operating condition to calculate the power provided by the array.

Other PV configurations, such as the Total Cross Tied (TCT) or the Bridge Linked (BL), may present better performances in comparison with the SP configuration for some operating conditions. However, there is no detailed procedures for modeling such configurations. In fact, the available techniques allow to analyze only one configuration which means that for each configuration a modeling algorithm is required, it making the evaluation of several configuration a complex and time consuming task. In other words, there is not a modeling procedure capable to represent any configuration. Therefore, a general modeling procedure for analyzing any PV configuration operating under uniform or shading conditions is introduced in this thesis. The possibility of studying any connection allows to consider structures without any connection pattern, in this way the thesis introduces the concept of irregular structure as a new option for obtaining improved power profiles at a particular operating condition. The general modeling procedure is a useful tool for reconfigurations analysis, planning and design of PV arrays.

All the modeling approaches presented in this work were validated through simulations and experimental tests. Most of them were implemented using Matlab scripts based on widely known programming structures and mathematical functions, those codes can be reproduced in languages such as *C* and *C++*.

Keywords: photovoltaic, module, array, modeling, shading, mismatching, bypass diode, equivalent circuit, algorithm.

Resumen

Técnicas de Modelado para Sistemas Fotovoltaicos Bajo Condiciones No Uniformes

Hay un creciente interés en los sistemas fotovoltaicos (PV) debido a que ellos representan una opción fuerte para abastecimiento al rededor del mundo. Por esto, también hay una necesidad creciente de desarrollar herramientas para analizar el comportamiento de dichos sistemas bajo condiciones realistas. Por tanto, mejor planeamiento, diseño y estrategias de operación pueden desarrollarse. Esta tesis aborda los problemas relacionados con el modelado de sistemas fotovoltaicos operando bajo condiciones uniformes y no uniformes. Mas aun, este trabajo considera el arreglo fotovoltaica conectado en diferentes configuraciones. De esta forma, la primer parte de la tesis presenta el estado del arte en técnicas de modelado, esto incluyendo las representaciones circuitales de las celdas y modelos fotovoltaicos y su comportamiento en diferentes escenarios, características de operación de diferentes configuraciones, los efectos de la operación bajo condiciones de sombreado, técnicas de modelado disponible, entre otros.

La configuración serie paralelo (SP) es una de las estudiadas, por tanto algunas técnicas para modelar arreglos SP son introducidas en esta tesis. Tales procedimientos permiten entender la operación de arreglos fotovoltaicos para detectar los aspectos principales que se deben considerar en un proceso de modelado. La primer técnica esta basada en el modelo ideal de un solo diodo pero considera la operación en el segundo cuadrante utilizando un modelo lineal para representar el diodo de bypass. Esta aproximación evita errores que provocan sobre estimación en el calculo de la potencia cuando el arreglo esta expuesto a condiciones de sombreado parcial. Una segunda aproximación introduce una combinación entre el modelo de un solo diodo y un modelo lineal para el diodo de bypass; las relaciones matemáticas entre voltajes y corrientes en el modulo son típicamente implícitas lo cual requiere el uso de funciones especiales como la función Lambert W. Sin embargo, la aproximación introduce un procedimiento para evitar el uso de tal funciona, lo cual permite reducir la carga computacional. La tercer aproximación esta basada en el modelo de un solo diodo para representar los módulos y el modelo Schottky para representar los diodos de bypass; se propone un procedimiento para calcular el punto de maxima potencia (MPP) para una condiciones de operación dada sin la necesidad de calcular toda la curva potencia vs voltaje como es realizado normalmente. En cambio, el procedimiento calcula algunos puntos en la vecindad de los puntos máximos locales (LMPP) para definir el MPP, logrando un calculo rápido de la potencia entregada por el array en una condición de operación. Mas aun, el procedimiento aplica tratamiento matemático introducida en la segunda aproximación para evitar el uso de la función Lambert W. Finalmente, la cuarta aproximación esta basada en versiones simplificadas del modelo de un solo diodo y el modelo Schottky; tales versiones

son llamadas modelo ideal de un solo diodo y modelo de interruptor ideal, respectivamente. El propósito principal de esta aproximación es introducir un procedimiento para modelar la sombra considerando su comportamiento dinámico lo cual permite obtener una condición de operación mas realista para calcular la potencia entregada por el arreglo.

Otras configuraciones PV tales como la Total Cross Tied (TCT) o la Bridge Linked (BL) pueden presentar mejor desempeño en comparación con la SP para algunas condiciones de operación. Sin embargo, no hay procedimientos detallados para modelar dichas configuraciones. De hecho, las técnicas disponibles permiten analizar solo una configuración lo cual significa que para cada configuración un algoritmo es requerido. Esto haciendo que la evaluación de diferentes configuraciones sea una tarea compleja y que consume mucho tiempo. En otras palabras, no hay un procedimiento de modelado capaz de representar cualquier configuración. Por esto, un procedimiento de modelado general para analizar cualquier configuración operando bajo condiciones uniformes o de sombreado parcial es introducido en esta tesis. La posibilidad de estudiar cualquier conexión permite considerar estructuras sin ningún patron de conexión, de esta forma esta tesis introduce el concepto de arreglo irregular como una nueva opción para obtener perfiles de potencia mejorados para ciertas condiciones de operación. El procedimiento de modelado general es una herramienta util para aplicaciones como reconfiguración, planeamiento y diseño de arreglos fotovoltaicos.

Todos las aproximaciones presentadas en este trabajo fueron validadas en pruebas de simulación y experimentales. La mayoría de ellas se implementaron en códigos de Matlab basados en estructuras de programación ampliamente utilizadas, estos códigos pueden ser reproducidos en lenguajes como *C* o *C++*.

Palabras clave: fotovoltaico, modulo, arreglo, modelado, sombra, irregular, diodo de bypass, circuito equivalente, algoritmo.

Preface

This thesis reports the results of my PhD studies at the Departamento de Ingeniería Eléctrica, Electrónica y Computación, Facultad de Ingeniería y Arquitectura, Universidad Nacional de Colombia. This work was carried out between February of 2013 to December of 2017, and it was funded by the **Beca doctorado Nacional Convocatoria 567** supported by Colciencias (Fondo nacional de financiamiento para ciencia, la tecnología y la innovación Francisco José de Caldas). This thesis was also supported by the Universidad Nacional de Colombia and Colciencias under the project **MicroRENIZ-25439 (Code 1118-669-46197)**.

The results of the thesis were published in one international journal and six national journals (see appendix B); in addition another five publications were supported by partial developments of this research work. The thesis format makes it easier for the reader to understand of the overall work and to identify the improvements in the state of the art. Moreover, the publications significantly improve the diffusion of the thesis results.

The thesis follows common publishing guidelines given by international journals. Similarly, the bibliographical citations have been numbered in alphabetical order; the equations, figures and tables have been numbered in order of appearance. Both roman and italic fonts appear in the text, the latter being used to highlight important issues, differentiate nouns and mark non-English words. Some simulations tests and writing process of papers were developed at the Università degli Studi di Salerno (Italy), during a research internship supported by Universidad Nacional de Colombia and Colciencias. Finally, the simulations of the photovoltaic systems and the implementation of the modeling techniques developed in this work have been carried out by using Matlab/Simulink and *C++*, while some simulations which include power electronics circuits have been carried out by using PSIM software.

Contents

| | |
|---|------------|
| Acknowledgments | IV |
| Agradecimientos | V |
| Abstract | VII |
| Resumen | IX |
| Preface | XI |
| Abbreviations and nomenclature | XV |
| 1. Introduction | 1 |
| 1.1. Basic concepts on PV devices | 2 |
| 1.2. PV modeling issues | 3 |
| 1.3. Thesis structure | 7 |
| 2. Operation and Modeling of PV Devices | 8 |
| 2.1. Introduction | 8 |
| 2.2. Photovoltaic cell and module operation | 9 |
| 2.3. Modeling of photovoltaic devices | 12 |
| 2.3.1. Single diode model | 12 |
| 2.3.2. Two diode model | 14 |
| 2.3.3. Bishop model | 15 |
| 2.3.4. PL model | 16 |
| 2.3.5. Alternative PV cell models | 17 |
| 2.3.6. PV arrays configurations | 17 |
| 2.3.7. The mismatching effect | 19 |
| 2.3.8. Operation and modeling of bypass diodes | 20 |
| 2.4. Modeling of photovoltaic arrays | 23 |
| 2.4.1. Modeling techniques for obtaining the electrical characteristics | 23 |
| 2.4.1.1. Solutions based on the single diode model | 24 |
| 2.4.1.2. Solutions based on the two diode model | 32 |
| 2.4.1.3. Solutions based on the Bishop model | 34 |

| | | |
|-----------|---|-----------|
| 2.4.2. | Modeling techniques oriented to energy yield analysis | 37 |
| 2.4.2.1. | Solutions based on the single diode model | 37 |
| 2.4.2.2. | Solutions based on other PV models | 40 |
| 2.4.3. | Modeling techniques for shading analysis | 42 |
| 2.4.3.1. | Solutions based on the single diode model | 42 |
| 2.4.3.2. | Solutions based on the Bishop model | 46 |
| 2.4.3.3. | Solutions based on the PL model | 51 |
| 2.5. | Conclusions | 51 |
| 3. | Modeling approaches for SP arrays | 55 |
| 3.1. | Introduction | 55 |
| 3.2. | A modeling approach considering the operation in the second quadrant . . . | 56 |
| 3.2.1. | PV string modeling | 58 |
| 3.2.2. | PV array modeling | 61 |
| 3.3. | Power estimation approaches | 65 |
| 3.3.1. | Approach 1: single diode model and linear bypass diode model | 66 |
| 3.3.2. | Approach 2: single diode model and exponential bypass diode model . | 71 |
| 3.3.3. | Approach 3: ideal single diode model and ideal bypass diode model . | 80 |
| 3.4. | Conclusions | 85 |
| 4. | Modeling of irregular PV arrays | 88 |
| 4.1. | Introduction | 88 |
| 4.2. | The concept of irregular PV array | 89 |
| 4.3. | Equivalent circuits for modeling irregular PV arrays | 93 |
| 4.3.1. | Computation of inflection points | 95 |
| 4.3.2. | Detection of the equivalent circuits and I-V, P-V curves reproduction | 98 |
| 4.3.3. | Dynamic simulation | 99 |
| 4.4. | General procedure for modeling PV arrays based on node voltage analysis . . | 102 |
| 4.4.1. | PV module model | 103 |
| 4.4.2. | Identification of independent sub-arrays and their parameters | 104 |
| 4.4.3. | Calculation of the sub-array current | 105 |
| 4.4.4. | Calculation of the array current | 108 |
| 4.4.5. | Application example of the proposed procedure | 108 |
| 4.4.6. | Validation of the proposed procedure | 111 |
| 4.4.7. | Application example: PV array reconfiguration | 113 |
| 4.5. | General procedure for modeling PV arrays based on mesh currents analysis . | 115 |
| 4.5.1. | PV module model | 116 |
| 4.5.2. | Calculation of the sub-array current | 117 |
| 4.5.3. | Calculate the array current | 119 |
| 4.5.4. | Application of the proposed modeling procedure | 120 |

| | |
|---|------------|
| 4.5.5. Validation of the proposed model | 121 |
| 4.6. Conclusions | 129 |
| 5. Conclusions and Future Works | 132 |
| A. System of equations and Jacobian matrix used in simulations | 137 |
| B. Publications | 141 |
| References | 143 |

Abbreviations and nomenclature

This section contains the abbreviations and nomenclature used along the thesis.

Abbreviations

| Abbreviations | Description |
|---------------|--|
| SP | Series Parallel |
| SD | Single Diode |
| ISD | Ideal Single Diode |
| TCT | Total Cross Tied |
| BL | Bridged Linked |
| HC | Honey Comb |
| MPPT | Maximum Power Point Tracking |
| MPP | Maximum Power Point |
| GMPP | Global Maximum Power Point |
| LMPP | Local Maximum Power Point |
| PV | Photovoltaic |
| STC | Standard Test Conditions |
| ASTM | American Society for Testing and Materials |
| AM | Air Mass |
| VBA | Visual Basic for Applications |
| DE | Differential Evolution |
| ABC | Artificial Bee Colony |
| PSO | Particle Swarm Optimization |
| PL | Piecewise Linear |
| RMSE | Root Mean Square Error |
| DLL | Dynamic Link Library |
| ANN | Artificial Neural Network |
| ESTI | European Solar Test Installation |
| NSSE | Normalized Sum of Squares Error |
| RAAE | Range Average Absolute Error |
| MAPE | Mean Absolute Percentage Error |
| P&O | Perturb and Observe |

| Abbreviations | Description |
|---------------|-------------------------|
| KVL | Kirchhoff Voltage Laws |
| KCL | Kirchhoff Current Laws |
| DAQ | Data Acquisition System |

Nomenclature

| Nomenclature | Description |
|--------------|---|
| I_{sc} | Short circuit current |
| I_{sat} | Saturation current |
| R_s | Series resistance |
| R_h | Parallel resistance |
| B | Thermal voltage |
| R_{da} | Activation resistance |
| V_{da} | Activation voltage |
| k | Boltzman constant |
| q | Electron charge |
| T | Temperature |
| T_{STC} | Temperature at STC conditions |
| V_{str} | String voltage |
| I_{str} | String current |
| I_{array} | PV array current |
| V_{array} | PV array voltage |
| V_{oc} | Open circuit voltage |
| V_{0k} | Inflection voltage of module k |
| V_{mpp} | Voltage at the maximum power point |
| I_{mpp} | Current at the maximum power point |
| I_{ph} | Photovoltaic current |
| V_t | Thermal voltage |
| P_{mpp} | Power at the maximum power point |
| I_d | Diode current |
| I_h | Parallel resistance current |
| I_{bk} | Blocking diode current |
| P_{GMPP} | Power at the global maximum power point |
| S | Irradiance |
| S_{stc} | Irradiance in STC |
| N_s | Number of cells in a PV module |
| N | Number of rows in a PV array |
| M | Number of columns in a PV array |

| Nomenclature | Description |
|---------------------|---|
| W_o | Lambert-W function |
| e_a | Positive terminal voltage in a PV module |
| e_b | Negative terminal voltage in a PV module |
| I_{db} | Bypass diode current |
| $I_{sat,db}$ | Saturation current of a bypass diode |
| $V_{t,bd}$ | Thermal voltage of a bypass diode |
| n | Ideality factor |
| n_{bd} | Ideality factor of a bypass diode |
| K_{Isc} | Temperature coefficient of the short circuit current in STC |
| K_{Vsc} | Temperature coefficient of the open circuit voltage in STC |
| M_{conn} | Connection matrix |
| N_{sa} | Number of sub-arrays |
| N_z | Number of columns of zeros in M_{conn} |
| SA_i | Sub-array i |
| $SA_{fc,i}$ | First column of sub-array i |
| $SA_{lc,i}$ | Last column of sub-array i |
| M_{Iph} | Matrix of photovoltaic currents |
| M_{Isat} | Matrix of saturation currents |
| M_{Vt} | Matrix of thermal voltages |
| M_{Rs} | Matrix of series resistances |
| M_{Rh} | Matrix of parallel resistances |
| M_{Isatbd} | Matrix of saturation currents of bypass diodes |
| M_{Vtbd} | Matrix of thermal voltages of bypass diodes |
| $M_{Iph,i}^{sa}$ | Matrix of photovoltaic currents of sub-array i |
| $M_{Isat,i}^{sa}$ | Matrix of saturation currents of sub-array i |
| $M_{Vt,i}^{sa}$ | Matrix of thermal voltages of sub-array i |
| $M_{Rs,i}^{sa}$ | Matrix of series resistances of sub-array i |
| $M_{Rh,i}^{sa}$ | Matrix of parallel resistances of sub-array i |
| $M_{Isatbd,i}^{sa}$ | Matrix of saturation currents of bypass diodes of sub-array i |
| $M_{Vtbd,i}^{sa}$ | Matrix of thermal voltages of bypass diodes of sub-array i |
| $M_{conn,i}^{sa}$ | Connection matrix of sub-array i |
| $I_{sa,i}$ | Current of sub-array i |
| $N_{n,i}$ | Number of nodes of sub-array i |
| $V_{n,i}$ | Vector of voltages nodes of sub-array i |
| $M_{nv,i}^{sa}$ | Matrix of nodes voltages identification of sub-array i |
| I_a | Mesh current at the right of a PV module |
| I_b | Mesh current at the left of a PV module |
| I_{by} | Current of bypass diode |
| $I_{sat,by}$ | Saturation current of a bypass diode |

Nomenclature **Description**

$N_{m,i}$ Number of meshes of sub-array i

1. Introduction

Photovoltaic (PV) systems have become a relevant research area due to the new energetic tendencies which promote the conservation of the environment and the reduction of the use of sources based on fossil fuels, this because of their negative environmental impact and their increasing price [97]. On the other hand, the incentive politics adopted by several countries around the globe increase the interest of the academic and industrial community on PV generation.

In the last two decades the intensification in the research PV systems has been remarkable. The exercise of searching the keywords “PV systems” in the Scopus provides a result of 123142 documents between papers and patents. PV systems have become a relevant research area due to the new energetic tendencies, which promote the conservation of the environment and the reduction of the use of sources based on fossil fuels because of their negative impact and their increasing price [17], [97]. Another reason for the current interest in PV systems concerns the incentive politics adopted by several countries in Europe and cities in United States. For some countries in Latin America, PV systems are also a priority, such is the case of Argentina, Ecuador, Honduras and Nicaragua, where a system based on feed-in tariffs have been implemented with the aim of strengthen the use of PV energy and other renewable sources [48], [75]. In the case of Colombia, in 2010 the Mines and Energy Ministry approved guidelines to the development of the Program for the Rational and Efficient Use of Energy and other forms of Non-conventional Energies (Programa de Uso Racional y Eficiente de la Energía y demás Formas de Energía no Convencionales - PROURE). This program promotes research and development activities in the non-conventional energies area such as the PV solar energy, identifying it as a key factor to make the participation of the non-conventional energies, in the interconnected system, reaches 6.5% for 2020 and 30% for the non-interconnected zones [23]. Moreover, the law 1715 of 2014 establishes the legal framework and the promotion instruments for the exploitation of the renewable energies and their integration with the Colombian energetic market [24].

At present the PV technology has been highly commercialized, according to the International Energy Agency (IEA) the global installed PV power during 2016 was 303 *GW* while in 2015 was 227.1 *GW*. Moreover, the IEA predicts that by 2030, the global installed capacity of PV will reach 1721 *GW* [44]. PV systems can be grouped in two general categories: off-grid and grid-connected PV systems. Off-grid PV systems are not connected to an electricity

network, in this kind of systems storage systems (batteries) are required to provide energy to the load during periods of no light (night) or low-light levels. DC-DC converters are also needed to implement control actions as maximum power point tracking (MPPT) strategies and regulation of the charge in batteries [58], [16]. On the other hand, grid-connected PV systems require of DC-AC inverters to convert the electricity from PV panels and inject it to the electrical grid. MPPT controllers, filters and bi-directional protection devices are also used [53], [57], [16]; other sub-categories of PV systems include: small and large PV systems, domestic and non-domestic PV systems, hybrid systems, grid-connected centralized and distributed PV systems, among others [16].

1.1. Basic concepts on PV devices

PV generation is based on electronic devices which transform sunlight into electricity. Then, PV devices are made of materials in which the absorption of light raises an electron to a higher energy state to be moved to an external circuit. Semiconductor materials in the form of a p-n junction are the most widely used in the production of PV devices [85]. At commercial scale, PV cells are normally made of monocrystalline and polycrystalline silicon with efficiencies of $26,3\% \pm 0,5$ and $21,3\% \pm 0,4$ respectively [39]. Other materials may achieve better performance but their high costs make production at large scale unfeasible [111]. Since the voltage and power of a single PV cell are small (0.6 V and 0.8 W approx.), in actual applications, several cells must be connected in order to fulfill the voltage and current requirements of a load. In this way, a group of series-connected cells connected in anti-parallel with a diode (known as bypass diode) form a module and typically groups of 2 or 3 modules in series connection form a panel which are the PV devices commercially available to form PV arrays for delivering significant amounts of power. The relationship between cells, modules and panels is illustrated in Fig. 1-1; such a relationship must be considered in the modeling process to define its *granularity*, in other words the basic PV unit considered to represent the relationships between the voltage and current in the PV array. Then, if a detailed analysis is required, the granularity of the model is typically at cell level or inclusive sub-cell level, on the other hand if a long-term analysis is required, the granularity of the model is typically at module level [72], [81]. In addition, the computational burden is highly related to the granularity of the model, in this way high granularity (more detailed) models require more robust processors than low granularity models.

The PV panels of an array can be connected in different structures. The most widely studied structure is the Series-Parallel (SP) array [50] which is formed by series-connected panels configuring strings that are connected in parallel. There are other common configurations: the Total Cross Tied (TCT) in which all panels in consecutive strings are connected in parallel through ties; the Bridge-Linked (BL) and Honey-Comb (HC) configurations, which are variations of the TCT where ties are located in interleaved fashion [88].

The PV conversion effect can be represented through an electric circuit in order to analyze the behavior of the current, voltage and power of an application. Several models have been reported in literature: the single diode model [111], [27], the two diode model [46], [78], the Bishop model [13], [99], among others. Each one of the aforementioned models have different parameters that must be defined to perform the required analysis on a PV system; therefore, different procedures for calculating the circuit parameters have been reported.

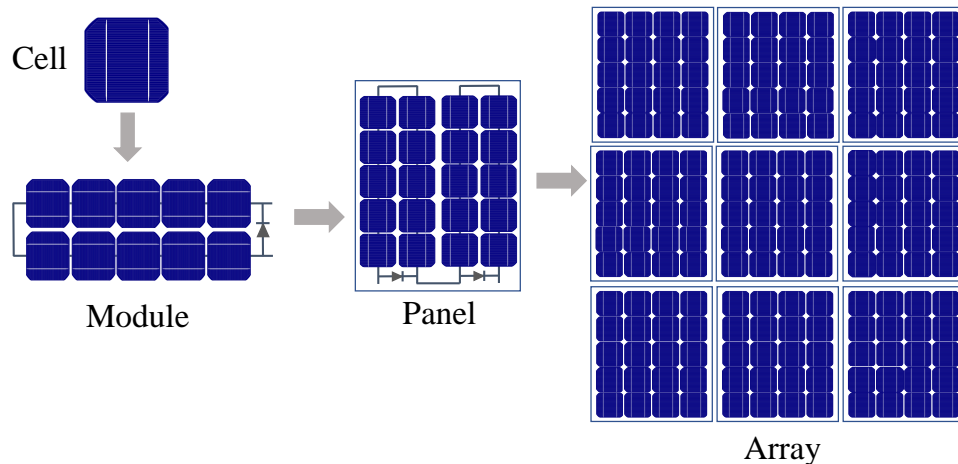


Figure 1-1.: Components of a PV array.

The more the complexity of the circuitual representation of the cell, the more the complexity of the procedure for computing the parameters. In the same way, such models have been scaled up to model PV modules allowing to define the level of detail for a particular analysis, evidently the analysis of a PV array at cell level will be more complex than a module level but it could provide useful information. Then, the selection of a model for analyzing a PV system must be done under the particular conditions defined by the user, in other words, the selection must be done to satisfy a desired relationship between accuracy and processing time.

1.2. PV modeling issues

In this context, modeling of PV systems has become one of the most important studying areas at present, due to the need of obtaining information concerning the performance and energy production of a PV system under different operating conditions. For this purpose, analytical and simulation methods have been used. In literature, around 25 different software packages or computational tools have been reported [31], [61], [106]. However, simulation packages have some limitations: high license cost, poor representation of panels operating at different irradiance levels, restrictions for interfacing the PV arrays models with power

electronics systems [79], time consuming and annoying process of connection and configuring circuitual elements, among others. Those limitations show the need of using analytical techniques, which in synergy with simulation packages and programming languages, allow providing suitable analysis of PV systems with a good balance between accuracy and computational cost.

In the process of modeling PV systems there are several aspects that must be considered: the size and connection of the array, the type of required analysis, the operation conditions, the computing resources available, among others. The size of the array could give a first idea about the complexity of the process and it could be a criterion for selecting the granularity, which normally varies between cell level or module level. Another relevant consideration is the type of required analysis since the study of PV systems can be mainly oriented to: the reproduction of the I-V and P-V curves and/or energy yield studies over the entire array.

On the other hand, independent of the connection, a PV array is normally formed by the same type of panels which have the same operating parameters. Moreover, if the irradiance condition is the same for all the panels in the array, it is considered that it operates under balanced or uniform conditions. However, in real applications such a condition is not always fulfilled since PV arrays are normally exposed to circumstances in which the balance is lost and the operating condition of the modules is non uniform, such a situation is better known as *mismatching conditions*. The non uniform conditions may be provoked by differences in the internal parameters of PV panels, but the difference in the irradiance level is the most common cause for mismatching conditions. This phenomenon is caused by partial shading due to objects (clouds, poles, buildings, trees, other panels on the PV structure, etc) in the neighborhood of the array, which project their shadow on the surface of the panels. When partial shading occurs, the shaded cells experiment negative voltages due to the excess of current imposed by the cells with higher levels of irradiance, this situation causes the shaded cells to consume power instead of produce it [13], in other words, those cells operate in the second quadrant.

To avoid in part the negative effect of partial shading, PV modules inside a PV panel, are connected in anti-parallel with a diode normally known as *bypass diode*; such a diode must be considered in the model of the module since their activation changes the behavior of the system. Fig. 1-2 shows the P-V curve of an array without shadow compared with the P-V curve of the same array exposed to partial shading. It can be observed the change of the maximum power point (*MPP*), such a behavior is a relevant aspect in the operation of the maximum power point tracking (*MPPT*) controller, but also for predicting the energy production of the array.

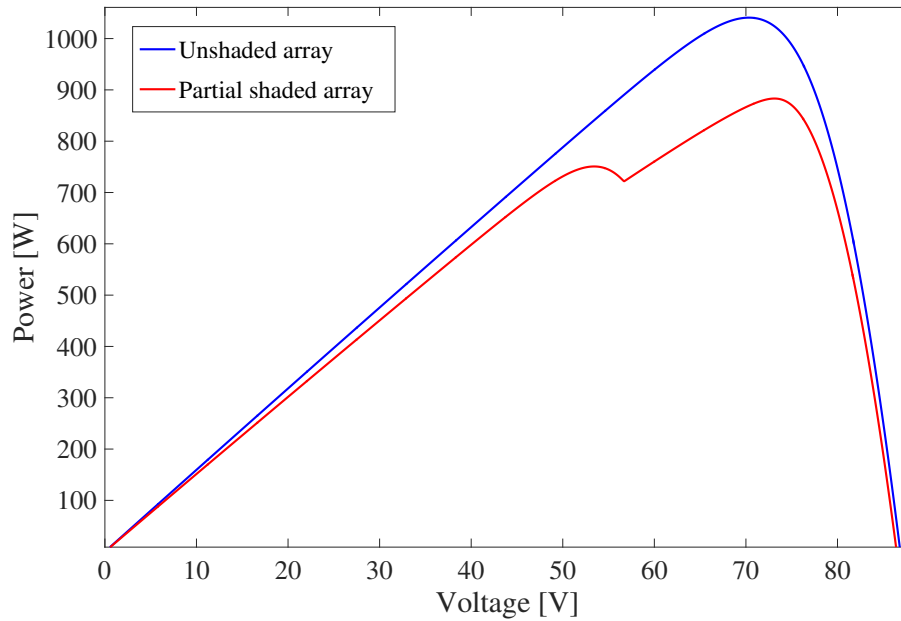


Figure 1-2.: Comparison of power curves in a PV array operating with and without shading.

The connection of the PV array is another concept that must be considered in the modeling process. As it was highlighted, there are four typical configurations: SP, TCT, BL and HC. However, other structures with different patterns of connection between strings or structures without any kind of pattern in the ties connecting the strings are physically possible as it is presented in [66], where the performance of hybrid structures operating under different shading scenarios is evaluated. Such hybrid structures are the result of combining SP with TCT configuration, BL with TCT configuration and BL with HC configuration. As an example, Fig. 1-3 shows a PV array which does not belong with the typically reported configurations i.e. *irregular configuration*. Fig. 1-4 shows a comparison of the power delivered of the same 4×4 PV array connected in SP, TCT, BL, HC and the irregular configuration. The five configurations are operating under the same irradiance and shading profiles; it can be seen that the maximum power point of the irregular connection has the highest power. This example puts into evidence that PV structures different from the conventional have a better performance under certain partial shading conditions.

Several techniques for modeling PV arrays under the typical configurations have been reported independently, i.e. techniques for modeling only one kind of PV array structure. A general procedure for modeling all the conventional configurations is not available yet. Moreover, due to the lack of analysis of new PV structures there are no information concerning the modeling of PV arrays under any (conventional or irregular) configuration. The development of a general procedure for modeling any PV array could be a useful tool for planning

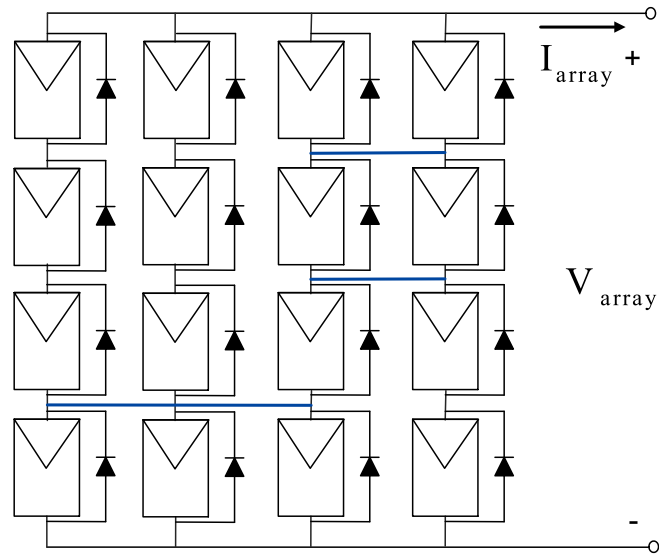


Figure 1-3.: Irregular PV array.

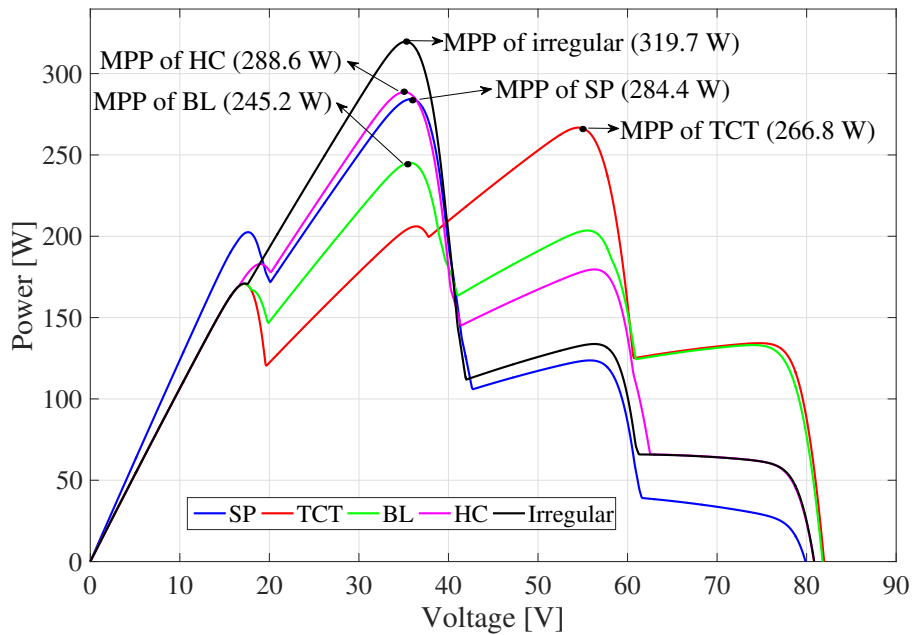


Figure 1-4.: Comparison of power provided by SP, TCT, BL, HC and an irregular 4×4 PV array under the same irradiance and shading profiles.

and design of PV systems since it will allow evaluating all the desired options for connecting the panels under the given operating conditions; so that the maximum achievable power is ensured, or the lower degradation is achieved. In this way, the suitable connection for the array can be defined; it can be also used for evaluation of *MPPT* control strategies and analysis of partial shading impact. Moreover, the procedure can be used in algorithms or techniques for reconfiguration of PV systems. In the same way, it can be combined with optimization methods for improving the computing times for large PV arrays.

1.3. Thesis structure

This thesis presents some concepts related with the modeling of PV systems with typical configurations as well as irregular structures. The analysis included in this work considers uniform conditions as well as mismatched conditions. In this way, Chapter 2 presents the basic concepts of the operation of PV devices, which must be considered in the modeling process: the different models for representing the PV cell, the modeling of bypass diodes, the scaling up process for modeling modules, the specific characteristics of SP, TCT, BL and HC arrays, among others. Chapter 2 also includes a review of the modeling techniques of PV systems, which enable to identify that the efforts have been focused on the modeling of SP arrays, confirming also that there is no a generalized procedure for modeling any PV array. Moreover, the review confirmed the tendency for using the single diode model due to its good compromise between complexity and accuracy. Other relevant aspects as the granularity, operation in the second quadrant and shading analysis are also addressed in Chapter 2. A new approach for modeling SP arrays is introduced in Chapter 3. Such an approach allows to reconstruct the I-V and P-V curves considering the operation in the second quadrant for improving the accuracy in the prediction of the power production. In addition, three approaches for power estimation in SP arrays are also proposed.

In the first part of Chapter 4, an initial approach of the analysis of irregular structures is given through a procedure that considers a simplification of the single diode model, known as ideal single diode model. The approach consists in the simplification of the PV array by lumping the panels connected in parallel and considering them as a single panel represented by a N – *diode* model, with N equal to the number of lumped panels; this procedure is validated through simulations tests. In the second part of the chapter, a procedure for modeling PV arrays under any connection is introduced. Such a procedure is based on the single diode model and it is divided in two approaches: solution by nodes voltages analysis and solution by meshes currents analysis. Both approaches are based on dividing the PV array in parts, named *sub-arrays*, which can be modeled and solved independently. The procedures are validated through simulations and experimental tests. Finally, the conclusions and future lines of researching derived from this work are given in Chapter 5.

2. Operation and Modeling of PV Devices

This chapter presents the basic concepts concerning the operation and modeling of photovoltaic (PV) devices. A fast overview of the most cited circuital models is given, as well as a description of the techniques for calculating the parameters of such models. On the other hand, the mismatching effect and the operation of the bypass diodes is also addressed giving special attention to the issue of partial shading.

A review of modeling techniques applied to PV arrays is presented. The techniques were classified into three categories in order to provide to the reader some basic elements that can be useful for defining a suitable solution for a given application. In the review the concepts considered as relevant were the level of detail for representing the PV panel (cell or module), the PV model, the final application structure (module or array) as well as its configuration and the operation in the second quadrant. The survey provides elements to identify key aspects as the most widely used PV model and PV array configuration studied.

Part of the analysis made in this chapter was published in Revista Tecnura in the paper: “Techniques for modeling photovoltaic systems under partial shading” [110].

2.1. Introduction

The analysis of PV systems covers different research areas, among which, modeling is one of the most important because it allows to predict the performance of a PV system in terms of energetic production. It supports the development of control techniques, sizing, planning, among others. The modeling of PV systems requires a set of concepts like PV basic models, PV system connection, operating and environmental conditions effects, etc. The main objective is to predict the PV array behavior with a suitable tradeoff between accuracy and calculation speed. Therefore, it is important to consider all the aspects related with the operation of PV systems: the principle of operation of PV devices, the available models and parameters to represent them, the configurations of those PV devices applied in actual applications and the phenomena that affect their performance. In this way, this chapter is devoted to explain the main concepts related with the operation of PV systems, this introducing the basic aspects of the operation of PV devices, their circuital models and

their key issues. In addition, special attention is given to the modeling techniques oriented to PV systems operating under shading conditions, since it is one of the main drawbacks of PV applications. The review of the concepts presented in this chapter allowed to define key points of this thesis and the specific subjects studied in the following chapters.

2.2. Photovoltaic cell and module operation

PV devices transform light into electricity. The PV cell is the basic unit of a PV system, its operation is basically the same as a semiconductor diode in which its p-n junction is exposed to light. PV cells are made of light-sensitive semiconductor materials that use photons to dislodge electrons to drive an electric current. There are two technologies typically used for manufacturing PV cells: crystalline silicon and thin film. Crystalline silicon PV cells are divided into polycrystalline and monocrystalline cells, which are the most popular for commercial PV panels [16], [111]. Thin film PV cells are divided into amorphous-Silicon (a-Si) cells, Cadmium Telluride (CdTe) cells, among others, with a lower commercial impact. Crystalline silicon PV cells show higher efficiency in comparison with other technologies: $26,3\% \pm 0,5$ for monocrystalline cells, $21,3\% \pm 0,4$ for polycrystalline cells, while a-Si cells and CdTe cells present efficiencies of $10,2\% \pm 0,3$ and $17,5\% \pm 0,3$ respectively [39].

The power production in a PV device depends on the irradiance, which in turns depends on the location. The distance between the sun and the earth varies with its motion and it causes irradiance also to change. However, the levels of annual energy due to sun radiation reach considerable amounts of $2300kW/m^2$ in some regions at the equator and $1700kW/m^2$ at southern Europe [47]. PV devices are generally evaluated under two standards: the direct-normal and global $AM1,5$ (Air Mass), defined by The American Society for Testing and Materials (ASTM) [111]. Both are used in PV industry to define the characteristics and parameters of commercial panels included on datasheets. Those parameters used as reference the Standard Test Condition (STC), which means an irradiance of $1000W/m^2$, at $25\text{ }^\circ\text{C}$ [68].

For practical applications, PV cells are connected in series to form modules, which in turn are connected in series to form panels; these are also connected in series to form strings. Finally, strings are connected in parallel to form arrays as is shown in Fig. **2-1**. The number of panels of a string will be defined by the voltage required for the load, while the number of the strings will be defined by the current conditions of the load. Fig. ?? shows how cells are connected in anti-parallel with a diode, named bypass diode, which is used to mitigate the negative effects of the mismatching conditions; such a concept will be discussed in detail in the following sections of this chapter.

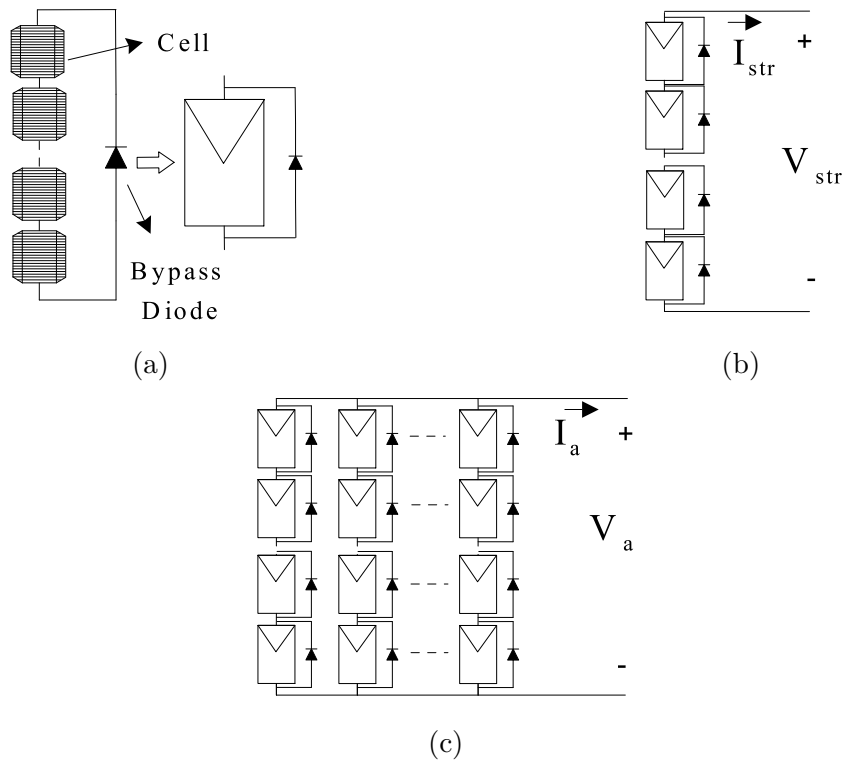


Figure 2-1.: Conformation of PV systems: (a) Module, (b) String, (c) Array.

The performance of a PV system is normally analyzed from the point of view of power generation. Then, the current vs. voltage (I-V) and power vs. voltage (P-V) curves become important tools. Those curves allow to analyze the behavior of a PV system for a given operating conditions of irradiance, temperature, shadowing, etc. Fig. **2-3** shows the characteristic curves of a PV cell. This kind of curves are also obtained for modules, strings and arrays. In such curves I_{SC} is the short-circuit current, V_{OC} is the open-circuit voltage, MPP the maximum power point, while I_{MPP} , V_{MPP} and P_{MPP} are the current, voltage and power at the maximum power point respectively.

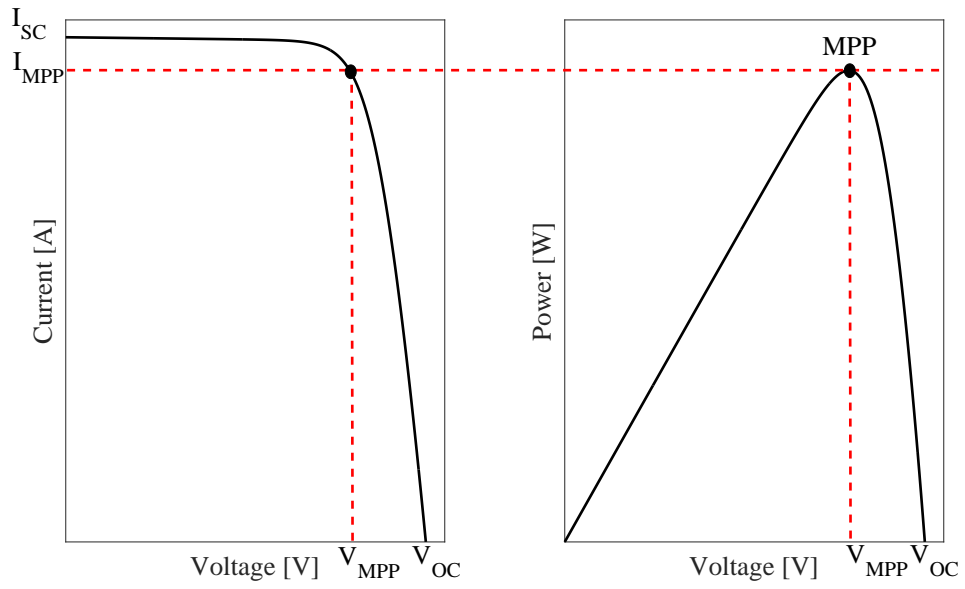


Figure 2-2.: Characteristic curves of a PV cell.

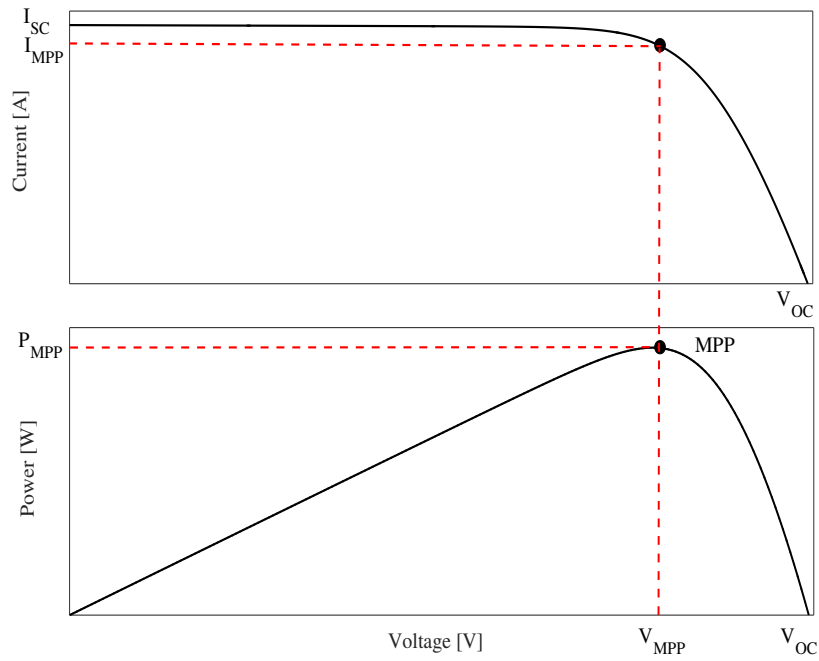


Figure 2-3.: Characteristic curves of a PV cell.

2.3. Modeling of photovoltaic devices

Due to the need of obtaining accurate information concerning the performance and energy production of PV systems under different operating conditions, analytical and simulation methods have been developed. The modeling process is commonly based on a circuitual representation of the PV cell. Therefore, it is convenient to consider all the elements that affect the behavior of the cell in a realistic way. In literature several models have been reported, the most widely adopted approaches are: the single diode model [111], [27], [83], [9], [42], the two diode model [46], [78], [116], [91], [21], the Bishop model [13], [99], [98], [63], [88] and the piecewise linear (PL) model [113], [5], [114].

According to some authors, some models are more suitable for certain cell technologies: in [33] authors propose a two diode model for modeling amorphous silicon cells, while the same model is used in [2] for modeling polycrystalline cells. Authors in [69] introduce a three diode model also for polycrystalline cells. The two diode model is also used in [104] for modeling amorphous, polycrystalline and monocrystalline PV cells. On the other hand, in [43] and [18] monocrystalline cells are modeled through the single diode model.

2.3.1. Single diode model

The single diode model is one of the most adopted approaches, since it is simple and accurate enough [111]. The equivalent circuit of the single diode model is shown in Fig. 2-4. By applying current and voltage Kirchhoff laws, equation (2-1) is obtained, which expresses the current of the cell (I_{cell}) in function of its voltage (V_{cell}). In (2-1) $I_{ph,cell}$ is the photovoltaic current which is directly proportional to irradiance, $I_{sat,cell}$ is the saturation current of the diode, $V_{t,cell}$ is the thermal voltage of the cell diode defined in (2-2), while $R_{s,cell}$ and $R_{h,cell}$ are the series and parallel resistances, respectively [9]. Series resistance $R_{s,cell}$ represents the ohmic losses, it has no effect on the open-circuit voltage, but reduces the short-circuit current; on the other hand, parallel resistance $R_{h,cell}$ represents the leakage currents, it has no effect on the short-circuit current, but reduces the open-circuit voltage [16].

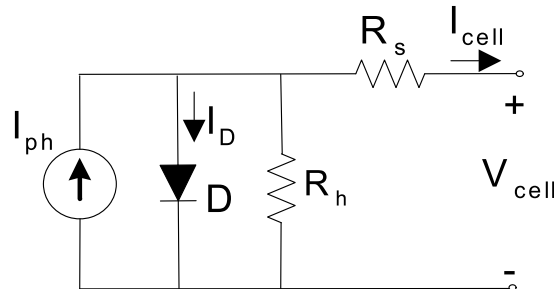


Figure 2-4.: Equivalent circuit of the single diode model.

$$I_{cell} = I_{ph,cell} - I_{sat,cell} \cdot \left(\exp \left(\frac{V_{D,cell}}{V_{t,cell}} \right) - 1 \right) - \frac{V_{D,cell}}{R_{h,cell}} \quad (2-1)$$

$$V_{t,cell} = \frac{n_{cell} \cdot k \cdot T}{q} \quad (2-2)$$

$$V_{D,cell} = V_{cell} + I_{cell} \cdot R_{s,cell} \quad (2-3)$$

In (2-2), n_{cell} is the diode ideality constant, k is the Boltzmann constant ($1,3806503 \times 10^{-23} J/K$), T is the temperature of the p-n junction in Kelvin degrees, and q is the electron charge ($1,60217646 \times 10^{-19} C$). This model can be scaled up to represent modules since they are formed by N_S series-connected cells and N_P strings of cells connected in parallel. For that purpose, the parameters of (2-1) and (2-2) can be re-defined as: $V_{mod} = N_S \cdot V_{cell}$, $I_{mod} = N_P \cdot I_{cell}$, $I_{ph} = N_P \cdot I_{ph,cell}$, $I_{sat} = N_P \cdot I_{sat,cell}$, $V_t = N_S \cdot V_{t,cell}$, $R_s = (N_S/N_P) \cdot R_{s,cell}$, $R_h = (N_S/N_P) \cdot R_{h,cell}$. In this way, the current of the module can be written as:

$$I_{mod} = I_{ph} - I_{sat} \cdot \left(\exp \left(\frac{V_{mod} + I_{mod} \cdot R_s}{V_t} \right) - 1 \right) - \frac{(V_{mod} + I_{mod} \cdot R_s)}{R_h} \quad (2-4)$$

This model is also known as the five parameters model, since there are five parameters required to solve (2-4) in order to know the current of the module for a given value of V_{mod} . Those parameters are: I_{ph} , I_{sat} , V_t , R_s and R_h . Unfortunately, such information is not included in the manufacturer's datasheet; the typical information given by manufacturer is the short-circuit current ($I_{SC,STC}$), the open-circuit voltage ($V_{OC,STC}$) and the voltage, the current and the power at the *MPP* ($I_{MPP,STC}$, $V_{MPP,STC}$ and $P_{MPP,STC}$) at STC; sometimes the open-circuit voltage/temperature coefficient K_v and the short-circuit current/temperature coefficient K_I are also included. Such an information is valid for the entire PV panel not for a single module, then in PV panels with multiple modules the parameters must be adjusted. Moreover for different operating conditions, some of those five parameters must be recalculated by using analytical methods. The basic structure of most methods reported in literature consists in solving a system of equations obtained by considering three key points of the characteristic curve of the PV device at STC: the short-circuit current point where $I_{mod} = I_{SC,STC}$ and $V_{mod} = 0$, the open-circuit voltage point where $I_{mod} = 0$ and $V_{mod} = V_{OC,STC}$ and the maximum power point where $I_{mod} = I_{MPP,STC}$ and $V_{mod} = V_{MPP,STC}$. In addition, the derivative of the power with respect to the voltage at the *MPP*, which is equal to zero, must be included [27], [26], [40].

Some variations of this procedure have been proposed: in [111] authors assumed that the photovoltaic current I_{ph} depends linearly on the irradiance and the temperature, they propose a new expression for calculating I_{sat} . In addition, a procedure based on successive iterations to calculate and adjust R_s and R_h values is also proposed. A similar technique is introduced

in [80] but including the use of the Lambert W function to solve the current equation. On the other hand, in [22] authors assumed that R_s , R_h and I_{sat} change with the irradiance to propose a new five parameter model, also defining new equations for the I_{ph} , I_{sat} including a thermal correction factor. In [18] and [42] authors proposed a set of equations for calculating the five parameters directly, it only considering the computation of the values of I_{SC} and V_{OC} for the specific irradiance operation point with respect to the STC values. A procedure based on tabular performance data is introduced in [74], the typical three points equations are defined but the value of R_s and R_h resistances are obtained from analytical correlations, which were defined on the basis of the performance data of more than one hundred surveyed PV panels; according to the authors the computer routines can be easily implemented even in VBA macros of Microsoft Excel.

2.3.2. Two diode model

This model has the same elements as the single diode model but an additional diode is included as it is shown in Fig. 2-5. The second diode represents the effect of recombination current loss in the depletion region, which is not taken into account in the single diode model; this model provides more accuracy at low irradiance values [46], [19].

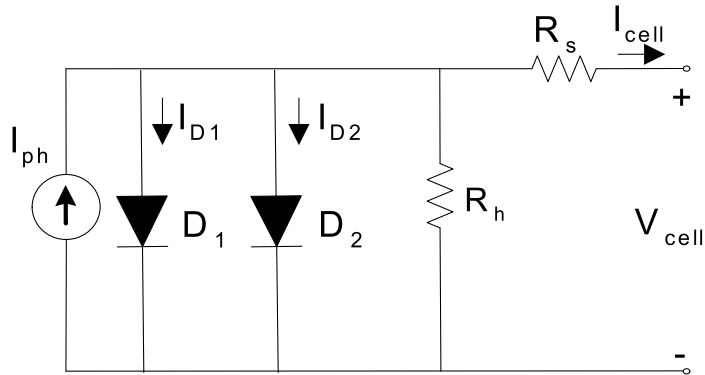


Figure 2-5.: Equivalent circuit of the two diode model.

Although the two diode model is more accurate it is also more complex due to the amount of variables to take into account and the increased number of parameters to be calculated. Equation (2-5) describes the relationship between the current and voltage in a PV module. Such an equation includes the considerations made for scaling up the parameters of the model as made for the single diode model.

$$I_{mod} = I_{ph} - I_{sat1} \cdot \left(\exp \left(\frac{V_{mod} + I_{mod} \cdot R_s}{V_{t1}} \right) - 1 \right) - I_{sat2} \cdot \left(\exp \left(\frac{V_{mod} + I_{mod} \cdot R_s}{V_{t2}} \right) - 1 \right) - \frac{(V_{mod} + I_{mod} \cdot R_s)}{R_h} \quad (2-5)$$

In (2-5) I_{ph} is the photovoltaic current, I_{sat1} is the saturation current of the diode D1, I_{sat2} is the saturation current of the diode D2, V_{t1} and V_{t2} are the thermal voltage of D1 and D2, respectively, both with the same definition used in the single diode model. Finally, R_s and R_h are the series and the parallel resistances, respectively. As it can be seen, the number of parameters to define is seven: I_{ph} , I_{sat1} , I_{sat2} , V_{t1} , V_{t2} , R_s and R_h .

To obtain the value of the seven parameters the three key points expressions (I_{SC} , V_{OC} and MPP) are also used along with other expressions [19], [37]. However, due to the complexity of the system, high computation times are required; this drawback has been the cause for the researchers to propose alternative solutions. In [46], an equation for the direct computation of I_{ph} has been proposed; in addition, it is assumed that $I_{sat1} = I_{sat2}$ and that the ideality factor is the same for both diodes. For obtaining the resistances values, two equations are proposed in order to find initial values; after that, a process of fitting is performed by solving the model equation (2-5) but considering I_{mod} as the independent variable. Merbah et. al. [41] proposed to divide the characteristic curve in two regions and then use two different equations for each one of the regions. The first region being close to the short circuit current and the second region being close to the open circuit voltage. In this way, one equation is defined as a $I(V)$ function and the other one is a $V(I)$ function. On the other hand, the techniques which define the problem as an optimization problem have been gained high popularity, such is the case of [21], where a method based on differential evolution (DE) optimization technique is presented, where I_{ph} , I_{sat1} and R_h are computed analytically, while V_{t1} , V_{t2} , I_{sat2} and R_s are optimized using the DE. In [73] artificial bee colony (ABC) theory is used to find the parameters while in [54], by using the information available in datasheet, a particle swarm optimization (PSO) based technique to find the parameters.

2.3.3. Bishop model

The circuital representation of the Bishop model is shown in Fig. 2-6. This model was introduced by Bishop in [13], it being the first approach to the analysis of the cell in the second and fourth quadrants. Those quadrants are relevant when the cells are exposed to partial shading because they consume power instead of producing it. As in the single diode model, the behavior of the cell is represented by a photovoltaic current source and the series and parallel resistances but it also includes a non-linear function (M) which describes the behavior in reverse mode. The model is represented by equations (2-6) and (2-7), where V_j is the voltage across the junction, V_{br} is the breakdown voltage, a is a fraction of ohmic current involved in avalanche breakdown and m the avalanche breakdown exponent. In [13], the parameters were extracted from an algorithm named PVNet developed by the Commission of the European Communities Joint Research Centre. A database of measured crystalline silicon cells is used to define the behavior of the parameters to obtain suitable values. However, there is not a technique or procedure to compute the parameters for a general case and the

relationship of the parameters with the irradiance or temperature is not well defined. This is due to the lack of data available in literature concerning the operation of PV cells in reverse mode. In [99] and [98] the Bishop model is used for analyzing the effect of shadowing but there is no a clear procedure to compute the parameters; in both papers the values of a , V_{br} and m are similar to the ones used in [13]. In the same way, the Bishop model is used in [63] and again the parameters are defined directly without giving a procedure for the computation; as in the last cited papers, the values of parameters are similar to the ones used in [13].

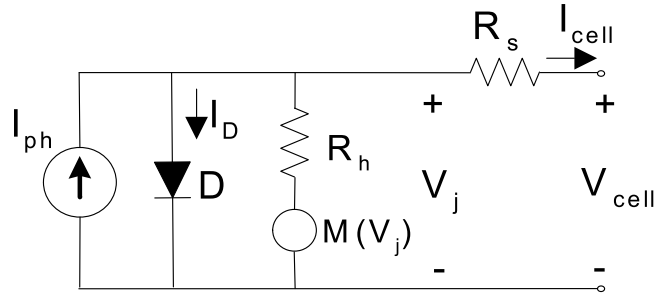


Figure 2-6.: Equivalent circuit of the Bishop model.

$$I_{cell} = I_{ph,cell} - I_{sat,cell} \cdot \left(\exp \left(\frac{V_{cell} + I_{cell} R_s}{V_{t,cell}} \right) - 1 \right) - I_{sh} \quad (2-6)$$

$$I_{sh} = \frac{V_j}{R_h} \cdot \left(1 + a \left(1 - \frac{V_j}{V_{br}} \right)^{-m} \right) \quad (2-7)$$

2.3.4. PL model

In [113], [5] and [114], the P-N junction nonlinear behavior is represented by means of a branch of voltage controlled resistors; such a model is known as piecewise linear (PL) model. In this way, this model allows to adopt n number of diodes for the representation of the PV device behavior. In Fig. 2-7 the circuit of the PL model is shown.

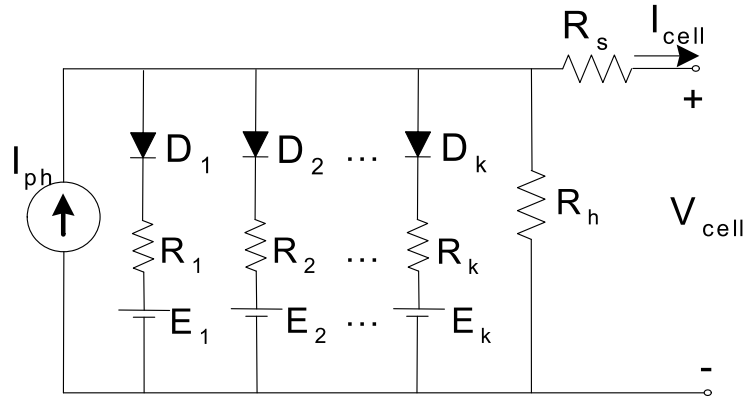


Figure 2-7.: Equivalent circuit of the Piecewise Linear model.

The basic idea of the PL model is to approximate the I- V curve by means of 2^k segments. The first approach is made by representing the I-V curve by two linear segments, then those segments are divided in two segments until the required accuracy is obtained, this considering that each diode in a branch is ideal. Authors in [113] define equations for compute the values of the resistances R_1 to R_k and the associated voltages E_1 to E_k , while in [5] the values of those parameters are obtained taking into account the *MPP* voltage and current points. However, there is not a systematic procedure for estimating the values depending on the number of branches the user wants to consider.

2.3.5. Alternative PV cell models

Some approaches inspired in the models presented in the previous sub-sections have been reported: in [82] an ideal model is used for proposing a technique for obtaining the energy production of PV systems under partial shading conditions. Such a model is a variation of the single diode model, where R_s and R_h are neglected; it simplifies the computation speed of the current since equation (2-4) becomes an explicit relationship which facilitates its processing. Another variation of the single diode model is the R_s model, which considers only the series resistance and neglects the parallel resistance. With this approach the last term in (2-4) is not considered and the model requires four parameters instead five [93], [20]. On the other hand, in [69] a three diode model is introduced with the aim of providing suitable accuracy levels, but due to the complex process for obtaining the parameters it is difficult to implement.

2.3.6. PV arrays configurations

As it was said at the beginning of this section, in practical applications several panels are inter-connected for providing the voltage and current levels that the load requires, such structures are known as PV arrays or PV fields. The typical configurations used in PV

systems applications are the Series-Parallel (SP), in which strings with the same number of modules are connected in parallel; therefore, for each module of a string flows the same current. The Total Cross Tied (TCT) configuration is derived from the SP configuration by connecting ties across each row, where the voltages across the ties are the same. In Bridge-Linked (BL) configuration the modules are connected in a bridge rectifier fashion, where four modules constitute a bridge; then, two modules in the bridge are connected in series and two strings are connected in parallel. Honey-Comb (HC) configuration combines characteristics from TCT and BL configurations [88]. Fig. 2-8 illustrate each one of the aforementioned configurations.

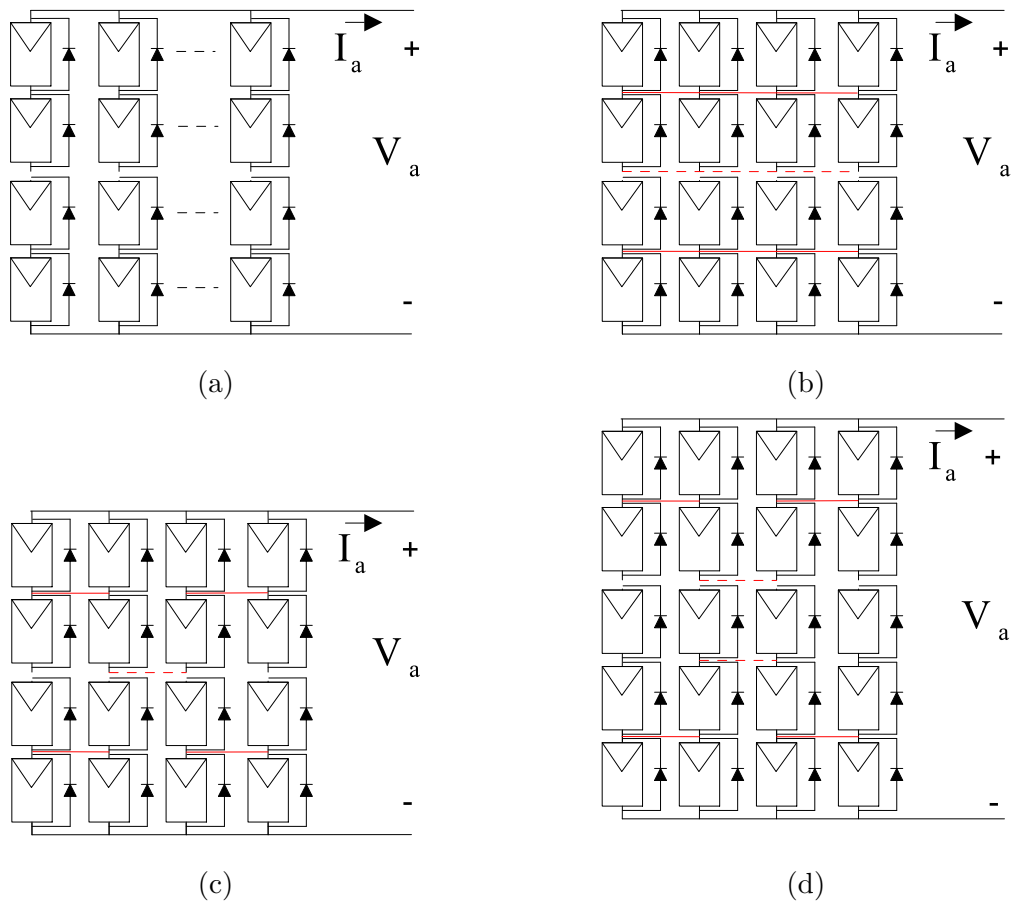


Figure 2-8.: Typical configurations of PV arrays: (a) SP, (b) TCT, (c) BL, (d) HC.

Therefore, the modeling of the modules must be scaled up in order to represent the entire array; the modeling of PV arrays allows to analyze the power and energy production for a given operation condition. Moreover, it can be considered as a tool for the design of maximum power point tracking algorithms and reconfiguration analysis.

2.3.7. The mismatching effect

The mismatching concept concerns aspects from PV panel parameters (circuitual values) to environmental conditions and other external situations (shading, soiling, etc). From the point of view of the circuitual parameters, the ideal condition corresponds to all the panels of the array having the same parameters (e.g. I_{ph} , I_{sat} , V_t , R_s and R_h), but due to fabrication tolerances this condition could be not fulfilled. From the point of view of the environmental conditions, since the power provided by a PV device depends on the irradiance, the ideal situation would be that all the panels of an array receive the same level of irradiance, unfortunately this condition is not always possible since PV arrays are normally exposed to shades. Other situations causing difference between the operating conditions may include lack of maintenance, dust, among others. These differences in the operating conditions of the panels of a PV array are commonly known as mismatching phenomenon, which is one of the most critical cause of the reduction of the energy production in PV systems [85].

The partial shading condition is one of the most common causes of mismatching, since the shadows projected over the surface of the panels cause a decreasing of the irradiance level, making the panels work under non-uniform operating conditions. The shadows can be produced by objects in the neighborhood of the PV system: clouds, elements which fall on the PV system surface such as leaves, or inclusive shadows projected from other modules in the PV structure (self-shading). When series-connected PV cells are under partial shading conditions, shaded cells can experiment negative voltages due to the excess of current imposed by the cells with higher levels of irradiance. This situation causes the shaded cells consume power instead of produce it [13], [112]. Moreover, undesirable conditions such as hot spots, aging or total cell damage can occur [115].

To avoid such negatives effects, bypass diodes are connected in anti-parallel with a series-connection of PV cells (PV module). The bypass diode provides a path for the excess of current, but due to the diode operation, it imposes a negative voltage to the cells (diode activation voltage). Such negative voltage is much lower than the breakdown voltage, but in any case it forces the cells to consume power. Fig. 2-9 shows a typical voltage vs. current curve of a PV cell in the first and second quadrant, where V_{br} is the breakdown voltage, V_{bda} is the bypass diode activation voltage, V_{OC} is the open circuit voltage, I_{SC} is the short circuit current and I_{STR} is the string current. The curve in the second quadrant is named cell reverse characteristic. In Fig. ?? the gray area represents the power losses occurring when the bypass diode is not connected to the module. In Fig. ?? the dark gray area represents the power losses caused by the bypass diode activation.

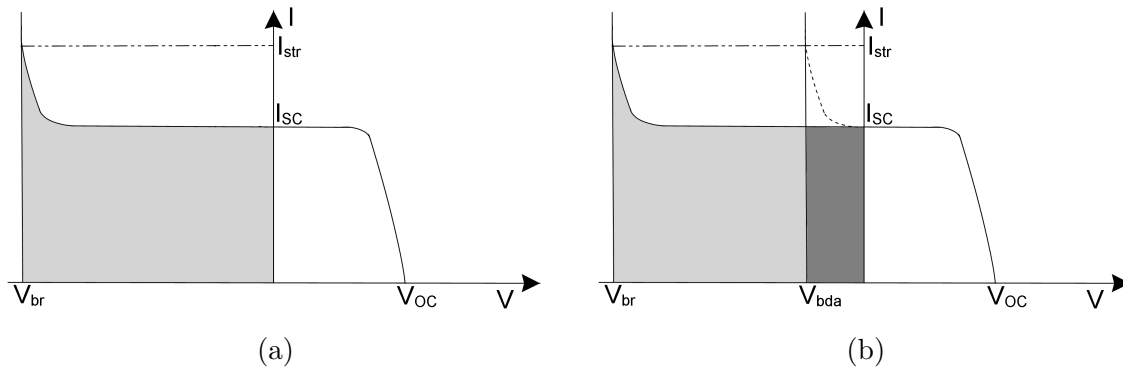


Figure 2-9.: I-V Characteristic of a PV cell (a) without bypass diode, (b) with bypass diode.

2.3.8. Operation and modeling of bypass diodes

In order to illustrate the activation of a bypass diode associated to a module in a string, Fig. 2-10 shows two modules connected in series. In Fig. ?? the modules are under the same irradiance conditions, therefore the bypass diodes remain inactive. In Fig. ?? the lower module is exposed to a shadow, therefore its irradiance level is lower than the irradiance of the module at the top, however its bypass diode remains inactive because the string current I_{str} is lower than its short-circuit current I_{sc2} . In Fig. ?? the shadow increases making the irradiance level of the lower panel decreases even more, in this case I_{str} is higher than I_{sc2} , which forces the bypass diode to become active.

Another important consideration concerning the bypass diodes activation is that, within a string or array, it causes multiple peaks in the Power vs Voltage curve, namely, multiple maximum power points as it is illustrated in Fig. 2-11. One major problem of such a condition is that the *MPPT* algorithm could be trapped in a local maximum [83]. Several bypass diode models have been reported in literature, in [63], [46], [12], the typical exponential model is used, while in [112] and [9] the linear model is selected, and the ideal switch model is used in [82] and [90]. Fig. 2-12 shows the characteristic curves of these models. Depending on the level of accuracy and speed calculation requirements, both the PV cell (or module) model and the bypass diode model must be selected.

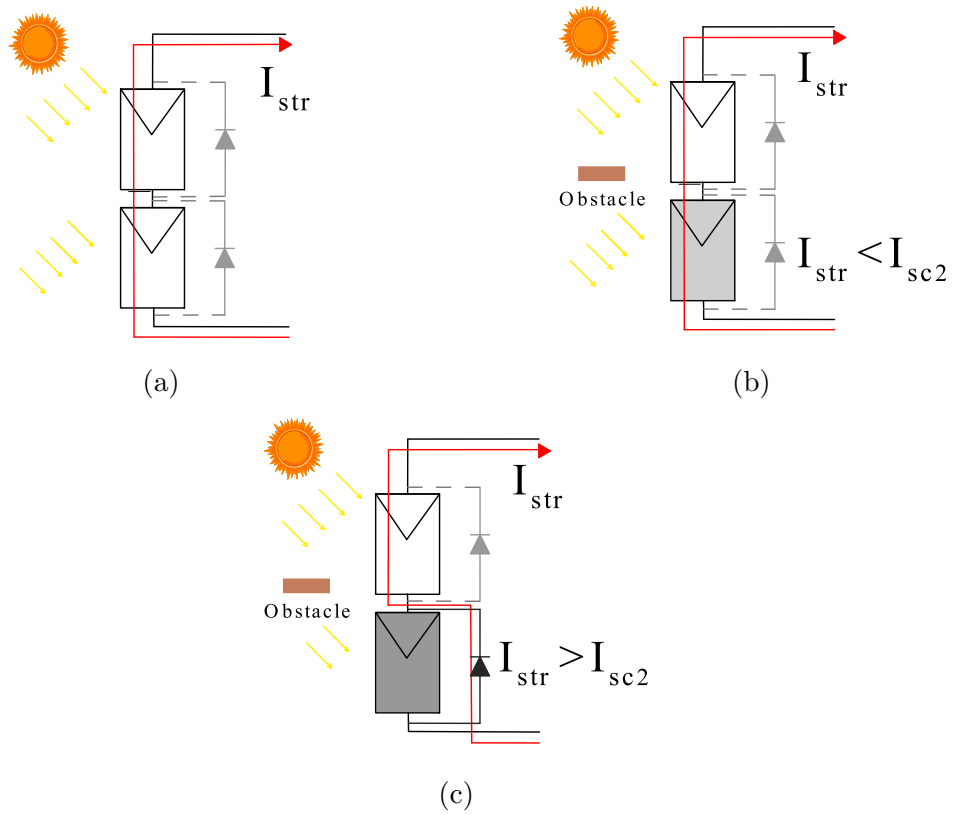


Figure 2-10.: Bypass diode activation scheme (a) Uniform conditions, (b) Mismatching conditions without bypass diode activation, (c) Mismatching conditions with bypass diode activation.

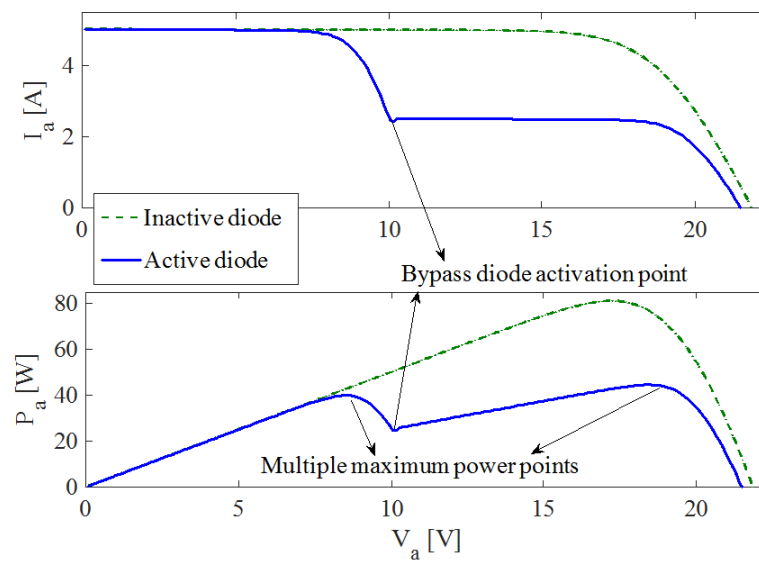


Figure 2-11.: Multiple MPP's caused by bypass diode activation.

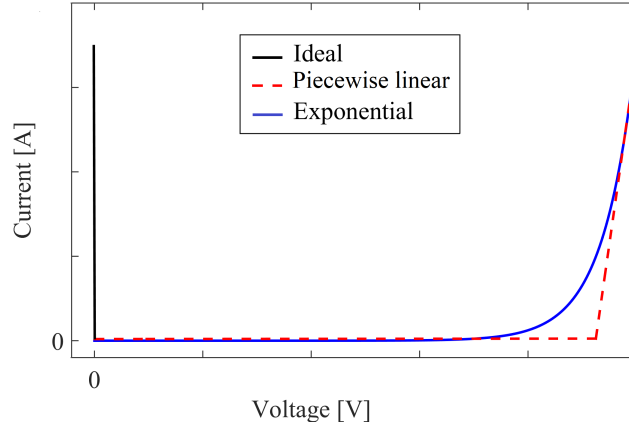


Figure 2-12.: Characteristic curves of different bypass diodes models.

In [83] the single diode model is used to represent a PV module. Authors included the bypass diode by using its exponential form. In this way, the equation which relates the current and voltage of the module is:

$$I_{mod} = I_{ph} - I_{sat} \cdot \left(\exp \left(\frac{\beta}{V_t} \right) - 1 \right) - \frac{\beta}{R_h} + I_{bd} \quad (2-8)$$

where

$$\beta = R_s \cdot (I_{mod} - I_{bd}) + V_{mod} \quad (2-9)$$

$$I_{bd} = I_{sat,db} \cdot I_{sat,bd} \left(\exp \left(\frac{-V_{mod}}{V_{t,bd}} \right) - 1 \right) \quad (2-10)$$

Equation (2-8) is a transcendental expression which can not be solve by trivial means. Therefore, authors proposed to use the Lambert W function to solve it. In this way, the current of the module is given by:

$$I_{mod} = -\frac{V_t \cdot W_0(\theta)}{R_s} + I_{sat,db} \cdot \left[\exp \left(\frac{-V_{mod}}{V_{t,bd}} \right) \right] - I_{sat,bd} + \frac{R_h \cdot (I_{ph} + I_{sat}) - V_{mod}}{R_h + R_s} \quad (2-11)$$

where

$$\theta = \left(\frac{R_h \cdot R_s}{R_h + R_s} \right) \cdot \frac{I_{sat}}{V_t} \cdot \exp \left[\frac{\alpha \cdot (I_{ph} + I_{sat}) + V_{mod} R_h}{V_t} \right] \quad (2-12)$$

2.4. Modeling of photovoltaic arrays

Several techniques for modeling PV arrays have been reported, due to their similar orientation or final purpose, three categories have been detected: Simulation to obtain the characteristic curves, Energy yield analysis and Shading effects analysis. This section presents a survey of the main aspects of the reported works oriented to identify key factors as the PV model, the level of detail (cell or module), the consideration of second quadrant operation and the final application, PV array configuration and the software or informatics tools used for their implementation. The works reported in this section were selected under the following factors: amount of citations, publication type (journal or conference), impact factor of the journal where the work was published, and year of publication. Fig. 2-13 shows the structure of this section in order to provide a guideline to the reader.

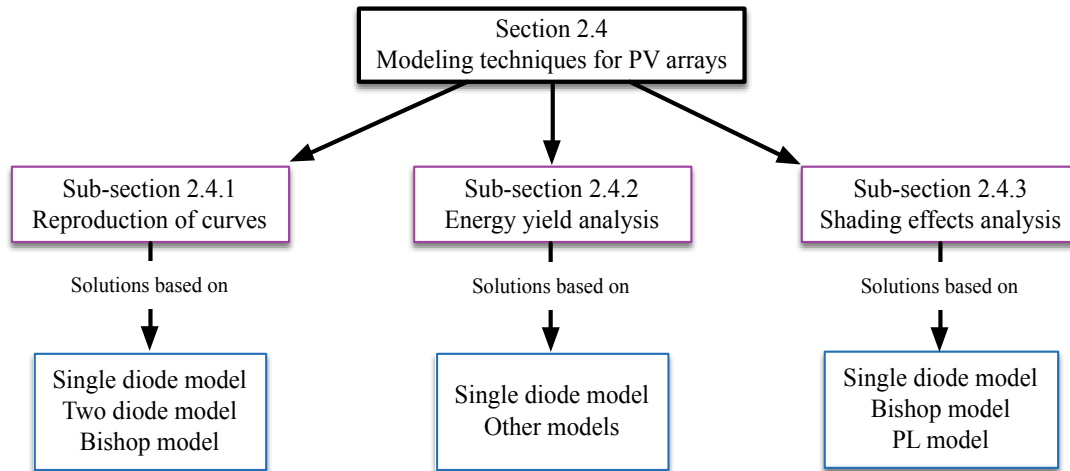


Figure 2-13.: Structure of section 2.4.

2.4.1. Modeling techniques for obtaining the electrical characteristics

The electrical characteristic curves I-V and P-V, provide useful information of the behavior of a PV system operating under a specific condition. In particular, the P-V curve allows to analyze the behavior of the maximum power point, which can be affected by the partial shading phenomenon. Through the information obtained from the P-V curve, it is possible to evaluate the performance of different connections in PV systems with one or multiples shading patterns to define which of them is less susceptible. Moreover, it is possible to analyze the performance of *MPPT* techniques designed to mitigate the effect of partial shading. Table 2-1 summarize all the techniques cited in this category.

2.4.1.1. Solutions based on the single diode model

In [50] the circuit theory and Brune's conditions are used to model a PV system at cell level. This technique is based on considering input or output ports in the system to obtain a set of matrix equations. The analysis is based on the single diode model and authors use an iterative method based on a system of equations from the open circuit condition equation, the short circuit condition equation and the MPP condition equation to obtain the five parameters of the model. For a group of N_s identical PV cells in series connection, the matrix representation of the equivalent voltage V_e and equivalent current I_e is given in (2-13) while (2-14) presents the matrix representation for a group of N_s identical PV cells in parallel connection, where V_D and I_D are the voltage and current of the single diode model respectively, and V and I are the voltage and the current of the string of cells. The parameters of both matrixes are defined as in section 2.3.1.

$$\begin{bmatrix} I_{ph,e} \\ V_e \end{bmatrix} = \begin{bmatrix} \frac{N_s}{R_h} & N_s \\ N_s & N_s R_s \end{bmatrix} \begin{bmatrix} V_D \\ I \end{bmatrix} + \begin{bmatrix} N_s I_D \\ 0 \end{bmatrix} \quad (2-13)$$

$$\begin{bmatrix} I_{ph,e} \\ I_e \end{bmatrix} = \begin{bmatrix} N_p \left(\frac{1}{R_s} + \frac{1}{R_h} \right) & \frac{N_p}{R_s} \\ \frac{N_p}{R_s} & \frac{N_p}{R_s} \end{bmatrix} \begin{bmatrix} V_D \\ V \end{bmatrix} + \begin{bmatrix} N_p I_D \\ 0 \end{bmatrix} \quad (2-14)$$

This model was implemented in Matlab and the user can enter the irradiance, the cell temperature, as well as the number of cells and their connection. The method was extended for modeling SP arrays; however, there are no details about the process which represents an important drawback for reproducing the procedure. As for the model of the bypass diodes authors do not give details concerning the model, but they considered the following condition: if the short-circuit current of a module is lower than the string current, a fixed voltage is assigned to it. In this way, it can be concluded that the bypass diode is modeled in a linear form, the operation in the second quadrant is not considered. To validate the modeling process, authors used a PV array of 3 modules, each one composed by 72 PV cells connected in series. The temperature is considered the same for all the modules while the irradiance levels are different ($1000W/m^2$, $700W/m^2$ and $400W/m^2$). Information concerning the computing times is not included.

The work reported in [49] is based on the single diode model with certain modifications and the reverse operation mode at cell level is considered. The modifications are based on the following concepts: (i) to express the avalanche effect of the partial shading, the number of shaded PV cells and the total number of PV cells in the PV module is included, (ii) to reflect the variations of the reverse-biased current, an additional resistance component is considered and (iii) the current simulated using the single diode model is gradually reduced near the open circuit voltage. Under the proposed modifications, the proposed circuit for modeling a PV cell is shown in Fig. 2-14 and the mathematical model is given in (2-15) to (2-19),

where N is the number of cells in the module, M is the number of partially shaded cells in the module, V_b is the breakdown voltage of a solar cell, the rest of variables are similar to the ones introduced in section 2.3.1. Constants α , β and γ are used for relating current due to avalanche effect of shaded solar cell and for relating current of resistance in PV module. However, authors do not provided a procedure for calculate their values.

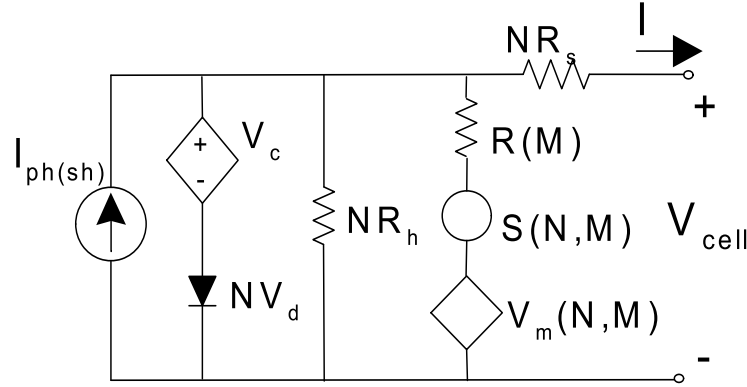


Figure 2-14.: Proposed circuit for modeling a PV cell.

$$R(M) = M (R_s + R_h) \quad (2-15)$$

$$V_m(N, M) = (N - M) V_{oc} \quad (2-16)$$

$$S(N, M) = \alpha \frac{(I_{ph} - I_{ph(sh)})}{I_{ph}} \left[\frac{MV_b}{V_b - (N - M) V_{oc} + V + NIR_s} \right]^\beta + \gamma \frac{(I_{ph} - I_{ph(sh)})}{I_{ph}} \quad (2-17)$$

$$V_c = \frac{nkT}{q} \ln \left(\frac{I_{ph} - I}{I_{ph(sh)} - I} \right) \quad (2-18)$$

$$I = I_{ph} - I_{sat} \left(\frac{I_{ph(sh)} - I}{I_{ph} - I} \right) \left[\exp \left(\frac{q(V/N + IR_s)}{nkT} \right) - 1 \right] - \frac{(V/N + IR_s)}{R_h} + S(N, M) \left[\frac{V_m(N, M) - (V/N + IR_s)}{R(M)} \right] \quad (2-19)$$

To validate the modeling technique, authors use a PV module of 30 poly-crystalline cells under different shaded areas affecting just one PV cell. The maximum root mean square error (RMSE) between the simulated and measured currents for the PV module with a completely shaded solar cell is approximately 2.37%. There is not a defined procedure to extend the modeling approach to a complete array, a possible reason may be the evident high complexity exhibit by the equations of the model. The implicit relationships between the voltage and current of the cell implies the use of specialized functions (e.g. Lambert-W function) or robust numerical methods. In this way, it is clear that a main drawback of this approach is its high complexity and the lack of a clear procedure for its reproduction and application.

In [79] a Matlab-based simulator at module level is presented, such a simulator is oriented to SP arrays. This is one of the most referenced works in the modeling of PV systems area, where authors developed a simulation tool in which the user to enter the PV system data: size, modules affected by shading and levels of shading. For this purpose, authors proposed to define the array characteristics through sub-terms to identify its parts: a subassembly is formed with several series-connected PV modules receiving the same level of irradiance. Such series-connected subassemblies, each with a different level of irradiance, form a series assembly. The series assemblies, having similar shading patterns, form a group. Multiple groups, having different shading patterns and being connected in parallel form a PV array. These concepts are illustrated in Fig. 2-15. The user must enter the data in a simple matrix form, all from the environment of Matlab. In addition, the approach considers the effect of blocking and bypass diodes, but the model for representing them is not described by authors; the user can include them through the initialization of a variable named *Diodes* equal to 1, otherwise the approach does not include the blocking and bypass diode in the analysis. There is not a description of the methodology to calculate the voltage and currents of the array in order to obtain its curves; however, the simulation tests performed with the tool were made with large PV arrays (300, modules, 900 modules and 1000 modules), which suggests the use of current sweeps to avoid the issues related with the complexity of the one diode model including the bypass diode. Finally, through the simulations tests, three concepts are studied: (i) the effect of the bypass and blocking diodes on the PV characteristics under partially shaded conditions, (ii) the behavior of the global MPP and (iii) performance of MPPT controllers. At the moment of the publication of this work, the code was available for free download which was a significant contribution, unfortunately at present it is not possible to download the information.

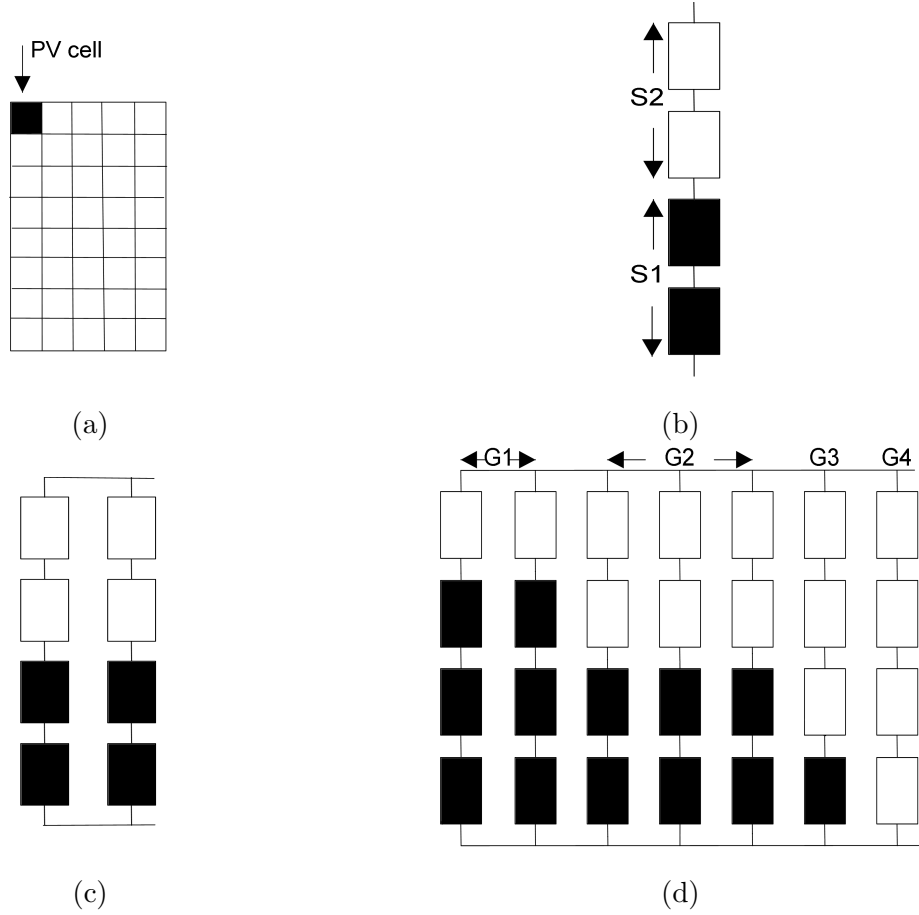


Figure 2-15.: PV array terms used in [79] (a) Module, (b) Series-assembly with two series-connected subassemblies S1 and S2, (c) Group, (d) PV array with groups G1 to G4.

The technique presented in [83] is based on the single diode model at module level including a bypass diode, which is modeled using the exponential form. In this way, the relation between the modules' voltage V_m and current I_m is given in (2-20), where $I_{sat,db}$ and $V_{t,db}$ are the saturation current and the thermal voltage of the bypass diode, respectively. The rest of parameters are defined as in section 2.3.1.

$$I_{mod} = I_{ph} - I_{sat} \cdot \left(\exp \left(\frac{V_{mod} + I_{mod} \cdot R_s}{V_t} \right) - 1 \right) - \frac{(V_{mod} + I_{mod} \cdot R_s)}{R_h} + I_{sat,db} \cdot \left(\exp \left(\frac{-V_{mod}}{V_{t,db}} \right) - 1 \right) \quad (2-20)$$

It is evident that the relation of the modules' current and voltage is a non linear implicit function. To overcome this issue, in this approach the Lambert W function is used to enable the explicit calculation of the current; such a function is available in well known simulation

softwares as Matlab or Maple. This technique is oriented to SP arrays and considers the effect of blocking diodes. The methodology to obtain the I-V and P-V curves is based on the construction of a system of non-linear equations by using the Kirchhoff laws for each string of the array. To find the current, the Newton-Raphson method is used, then a system F and its Jacobian matrix must be defined as in (2-21) and (2-22), where $X = [V_1, \dots, V_n, V_{diode}]$. The structure of the system allows to simplify the structure of the Jacobian in order to reduce the computing burden because such a matrix must be inverted for performing the Newton-Raphson method.

$$F(X) = \begin{bmatrix} V_1 + V_2 + \dots + V_n + V_{diode} - V = 0 \\ I_1(V_1) - I_2(V_2) = 0 \\ \dots \\ I_1(V_1) - I_n(V_n) = 0 \\ I_1(V_1) - I_{diode}(V_{diode}) = 0 \end{bmatrix} \quad (2-21)$$

$$J = \begin{bmatrix} 1 & 1 & \dots & 1 & 1 \\ \frac{\partial I_1}{\partial V_1} & -\frac{\partial I_2}{\partial V_2} & \dots & 0 & 0 \\ \vdots & \vdots & \dots & \vdots & \vdots \\ \frac{\partial I_1}{\partial V_1} & 0 & \dots & -\frac{\partial I_n}{\partial V_n} & 0 \\ \frac{\partial I_1}{\partial V_1} & 0 & \dots & 0 & -\frac{\partial I_{diode}}{\partial V_{diode}} \end{bmatrix} \quad (2-22)$$

The validation of the technique was made through simulations performed in Matlab for a string with two modules exposed to different irradiance levels. The results allowed to conclude that the approach is accurate and requires a moderate computational burden. In addition, the model was implemented in a dynamic link library (DLL) in PSIM to analyze the performance of an MPPT controller. This puts into evidence the versatility and usefulness of the proposed modeling procedure.

The solution presented in [76] is based on the concepts introduced in [83], but improving the procedure for calculating the inverse of the Jacobian matrix (2-22), which allows a reduction in the computing time. Considering the concept of differential resistance for the modules and the blocking diode given in (2-23) and (2-24), the Jacobian matrix shown in (2-22) can be expressed in parts as is presented in (2-25) to (2-29).

$$\frac{\partial I_1}{\partial V_1} = \frac{1}{R_1}, \dots, \frac{\partial I_n}{\partial V_n} = \frac{1}{R_n} \quad (2-23)$$

$$\frac{\partial I_{diode}}{\partial V_{diode}} = \frac{1}{R_{diode}} \quad (2-24)$$

$$A = [1]_{1 \times 1} \quad (2-25)$$

$$B = [1 \ 1 \ 1 \ \dots \ 1 \ 1 \ 1]_{1 \times n} \quad (2-26)$$

$$C = \frac{1}{R_1} [1 \ 1 \ 1 \ \dots \ 1 \ 1 \ 1]_{1 \times n}^T \quad (2-27)$$

$$D = \begin{pmatrix} -\frac{1}{R_2} & 0 & 0 & 0 & 0 & 0 \\ 0 & -\frac{1}{R_3} & 0 & 0 & 0 & 0 \\ 0 & 0 & \dots & 0 & 0 & 0 \\ 0 & 0 & 0 & \dots & 0 & 0 \\ 0 & 0 & 0 & 0 & -\frac{1}{R_n} & 0 \\ 0 & 0 & 0 & 0 & 0 & -\frac{1}{R_{diode}} \end{pmatrix} \quad (2-28)$$

$$J = \begin{pmatrix} A & B \\ C & D \end{pmatrix} \quad (2-29)$$

Authors propose to use the Schür Complement tool to explicitly calculate the inverse of the Jacobian matrix, achieving an improvement in the computing time. In addition, the work focuses in two problems: the calculation of the whole I-V curve of string operating under different irradiance levels, and the calculation of a single value of the I-V curve. For the first problem, the proposed technique is compared with the solution obtained by using the *fsolve* function of Matlab with different algorithms (Trust-region dogleg, Levenberge-Marquardt and Gauss-Newton). Results show that the proposed algorithm allows obtaining the right solution in less than the 47% of the time needed by *fsolve* function. For the second problem the authors develop an analysis concerning the guess solution of Newton-Raphson method, adopting a technique based on the inflection points of the I-V curve presented in [82]; in this way, the I-V curve can be analyzed by sections depending on the bypass diodes activation.

The work presented in [51] proposes an artificial neural network (ANN) to find the circuit parameters of the single diode model to represent a PV module achieving a satisfactory performance when comparing the calculated parameters with those provided by the Sandia's PV module electrical performance model [55], which was developed at Sandia National Laboratories (New Mexico, US.). The second part of this research presents a an algorithm to

analyze PV modules at cell level where the inputs are the number of series connected cells and the number of solar cells per bypass diode. Authors present a set of seven equations based in the Kirchhoff's voltage and current laws, which conform the module model. However there is a lack of detail in the procedure since is not defined what of the variables (current or voltage) is the independent variable; in the validation example authors consider a PV panel consisting on 36 cells and two bypass diode which divide the panel into two modules, then the system to solve consists of 39 unknowns that are calculated by means of a trust region method. A third part of this work is devoted to apply the extension of the previous modeling procedure for its application in SP, TCT and BL arrays. In such a process it is assumed that the panels forming the array contain two modules (two bypass diodes) and once again the Kirchhoff's voltage and current laws are applied to define expression for each configuration considering sum of the voltages in each mesh and sum of currents in each node of the array. The model is finally formed by ten equations but unfortunately there is a lack of detail of the process for solving the systems of equations obtained. Finally, the modeling procedure is used to perform an analysis of power production considering 30 shading scenarios on 12 different PV array configurations; the results show that the TCT configuration provided a better performance for a significant number of scenarios; simulations results were not compared with circuital or experimental test.

The modeling technique presented in [88] is based on the single diode model for representing the operation under uniform irradiance conditions and also it is based on the Bishop model for representing the operation under partial shading conditions. The parameters for the single diode model are calculated based on the theory introduced in [111] while the calculation of the parameters a , m and V_{br} of the Bishop model are calculated through the analysis of real I-V curves of solar cells operating under shading conditions and adjusted with a trial and error process. A special terminology is used in this work which is very similar to the one presented in [79]: modules under the same irradiance connected in series form a substring, several substrings under different irradiance but connected in series form a string, identical strings that are connected in parallel form an assembly, and assemblies that are connected in parallel form an array. The technique presented in this work is applied to SP, TCT, BL, and HC configurations under shading conditions at module level. In this work the current is considered the independent variable, therefore the introduced procedures are aimed to find the voltage of the system. The first stage of the procedure is common to all the configurations studied, Fig. **2-16** illustrate the actions required in such a stage.

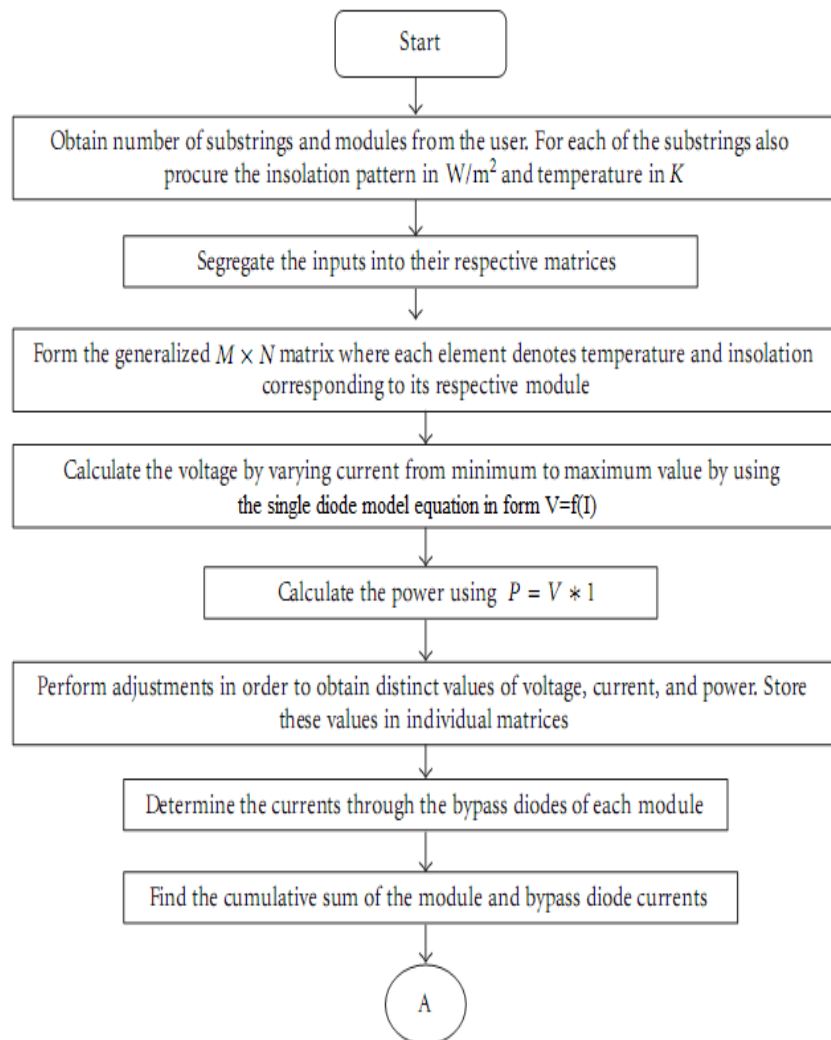


Figure 2-16.: Initial procedure of the technique proposed in [88].

The procedures for simulating SP, TCT configurations are summarized in the flowcharts of Fig. 2-17 while the procedure for BL and HC configurations is depicted in Fig. 2-18; the implementation of the algorithms were made in Matlab code. As it was mentioned, the Bishop model is used for modeling the operation under partial shading conditions, however it is not clear how the model is included in the different methodologies proposed for modeling different PV arrays configurations. Several simulations was performed using different arrays sizes and configurations and also using different shading patterns, this with the aim of define what array presents better performance; this is one of the features the author highlights since there are few tools for performing analysis of different configurations. The results were validated through experimental tests providing good agreement, in addition the effect of using different number of bypass diodes per module was also studied.

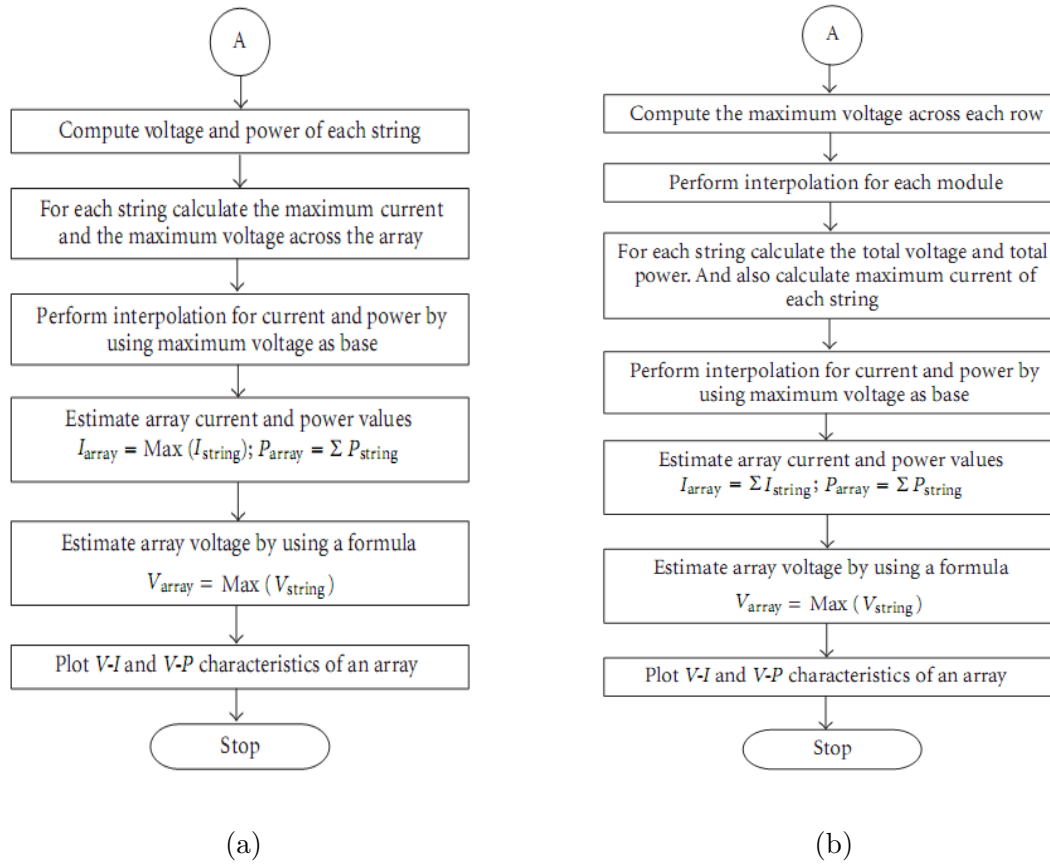


Figure 2-17.: Flowcharts of the procedure proposed in [88] for (a) SP configuration, (b) TCT configuration

2.4.1.2. Solutions based on the two diode model

The work presented in [46] is an approach based on the two diode model to represent the PV cell, it uses the voltage as the dependent variable and the current as the independent variable. Authors justify the use of the two diode model since it presents a better accuracy than other models at low irradiance levels. The first part of the work describes a methodology to obtain the parameters of the two diode model through a set of equations which are then use for constructing a system of equations which is solved by means of the Newton Raphson method. The modeling procedure proposed by authors consider the following stages: (i) determination of shading patterns and temperature for a particular shading affecting group of modules, (ii) calculation of voltage and current for each group of modules, based on the two-diode model and exposed to a known shading pattern and (iii) performing linear interpolation with extrapolation techniques to form the continuous I-V and P-V curves. SP, TCT and BL 20×3 arrays exposed to four different shading levels were simulated and analyzed. The approach was implemented under the dSPACE platform and the simulations results

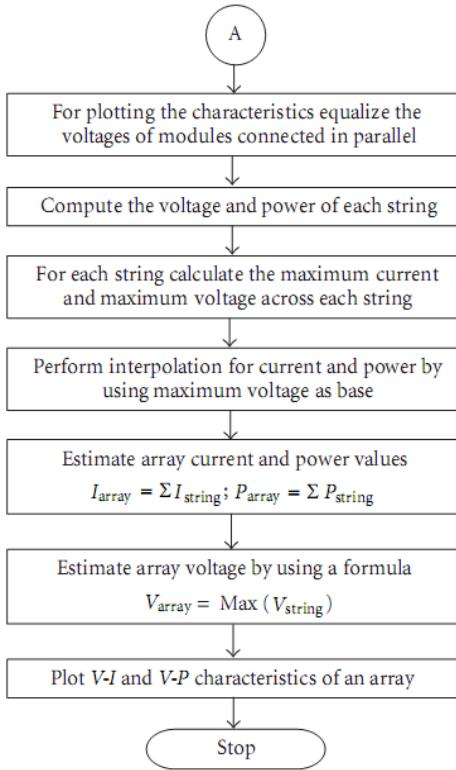


Figure 2-18.: Flowcharts of the procedure proposed in [88] for BL and HC configuration.

were compared with the ones obtained in [108] where a simulator for PV system simulator based on an artificial neural network and also with the approach presented in [79] which is based on the diode model. In the work, only the results of the simulation on the SP array was shown, the authors analyze the changes in the MPP due to the different shading profiles and different temperature levels affecting the modules. The results show good agreement with the ones presented in [108] with an error of less of 5%. The information concerning the TCT and BL arrays is not given, as well as the process for performing the interpolation and the issues associated to it. Finally, the modeling technique is used for the evaluation of a MPPT strategy evaluation.

In [45], the two diode model is used to develop a simulator in Simulink at module level oriented to SP arrays. The computation of series and parallel resistances are based in the set of equations presented in [111], it taking into account the new terms appearing due to the second diode. In this way, the first part of this work is devoted to the process for obtaining the parameters of the model and its validation at different irradiance and temperature values. The model is based on performing a current sweep to find the voltage at each module in the string, the entire method is developed under the Simulink environment and the user is able

to enter the information of the system through a dialog window as is shown in Fig. 2-19, the shadowing is assumed to affect groups of entire modules; the bypass and blocking diodes are also included through block functions available in Simulink. The implementation is then used for analyze the effect of shading and the effect of bypass and blocking diodes in the I-V and P-V curves through several simulations with a 3×3 SP array, but authors did not include an error analysis. An analysis on power losses due to the operation in the second quadrant was not presented either. Finally, an application with a MPPT controller was also described to highlight the usefulness of the simulator.

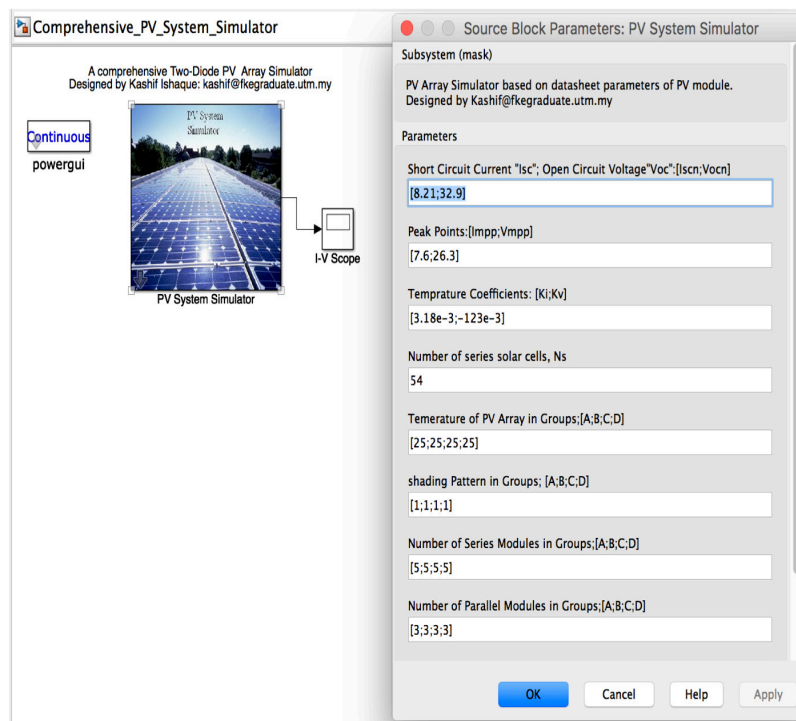


Figure 2-19.: Interface of the simulator proposed in [46].

The Simulink files were put online available for free download, however at the moment of this review the system did not work since the simulator was developed in a previous version of Simulink, which is a considerable drawback for the application of this tool.

2.4.1.3. Solutions based on the Bishop model

The technique introduced in [63] is applied to the analysis of modules or SP arrays including bypass and blocking diodes. A system of equations is constructed to represent the operation of each string in the array; where the unknown variables are the voltage and current of cells or modules. The damped Newton method is applied for calculating the solution of the system. In this work authors consider that the circuit of a PV array consists of two layers:

the layer of cell to module and the layer of module to array. In this way, in the layer of cell to module, a cell or diode is called *unit* and, in the layer of module to array, a module or diode is called *unit*. Another entity called *block* is defined to describe two types of wire connection in a string: a loop yielded by a bypass diode across a number of modules (or cells) and, otherwise, a module (or cell) or a blocking diode. Then, the array or the module is defined with three layers: strings, blocks and units. Each unit is encoded by using four elementary flags: the first flag denotes the specific string that contains a unit (cell or module), the second flag the specific block that contains the unit, the third flag the type of the block and the last value the unit. Fig. 2-20 illustrates the encoding process. In addition, the irradiance and temperature are also encoded in a geometrical form to capture the physical installation information of the PV array. Then, a cell or module is labeled by a subscript i with its coordinates (X_i, Y_i, Z_i) . Those are used to determine the irradiance $G(X_i, Y_i, Z_i)$ and the temperature $T(X_i, Y_i, Z_i)$ conditions; other parameters as the series and parallel resistances are stored in a following sequence along with the identification flags of the cell or module. At this point, certain level of complexity for the definition of the array and its parameters can be identified. Moreover, it is not completely clear the difference in the use of flags for modules and cells. The model was developed in Matlab and it was validated with simulation tests; authors affirm that the procedure has low computational cost but they did not give any information concerning the simulation time as well as details concerning the calculation of the Bishop model parameters. Finally, the work highlights the use of the damped Newton method as a tradeoff between convergence speed and robustness. Analysis related with the operation of cells or modules in the second quadrant are not presented.

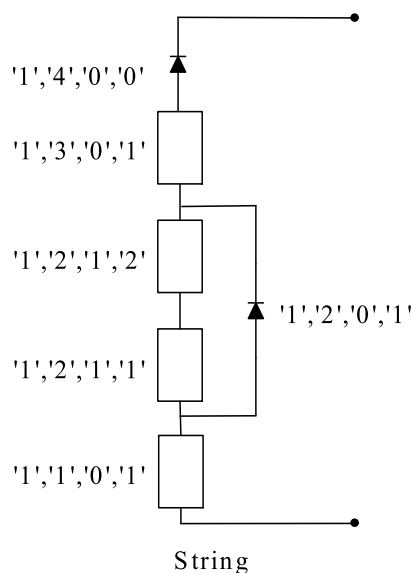


Figure 2-20.: Illustration of the flags system proposed in [63].

In [77] a modeling technique including the reverse mode operation at cell level is presented.

It can be said that this work is an improvement of the approach introduced in [76] for the following reasons: (i) the technique considers the modeling at cell level, (ii) the Bishop model is used to represent the PV cell, which allows to analyze the second quadrant operation and (iii) the cell-by-cell analysis performed in this work allows to include parametric tolerances and a detailed mismatching profile. The analysis is based on obtaining a system of equations in which the cells and bypass diode voltages are the unknown; such a system of equations is solved by using an iterative process, eg. Newton's technique. As in in [76], the Schür Complement tool is adopted to obtain the inverse of the Jacobian matrix, which improves the speed calculation. The performance of the proposed approach was evaluated through simulations and comparisons with the *fsolve* function of Matlab using a PV array of 3 panels, each one formed by three modules, each one of 24 series-connected cells; the execution time was 7.7 s with a mean squared relative error equal to 6.0814×10^{-21} . Since the proposed technique is based on the Bishop model, other simulations were made in order to evaluate the performance of the proposed technique for analyzing cell power losses in shadowed conditions; the cell-by-cell analysis enables to include a more detailed mismatching profile for a more realistic study of the power production and also of possible wrong operation (hot spots, aging, etc). Therefore, it can be concluded that the proposed technique is also applicable for energy yield prediction and to analyze of hot-spot heating due to shading and parametric tolerances. In addition, authors provide a clear description of the technique which allows its implementation on different environments different from Matlab. However, it is worth to point that there is no details concerning the selection of the parameters α and m used in the Bishop model equation.

Table 2-1.: Modeling techniques for obtaining the characteristic curves

| Ref. | Level | Model | Final application |
|------|--------|-------------------------|----------------------------|
| [50] | Cell | Single diode | Array (SP) |
| [49] | Cell | Single diode modified | Module |
| [46] | Cell | Two diode | Array (SP, TCT and BL) |
| [63] | Cell | Bishop | Array (SP) |
| [77] | Cell | Bishop | Array (SP) |
| [83] | Module | Single diode | Array (SP) |
| [76] | Module | Single diode | Array (SP) |
| [51] | Cell | Single diode | Array (SP, TCT and BL) |
| [79] | Module | Single diode | Array (SP) |
| [88] | Module | Single diode and Bishop | Array (SP, TCT, BL and HC) |
| [45] | Module | Two diode | Array (SP) |

2.4.2. Modeling techniques oriented to energy yield analysis

Energy prediction is one of the most important topics in PV systems planning. Designers require this kind of information to calculate the size of the arrays, the return-of-investment time, among others. Therefore, obtaining the I-V and P-V curves is not the final goal. Table 2-2, summarizes the survey presented in this category.

2.4.2.1. Solutions based on the single diode model

The work presented in [12] proposes the use of a PV model based on the single diode model in addition with a term to represent the negative diode breakdown operation similar to the Bishop model, in addition the bypass diode is represented in an exponential form. The circuit adopted in this approach is shown in Fig. 2-21. The operation of the cell is then described by (2-30), where the first terms are identical to the ones defines for the single diode model in section 2.3.1, while the last term represent the operation in the second quadrant by means of coefficients b , V_{br} and m , but authors do not describe the process to calculate them.

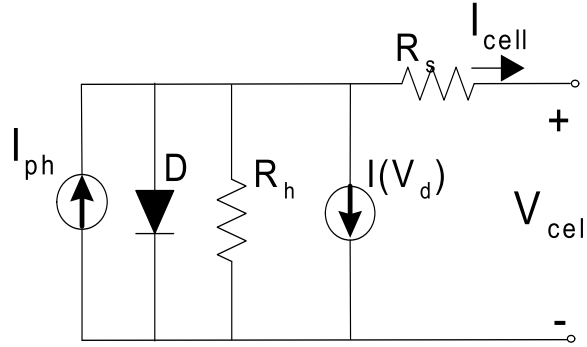


Figure 2-21.: PV cell circuit adopted in [12].

$$I_{cell} = I_{ph} - I_{sat} \left(\exp \left(\frac{V_{cell} + IR_s}{V_t} \right) - 1 \right) - \frac{V_{cell} + IR_s}{R_h} - b(V_{cell} + IR_s) \left(1 - \frac{V_{cell} + IR_s}{V_{br}} \right)^{-m} \quad (2-30)$$

As it can be seen (2-30) is an implicit equation, then authors propose to use the Lambert W-function to obtain an explicit relationship between current and voltage; moreover, the form $V = f(I)$ is proposed and finally equation (2-31) is obtained, where z is the minimum root of a quartic equation which characterized the operation in the second quadrant.

$$V_{cell} = \begin{cases} R_h (I_{ph} + I_{sat}) - (R_s + R_h) I - V_t \cdot W \left(\frac{R_h I}{V_t} \exp \left(\frac{R_h (I_{ph} + I_{sat} - I)}{V_t} \right) \right) & I \leq I_{ph} \\ V_{br} - IR_s - z & I > I_{ph} \end{cases} \quad (2-31)$$

The analysis perform leads to the following conclusions: in the first and fourth quadrants, the voltage of a group of series-connected cells or cell string is the sum of the individual cell voltages $V_{cell,i}$, while in the second quadrant, the short circuit current of the cell group may be considered equal to the minimum short circuit current of the individual cells in the string. In this way, a PV module formed by N_{cs} cell strings in series connection can be described by (2-32), while a PV string formed by N_m modules in series connection can be described by (2-33).

$$V_{mod} = \sum_{i=1}^{N_{cs}} V_{cell,i}(I) \quad (2-32)$$

$$V_{str} = \sum_{i=1}^{N_m} V_{mod,i}(I) \quad (2-33)$$

In this way, a PV string is modeled in an explicit form and the values of its voltage can be calculated without needing iterative methods. Authors propose two alternatives for the application of this technique in SP arrays: (i) predetermination of the I-V curve of each string and graphical superposition of the individual curves to construct the array I-V characteristic as in [79] and (ii) iterative solution of each string equations for a given terminal voltage and then summation of the individual currents as in [83]; the technique is validated through simulation and experimental tests but there is no details concerning the execution times. Authors highlight the main differences of the proposed procedure in comparison with other works such [83], [82], [9] and [76], pointing out that the main contribution is the detail of the model (cell level) and the explicit procedure to calculate de voltage and currents of the array avoiding the use of iterative methods; in addition the Lambert W function is expressed as a series expansion accurate enough, this with the aim of reduce the computational burden. Finally, authors present an analysis which allowed to define mathematical expressions for evaluating the voltage and current of the MPP's of a string exposed to partial shading conditions.

The technique described in [82] is based on the ideal single diode model (neglecting the series R_s and parallel R_h resistances) at module level. In this way, the relationship between the voltage and current of a PV module can be expressed in an explicit form as is given in (2-34), the nomenclature of such equation is the same introduced in section 2.3.1. In this way, the is no need of using the Lambert W function. The blocking diode is included in its exponential form and the bypass diodes is modeled as an ideal switch, namely, it could be open or closed. Therefore, if the bypass diode associated to a module is turn on, the module becomes inactive.

$$I_{mod} = I_{ph} - I_{sat} \left(\exp \frac{V_{mod}}{V_t} \right) \quad (2-34)$$

In addition, authors provide an interesting contribution when introducing the *inflection points concept*, which refers to those points of the I-V curve changes is behavior due to the effect of the activation of bypass diodes when the modules are exposed to partial shading. Fig. 2-22 illustrate the behavior of the I-V curve of the same string formed by 4 modules with and without partial shading, it is evident that the I-V curve changes when it is exposed to partial shading; in this specific example 3 of the 4 modules has different levels of irradiance. The points where the I-V curve changes is monotonically decreasing behavior are then called inflections points.

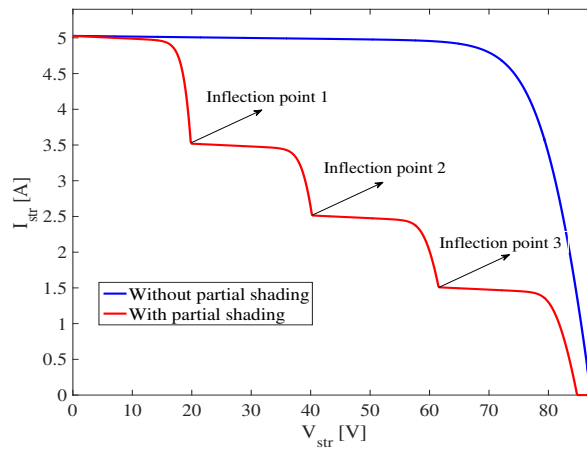


Figure 2-22.: I-V curves of a string with and without partial shading.

This technique is oriented to SP arrays by modeling each string and then added the currents. The string modeling is based in the same principle of [83]: applying the Kirchhoff laws to obtain a system of equations, but considering that the activation of a bypass diode implies the deactivation of a module, the size of such a system of equations is not fixed, it depends on the number of active modules. Then, authors propose a procedure to find the voltages values in which the bypass diodes become active, such voltages are then called inflection voltages. The system of equations obtained to evaluate a given voltage value is then solved by means of Newton Raphson method or other iterative algorithms. In addition, authors proposed to use a LU-type factorization in order to reduce the time computation of the inverse of the Jacobian matrix. Simulation results validate the approach, however there is no information concerning the computing time reduction achieved in comparison with other approaches; the analysis of the error introduced by using ideal models for the module and the bypass diode is not described either.

The work presented in [9] is inspired on the inflection points technique introduced in [82], but with the following remarkable differences: (i) the complete single diode model is used (R_s and R_h are considered), (ii) the bypass diode is considered in a piecewise linear form defined by a resistance R_{bd} and a voltage source V_{bd} and (iii) the PV array modeling is made

by only one equation, which can be solved by a numeric technique. Applying a mathematical procedure, described in detail in the paper, the voltage of a string j with n modules (in a SP array) as function of its current I_j is given by (2-35); V_{am} corresponds to the voltage of the active modules, i.e. the modules in which the bypass diode is not active; V_{im} corresponds to the voltage of the inactive modules, i.e. the modules with active bypass diodes, which in turns depends on the current of the string as given in (2-36) and V_{bk} correspond to the blocking diode voltage which is given by a linear approach. In this way, a better approach of the operation in the second quadrant due to the effect of partial shading is introduced.

$$V_{str,j} = \sum_{i=1}^{ac} V_{am,i}(I_j) + \sum_{k=ac+1}^n V_{im,k}(I_j) - V_{bk,j} \quad (2-35)$$

$$V_{im} = - (I_j R_{bd} + V_{bd}) \quad (2-36)$$

Authors proposed to define the string voltage V_{str} as the independent variable since in most of applications such a voltage is fixed by a power converter. Then, the string current must be obtained by solving (2-35) by means of methods such as Newton Raphson. The performance evaluation was made by means of experimental and simulations tests for small, medium and large arrays; for a large PV array form by 50 string of 50 modules each the computing time was almost 8 hours and 40 minutes, such result was compared with the results provided by the techniques proposed in [83] (named Complex) and [82] (named Fast) with which the computing times were 47 hours and 13 seconds, respectively. The error in the prediction of the MPP power, taking as reference the value provided by a circuital simulation using Simulink, was $4.4 \times 10^{-2} \%$ while for the Complex method and Fast method the error was $1.59 \times 10^{-2} \%$ and 4.4% , respectively. Considering the results authors define the introduced approach as a tradeoff between a complex but accurate technique [83] and a fast but less accurate technique [82]. Finally, authors demonstrate the usefulness of the proposed modeling method by means of a simulation of a battery charger controlled by a MPPT algorithm; such a simulation allowed to highlight that the procedure can be implemented in C++ language to generate a DLL block to be used in simulation environments as PSIM.

2.4.2.2. Solutions based on other PV models

The technique described in [65] is based on the estimation of the losses caused by the partial shading, it by calculating the power P of a SP array directly by using an heuristic model. The basic equation which authors define for the model are given in (2-37), where P_{NS} is the power of the array without shading, F_{ES} is the effective shading factor which in turn is defined in (2-38), where F_{GS} is a geometrical shading factor, N_{TB} is the total number of modules in the array and N_{SB} is the number of modules of shaded modules. Since the

purposes in to analyze the power and the geometrical characteristics of shade, this technique does not addresses the issue of obtaining the whole I-V or P-V curve.

$$P = P_{NS} (1 - F_{ES}) \quad (2-37)$$

$$(1 - F_{ES}) = (1 - F_{GS}) \left(1 - \frac{N_{SB}}{N_{TB} + 1} \right) \quad (2-38)$$

The geometrical shading factor F_{GS} is obtained empirically but the process is not described, this can be a drawback since in actual applications the shadow can exhibit different behaviors. The model was validated through experimental tests with 3 different sizes SP arrays. The model presents an error between 12 % and 23 % with respect to the power predicted by the real curves of the arrays.

In [28] the inter-row shading effect is analyzed through a simplified heuristic PV model, which allows to reduce the computing time for the study of power production in large PV arrays. This is very useful to perform calculations of energy yield for long periods, e.g. years, then this technique is developed at module level. One assumption made by authors to simplify the calculation is that each parallel string in the PV installation contains the same percentage of shaded submodules, because of that it is not possible to model irregular shading patterns. Another assumption is that partial shading on a given submodule can be represented in a binary condition. In this way, the model is based on four variables: (i) fraction of submodules shaded in a string S , (ii) fraction of parallel strings shaded X , (iii) irradiance fraction reaching the shaded submodule E_e and submodule fill factor FF_0 , defined as $FF_0 = P_{mpp,0}/V_{oc,0}/I_{sc,0}$. Then, the model focuses on the reduced power of the partially shaded strings $P_{str}/P_{str,0}$ which depends on the four variables previously defined and finally the power of the array can be found by adding the power of the shaded and unshaded strings as given in (2-39). In this model, it is assumed that the unshaded strings produce their peak power.

$$\frac{P_{array}}{P_{array,0}} = X \left(\frac{P_{str}}{P_{str,0}} \right) + (1 - X) \quad (2-39)$$

In order to include the effect of the activation of bypass diode when a module is shaded, authors propose to recalculate the operation voltage of the modules: for the unshaded modules the voltage increase in a proportion related with the number of shaded modules. The voltage for the shaded modules is assumed equal to zero, which leads to define that the bypass diode is modeled as an ideal switch and the power of the entire string is equal to the power delivered by the unshaded modules. This situation is very similar to the one presented in [82], then it can be concluded that the operation in the second quadrant is neglected which can introduce errors in the prediction of the array power. Simulations and experimental tests

validate the proposed approach, however it must be highlighted that the assumptions made for the development of the model limit it to the application only to certain shading profiles.

Table 2-2.: Models oriented to energy yield analysis

| Ref. | Level | Model | Final application |
|------|--------|--------------|-------------------|
| [12] | Cell | Single diode | Array (SP) |
| [82] | Module | Single diode | Array (SP) |
| [9] | Module | Single diode | Array (SP) |
| [65] | Module | Heuristic | Array (SP) |
| [28] | Module | Heuristic | Array (SP) |

2.4.3. Modeling techniques for shading analysis

Another interesting topic in the study of PV systems is the analysis of the shading effects since, as it was said before, shading is one of the most important issues to take into account in the design and planing of PV systems. Shading effects include power losses, accelerated aging of the PV panels, wrong operation of the control systems, among others. Table **2-3**, summarizes the techniques presented in this category.

2.4.3.1. Solutions based on the single diode model

In [4], the single diode model is used for representing the operation of the solar cell when operating in direct bias, while equation (2-40) has been proposed to represent the reverse operation of the cell, where B_e is a non-dimensional quasi-constant parameter (equal to 3 in this work), V_b is the breakdown voltage of the cell and ϕ_T is the built-in junction voltage considered equal to 0.85 V in this work. The bypass diode is modeled as a straight line with infinite slope and intercept at -0.8 V.

$$I_{cell} = \frac{I_{ph} - R_p^{-1} V_{cell} + c V_{cell}^2}{1 - \exp\left(B_e \left(1 - \sqrt{(\phi_T - V_b) - (\phi_T - V_{cell})}\right)\right)} \quad (2-40)$$

The first concept analyzed in this work is the influence of the amount of shading, for this purpose the authors considered a string of 18 cells supposing that one of the cells is 25 %, 50 %, 75 % or 100 % shaded. From the analysis authors conclude two main effects of the shading: reduction on the photovoltaic current in the shaded cell and the displacement of the maximum power point of the string, which is one major issue to be considered in MPPT strategies design. A second analysis performed was the influence of the reverse characteristic of the shaded cell, in which the authors conclude that cells with high shunt conductance produce less effect in the deformation of the I-V characteristic. The next analysis presented

in this paper was the influence of the string length, this effect has been analyzed by shading completely one cell in a system formed by 108 PV cells, changing the number of cells connected to the bypass diode in four cases; the conclusion of this analysis is that increasing the number of cells protected by the bypass diode produces a higher deformation in the I-V characteristic, which in turn, causes a higher reduction in maximum power. Moreover, higher power is dissipated in the shaded cell and less current flows through the bypass diode. Finally, the influence of the number of shaded cells is also analyzed. It is made by using five configurations for a string of 18 cells. The authors conclude that the deformation of the I-V characteristic increases with the number of shaded cells, which is a consequence of the decrease in the string short circuit current when the number of shaded cells is increased.

The work reported in [64] presents an investigation on the mismatch losses and the power losses in tracking of a local maximum power point instead the global maximum. The analysis was made by simulations in Simulink considering the single diode model for representing the PV cell. A large string formed by 18 cells and a 6×3 SP array were the structures used by authors in this work. The values of the parameters for the cell were calculated using the procedure introduced in [111], taking as reference the values of the datasheet of the NAPS NP190GKG PV module which contains 54 cells. Each module contains three bypass diodes connected in anti-parallel with 18 series-connected cells. In addition, each bypass diode was represented by the exponential form. The mentioned structures were exposed to different shadow levels. The analysis of the simulation were focuses on three main concepts: (i) power of the global MPP, (ii) the mismatch losses and (iii) the power difference of the local MPPs. The main conclusions are that at low voltages decreases as system shading increases and at high voltages it decreases as shading strength increases; in addition, the fact that every block of PV cells does not operate in its own MPP, although the whole PV power generator operates in its global MPP, generates losses which mainly depends on the number of cells affected by shaded and the strength of the shadow (level of irradiance blocked by shadow), but in general the losses in multi-strings arrays are lower than the losses in a single large string.

In the previous sub-sections, the work presented in [12] was discussed from the point of view of the energy yield analysis. However, in that work the authors also show the results of the partial shading analysis, from which they propose some expressions to calculate the MPP's of a partially shaded PV string. Their analysis begins by using the case of two levels of irradiance (shaded and unshaded), after that an extension of the analysis is made considering n irradiance levels. In this way, the voltage, the current and the power of the n MPPs are given by (2-41) to (2-43) with $j = 1, 2, 3...n$; S is the irradiance, ΔV_D is the voltage drop on a conducting bypass diode, λ is an empirical coefficient for $I_{mpp,j}$ typically equal to 0.06, N_m is the number of PV modules in the PV string, N_{cs} is the number of cells in the module and the rest of parameters $V_{mpp,0}$, $I_{mpp,0}$, $V_{oc,0}$ are the voltage and current at MPP and the open

circuit voltage, respectively, according to the datasheet of the PV panel. The performance of the proposed expressions was satisfactory since the root mean squared error was lower than 2% and for extreme conditions of partial shading a RMSE up to 9% was obtained.

$$V_{mpp,j} = \sum_{i=1}^j N_i \left[\frac{S_j V_{mpp,0}}{S_i N_{cs}} + \left(1 - \frac{S_j}{S_i}\right) \frac{V_{oc,0}}{N_{cs}} \right] - \sum_{i=j+1}^n N_i \Delta V_D \quad (2-41)$$

$$I_{mpp,j} = S_j I_{mpp,0} \left[1 + \lambda \frac{\sum_{i=1}^{j-1} N_i}{N_m N_{cs}} \right] \quad (2-42)$$

$$P_{mpp,j} = V_{mpp,j} \cdot I_{mpp,j} \quad (2-43)$$

On the other hand, in [67] a technique to obtain the power peaks of PV arrays (SP, TCT and BL) with equations to the meteorological data is introduced; the model is based on the single diode model at cell level as defined in section 2.3.1. The power peak prediction technique is based on the fact of the number of power peaks in a partially shaded serial connection of modules is equal to the number of different irradiance levels over the modules and that each power peak corresponds to the operation of a group of modules at their MPP. Therefore, the model calculates each power peak assuming that the modules with a certain irradiance level are operating at their MPP. The first stage of the procedure has the aim of calculate the parameters of the single diode model, in addition explicit equations for calculate the short-circuit current I_{sc} , the MPP current I_{mpp} , the MPP voltage V_{mpp} and the open circuit voltage V_{oc} are introduced. At this point the model is scaled up for modules representation by performing a simple product or division of the parameters for the series or parallel connection of cells. Then, authors define the first basic expression of the technique under the following aspect: for modules in series connection, the voltage at each power peak is calculated when one group of modules with the same irradiance level operates at their MPP. Thus, a string exposed to m different irradiance levels S_1 to S_m , the terminal voltage V_i at which the modules exposed to the S_i irradiance level (operating at their MPP) is defined by (2-44), where n_j is the number of modules with the S_j irradiance level and V_D is the forward voltage of the bypass diode.

$$V_i = V_{oc} \sum_{j=1}^{i-1} n_j + V_{mpp} \cdot n_i + V_D \sum_{j=i+1}^m n_j \quad (2-44)$$

The second basic expression of the this model defines the current at the power peak; such an equation was obtained through empirical process, then for a string exposed to n irradiance levels the current is given by (2-45), where $I_{mpp,i}$ is the current I_{mpp} of the modules under

the irradiance level S_i , V_T is the given terminal voltage and V_1 to V_n re the terminal voltages when modules exposed to irradiance levels S_1 to S_n operate at their respective MPP which are calculate using (2-44). In addition, $S(x)$ and $R(x)$ are functions defined in (2-46) and (2-47), respectively.

$$I = I_{mpp,1}S(V_1 - V_T) + I_{mpp,2}S(V_2 - V_T)R(V_T - V_1) + I_{mpp,3}S(V_3 - V_T)R(V_T - V_2) + \dots + I_{mpp,n}S(V_n - V_T)R(V_T - V_{n-1}) \quad (2-45)$$

$$S(x) = \begin{cases} 1,05, & x > 0 \\ 1, & x = 0 \\ 0, & x < 0 \end{cases} \quad (2-46)$$

$$R(x) = \begin{cases} 1, & x > 0 \\ 0, & x \leq 0 \end{cases} \quad (2-47)$$

Based on (2-44) and (2-45), a large set of equations is defined for SP, TCT and BL arrays; each configuration was evaluated experimentally using Sanyo HIT 200-W PV modules. Results showed that the accuracy of the model was higher than 95 % in the calculation of the global power peaks and 90 % in the calculation of the voltage associated with the global power peak for the tested partial shading conditions. However, the large amount of equations required and the lack of detail for defining some parameters as functions $S(x)$ and $R(x)$ can be a drawback of this technique.

In [29] a modification of the single diode model is introduced in order of representing PV cells under partial shading condition. Authors assume that PV cells can be exposed to three conditions: uniform irradiance, completely shading and partial shading. Since, the probability of the three kinds of conditions appear on one PV cell at the same time is negligible, the authors focus on modeling the third condition: partial shading. In this way, the cell is represented by (2-48), where the variables with subindex 1 are related with the partial shading operation, while the variables with subindex 2 correspond to the uniform irradiance condition. The rest of parameters are the same described in section 2.3.1.

$$I_{cell} = A_1 I_{ph1} - A_1 I_{sat1} \left[\exp \left(\frac{V_{cell} + I_{cell} R_s}{V_{t,cell}} \right) - 1 \right] + A_2 I_{ph2} - A_2 I_{sat2} \left[\exp \left(\frac{V_{cell} + I_{cell} R_s}{V_{t,cell}} \right) - 1 \right] - \frac{V_{cell} + I_{cell} R_s}{R_h} \quad (2-48)$$

This model was implemented in Simulink to validate its accuracy. For this purpose, a module formed by 72 cells was simulated, in addition the simulation considers three cases: the module

without bypass diode, the module with 3 bypass diodes (each bypass diode connected to 24 cells) and the module with 4 bypass diodes (each bypass diode connected to 18 cells). The level of shading was 85% for all simulations and the number of cells shaded was changed from 0 to 72. The simulation results evidence that the use of bypass diodes mitigates in part the negative effect of partial shading on the global MPP power. One of the interesting conclusion of the analysis was the fact that when the module was exposed to a shade with an area of 60% or more, the global MPP was located at a voltage too low to be traced by the DC-DC converter, this forcing the system to operate at the local MPP causing power losses, which leads to considering a deeper analysis on the suitable number of bypass diode which must be connected in the module.

2.4.3.2. Solutions based on the Bishop model

In [13] the Bishop model is introduced. Such model, described in section 2.3.3, is considered one of the most suitable models for describing the operation of PV cells in the second quadrant due to partial shading conditions. In addition, the work introduces a tool to model the electrical behavior of solar cell interconnection circuits based on Pascal language. The tool, named PVNet, allows to obtain the I-V curves of PV panels in three quadrants by performing a voltage sweep. PVNet identifies the interconnections of a PV panel through a code of four integer numbers: the first number identifies the number of bypass diodes (represented by the exponential model), the second one identifies the number of groups of series-connected cells bridged by each bypass diode, the third number identifies the amount of strings of cells connected in parallel and the last digit is the number of cells in each group. Fig. 2-23 illustrate some examples of the encoding process.

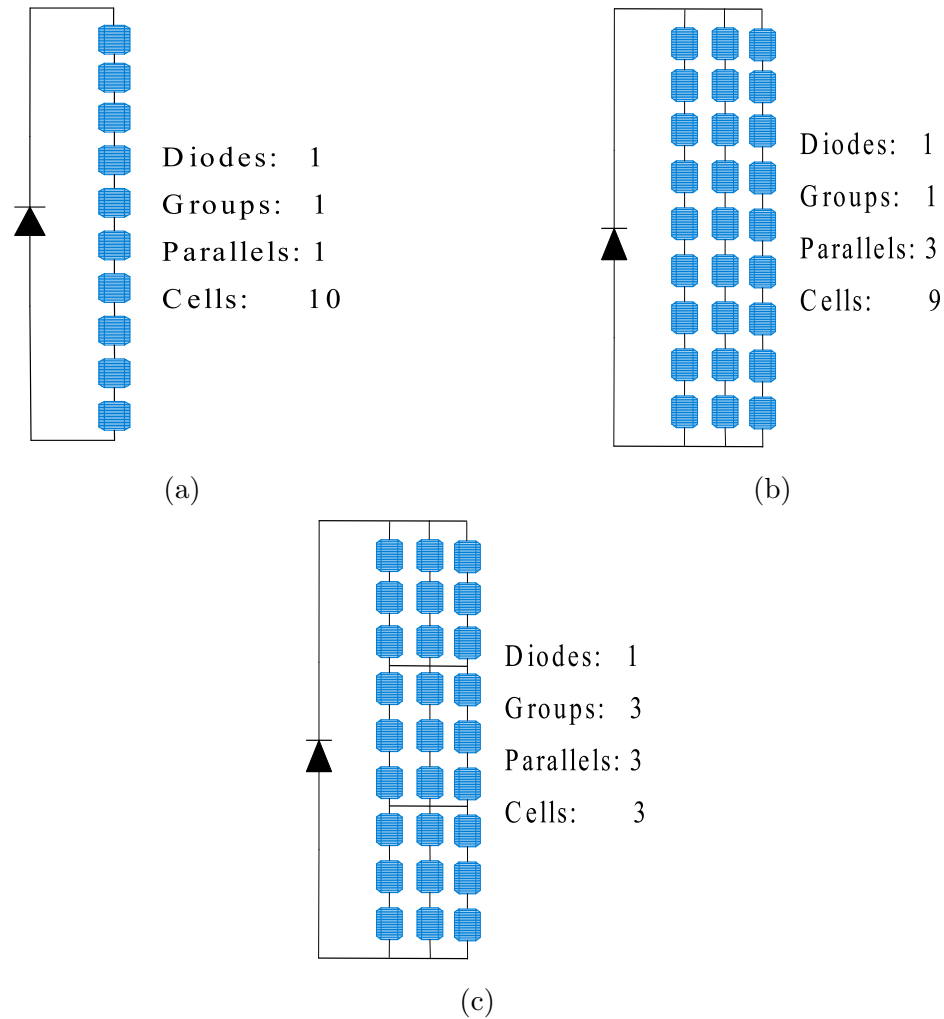


Figure 2-23.: Encoding examples used by PVNet.

The algorithm calculates the circuit parameters through statistical processes which are based on a large data base of different monocrystalline PV cells provided by the European Solar Test Installation (ESTI). The procedure for obtaining the I-V characteristics is based on the basic circuital principles of summation of voltages in series connection and summation of currents in parallel connection; therefore, the initial information concerning the connection of the cells inside the module must be precise. In addition, the method is able to perform the analysis when the cells are modeled with different parameters, which implies to interpolate voltage and current values. Several simulations were performed using the structures shown in **2-23**. Those simulations allowed to analysis the different effects of the partial shading and recognize the importance of the operation in the second quadrant, the differences in the temperature operation between the shaded and unshaded cells and the current imbalance which not only affect the power production, but also causing deterioration of the cells and irreversible damages; the effect of the connection of bypass diodes is not enough to mitigate

the shading effects, then author proposed to analyze the effect of modifying the value of shunt resistance or the value of its breakdown voltage which mainly concerns to manufactures; this work also introduces a short analysis of the operation of blocking diodes in a string which results in a proper way of eliminating the current imbalance.

In [99] the power losses related with the series and parallel resistances under shading conditions are studied. The Bishop model with a modification is used, such as modification is illustrated in Fig. 2-24. In this way, the behavior of the cell is represented by (2-49) and (2-50), where V_b is the breakdown voltage and n is the Miller constant.

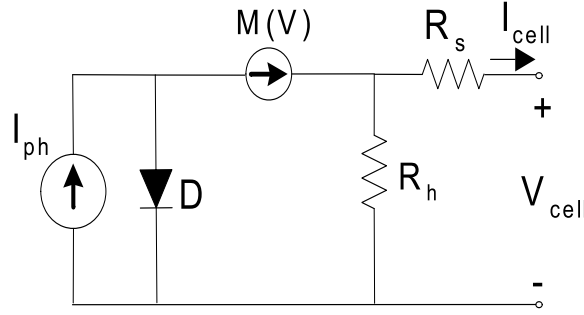


Figure 2-24.: Equivalent circuit of a PV cell used in [99].

$$I_{cell} = \left(I_{ph} - I_{sat} \left(\exp \left(\frac{V_{cell}}{V_t} \right) - 1 \right) \right) M(V) - \frac{V_{cell}}{R_h} \quad (2-49)$$

$$M(V) = \frac{1}{(1 - (|V|/V_b)^n)} \quad (2-50)$$

The implementation of the model was performed in Simulink where a current sweep was performed in order to obtain the voltages of the cells. The performance of the module was made by using a module formed by 36 cells in series connection and the results show a good agreement compared with real measurement. From multiple simulations with using different level of shading and number of shaded cells authors conclude: a single solar cell totally shaded does not cause a significant maximum power loss, which is less than 10 % at lower irradiation. However, the power losses increase with increments in the irradiation and shadow rate. The variations of the series and parallel resistance have a relationship between the losses on partial shading conditions: the effect of a reduction in the parallel resistance not only increases the slope of the reverse I-V characteristic of the PV module, but also modifies the I-V characteristic in direct polarization. Another relevant conclusion is that the series resistance increases at the same time the shadow rate does; in contrast, the parallel resistance presents a clear reduction due to shadowing, which increases the probability of

hot spot apparition in the PV module.

In [98], an analysis of the I-V curves for different connections of the bypass diodes, in the first and second quadrant, is presented. The analysis is based on the Bishop model but considered two diodes as is illustrated in Fig. 2-25; the relation between the current and voltage in the cell is then given by (2-51) where parameters are described in section 2.3.2 and 2.3.3.

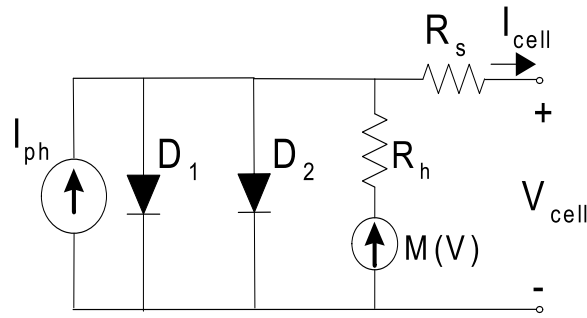


Figure 2-25.: Equivalent circuit of a PV cell used in [98].

$$I_{cell} = I_{ph} - I_{sat,1} \left(\exp \left(\frac{V_{cell} + R_s I_{cell}}{V_{t,1}} \right) - 1 \right) - I_{sat,2} \left(\exp \left(\frac{V_{cell} + R_s I_{cell}}{V_{t,1}} \right) - 1 \right) - \left(\frac{V_{cell} + R_s I_{cell}}{R_h} \right) \left[1 + a \left(1 - \frac{V_{cell} + R_s I_{cell}}{V_b} \right)^{-m} \right] \quad (2-51)$$

The model was implemented in PSpice and the results were compared with experimental tests carried out in a commercial panel formed by 60 cells and 2 bypass diodes, the results show good agreement with the real I-V curves, obtaining a root mean squared error of 3.1 % for the module current. After the preliminary validation of the model, authors analyzed several cases considering different shadow levels for a module with different configurations in the connection of the bypass diodes, for this analysis a module formed by a 36 cells was considered. One of the cases under studied was the connection of bypass diodes with overlapped cells; such a case is illustrated in Fig. 2-26.

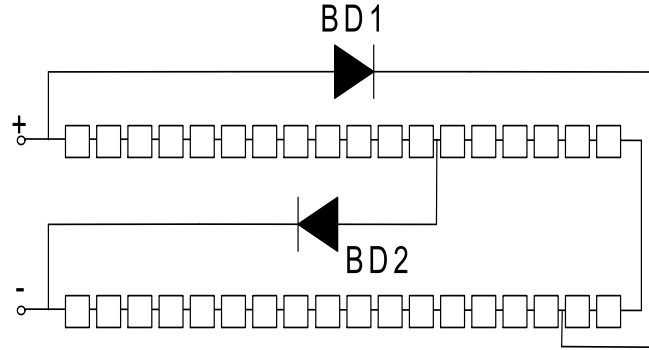


Figure 2-26.: PV module with two bypass diodes and overlapped cells.

The results showed that for the case of Fig. 2-26 with one overlapped cell exposed to shading, depending on the level of the shadow, for low voltages values both bypass diodes become active and their current is the same which results in an increase of the short circuit current of the entire module; when the voltage increases $BD2$ becomes inactive reducing the output current of the module. Authors also proposed an expression to estimate the maximum number of solar cells, n_{max} , protected by one bypass diode in a PV module under the following analysis: in reverse bias, the current across the solar cell does not increase drastically until the breakdown voltage is achieved, if a safety factor of 80% of the breakdown voltage V_b is fixed as maximum breakdown voltage supported by a cell, the dissipated power will below the maximum allowed and the cell will not be damaged. Then, to force the bypass diode to become active, the reverse voltage of the shaded cell V_s can be defined as in (2-52), where V_d is the voltage at the bypass diode in conduction state and n the number of cells covered by the bypass diode. In addition, considering that the open circuit voltage V_{oc} as the maximum voltage allowed at each unshaded cell, (2-52) can be redefined as (2-53).

$$V_s \geq V_d + \sum_{i=1}^{n-1} V_i \quad (2-52)$$

$$V_s \geq V_d + (n-1) V_{oc} \quad (2-53)$$

Considering the safety factor of 80% the maximum number of cells protected by a bypass diode can be defined as:

$$n_{m\acute{a}x} \leq 1 + \frac{0.8V_b - V_d}{V_{oc}} \quad (2-54)$$

Finally, the model is extended to perform some simulations on SP arrays where the changes in the behavior of the MPP due to different shading profiles were studied, but the is not a

detailed discussion over the implementation of this procedure on PSpice.

The technique described in [94] is used to calculate the shading losses in PV arrays with SP connection. A geometric shading factor is defined, which allows to include the information about the area of the module affected by the shadow. In addition, different kinds of shadows are considered: the real shadow, the most concentrated shadow, the most distributed shadow and the approximated real shadow. The modeling technique considers several set of equations: (i) the equations of the partially shaded solar cells, (ii) the equations of the bypass diodes and (iii) the equations that relate the system currents and voltages obtained from the Kirchhoff laws. Then, by solving the system of equations, a shading power losses factor of the array is obtained.

2.4.3.3. Solutions based on the PL model

In [113] authors suggest to use this model in PSIM or EMTP. The considered cases were: (i) influence of percentage of shading, (ii) effect of the number of shaded cells, (iii) effect of bypass diodes, and iv) effect of the configuration of cell connection. The main conclusion is that when overlapped cells are shaded, the short-circuit current can be much higher than the reference case (unshaded case) because when one or more overlapped cells are shaded, the circuit structure changes from a series string to two parallel strings. The analysis also include simulations for SP, TCT, BL and HC arrays under different shading conditions. The authors compare two aspects for each connection: fill factor and maximum power, concluding that TCT configuration has a better performance compared to the rest. SP has the poorest performance, while BL and HC have comparable performance. On the other hand, [114] is a second stage of the work presented in [113], where a comparison between the PLPB model and the single diode model is performed for the four typical PV arrays configurations. The authors provide detailed mathematical models based on the single diode model, which are solved by using the Newton-Raphson method, then the results are compared with the performance of simulations of the same configurations made in EMTP using the PLPB model.

2.5. Conclusions

This chapter has presented the main concepts concerning the operation and modeling of PV devices. The most relevant PV cell models were explained and an overview of the procedures for computing their parameters was also given. Since the parameters provided from the manufacturers in datasheets are reference values at STC, it is necessary to apply a procedure for obtaining the values of the parameters for the actual operating point. The complexity of the PV model will define the complexity of the procedure for obtaining the parameters and the accuracy of the results.

Table 2-3.: Models for shading analysis

| Ref. | Level | Model | Final application |
|-------------|--------------|-----------------------|----------------------------|
| [4] | Cell | Single diode | Array (SP)/Module |
| [64] | Cell | Single diode | Array (SP) |
| [12] | Cell | Single diode | Array (SP) |
| [67] | Cell | Single diode | Array (SP, TCT and BL) |
| [29] | Cell | Single diode modified | Module |
| [13] | Cell | Bishop | Module |
| [99] | Cell | Bishop | Module |
| [98] | Cell | Bishop | Array (SP) |
| [113] | Cell | PL | Array (SP, TCT, BL and HC) |
| [114] | Cell | PL | Array (SP, TCT, BL and HC) |
| [94] | Module | Bishop | Array (SP) |

Most of the procedures reported in literature are based on the single diode model, which requires five parameters. In the same way, most of those procedures are based on solving a system of equations defined from the three key points (I_{SC} , V_{OC} , and MPP), [111], [27], [26], [40]. On the other hand, the use of the two diode model increases the complexity of the procedures for obtaining its parameters since such a model requires seven parameters instead of five. However, such a model increases the accuracy at low irradiance values [46], [19]. Due to the complexity to find the parameters of the two diode model, some authors have proposed approaches based on fixed set of equations which only require basic information from datasheet [19], [37], [41]. The Bishop model has been used for analyzing the reverse mode of the cell when it is exposed to partial shading, since it allows to obtain the characteristic curve for the first, second, and fourth quadrant. However, there is not a clear reported procedure to find the parameters of the model, in particular the avalanche breakdown parameters. Another models have been proposed such as the PL model [113], [5] and some variations of the single diode model [93], [20], [82]. They have been used in order to avoid the complexity of the other models or for analyzing in detail some specific condition of the cell [107], [103].

The mismatching effect, in particular the partial shading, causes PV cells operate in the second quadrant. Therefore, they do not produce power but instead they consume it. Then, in order to mitigate such a negative effect, bypass diodes are used. Considering that PV systems are commonly exposed to partial shading, it is important to include the bypass diodes in the model of the module. In the literature survey on modeling techniques for PV arrays, also presented in this chapter, three application categories were identified: Simulation to obtain the characteristic curves, Energy yield analysis and Shading effects analysis. From all the

techniques presented in the survey, 14 works used the single diode model for modeling the PV cell or module, while in 2 works the two diode model was selected for the representation of the PV cell or module. On the other hand, 7 works include the Bishop model and 2 include the PL model for analysis. Those results show a clear tendency to use the single diode model for the modeling of PV arrays, which in turn allows to consider that the single diode model is, in fact, a suitable way for representing the PV cell or module because it provides a good compromise between accuracy and complexity. The Bishop model is the second model most used in the works included in this survey because such model is suitable for representing the operation of the PV cell or module when the system operates under partial shading. However, only in [13] the authors presented an analysis of the system operation in the second and third quadrant, while in [98] and [77] the authors studied operation of PV modules in the second quadrant. A common fact detected in the works based on Bishop model was the lack of detail in the procedure for calculating the parameters a and m which define the avalanche breakdown operation. The variations of the typical PV models as the R_s model and the ideal model were employed for improving the calculation speed in algorithms for energy prediction [82]. In addition, procedures as the presented in [65] and [28] introduced models which do not represent the operation of an equivalent circuit, instead they are based on empirical equations.

The literature review presented in this chapter also allows to identify the tendency in the level of detail in the modeling techniques, i.e. cell level or module level. In this way, in 16 works the modeling was performed at cell level while in 8 works the modeling was performed at module level. However, from the 11 techniques presented for obtaining the characteristic curves, 6 of them were implemented at cell level and the other 5 were implemented at module level. The techniques oriented to energy yield analysis do not show a defined tendency; however, considering that power production analysis is a relevant issue in large PV fields, techniques developed at module level can be a suitable option in order to improve the computational time. On the other hand, from 11 works included in techniques for shading analysis, 10 considered modeling at cell level and 1 at module level since such techniques were generally focused on the behavior of *MPP* and impact of the connection of bypass diodes in different sections of the PV module.

Aspects that may be subjective as the complexity or the detailed information concerning the modeling procedures were also identified: the techniques presented in [67], [94], [51] are based on large set of equations which difficult the understanding of the procedure, besides it can be a drawback for the implementation in embedded processors. On the other hand, techniques described in [51] and [88] are oriented to SP, TCT and BL configurations and their results were satisfactory, however the lack of detail on the proposed procedures implies a drawback for users or researchers to reproduce them. Finally, modeling techniques based in environments as Simulink [45], [98] have a major drawback consisting in the fact that the

files can become obsolete since the permanent (at least twice in one year) upgrade of the simulation environment.

Finally, with respect to the final application structure of the modeling techniques included in this chapter, most of the techniques were applied to SP arrays. TCT and BL structures were discussed in [46], [51], [88], [67], [113] and [114], while HC connection was considered in [88], [113], [114]. It is clear that SP configuration is the most widely studied array, and it is clear also that there is no a procedure for modeling a PV array under any (or different) configuration. Moreover, this survey allows to establish that analysis of PV arrays has been oriented to the regular SP, TCT, BL and HC configurations. Structures under irregular connections have not been considered, in consequence techniques for modeling such structures have not been developed. The performance of irregular PV structures under mismatching conditions has not been analyzed, then the behavior of such structures under partial shading conditions is unknown. Such kind of structures can represent an option for mitigate the negative effects of shadows or another mismatching conditions; thus, analysis of irregular or no conventional PV structures can be considered as a new field of researching on the field of PV systems. This field is addressed in Chapter 4 of this thesis.

3. Modeling approaches for SP arrays

In the previous chapter it was detected that SP array is the most used and studied PV configuration. However, there is still a lack of analysis of some aspects as the operation of the cells in the second quadrant, the bypass diodes models and the shadow representation. Therefore, this chapter is devoted to the analysis and modeling of SP arrays; some approaches at module level are introduced. Such approaches use different module models and bypass diode representations, this for exploring different levels of performances and complexity. The procedures presented in this chapter are oriented to the reproduction of the electrical characteristics and energy yield analysis.

The analysis and results presented in this chapter have been published in *Revista Tecnológicas* in the paper: “Modeling of PV systems based on inflections points technique considering reverse mode” [92], *Revista Tecnológicas* in the paper: “Energy prediction in urban photovoltaic systems” [90], *Revista Dyna* in the paper: “Estimating the produced power by photovoltaic installations in shaded environments” [89] and in *Revista Ingeniería e Investigación* in the paper “Fast calculation of the maximum power point of photovoltaic generators under partial shading” [90].

3.1. Introduction

The SP is the most widely studied PV array configuration, fact that was demonstrated in the previous chapter. Such a configuration has been studied from different points of view: reconstruction of the characteristic curves, energy yield analysis and shading effects analysis, also at different level of detail (cell and module level). Moreover, such a configuration can be consider as the simplest one which makes it suitable for performing a first analysis of the operation of PV devices and all the associated phenomena described in Chapter 2. Therefore, in this chapter the SP configuration is used to analyze the aspects that must be included in a modeling process: PV module models, mismatching phenomenon, bypass diode models and mathematical tools for analysis. Those factors have to be taken into account for modeling any PV array as will be discussed in Chapter 4.

In this chapter modeling approaches for SP arrays at module level are proposed. Such approaches can be defined as procedures for reproduction of the electrical characteristics and

energy yield analysis or power estimation. For this purpose, section 3.2, introduces a modeling approach that considers the operation in the second quadrant. Such an approach is based on the technique presented in [82], in which the PV module is represented by the ideal single diode model and the bypass diode is considered as an ideal switch. The proposed approach uses the same model for the PV module but considers a linear representation for the bypass diode, this with the aim of analyzing the operation in the second quadrant of the modules exposed to partial shading conditions.

Moreover, in section 3.3, three approaches also oriented to power estimation analysis are presented. However, the operation in the second quadrant of the modules operating under mismatching conditions is not considered since those models have two aims: analyze the effect of the bypass diode model and improve the calculation speed for first-attempt energy estimation. In the first approach, the module is represented by the single diode model and the bypass diode by a linear model. The second approach uses the single diode model for the modules and the exponential model for the bypass diode. Finally, the third approach presents a solution for improving the processing time, which avoids to calculate the whole power curve to detect de GMPP. For that third approach the module and the bypass diode are represented through ideal models, but special attention is given to the modeling of the partial shading conditions. Therefore, the dynamic behavior of the shadows due to the sun translation is considered to reduce the error produced by the assumption of average shading profiles. All the approaches introduced in this chapter were validated through simulations tests.

3.2. A modeling approach considering the operation in the second quadrant

Despite the amount of reported techniques for modeling SP arrays, a lack of analysis of the operation in the second quadrant was identified in the overview given in Chapter 2; only in [13] and [98] some concepts are given. The approach presented in this section is aimed to improve the approach presented in [82] by including the reverse mode of the module in the modeling procedure. In this way, as in [82], this approach considers the ideal single diode model, which neglects the series and parallel resistances R_s and R_h . However, instead represent the bypass diode as an ideal switch, in this approach the effect of the bypass diode is considered through a linear approximation of the exponential model. Fig. 3-2 illustrates the PV module circuit. It is worth to precise that the procedure presented in [77] also considers the operation in the second quadrant. However, that paper was published after the approach given in this section was reported in [92].

The *inflections points concept* is related to the voltage at which the bypass diode of a module

exposed to shadows turns on. Fig. **3-1** shows the I-V curve of a string formed by 4 modules where 3 of them operate under partial shading conditions; the short-circuit currents of the modules are: 5.031 A, 3.52 A, 2.51 A and 1.5 A. Such an operating condition causes the bypass diodes associated to the three modules affected by partial shades to become active. It can be observed that the curve in Fig. **3-1** presents a discontinuous behavior as it was explained in Chapter 2. Moreover, Fig. ?? shows the diode current (exponential model) vs. array voltage curve of the bypass diode associated to each module. Each voltage value in which the current of the bypass diode becomes 0 A is related with the operating point in which the I-V curve of the whole string changes its derivative. Considering that the voltage of a PV array is typically imposed by a dc-dc converter (e.g. to perform the MPPT control), the analysis of the inflections points is made in terms of the voltages in which the bypass diodes turn on. In this way, each voltage in which the I-V curve changes its derivative is named *inflection voltage*; for the case shown in Fig. **3-1**: V_{o_2} , V_{o_3} and V_{o_4} .

Taking into account the ideal single diode model, the current of the k th module $I_{pv,k}$ of a string is given by (3-1). In a PV string formed by N modules, the bypass diode of module k turns on when the inequality defined in (3-2) holds for $j, k \in [1, N]$. In this way, such a consideration requires to organize the modules of the string according to their short-circuit current in descending order.

$$I_{pv,k} = I_{sc,k} - I_{sat,k} \cdot \exp(B_k \cdot V_{pv,k}) \quad (3-1)$$

$$I_{pv,j} > I_{pv,k} \quad (3-2)$$

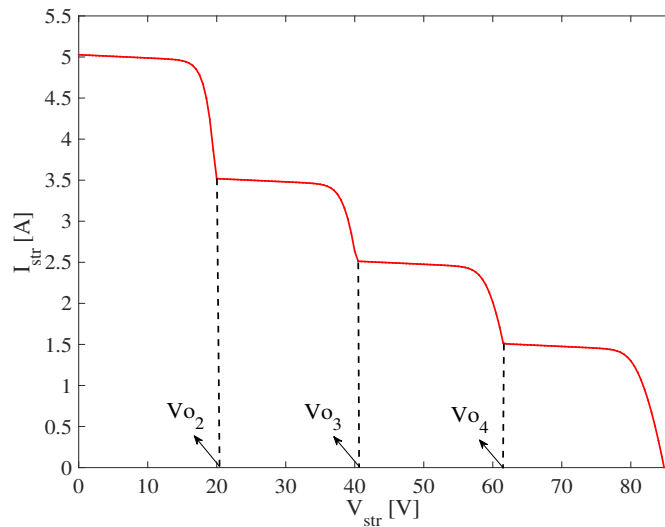


Figure 3-1.: Inflections voltages of a string formed by 4 modules with 3 of them operating under mismatching conditions.

In [82], the behavior of the bypass diode was assumed as an ideal switch. Therefore, if the bypass diode of the k th module becomes active, the voltage of the k th module ($V_{pv,k}$) is zero. Under that assumption, and considering (3-1) and (3-2), the conditions for obtaining the value of the maximum voltage in which the bypass diode will remain active are given in (3-3) to (3-5).

$$I_{pv,j}=I_{pv,k} \wedge V_{pv,j}=V_{o_{j,k}} \wedge V_{pv,k}=0 \quad (3-3)$$

$$I_{sc,k}-I_{sat,k}k=I_{sc,j}-I_{sat,j} \cdot \exp(B_j \cdot V_{o_{j,k}}) \quad (3-4)$$

$$V_{o_{j,k}}=\frac{1}{B_j} \cdot \ln\left(\frac{I_{sc,j}-I_{sc,k}+I_{sat,k}}{I_{sat,j}}\right) \quad (3-5)$$

However, $V_{o_{j,k}}$ correlates the behavior of the j th and the k th modules, then it is necessary to take into account the contributions of the other modules in the string. In this way, equation (3-6) defines the inflection voltage for the k th module in a string of N modules. Finally, with the definition of the inflections voltages in [82], it is considered that for obtaining the I-V curve of a string it not necessary to solve a system of $N+1$ equations (considering the blocking diode), instead the size of the system to be solve will change depending on the array voltage (V_{array}) to be evaluated. The module or modules for which the condition given in (3-7) is fulfilled are not considered for the equations system, this because such modules are in short-circuit and their voltages are zero.

$$V_{o_k}=\sum_{m=1}^{k-1} V_{o_{m,k}}, \quad k \in [2, N] \quad (3-6)$$

$$V_{array} < V_{o_k} \quad (3-7)$$

3.2.1. PV string modeling

From the circuit shown in Fig. 3-2, the relationship between the voltage and current in the module is given by (3-8), where I_{sc} is the short circuit current, I_{sat} is the saturation current of the diode D and B is the thermal voltage defined as $B = n \cdot k \cdot T/q$, series and parallel resistances are neglected in this case. The same nomenclature applies for the rest of equations in this approach. The ideality factor of the diode n can be obtained from the diode datasheet, while the Boltzmann constant k is $1,3806503 \times 10^{-23} J/K$, the electron charge q is $1,60217646 \times 10^{-19} C$ and the module temperature in Kelvin degrees T depends on the operation conditions. The bypass diode is represented by two parameters: an activation voltage V_{da} , represented by a voltage source, and an activation resistance R_{da} defining the slope of the voltage - current characteristic of the diode. Both parameters can be extracted from the diode datasheet or estimated using a computational tool [14], [9], [25].

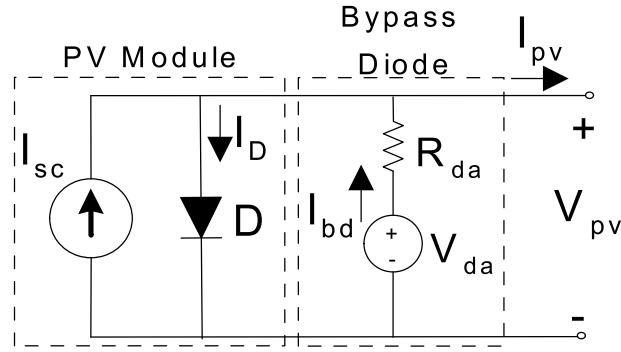


Figure 3-2.: Circuital approach for the PV module.

$$I_{pv} = I_{sc} - I_{sat} \cdot \exp(B \cdot V_{pv}) \tag{3-8}$$

Such an explicit expression does not require the use of mathematical tools like the Lambert-W function, which simplifies the computation of the voltages and currents for a given operating condition. Now, considering the array shown in Fig. 3-3, the voltage of a string formed by N modules is defined as the sum of the voltages of each module and the blocking diode voltage as given in (3-9). Moreover, since the modules and the blocking diode are connected in series, the current is the same for all the elements in the string as it is defined in (3-10). The current flowing through blocking diode I_d can be modeled using the classic Schottky equation given in (3-11) [83].

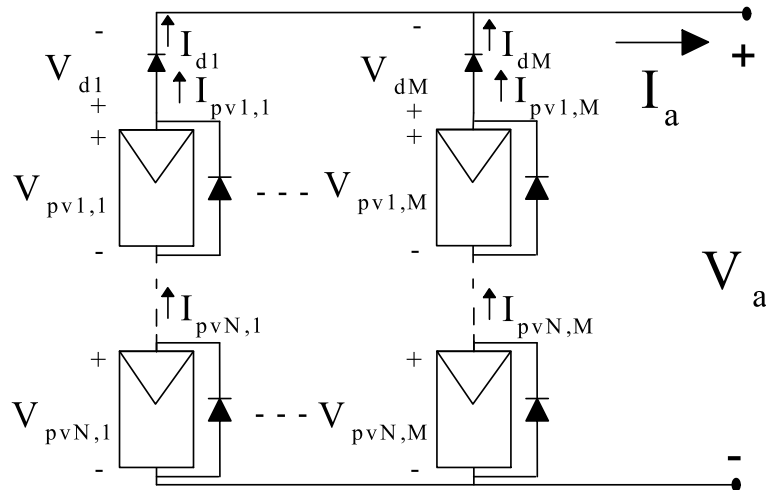


Figure 3-3.: $N \times M$ SP array including blocking diodes

$$V_{str} = \sum_{k=1}^N V_{pv,k} + V_{diode} \quad (3-9)$$

$$I_{pv,1} = I_{pv,k} = I_d, \forall k \in [2, N] \quad (3-10)$$

$$I_d = I_{sat,d} \cdot (\exp(B_d \cdot V_d) - 1) \quad (3-11)$$

In order to analyze the operation in the second quadrant, the activation of the bypass diode of each module must be considered. In this way, equation (3-12) defines the conditions for the activation of the bypass diode associated to module k .

$$I_{str} = I_{pv,k} = I_{sc,k} - I_{sat,k} \cdot \exp(B_k \cdot V_{pv,k}) \quad (3-12)$$

Then, if I_{str} is higher than the short-circuit current of module k ($I_{sc,k}$), the voltage $V_{pv,k}$ of such a module is given by the negative voltage of its bypass diode as it is shown in Fig. 3-4, where V_{da} and V_{br} are the activation and the breakdown voltage, respectively and V_{op} is the voltage at which the module operates depending on the string current I_{str} . In that figure, the gray area represents the dissipated power of the module, in other words, the power losses caused by the mismatching condition.

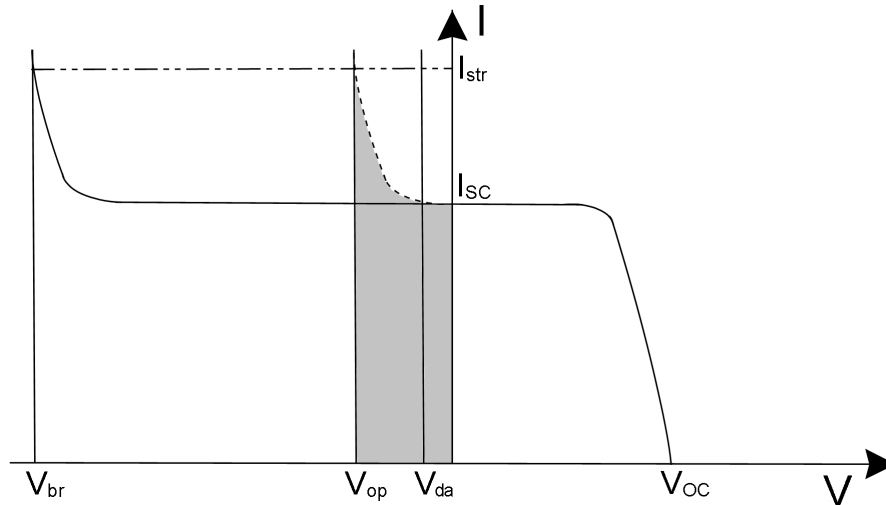


Figure 3-4.: Operation of PV module in the second quadrant due to bypass diode activation

Considering the inflection points concept given in [82], the inflection voltage, or the minimum string voltage at which the bypass diode becomes active, is rewritten as given in (3-14), which takes into account the non-ideal model of the bypass diode.

$$V_{0j,k} = \frac{1}{B_j} \cdot \ln \left(\frac{I_{sc,j} - I_{sc,k} + I_{sat,k} \cdot \exp(B_k \cdot V_{da})}{I_{sat,j}} \right) \quad (3-13)$$

$$V_{0k} = \sum_{m=1}^{k-1} V_{0m,k} \quad (3-14)$$

3.2.2. PV array modeling

Considering equations (3-8) to (3-11), the equations system formed by $N + 1$ non-linear equations is proposed in (3-15), for modeling a SP array with N rows and M strings, in which the voltages of the modules are the unknown variables.

$$\left\{ \begin{array}{l} F_1(V) : \sum_{k=1}^{N+1} V_k - V_{str} = 0 \\ F_2(V) : -I_{sat,1} \cdot \exp(B_1 \cdot V_{pv,1}) + I_{sat,2} \cdot \exp(B_2 \cdot V_{pv,2}) + I_{sc,1} - I_{sc,2} = 0 \\ \vdots \\ F_{N+1}(V) : -I_{sat,1} \cdot \exp(B_1 \cdot V_{pv,1}) + I_{sat,N+1} \cdot \exp(B_{N+1} \cdot V_{pv,N+1}) + I_{sc,1} - I_{sc,N+1} = 0 \end{array} \right. \quad (3-15)$$

This system can be solved by means of the Newton-Raphson method. For that purpose, the Jacobian matrix must be defined as a $(N + 1) \times (N + 1)$ matrix with the structure shown in (3-16), in which the elements in the first column are given by (3-17), the elements in the diagonal are given by (3-18) and the elements in the first row are equal to 1. The remaining elements are equal to zero.

$$J = \begin{bmatrix} \frac{\partial F_1}{\partial V_{pv,1}} & \cdots & 1 & \cdots & 1 \\ \vdots & \ddots & \vdots & \vdots & \vdots \\ \frac{\partial F_k}{\partial V_{pv,1}} & \cdots & \frac{\partial F_k}{\partial V_{pv,k}} & \cdots & 0 \\ \vdots & \vdots & \vdots & \ddots & \vdots \\ \frac{\partial F_{N+1}}{\partial V_{pv,1}} & & 0 & & \frac{\partial F_{N+1}}{\partial V_{pv,N+1}} \end{bmatrix} \quad (3-16)$$

$$\frac{\partial F_k}{\partial V_{pv,1}} = -I_{sat,1} \cdot B_1 \cdot \exp(B_1 \cdot V_{pv,1}) \quad (3-17)$$

$$\frac{\partial F_k}{\partial V_{pv,k}} = I_{sat,k} \cdot B_k \cdot \exp(B_k \cdot V_{pv,k}) - \frac{1}{R_{da,k}} \quad (3-18)$$

Where, $R_{da,k}$ is the activation resistance of the bypass diode in the k th module. In addition, considering the information given by the inflection points, if the bypass diode of k th module

is inactive its current is given by (3-12), otherwise its current is calculated from (3-19), where $V_{da,k}$ is the activation voltage of the bypass diode in the k th module.

$$I_{pv,k} = I_{sc,k} - I_{sat,k} \cdot \exp(B_k \cdot V_{pv,k}) + \frac{1}{R_{da,k}} (V_{pv,k} - V_{da,k}) \quad (3-19)$$

The approach described in this section (named SQ approach) was implemented in Matlab and its performance was compared with the technique reported in [82] (named Fast approach). The validation was made by using the PV array shown in Fig. 3-5; the irradiance values for each module in the array in W/m^2 are given in (3-20). The parameters of the PV system are presented in Table 3-1.

$$S = \begin{bmatrix} 980 & 980 & 980 \\ 362,6 & 392 & 392 \\ 98 & 196 & 196 \end{bmatrix} \quad (3-20)$$

Fig. 3-6 shows the P-V curve of the array provided by both the Fast and the SQ approaches, where it is evident the overestimation of the Fast approach. In this particular case the overestimation in the power of the MPP was 5.72 W which can be negligible, but for long period analysis the overestimation can introduce errors in the energy projection as it is illustrated further; the error introduced by the Fast approach is due to the ideal representation of the bypass diode which does not consider the operation in the second quadrant. Fig. ?? (a,b and c) shows the behavior of the voltage of modules $m1$, $m4$ and $m7$ (first string of the evaluated array) with respect to the array current I_a ; module $m1$ is not exposed to shading condition while modules $m4$ and $m7$ are exposed to different levels of shading. Therefore, for certain values of the array current they operate in the second quadrant due to the activation of their bypass diodes as it is shown in the zoom area of Fig. ?? and Fig. ??.

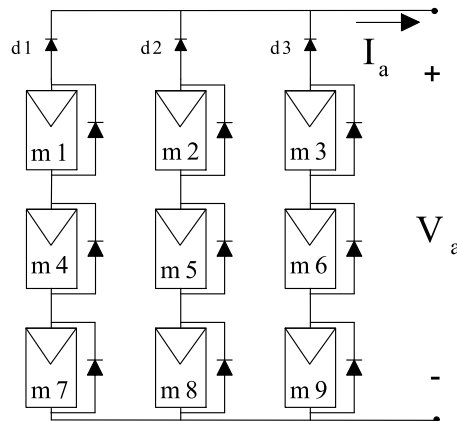


Figure 3-5.: PV array used for validating of the SQ approach

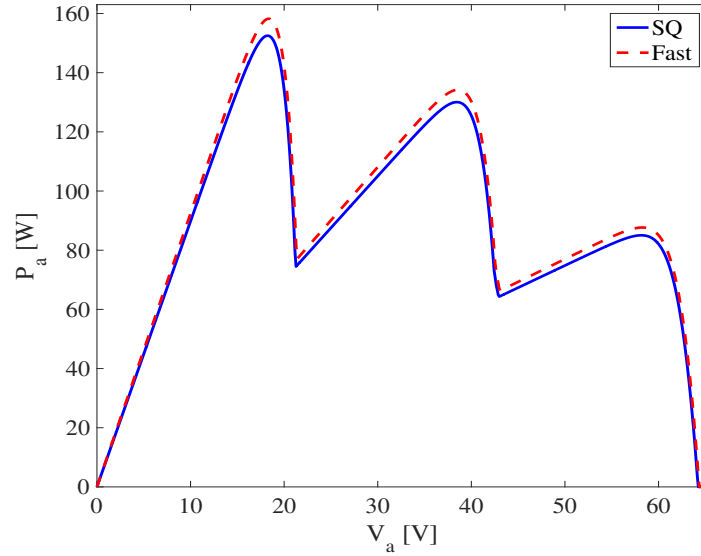


Figure 3-6.: P-V curves of Fast and SQ approaches

Table 3-1.: Parameters for simulation

| Parameter | Value |
|--|--------------------------|
| Short-circuit current I_{sc} | 5.13 A |
| Open circuit voltage V_{oc} | 21.78 V |
| Saturation current A | 2.28×10^{-7} A |
| Thermal voltage B | 0.7782 V ⁻¹ |
| Blocking diode saturation current A_d | 1×10^{-6} A |
| Blocking diode thermal voltage B_d | 0.015 V ⁻¹ |
| Bypass diode activation voltage V_{da} | 0.2166 V |
| Resistance of bypass diode R_{da} | 0.003 Ω |

Fig. **3-7** shows an irradiance profile at the center of Colombia, for 7 days, with samples taken hour by hour, while Fig. **3-8** shows the prediction in power provided by the two approaches for the same 3×3 array of Fig. **3-5** operating under the shading profile Sh given by (3-21).

$$Sh = \begin{bmatrix} 100\% & 100\% & 100\% \\ 37\% & 40\% & 40\% \\ 10\% & 20\% & 20\% \end{bmatrix} \quad (3-21)$$

The computing time required by the SQ approach to evaluate each irradiance value was 30 s while the time required by the Fast approach was 1.7 s. However, in the evaluated period the power estimation provided by the SQ approach is 3990.4 W while the power estimation

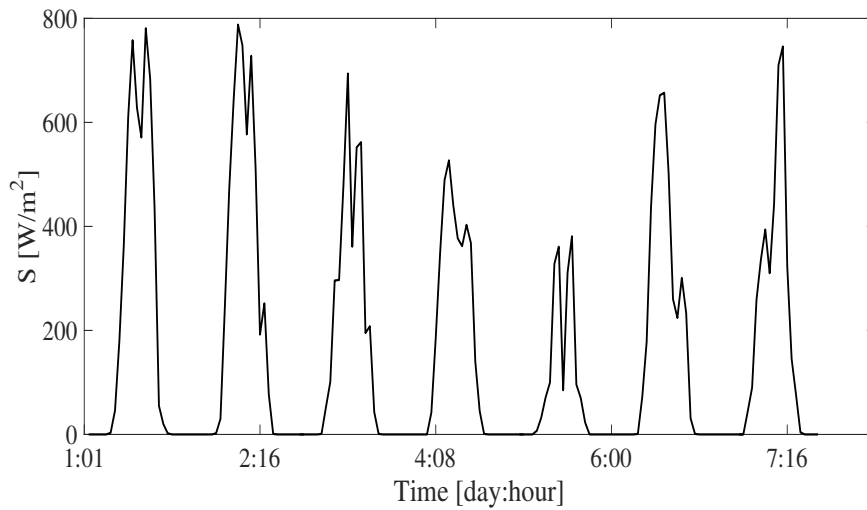


Figure 3-7.: Irradiance profile evaluated

provided by the Fast approach is 4180.3 W which means a difference of almost 200 W. Taking into account that the evaluated array evaluated is a small array, it can be expected that the overestimation will be considerable for larger PV fields.

The use of modeling procedures which consider the operation in the second quadrant allows the analysis of other phenomena associated with the issue of partial shading. Such issues may include hot spots and aging; this subject has been addressed from different methods, among which I-V curves analysis based methods have emerged as complementary tools for methods based on infrared thermography or similar procedures which requires specialized equipment [15]. The analysis of the I-V curves for detection of hot spots requires to consider the modules operation in the second quadrant since it is necessary to take into account the power losses [30], [105] and behavior of bypass diode. The analysis of configurations for connection of bypass diodes is another issue in which the operation on the second quadrant is required; some works devoted to this matter are based on the Bishop model [98] or the one diode model [38] and the exponential form of the bypass diode; the high complexity of the mathematical procedure for establishing the mathematical relations between the voltages and currents implies high computational effort. On the other hand, if the analysis is performed at cell level, the complexity of the procedure increases even more; at this point it is important to evaluate and consider the relationship between accuracy and computational effort.

The modeling techniques based on the Bishop or the one diode model including with the exponential model of the bypass diode provide suitable levels of accuracy. However, as it was pointed out in Chapter 2, the procedure for calculating the model parameters is complex (one diode model) or not enough clear or accurate (Bishop model). The approach introduced

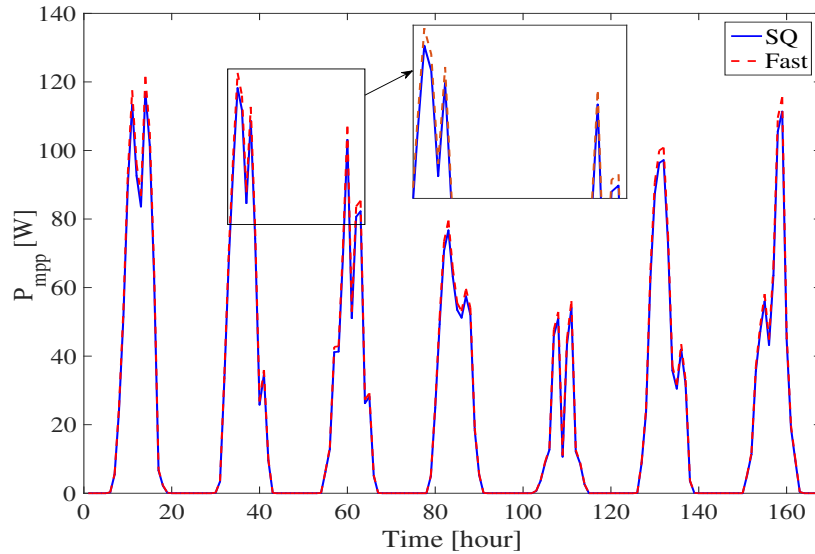


Figure 3-8.: Energy prediction of both Fast and SQ approaches

in this section allows to reproduce the I-V and P-V curves of a PV array operating under mismatching conditions. In addition, it offers a different and simple option for analyzing the operation of PV modules in the second quadrant.

3.3. Power estimation approaches

Analyzing the energy production of a PV system must consider the effect of partial shading due to the significant power losses it introduces [9]. In some works the estimation of the power is addressed by averaging the shade impact on the effective irradiance that reaches the PV modules, providing simplified equations to estimate the PV power production [35]. However, such an approach introduces significant errors since the power losses are not proportional to the shade size, for instance, small shades could produce large power losses [98].

As it has been shown in the previous chapter, the PV circuital representation defines the complexity of the analysis of a PV array. Complex cell or module models provide high accuracy but the required computational effort requires long simulation times, which makes impossible to estimate monthly or yearly performances to provide a long-term analysis. On the other hand, the use of simplified models significantly reduces the simulation times, as the technique presented in [82] does in the estimation of long-term performances, but it introduces errors that could lead to wrong designs or non-profitable decisions. Such conflictive objectives, i.e. high accuracy and fast processing, are addressed in this section through different options. In that way, three approaches for estimating the PV power in SP arrays are presented; in such approaches a combination of different models for the PV module

and the bypass diode are introduced. In this way, approaches 1 and 2 are based on the complete single diode model but the bypass diode is represented through its linear model and its exponential model, respectively, which enables to consider the operation of the shaded modules in the second quadrant. On the other hand, approach 3 is based on the ideal single diode model and the ideal bypass diode model but it considers a dynamic shadowing model instead of the common average model.

3.3.1. Approach 1: single diode model and linear bypass diode model

The approach presented in this section is a tradeoff between the technique presented in [83] (Lambert-W approach) and in [82] (Fast approach). The first is based on the complete single diode model and the Schottky model for the bypass diode, while the latter is based on the ideal single diode model (ISD) and the ideal switch model for representing the PV modules and the bypass diode, respectively; in addition, the inflection points concept is introduced. Both procedures provide different compromises between accuracy and speed calculation: Lambert-W approach provides high accuracy, but its long simulation times makes impossible to evaluate monthly or yearly profiles. In contrast, the Fast approach provides short simulation times to evaluate long power profiles, but it introduces errors due to the simplification made for modeling the modules and the bypass diode.

The proposed solution, uses the single diode model for representing the PV modules, while the bypass diodes are modeling by a modified switch. The equivalent circuit of the proposed solution is shown in Fig. 3-9. In this way, the behavior of the module is given by (3-22) to (3-25), where I_{sat} and V_t are the saturation current and the thermal voltage of the diode D_j . The parameters of the circuit can be calculated by using procedures as the reported in [27] or [111]. In addition, in this approach a blocking diode (D_{bk}) connected in series with each string is considered.

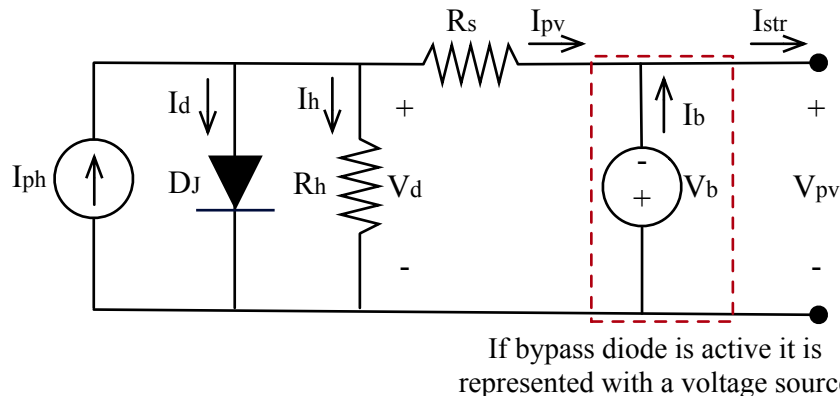


Figure 3-9.: Single diode model with linear bypass diode model

$$I_d = I_{sat} \cdot \left(\exp\left(\frac{V_d}{V_t}\right) - 1 \right) \quad (3-22)$$

$$I_h = \frac{V_d}{R_h} \quad (3-23)$$

$$I_{pv} = I_{ph} - I_d - I_h \quad (3-24)$$

$$V_{pv} = V_d - I_{pv} \cdot R_s \quad (3-25)$$

Fig. ?? shows the comparison between the three module models. In Fig. ??, the $I - V$ curves show that the three models accurately describe the short-circuit current (I_{sc}), open-circuit voltage (V_{oc}) and maximum power point (MPP). Such a figure also put in evidence the high accuracy provided by the proposed approach, in comparison with the Fast approach, for the reproduction of the PV module behavior as power source (first quadrant: positive current and voltage).

Fig. ?? presents the approaches behavior at the second quadrant (positive current and negative voltage), in which the PV module operates as a load. Such results show the improvement provided by the proposed model over the Fast approach: since the diode voltage is negative, it forces the module to dissipate power. This feature is introduced by assigning a voltage V_b when the diode becomes active. Moreover, taking into account that the string current imposes the module current, the diode current will be always lower than the maximum I_{ph} value. In the simulation presented in Fig. ?? $I_{ph} = 5.13 \text{ A}$, therefore the difference between the proposed and Lambert-W approach is negligible.

The modules in which the bypass diode becomes active will operate in the second quadrant (as a load, $P_{pv} < 0$) since $V_{pv} < 0$. Such a condition is considered by both the Lambert-W and the proposed approaches; instead, the Fast approach considers the PV module inactive ($P_{pv} = 0$) for $V_{pv} < 0$ as depicted at the right of Fig. ?. In general, in this approach the following consideration is adopted: the bypass diode is closed when its voltage is higher than a real diode threshold voltage V_b , otherwise the diode is open. Fig. **3-10** shows the current - voltage (I-V) characteristics of the bypass diode models used in the Lambert-W approach, the Fast approach and the proposed approach. The improvement over the ideal switch approach is evident ($V_b = 0.2 \text{ V}$).

For evaluating the power in an entire $N \times M$ array, each one of the strings must be analyzed [83], each of them modeled by the $N + 1$ non-linear equations given in (3-26) and (3-27).

$$I_{str} = I_{pv,k} + I_{b,k} = I_{pv,k+1} + I_{b,k+1} \quad (3-26)$$

$$V_{str} = \sum_{k=1}^N V_{pv,k} + V_{t,bk} \cdot \ln\left(\frac{I_{str}}{I_{sat,bk}} + 1\right) \quad (3-27)$$

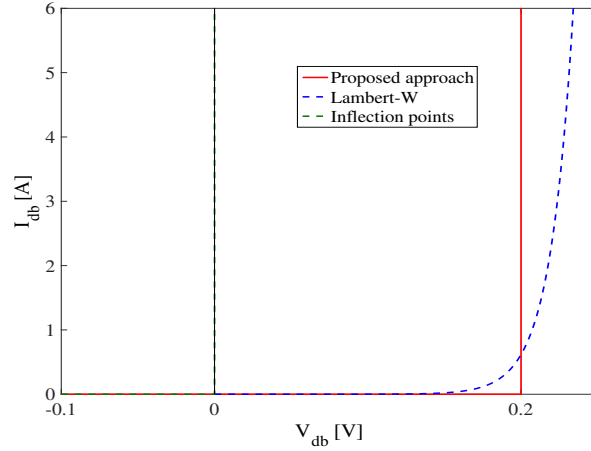


Figure 3-10.: Comparison of the bypass diodes models.

Where, $I_{b,k}$ is the current of the current of the bypass diode associated to module k and $I_{sat,bk}$ is the saturation current of the blocking diode associated to module k .

The literature review presented in Chapter 2 showed that the main drawback of the Lambert-W approach is the high computational effort required to find the MPP for a given irradiance condition. This because it is required to calculate the string current for the evaluated string voltage by solving $N + 1$ non-linear equations which in turns requires the use of the Lambert-W function N times. On the other hand, the Fast approach does not require the Lambert-W function; moreover, the number of equations to solve changes inversely with the number of bypass diodes active which reduces significantly the simulation time, but calculation errors are introduced due to the simplifications adopted. In any case, both techniques still require to solve a non-linear equations system, which implies the use of algorithms such as the Newton-Raphson or trust-region methods.

The proposed procedure is divided in three parts as depicted in Fig. **3-11**: the first process is used to obtain the $I - V$ curve of each PV module independently, it using (3-22) to (3-25), which are explicitly evaluated for different values of V_d without introducing simplification errors and avoiding the use of the Lambert-W function. In this part of the process, the modules voltages are compared with the threshold voltage V_b to simulate the bypass diode operation. The second procedure is used to obtain the string $I - V$ curve by adding the voltages of the modules at the evaluated string current. Since all the modules are in series their current is the same, hence the modules voltages are explicitly extracted from the modules $I - V$ curves generated by the first procedure. Finally, the third process calculates the power and energy. This procedure must be executed for each string in the SP array, then the global power is calculated by adding the power of each string. The proposed approach does not require to solve a non-linear equation system, hence it provides high accuracy and

short simulation times.

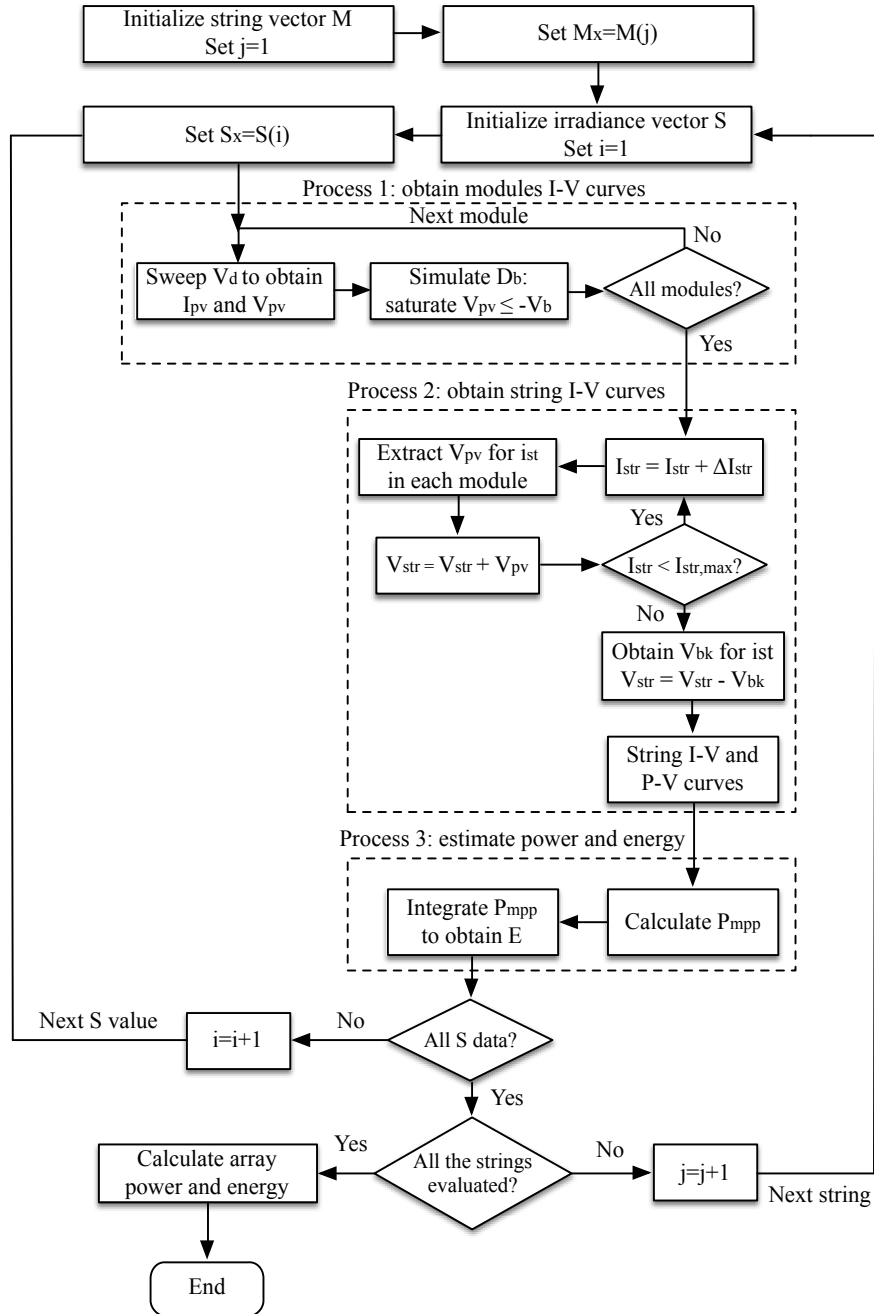


Figure 3-11.: Proposed approach to estimate the string power and energy production.

The performance of the proposed approach is evaluated in contrast with both the Lambert-W and the Fast approaches using the ERDM85 PV panel to perform the simulations. Fig. 3-12 shows the simulation of a string with $N = 5$, an irradiance of $1000W/m^2$ and the presence of several shade sources that generate the following shading profile: the module PV1 receives

the 94 % of the irradiance, while the modules $PV2$ to $PV5$ receive 60 %, 40 %, 20 % and 10 %, respectively. The figure illustrates the accurate simulation performed by the proposed approach, which results are indistinguishable from the Lambert-W simulation, while the Fast approach introduces significant errors.

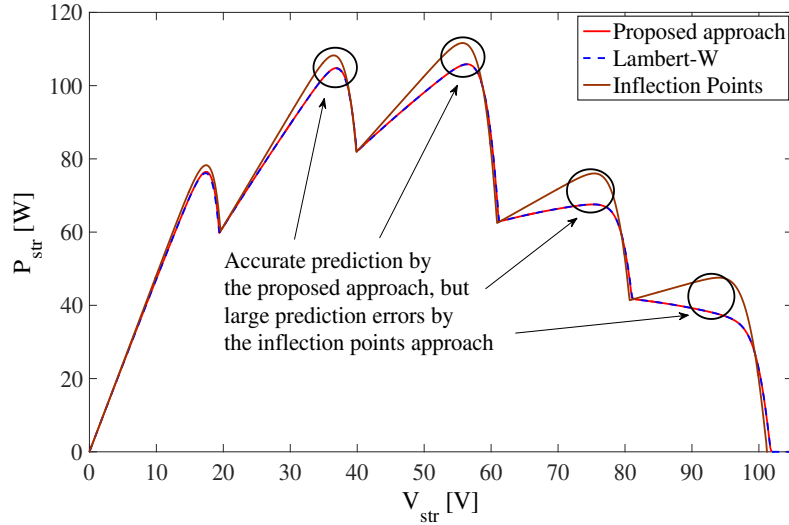


Figure 3-12.: Simulation of string with 5 modules

To provide a more general comparison, Fig. ?? presents the simulation times T_p and normalized errors $NSSE$ [96] for PV string sizes between 2 and 10 modules.

All the solutions were implemented in Matlab scripts where the Lambert-W function available in Matlab was adopted. The results put into evidence the strong reduction of the simulation time provided by the proposed approach: in Fig. ?? the T_p of the Lambert-W approach is divided by 100 to allow its plotting in the same scale of both, the Fast and the proposed approaches. For example, for $N = 6$ the proposed approach requires 0.034 s, while the Fast and Lambert-W solutions require 1.40 s and 191.95 s, respectively. Similarly, the error generated by the proposed approach, with respect to the more accurate Lambert-W, is much smaller than the error introduced by the Fast approach. In any case, the error generated by the proposed approach is negligible: for example, for $N = 6$ the proposed approach introduces an error of 0.12 %, while the Fast solution introduces an error of 2.88 %. In addition, the results show that for larger N values the difference between the simulation times increases, but the errors are almost constant. Hence, the proposed approach provides accurate results in very short times, which allows to estimate the power production of large PV strings in long periods. Finally, to illustrate the use of the proposed solution, a realistic application is considered: a commercial PV inverter (SolarEdge SE2200) that requires 350V to operate, 20 BP585 PV modules must be used to form the string. Considering several shade sources in the available area that produces the profile described in Table 3-2, it is required

to estimate the yearly energy production to evaluate the economic convenience of the PV installation.

Table 3-2.: Shading profile for the application example

| | | | | | | | | | | |
|------------------|------|------|------|------|------|------|------|------|------|------|
| PV1-PV10 | 94 % | 86 % | 66 % | 61 % | 44 % | 42 % | 41 % | 40 % | 39 % | 38 % |
| PV11-PV20 | 37 % | 33 % | 31 % | 28 % | 27 % | 26 % | 20 % | 10 % | 5 % | 4 % |

The simulation of a single irradiance condition takes 1380 s (23 minutes) with the Lambert-W approach, 6.5 s with the Fast approach, while the proposed approach requires 0.0061 s with an error of 0.1 %. To simulate a day (8.5 hours with data each 30 s), the Lambert-W approach will require 391 hours (16.3 days), the Fast approach will require 1.84 hours, while the proposed approach requires 6.24 s. Finally, to simulate a year (365 days), the Lambert-W approach will require 16.4 years, the Fast approach will require 28 days, while the proposed approach requires 37 minutes. Therefore, the yearly simulation of the string with $N = 20$ is not practical with both the Lambert-W or Fast approaches. Instead, the proposed approach makes possible to perform the evaluation: Fig. ?? shows the irradiance profile of a day in southern Italy, while Fig. ?? shows the power production estimated through the calculation of the global *MPP* for each irradiance value; such a simulation was performed in 6.24 s and the energy produced by the system was 0.77 kW/h.

Similarly, Fig. 3-13 shows the yearly energy production, where the irradiance profile in Fig. ?? changes depending on the month. Such a simulation was performed in 37 minutes and the total energy estimated was 371 kW/h. Finally, with the information provided in Fig. 3-13 it is possible to calculate the return-of-investment time (in years) using the costs of the PV system and the cost of electricity in the geographical region under evaluation.

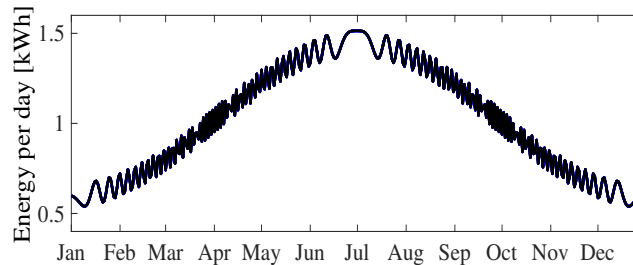


Figure 3-13.: Simulation of a year for a string with $N = 20$ performed in 37 min

3.3.2. Approach 2: single diode model and exponential bypass diode model

The second approach introduced in this section is an improvement to the approach 1 because the bypass diode is now modeled in its exponential form, the equivalent circuit is shown in

Fig. 3-14. The current and voltage values of the modules of the PV array are calculated without using the Lambert-W function as it will be explain further. In addition, this solution introduces a procedure to obtain the power at the global maximum power point *GMPP* through the calculation os the power in the vicinity of the maximum power points; this avoiding the need to calculate the whole P-V curve which results in a significant reduction of execution time.

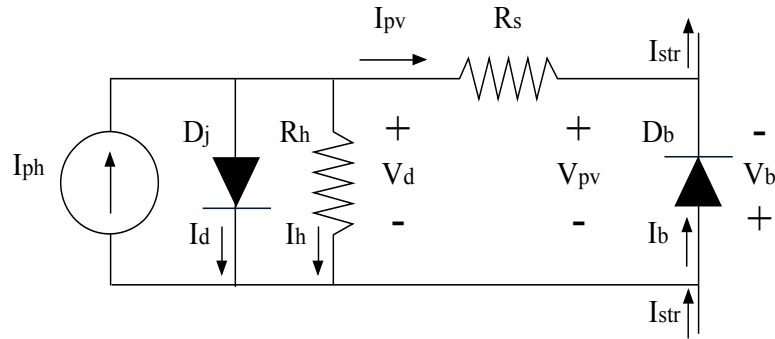


Figure 3-14.: Equivalent circuit used in approach 2

The module behavior is represented through (3-22) to (3-25), while (3-28) represents the current of the bypass diode, where $I_{sat,b}$ and $V_{t,b}$ are the saturation current and the thermal voltage of the bypass diode, respectively, and $V_b = -V_{pv}$. In this way, the current flowing through the string is now given by (3-29).

$$I_b = I_{sat,b} \cdot \left(\exp\left(\frac{V_b}{V_{t,b}}\right) - 1 \right) \quad (3-28)$$

$$I_{str} = I_{pv} + I_b \quad (3-29)$$

The classical procedure to calculate the power in each string of the array is based on obtaining the relations between the current and the voltage of each module in the string by applying the Kirchhoff laws, i.e. the current flowing through the modules ($I_{pv,k}$) and the blocking diode (I_{bk}) is equal to the string current I_{str} while the string voltage V_{str} is equal to the sum of the modules and blocking diode voltages ($V_{pv,j}$ and V_{bk}). In this way, such relations form the non-linear system of equations F given in (3-30), with $x = [V_{pv,1}, V_{pv,2}, \dots, V_{pv,k}, \dots, V_{pv,N}, V_{bk}]$.

$$F(x) = \left\{ \begin{array}{c} I_{pv,1} = I_{pv,2} \\ I_{pv,2} = I_{pv,3} \\ \vdots \\ I_{pv,k} = I_{pv,k+1} \\ \vdots \\ I_{pv,N-1} = I_N \\ I_{pv,N} = I_{bk} \\ V_{pv,1} + V_{pv,2} + \dots + V_{pv,k} + \dots + V_{pv,N} + V_{bk} = V_{str} \end{array} \right\} \quad (3-30)$$

There are several proposed techniques which deal with the solution of (3-30), with two main approaches: using the exact system Jacobian shown in (3-31) [83], [76], or simplifying it through the use of linear or ideal models for the bypass diode to speed up the calculation [9], [82]. In both cases, numerical methods (e.g Newton Raphson or Trust-region) are required.

$$J = \left\{ \begin{array}{ccccc} \frac{\partial I_{pv,1}}{\partial V_{pv,1}} & \frac{\partial I_{pv,2}}{\partial V_{pv,2}} & \dots & 0 & 0 \\ \vdots & \vdots & \ddots & \vdots & \vdots \\ 0 & 0 & \dots & \frac{\partial I_{pv,N}}{\partial V_{pv,N}} & \frac{\partial I_{bk}}{\partial V_{bk}} \\ 1 & 1 & \dots & 1 & 1 \end{array} \right\} \quad (3-31)$$

The size of J is $(N + 1) \times (N + 1)$, e.g. for a string of 2 modules the Jacobian is a 3×3 matrix, for a string of 7 modules the Jacobian is a 8×8 matrix and so on. Therefore, the computational effort to solve the system, mainly by inverting J and multiplying and adding matrices, significantly increases with the number of modules in the string.

In order to avoid the use of the Lambert-W function to calculate each module voltage and current, the approach introduced in this section proposes to perform a sweep over V_d to calculate I_{pv} from (3-22), (3-23) and (3-24), which are explicit equations. Then, the module voltage V_{pv} is calculated from (3-25) and the string current is calculated from (3-26). With this procedure all the modules are characterized in terms of the string current, without any simplification to the single diode model, using two ordered vectors: PV voltage and string current vectors. However, since the modules are in series, they operate at the same string current I_{str} . Therefore, the electrical characteristics of the modules must be interpolated in order to calculate the voltage of the modules at the same current I_{str} . Moreover, the voltage drop introduced by the blocking diode must be also taken into account, which is an explicit equation as it is shown in (3-32) and (3-33). Finally, all the modules and blocking diode voltages are added to obtain the string voltage as is given in (3-27); which eventually enables to calculate the string power.

$$I_{bk} = I_{sat,bk} \cdot \left(\exp \left(\frac{V_{bk}}{V_{t,bk}} \right) - 1 \right) \quad (3-32)$$

$$V_{bk} = V_{t,bk} \cdot \left(\ln \left(\frac{I_{str}}{I_{sat,bk}} \right) + 1 \right) \quad (3-33)$$

The previous procedure has two main parts: first, the characterization of the modules by performing a sweep on each point of V_d ; such a process must be done one time for a given irradiance condition S independent of the string current to be tested; and second, the calculation of the string voltage, which depends on the string current. The flowchart in Fig. 3-15 summarizes the string voltage calculation procedure.

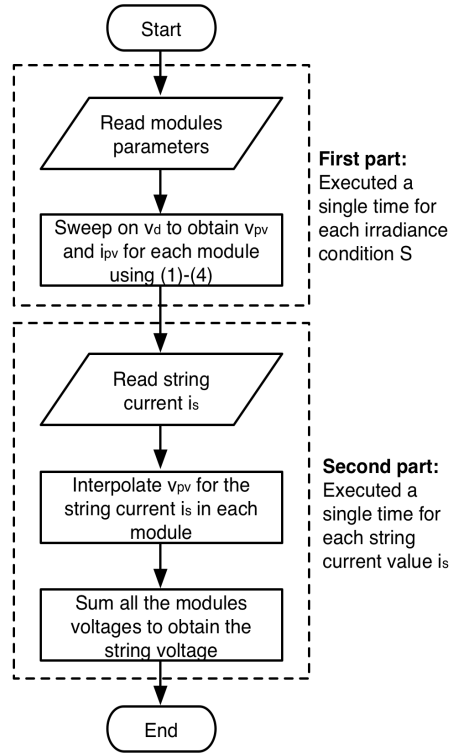


Figure 3-15.: Fast procedure to calculate the string voltage.

In order to analyze the accuracy of the proposed modeling procedure Fig. ?? presents the performance comparison between the proposed fast method and the classical method using the Lambert-W function, for calculating the complete $P - I$ curve for strings with different number of modules (2 to 20). The results presented in Fig. ?? show that the approach presented in this section requires processing times between 4 and 5 orders of magnitude shorter. For example, with 2 PV modules the classical method requires $2,47 \times 10^6$ % more time than the proposed approach, while with 20 modules the classical method requires $2,03 \times 10^7$ %

more time. In fact, for PV systems up to 20 modules, the proposed fast method never requires more than 1 *ms* to obtain the solution; instead, the classical method requires from 2,63 minutes (2 modules) up to 4,58 hours (20 modules).

To validate the procedure accuracy, three characteristics were evaluated: string voltages V_{str} and power P_{str} for each current value and the global maximum power P_{GMPP} . Since the PV voltage and power are zero at the short-circuit current, a suitable error formula must be used to avoid divisions by zero for this type of calculations.

The Range Average Absolute Error (RAAE) is adopted [95], which normalizes the difference between the signal vectors over the maximum variation range of the reference data to provide a fair comparison between different operation conditions. The RAAE expression is given in (3-34), where h is the number of data, while y_k^* and y are the predicted and reference signal vectors, respectively. Figure ?? presents the errors between the proposed approach and the classical Lambert-W approach for V_{str} , P_{str} and P_{GMPP} , in which the differences between the results of both methods are under 0,0001 %, i.e. a negligible difference.

$$RAAE [\%] = 100 \cdot \frac{\frac{1}{h} \sum_{k=1}^h |y_k^* - y_k|}{|MAX(y) - MIN(y)|} \quad (3-34)$$

Those results put in evidence the high accuracy and fast processing time provided by the proposed solution (fast solution). However, the calculation of the P_{MPP} is based on performing a complete sweep to the string power curve, which requires calculating a large number of unnecessary points far from the $GMPP$. Avoiding such unnecessary calculations will enable to improve, even more, the performance of the proposed algorithm in terms of speed and required memory. Therefore, a procedure to estimate the neighborhood of the $GMPP$ is proposed, such a method allows to reduce the number of P-I points to be calculated.

Since PV strings are formed by modules connected in series, the current in which the MPP of each module occurs is near to the string currents in which the $LMPPs$ (and $GMPP$) occur. This condition is due to the large change in the module power curve derivative present at the module MPP as reported in [76]: for voltages lower than the MPP voltage the slope is positive and for voltages higher than the MPP voltage the slope is negative having a higher amplitude. Therefore, the power slopes around the module MPP cause a change in the sign of the power slope of the string that produces a $LMPP$ (or $GMPP$). In order to illustrate such a situation, Fig. ?? shows the $V - I$ and $P - I$ curves of a ERDM85 PV panel operating under two different solar irradiance conditions, $943 W/m^2$ ($I_{ph} = 5 A$) and $566 W/m^2$ ($I_{ph} = 3 A$). Fig. ?? and Fig. ?? present the curves of each panel while Fig. ?? and Fig. ?? present the curves of a string formed by the two panels under the aforementioned conditions.

The MPP of each module in ?? produces a MPP , at almost the same current, in the string power curve depicted in ?. Using that information, it is possible to estimate the vicinity of

the string *LMPPs* (and *GMPP*) currents by estimating the currents at which the *MPPs* occur. Then, starting from those currents, a hill-climbing algorithm is used to reach the *LMPP* without evaluating the complete power curve, thus avoiding the evaluation of an unnecessary large number of points. The first approximation used to find the vicinity of the *MPP* current is to neglect the effect of the series resistance R_s and the bypass diode, i.e. $P_{pv} \approx P_d = I_{pv} \cdot V_{pv}$ as given in (3-35), which leads to an explicit relation. Then, at the maximum P_d value its derivative with respect to V_d is zero as given in (3-36). Hence, (3-36) must be solved for each panel to find the V_d values near the *MPP*. However, (3-36) is an implicit expression that cannot be solved explicitly even using the Lambert-W function. Therefore, some simplifications must be introduced into (3-36) to avoid the use of recursive solvers: first, since the *MPP* voltage of a commercial PV panel is commonly larger than 16 V, and the thermal voltages $V_{t,d}$ of commercial modules is around 1,1 V [32], the relation $V_d \gg V_{t,d}$ holds and $V_d/V_{t,d} + 1 \approx V_d/V_t$. Moreover, based on the Fractional-open-circuit MPPT analysis [34], it is expected that V_d at the *MPP* be near to 78% of the open circuit voltage of the PV module. Hence, the term $V_d/R_h \approx (0,78 \cdot V_{oc,STC})/R_h$ where $V_{oc,STC}$ represents the open circuit voltage in STC. With such approximations introduced in (3-36), the $V_{d,MPP}$ value near to the *MPP* is given in (3-37). Then, such $V_{d,MPP}$ values for each module are replaced into (3-22) to (3-25), (3-28) and (3-29) in order to obtain the vicinity of the *MPP* currents $I_{MPP,approx}$ for the string.

$$P_d = V_d \cdot \left(I_{ph} - I_{od} \cdot \left[\exp\left(\frac{V_d}{V_t}\right) - 1 \right] - \frac{V_d}{R_h} \right) \quad (3-35)$$

$$\frac{\partial P_d}{\partial V_d} = -I_{od} \cdot \exp\left(\frac{V_d}{V_t}\right) \cdot \left[\frac{V_d}{V_t} + 1 \right] - \frac{2 \cdot V_d}{R_h} + (I_{ph} + I_{od}) = 0 \quad (3-36)$$

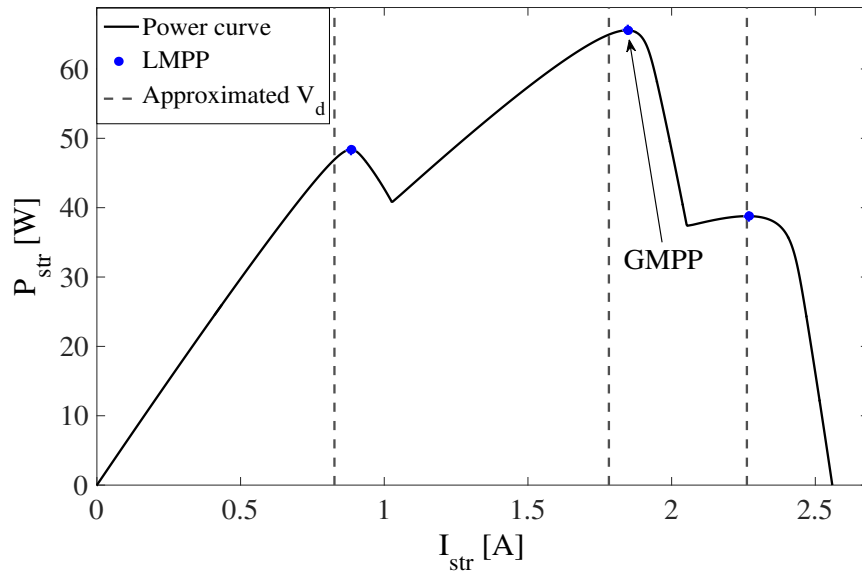
$$V_{d,MPP} \approx V_t \cdot W \left(\frac{1}{I_{od}} \cdot \left[\frac{-2 \cdot (0,78 \cdot V_{oc,STC})}{R_h} + I_{ph} + I_{od} \right] \right) \quad (3-37)$$

In order to validate the estimation of the *MPP* vicinity procedure, a simulation of a string formed by three modules was performed. The parameters of the modules are presented in Table 3-3, while Fig. 3-16 shows the power curve of the string. For the sake of simplicity, the three modules have the same parameters, which does not introduce any distortion to the calculation results. To force the mismatching condition, the three modules are considered under different irradiance levels (i.e. partial shading): 500 W/m^2 , 400 W/m^2 and 200 W/m^2 , hence three *LMPP* exist.

The simulation also shows the approximated *MPP* currents obtained with (3-37), which are very close to the exact *MPP* currents. With the previous results, the search of each *LMPP* can be started from the $V_{d,MPP}$ values, which strongly reduces the number of points of the power curve to be calculated in comparison with a full sweep of the curve as performed in traditional approaches.

Table 3-3.: Shading profile for the application example

| Parameter | Value |
|--|---------------------------|
| Saturation current I_{od} | $1,5415 \times 10^{-8} A$ |
| Thermal voltage V_t | $1.1088 V$ |
| Series resistance R_s | 0.0045Ω |
| Parallel resistance R_h | 109.495Ω |
| Open circuit voltage at STC $V_{oc,STC}$ | $21.78 V$ |
| Bypass diode saturation current I_{ob} | $1 \times 10^{-6} A$ |
| Bypass diode thermal voltage $V_{t,b}$ | $0.015 V$ |
| Blocking diode saturation current $I_{o,bk}$ | $1 \times 10^{-6} A$ |
| Blocking diode thermal voltage $V_{t,bk}$ | $0.15 V$ |

**Figure 3-16.:** Approximation of V_d values at the $LMPPs$.

Taking into account that the $V_{d,MPP}$ values are near to the $LMPP$ conditions, a simple hill-climbing algorithm is used to detect the $LMPP$ power: increase (or decrease) the string current while the power increases. Fig. 3-17 presents the flowchart of the proposed algorithm, which is divided in modular blocks to evaluate all the $LMPP$ possible conditions.

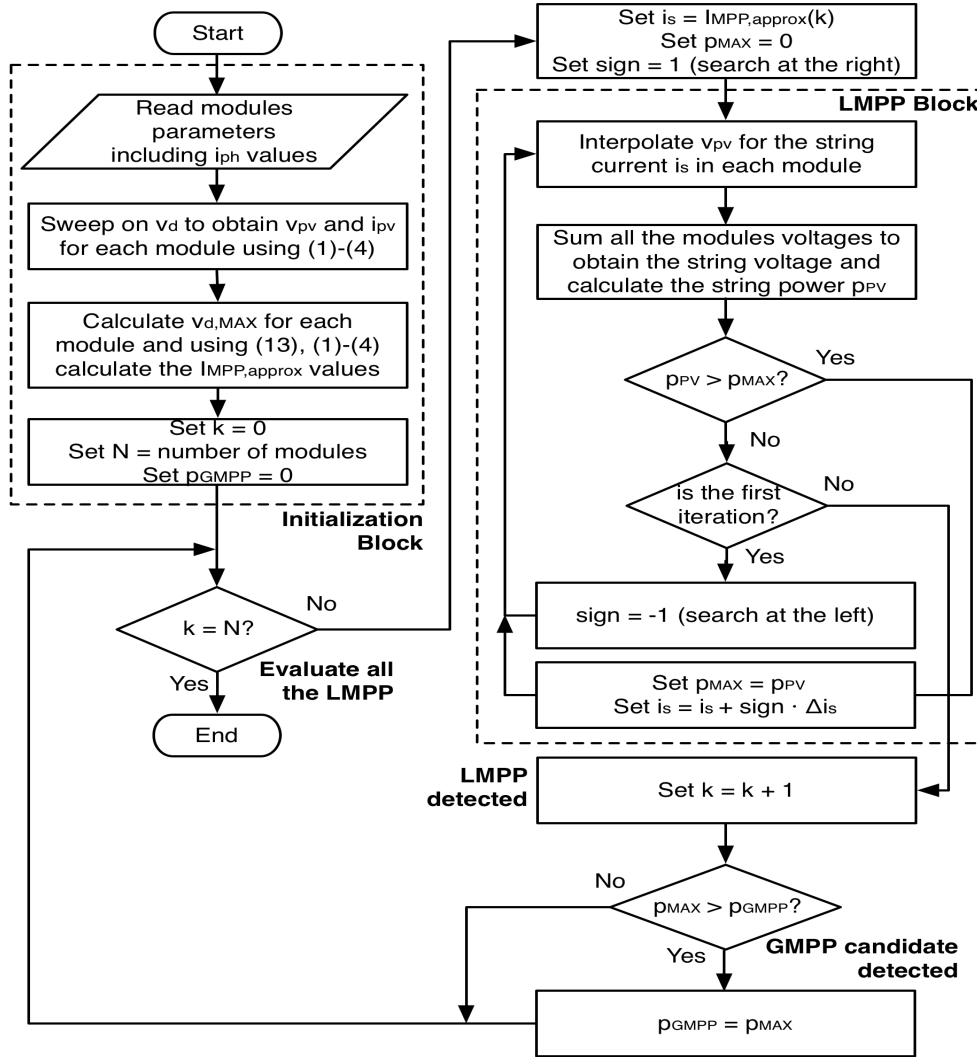


Figure 3-17.: Complete algorithm for calculating the maximum power.

The first block, named initialization block, characterizes the PV modules in the same way as the algorithm presented in Fig. 3-15, where a V_d sweep to each module is performed. The initialization block also calculates the *LMPP* vicinity in terms of $V_{d,MAX}$ values as described in the previous section. Finally, the control variables N (number of modules), k (*LMPP* in evaluation) and P_{GMPP} (maximum power) are initialized. After detecting the zones of the *LMPPs*, the algorithm evaluates each zone to calculate the corresponding *LMPP* with the *LMPP* block, in which the string current is calculated in the same way previously proposed in the flowchart of Fig. 3-15: the modules voltages are interpolated at the same string current value. This process starts at the approximated *LMPP* currents $I_{MPP,approx}$, increasing the string current while the power increases. However, in the case that the first iteration produces a power reduction, it means the *LMPP* is at a lower current, hence the current is decreased while the power increases. When the *LMPP* is detected it is contrasted with the other

$LMPPs$ to update the $GMPP$. This process is repeated until all the $LMPPs$ are evaluated.

To evaluate the performance of the proposed procedure, a PV string formed with four modules is simulated, where the parameters are the same ones described in Table 3-3, but the irradiances of the modules are $940 W/m^2$, $600 W/m^2$, $400 W/m^2$, and $200 W/m^2$. Fig. 3-18 illustrates the number of $P - I$ points calculated using the complete sweep and the proposed (reduced) approaches, where the reduced number of calculations can be appreciated. In fact, for the string made of four modules the sweep approach calculates 950 $P - I$ points, while the reduced approach only calculates 58 points.

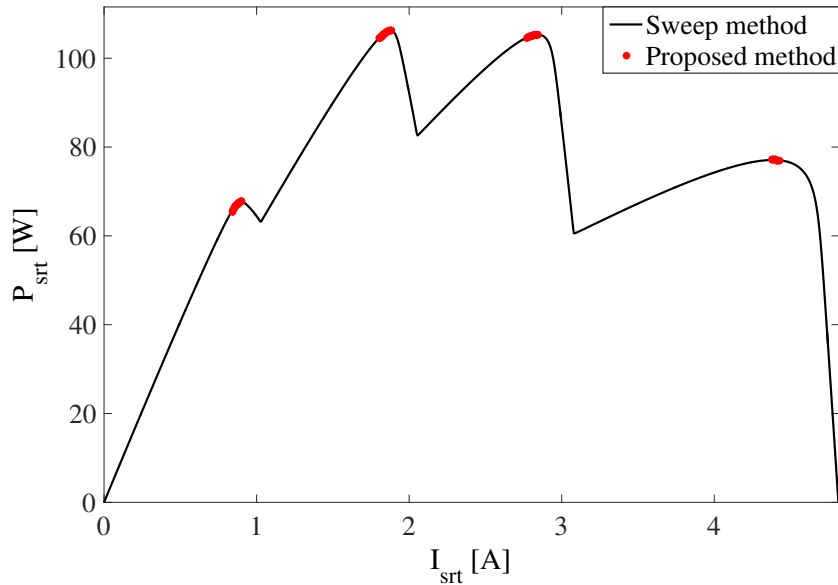


Figure 3-18.: Calculation of the $GMPP$ with a reduced number of $P-I$ points.

Since the number of $P - I$ points calculated by the reduced solution depends on the approximation of $I_{MPP,approx}$, multiple simulations were performed to provide an average relation between the number of points calculated by both approaches to reach the same result: the reduced approach calculates an average of 6,39% of the $P - I$ points calculated by the sweep solution. Therefore, the proposed $GMPP$ calculation algorithm, i.e. Fig. 3-17, improves significantly the performance in comparison with classical solutions based on implicit expressions for I_{pv} recursive solvers and sweeps for calculating the string power.

A comparison of the approaches 1 and 2 is presented. This, since the two approaches are based on the single diode circuit but use different bypass diode models. Fig. 3-19 shows the $P-V$ curve for the sample string example in Fig. 3-18. In this case the sweep in the approach 1 has 484 points while the approach 2 calculated 34 points which corresponds to 7% of the whole sweep. The execution time required for the approach 1 was 0.04 s and the execution

time of the approach 2 was 0.03 s. Finally, the MAPE in the *GMPP* of the approach 2 with respect to approach 1 is 0.5 %.

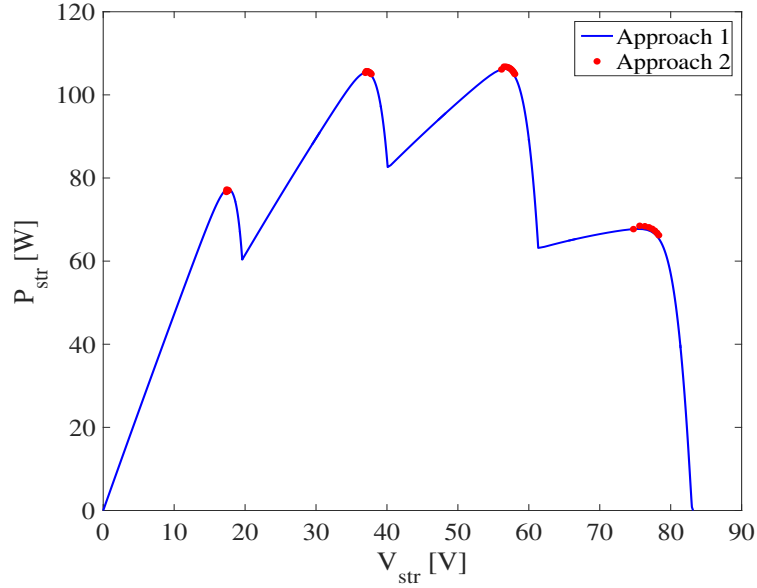


Figure 3-19.: Comparison between Approach 1 and Approach 2.

The results show that the effectiveness of the proposed process to identify the starting point of V_d to perform the sweep. Finally, it can be said that both solutions are suitable options to perform a fast calculation of the amount of power provided for a SP array.

3.3.3. Approach 3: ideal single diode model and ideal bypass diode model

The third approach considers the ideal single diode model and the ideal switch model for representing the PV modules and the bypass diodes, respectively. Fig. **3-20** illustrates the circuit of the model adopted in this approach, which is based on the inflections points technique [82] explained in section 3.2 but without considering the blocking diode for the sake of simplicity.

As it was pointed in the previous sections and chapters of this thesis, the partial shading conditions must be considered since its effect significantly affect the power production of a PV array. The aim of this approach is to introduce a procedure for including the partial shading conditions in a suitable manner; for this purpose, the dynamic behavior due to the sun translation is considered. Fig. **3-21** shows the shading generated by a building over a set of PV modules for different instants of the day.

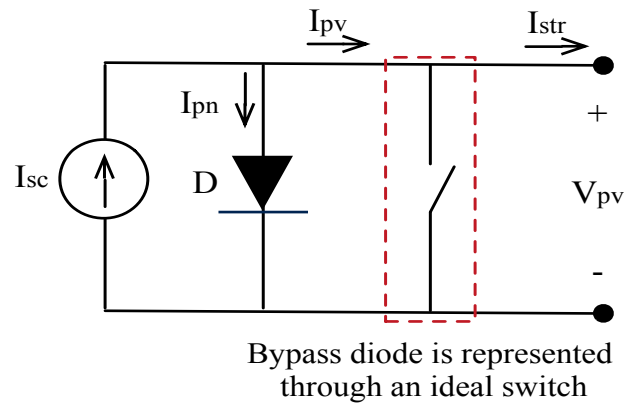


Figure 3-20.: PV array in series-parallel structure.

The dynamic behavior of the shading is commonly neglected and average profiles are assumed for analysis [67], [35]. Such an assumption can lead to errors in the prediction of the power production.



Figure 3-21.: PV array in series-parallel structure.

The classical prediction model used to estimate the power and energy profiles in a PV installation are depicted in the top of Fig. 3-22. In such a structure, the modules are assumed uniformly irradiated. Such a model is fed by an irradiance forecast to evaluate the PV installation in a specific place. Then, the *MPP* power P_{mpp} for each irradiance condition is registered to provide a power profile, which eventually is integrated to predict the energy production. For PV arrays without mismatching, the classical model is accurate enough since the P_{mpp} is correctly predicted. The black trace in the bottom of Fig. 3-23 corresponds to the power curve of a four-modules string predicted with the classical model. A shading across the modules occurs provokes the following irradiance for each module in the string: 1000 W/m^2 , 700 W/m^2 , 500 W/m^2 and 300 W/m^2 ; the classical model addresses such a condition by reducing the irradiance of the modules to an average irradiance value in the

array.

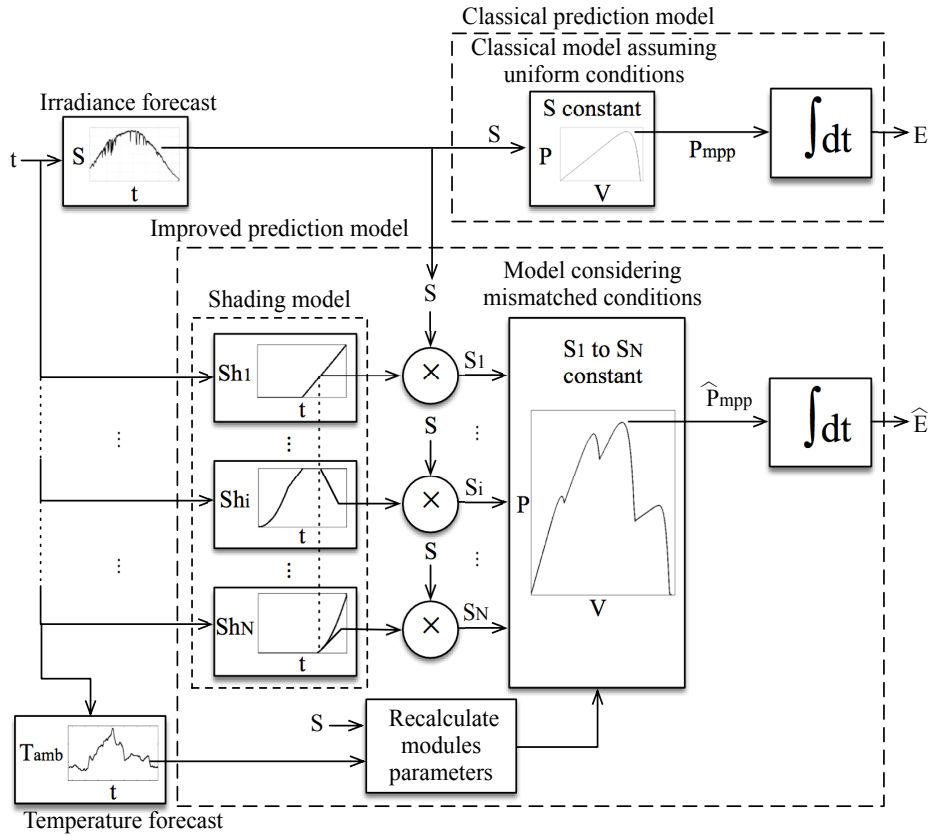


Figure 3-22.: Prediction structures to estimate PV power profile and energy.

Such an approach is illustrated by the red dotted trace in Fig. 3-23 which represents the new power curve predicted for an average irradiance condition generated by a shading profile. Finally, the blue trace in Fig. 3-23 presents a more precise power curve obtained taking into account the irradiance condition in each module. Such a trace put into evidence the large errors introduced in the power estimation by the classical model in both non-shading and average-shading approaches.

Under the light of the previous analyses, and taking into account that the sun translation changes the shading shape in a particular place along the day, the improved prediction model illustrated at the bottom of Fig. 3-22 is proposed. Such a structure considers dynamic shading conditions for each module, which affects the effective irradiance in each module. Then, the environmental irradiance value provided by the forecast is modified in agreement with the shading profile to generate the irradiance vector $[S_1, \dots, S_i, \dots, S_N]$ to feed the procedure based on the inflection points technique for computing the power of the array. A forecast of temperature was also considered to recalculate the PV module parameters for each irradiation

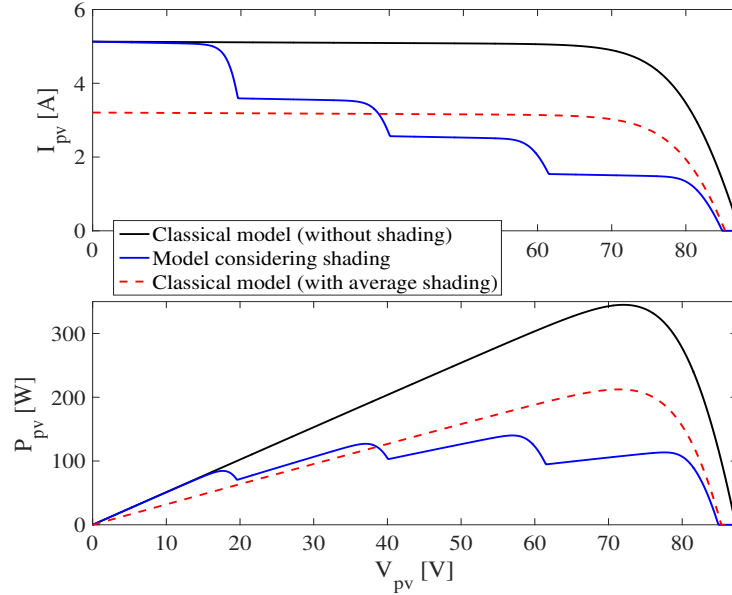


Figure 3-23.: Electrical characteristics predicted under shading conditions.

ce condition which also improve the accuracy of the prediction model. In this way, the MPP power for each irradiance condition forms the power profile to predict the energy production.

Then, to provide an improved prediction of the power profile, the proposed approach includes a first layer to model the dynamic change of the shades. To generate such shading models, data from the place to evaluate is required. Two options are considered: PV arrays already installed or suitable places for new PV installations. In both cases, the effective irradiance available in the position of each module must be registered along the day. Such a procedure could be done at any moment while the irradiance forecast for the place is available. In the case of an array already installed, each PV module must be short-circuited to register the dynamic profile of the short-circuit current using an ammeter. The lower the time intervals used to register the current, the higher the resolution of the shading model. In the case of suitable places for new PV installations, one or several modules could be used to register the short-circuit currents generated in the positions where the modules will be installed.

Then, the effective irradiances for the modules are calculated from (3-38) using both the measurements and STC short-circuit currents, and using both the forecast and STC temperatures. Fig. 3-24 illustrates the measurement architecture: the short-circuited modules are used to register the effective irradiance profiles $S_{test,i}(t)$ along the day. Then, using such profiles and the forecast irradiance profile $S(t)$, the shading profile $Sh_i(t)$ for each module is calculated as is given in (3-39).

$$I_{sc} = I_{STC} \cdot \frac{S_{pv}}{S_{STC}} (1 + \alpha_I \cdot (T_{pv} - T_{STC})) \quad (3-38)$$

$$Sh_i(t) = \frac{S_{test,j}(t)}{S(t)} \quad (3-39)$$

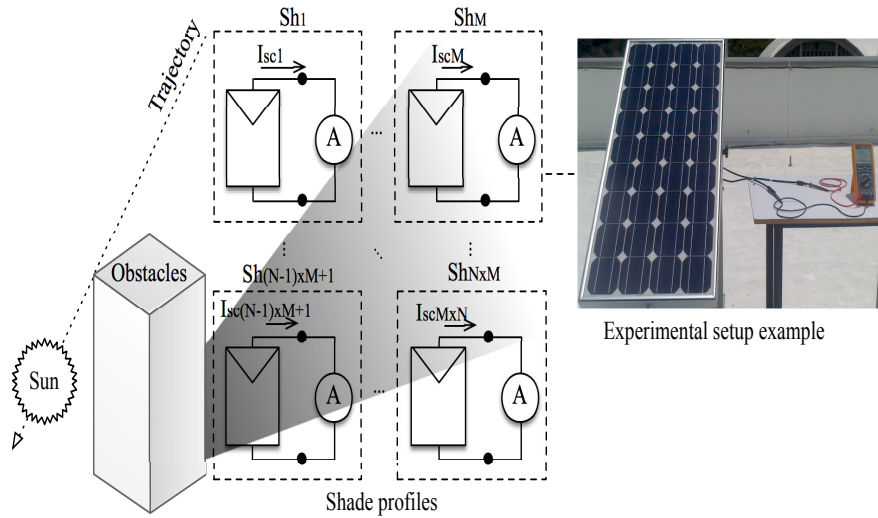


Figure 3-24.: Shade measurement architecture.

To illustrate the shading profiles, Fig. **3-25** shows a simulation considering a PV array composed by two parallel strings with three modules each, where the shading profile begins at 8:24 in the left-bottom corner of the array.

The shade flows towards the top-right corner of the array, it covering the six modules at 16:00. The simulation shows that the bottom-left module is completely shaded at 12:00, while the top-right module is not shaded almost all the time. Fig. **3-25** also illustrates the non-linearity of the shading profiles, as well as the difference among the patterns in each module. These shading profiles were taken on a winter day in central Colombia, where the angle of the sun allows the projection of the shadows. **In this simulation, 100 % corresponds to absolute shade which is not the case for a real environment but it is assumed in this case to illustrate the concept.**

To evaluate the performance of the proposed prediction model, an experimental irradiance and temperature profiles shown in ?? and ??, taken in the south of Italy on a summer day, were used to estimate the power production of a PV array using both the classical and the improved approaches. The improved prediction model considers the shading profiles given in Fig. **3-25**, while the classical model was considered with average shading among such profiles.

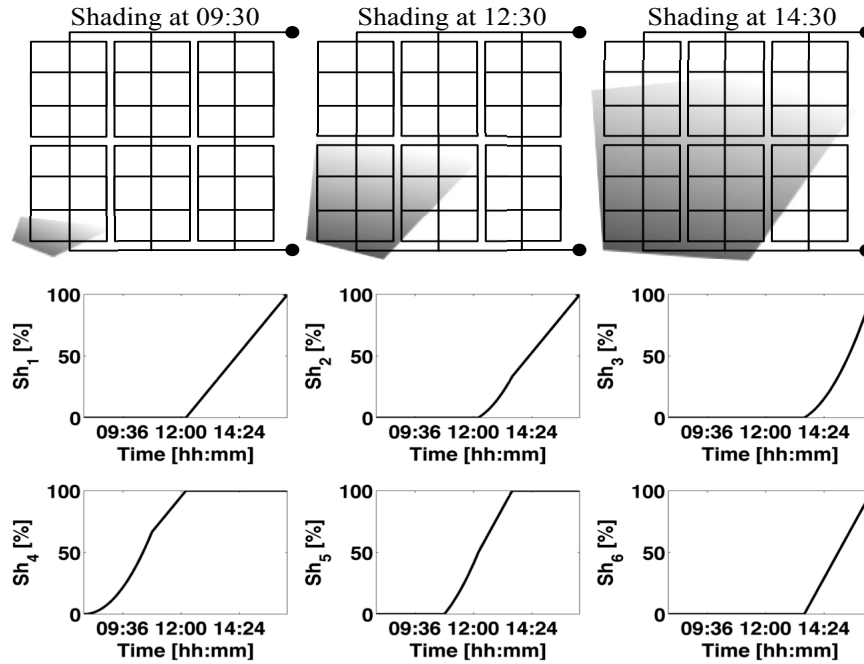


Figure 3-25.: Shading profiles of the affected PV modules.

The predicted power profiles obtained in Fig. ?? put into evidence the overestimation made by the classical approach with respect to the proposed solution. In such an example, the classical model overestimates by 23% the energy produced by the array under the forecast irradiance and shading profiles. Therefore, the proposed solution allows a PV installation to be accurately designed, and provides precise information to plan the energy delivery to the consumer or to the grid.

3.4. Conclusions

In this chapter some approaches for modeling SP arrays at module level were presented. The concepts analyzed in this chapter allowed to achieve a better understanding of the operation of PV devices and the process of modeling SP arrays. Different PV module and bypass diode models were used in the approaches.

The SQ approach is an improvement of the Fast approach introduced in [82], because the bypass diode is modeled through a linear representation which allows to considering the module operation in the second quadrant. In this way, the predicted power obtained by the SQ approach has less overestimation than the Fast approach as it is shown in the simulation results: for a 3×3 array evaluated under 7 days, the Fast approach introduced an overestimation in the predicted energy of 200 W. The simulation times were 30 s and 1.7 s for the SQ approach and the Fast approach, respectively, which shows that relative low computation

times are still achieved. The SQ approach enables to analyze SP arrays under partial shading conditions for power prediction, with a good balance between accuracy and speed calculation.

Section 3.3 introduced three approaches mainly oriented to perform power prediction analysis considering mismatching conditions. In this way, the first approach of section 3.3 is a tradeoff between the techniques presented in [83] (Lambert-W approach) and [82] (Fast approach). The proposed solution combines the single diode model for representing the PV modules and a linear model for the bypass diodes to take into consideration the operation of the modules in the second quadrant. A mathematical procedure is introduced to avoid the use of the Lambert-W function which allows to reduce the processing times, this without losing accuracy in the predicted power. The proposed solution was validated through two application cases. In the first case, a small string formed by 5 modules with a single irradiance profile was considered; the error of the proposed approach with respect to the Lambert-W approach was 0.12 %, while the Fast approach error was 2.88 %. The simulation times were 191.95 s, 1.4 s and 0.034 s for the Lambert-W, the Fast and the proposed approach. In the second case, the inverter SolarEdge SE2200, which requires a string of 20 PV modules to operate was considered. An irradiance profile of one day was evaluated with the Lambert-W, the Fast and the proposed approach, the processing times were: 391 hours (16.3 days), 1.84 hours and 6.24 s, respectively. The results put into evidence the good performance of the proposed approach to simulate short or long periods with high precision.

The second procedure introduced in section 3.3 is based on the single diode model, but the exponential model was used for representing the bypass diode. In this approach, the Lambert-W function is not required and only the string power within the neighborhood of the LMPPs are calculated; after that, a mathematical procedure is employed to define the GMPP without the need of calculating all the points of the I-V curve. These two characteristic allow to achieve a significant reduction in the simulation times. The proposed approach calculates an average of 6.39 % of the points calculated by the conventional sweep method; in the case of a string of 20 modules the conventional sweep method requires hours while the proposed approach requires less than 1 ms as it is shown in Fig. ???. In the same way, the error (RAAE) introduced by the assumptions made in the proposed solution is lower than 0.0001 %, which is a negligible difference. Since the proposed approach enables to obtain the GMPP in a fast and accurate way, large PV systems can be analyzed in terms of economic viability accounting for partial shading conditions, which was not possible with classical methods. Such analysis could include Monte Carlo simulations to quantify the impact of shading on the power production of the PV installation to select the best location for the PV array. In addition, this method can be used in dynamic reconfiguration of PV systems to reduce the impact of partial shading in the power production. Finally, it is worth to consider that the simplicity of the method makes it suitable for implementation in software packages like Matlab and other programming languages such as C or C++, which is proposed as future

work.

The last approach presented in this chapter is also devoted to energy yield analysis, such an approach is based on the ideal models of the PV module and the bypass diode. The procedure for estimating the power is improved by considering dynamic shading conditions for each module, since classical solutions usually assume average shading profiles, which can introduce errors in the estimation. The proposed solution uses short-circuit current measurements to define the behavior of the shading pattern for each module. The accuracy of the proposed approach for the estimation of the power is demonstrated in an example where the classical approach over-estimates the energy production in 23%. Thus, the proposed approach is a tool for supporting the installation designers and grid planning engineers by giving an accurate estimation of the power production: the former ones profit from an accurate return-of-investment calculation and well-sized equipment design, which permits an evaluation of the economic and technical viability of an installation. The later ones profit from the accurate power estimation to avoid unexpected power drops that trigger undesired and costly contingency plans.

In general, all the approaches included in this chapter have a good agreement with solutions that have been reported in literature: [83], [82], [9]. The approaches presented in this Chapter are mainly oriented to power prediction, but they can be also used for reproducing the I-V and P-V curves. Finally, the concepts analyzed through the implementation of the presented solutions enable to achieve a better understanding of the operation of PV devices.

4. Modeling of irregular PV arrays

In this chapter the main contributions of this thesis are presented. After considering the state of the art of modeling PV arrays, it was detected that there is no a unique technique or procedure for modeling PV arrays under any configuration. On the other hand, the lack of analysis on PV irregular configurations was also detected. Then, the procedures presented in this chapter are also oriented to such configurations. The first part of this chapter describes the concept of irregular PV configurations while the remaining of the chapter introduces some approaches for modeling irregular and regular PV arrays. All approaches introduced in this chapter are able to model PV arrays under both uniform or mismatched conditions.

Part of the analyses and results achieved in this chapter have been published in *Revista Tecnológicas* in the paper: “Equivalent circuits for simulating irregular PV arrays under partial shading conditions” [109] and in the paper “General modeling procedure for photovoltaic arrays” published in *Energy Power Systems Research* [11].

4.1. Introduction

In chapter 2 an overview of the state of the art of PV arrays modeling was presented. Such an overview allowed to detect two main aspects which helped to define the orientation of the research work developed in this thesis. First, the modeling techniques reported in literature are able to represent the electrical behavior of only one kind of PV array, i.e. SP, TCT, BL or HC; in fact, the most widely studied is the SP connection. Then, if for a particular application, the evaluation of different configurations is required, multiple algorithms or procedures must be implemented; such an implementation can consume significant amount of time and inclusive can produce a inefficient use of resources as processor or computing tools, since the programming of different algorithms in such devices can occupy valuable space that could be used in other tasks. Such is the case of systems aimed at executing reconfiguration analysis and *MPPT* control strategies under the same platform [3]. A concept associated to the modeling techniques analyzed in Chapter 2 was the strong tendency for the use of the single diode model for representing either a PV cell or the PV module. It could lead to consider the single diode model as a suitable option since it has a good compromise between complexity and accuracy. In the same way, from the concept of granularity, it can be said that for applications requiring the reproduction of the $I - V$ and $P - V$ curves and energy yield analysis, modeling a PV array at module level is widely accepted [81]. The second aspect is the lack

of analysis on other PV configurations or structures different from conventional ones, i.e. configurations which do not follow a regular pattern of connection, such configurations are named *irregular configurations* in this chapter. The possibility of achieving a better performance for a given operating conditions using an irregular PV array has been barely discussed.

Therefore, the main scope of this chapter is to propose different approaches for modeling PV arrays under any connection, at module level, and exposed to both uniform or mismatched conditions. In the first part of this chapter the concept of irregular array is explained in detail, and analyzed from the point of view of the actual connections of PV arrays considering the internal connection of commercial PV panels. In the second part, a first approach for modeling irregular PV arrays is introduced; such an approach uses the ideal single diode model and is able to model either regular or irregular arrays, however its application in this chapter is oriented to model irregular arrays; simulations results validate the proposed procedure. The rest of the chapter is devoted to explain another modeling approach, which is based on the classic nodes voltages and meshes currents analyses. In this case, the modules are modeled through the complete single diode model and it is also able to model PV arrays with any connection under uniform and mismatched conditions. The validation of such an approach is made through simulations and experimental tests. Finally, considering that in Chapter 2 at least three main application of modeling techniques were identified (reproduction of characteristic curves, energy production analysis and shading analysis), it can be said that the approaches introduced in this chapter belong to the former groups.

4.2. The concept of irregular PV array

PV array configurations such as SP, TCT and BL have been widely discussed and, as it was shown in Chapter 2, several techniques for modeling those structures have been reported. The aforementioned PV structures follow a pattern for the connection of PV panels, which makes them *regular configurations*. On the other hand, there are no evidences of the use of different connections in which unlike conventional or regular configurations, any pattern is followed and the PV panels are connected arbitrarily forming structures which can be considered as *irregular configurations*. Only in [66] a study on the performance of hybrid structures operating under different shading scenarios is presented. The hybrid structures are the result of combining conventional configurations: SP-TCT, BL-TCT and HC-TCT. However, there are no information concerning the performance of other irregular configurations operating under mismatching conditions. Fig. 4-1 shows the P-V curves for SP, TCT, BL and an irregular 4×4 PV array operating under the same partial shading profile, which is represented by the irradiance matrix shown in (4-1) in W/m^2 . It is evident that the maximum power of the irregular array is higher than the maximum power of the other arrays; the difference in the maximum power value between the irregular array and the SP, TCT and BL arrays, for this particular case, is 27, 7 %, 15 % and 32 %, respectively.

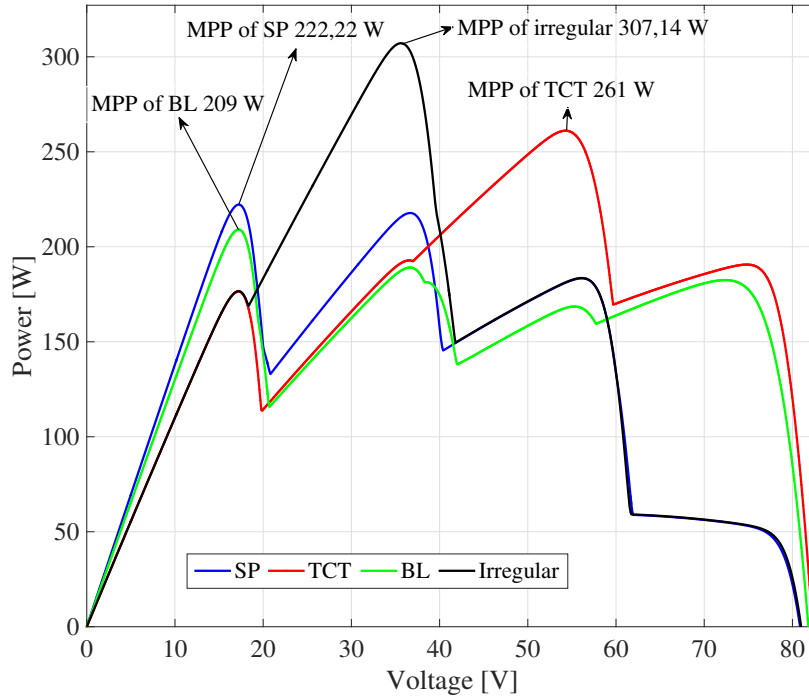


Figure 4-1.: P-V curves of different configurations under the same mismatching pattern.

$$S = \begin{bmatrix} 10 & 100 & 300 & 300 \\ 400 & 30 & 500 & 500 \\ 200 & 900 & 100 & 100 \\ 600 & 200 & 1000 & 1000 \end{bmatrix} \quad (4-1)$$

From the irradiance matrix it can be seen that the modules in the last two strings of the array (from left to right) are exposed to the same shadow levels while the modules in the two first strings are exposed to different shadow levels. Such a condition is common in PV arrays surrounded by trees as it is illustrated in Fig. 4-2, or surfaces with spaces through which the sunlight reaches the PV panels producing a non-uniform shadow. Then, in order to mitigate the effect of shadow on the power provided by the array, an irregular structure can be useful.

Commercially available PV panels have different number of modules, e.g. the BP585 and JS65 Yingli Solar panels are formed by two series-connected modules of 18 cells each, so the panels have 36 cells, while the ERDM85 panel is formed by a single module with 36 cells. Fig. ?? shows a TCT connection made with two-module PV panels: in the left, the physical connection from panels terminals is shown while in the right the actual connection considering the internal configuration of the panels is illustrated.



Figure 4-2.: Non-uniform shadow due to a tree.

The P-V curves of such arrays operating under the same irradiance conditions are shown in Fig. 4-3; the power at the MPP of the physical connection is 2,5% higher than the one provided by the actual connection. This means that if the internal configuration of the PV panels is not considered, inaccurate results are achieved. Moreover, if a modeling technique developed for TCT arrays is applied to TCT arrays formed with panels containing more than one module, results will not be correct. Inaccurate analyses can introduce significant errors in larger arrays, this affecting power prediction, planning or payback time studies.

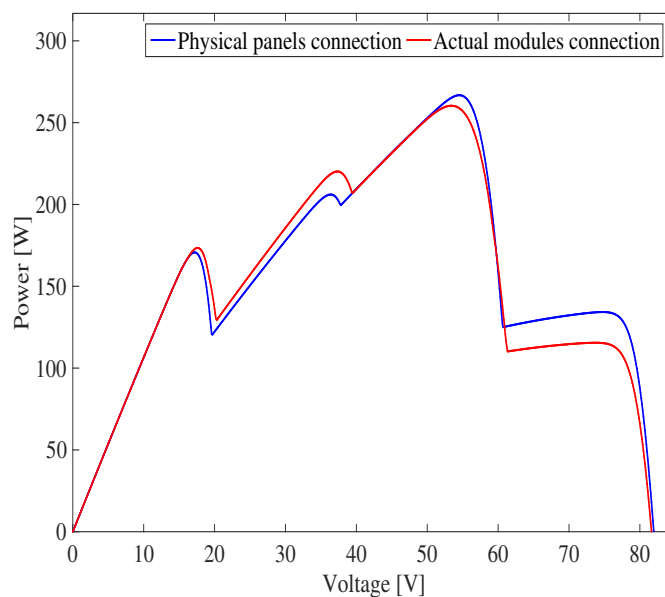


Figure 4-3.: P-V curves of single and two bypass diode panels of TCT array under the same operating conditions.

In this way, by considering the internal connection of PV panels such as the BP585 or the

JS65 or any multi-module PV panel, TCT, BL or HC arrays are in fact irregular connections and conventional modeling techniques associated to this kind of arrays cannot be applied. Then, modeling techniques which consider the internal connection of the PV panels must be adopted to achieve reliable analyses of the electrical behavior in PV systems.

On the other hand, when a panel fails and it requires to be replaced, it is possible that the new panel, despite providing the same current and voltage, has a different internal composition. For example, the BP585 can be replaced by the ERDM85 since both have similar characteristics. However, the ERDM85 has one module, which would change the configuration of the array drastically. This situation is illustrated in Fig. 4-4, where the same TCT configuration of Fig. ?? is considered but replacing the upper left corner and the central panels with ERDM85 panels. The previous examples put into evidence the existence of irregular PV arrays in practical applications; hence it is necessary to develop a modeling procedure for analyzing such arrays. Such a general model will be a useful tool for planning and design PV systems, since it would give the possibility of evaluating all the desired configurations to find the suitable one for certain operating conditions. In addition, the procedure can be also used for evaluation of *MPPT* control strategies and analysis of partial shading impact. Moreover, reconfiguration techniques can be improved since more options for connecting the PV panels can be validated.

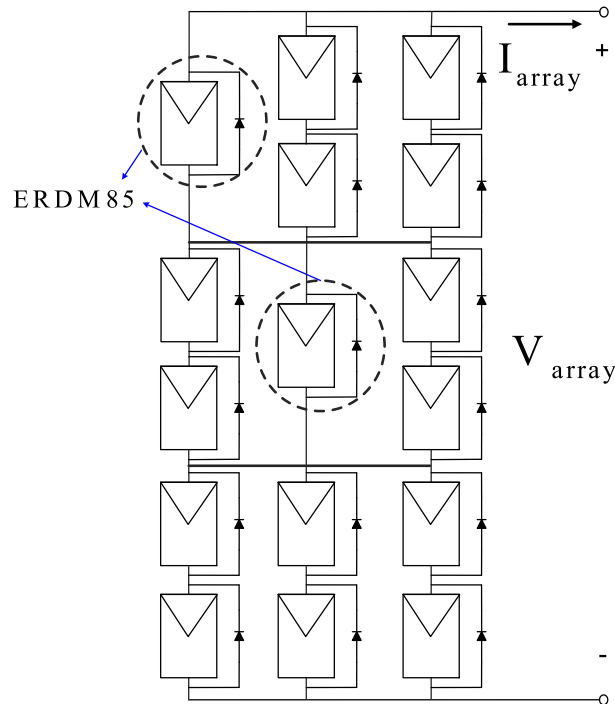


Figure 4-4.: Modules connection after replacing BP585 panels with ERDM85 panels.

4.3. Equivalent circuits for modeling irregular PV arrays

The inflection points technique was introduced in [82] and it was applied to SP arrays. It is based on the calculation of the modules voltages at which the I-V curve becomes discontinuous. These discontinuities are caused by the activation of the bypass diodes due to the different irradiance levels affecting the PV modules, this caused by partial shading. The details of such a technique were discussed in chapter 3. Fig. 4-5 shows a pilot PV array used to illustrate a first approach for modeling irregular PV arrays based on the inflection points concept. It must be noted that such a PV array does not correspond to any of the typical configurations (SP, TCT, BL or HC). Instead, it is formed by three parallel-connected modules at the top, two parallel-connected modules at the center, two parallel-connected modules at the bottom and two series-connected modules at the bottom right.

This approach considers the ideal single diode model for representing the modules, while the bypass diode is modeled as an ideal switch; such models were adopted to simplify the mathematical operations. In addition, a procedure for obtaining equivalent blocks of modules connected in parallel is introduced. Such a process consists in lumping the parallel-connected modules into a single equivalent block as it is shown in Fig. ??, where the case for two modules is illustrated. It is worth to note that both $BD1$ and $BD2$ bypass diodes can be accurately represented by a single equivalent bypass diode BD . In this way, the current of an equivalent block of N parallel-connected modules can be defined as given in (4-2).

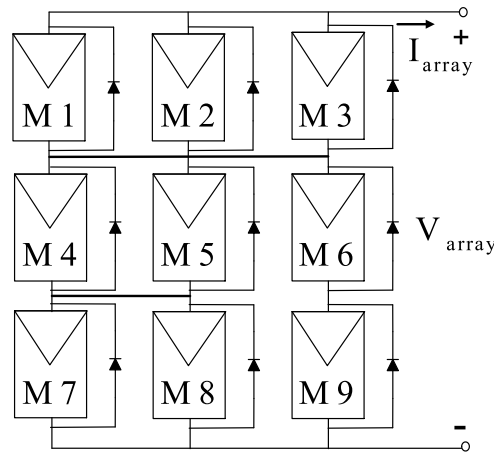


Figure 4-5.: Irregular array used for introducing the modeling approach.

$$I_{eq} = \sum_{i=1}^N I_{sc,i} + \sum_{i=1}^N (I_{sat,i} \cdot (1 - \exp(B_i \cdot V_{mod}))) \quad (4-2)$$

Then, the three modules at the top row of Fig. 4-5 were lumped in a single equivalent module modeled by a triple diode model. The two modules at the center and at the bottom

were lumped in equivalent modules modeled by a double diode model. The bypass diodes connected to each module, in the original array, were replaced by a single bypass diode since the activation of any of them deactivates the others. Then, considering the numeration given at each module in the array, the operation of the block formed by the three parallel-connected modules is given by (4-3), while the operation of the two blocks formed by two parallel-connected modules is given by (4-4) and (4-5).

$$I_{eq1} = \sum_{i=1}^3 I_{sc,i} + \sum_{i=1}^3 (I_{sat,i} \cdot (1 - \exp(B_i \cdot V_{mod1}))) \quad (4-3)$$

$$I_{eq2} = \sum_{i=4}^5 I_{sc,i} + \sum_{i=4}^5 (I_{sat,i} \cdot (1 - \exp(B_i \cdot V_{mod2}))) \quad (4-4)$$

$$I_{eq3} = \sum_{i=7}^8 I_{sc,i} + \sum_{i=7}^8 (I_{sat,i} \cdot (1 - \exp(B_i \cdot V_{mod3}))) \quad (4-5)$$

In (4-3) to (4-5) I_{sc} is the short circuit current, $I_{sat,i}$ is the diode saturation current of module i and B_i is defined as $1/(n_i \cdot V_{t,i})$ where n_i is the ideality factor and $V_{t,i}$ is the thermal voltage of module i . V_{mod} is the block voltage, which is the same voltage of all modules lumped in the equivalent one since they are connected in parallel. Fig. 4-6 shows the new configuration of the PV array due to the lumping process. As it can be seen, the obtained configuration is still irregular so it cannot be modeled using a modeling technique for conventional PV arrays. The modules have been re-named according to the equivalent ones: $M1$, $M2$ and $M3$ were lumped in M_{n1} ; $M4$ and $M5$ were lumped in M_{n2} ; $M7$ and $M8$ were lumped in M_{n3} . Modules $M6$ and $M9$ remain the same, but they were re-named as M_{n4} and M_{n5} , respectively, for nomenclature consistency. In addition, the string formed by M_{n2} and M_{n3} and the string formed by M_{n4} and M_{n5} are named sub-arrays, SA_1 and SA_2 respectively.

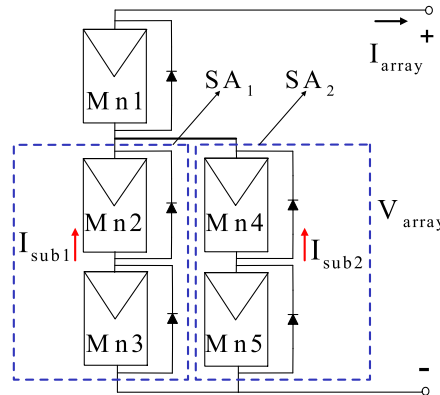


Figure 4-6.: Configuration adopted by the array after the lumping process.

The inflection points concept considers that, depending on the irradiance profile and the activation of the bypass diodes, a PV array can change its structure for a given voltage

operation; this taking into account that the analysis of the system is made through a voltage sweep. In this way, the new array, shown in Fig. 4-6, is formed now by 5 modules with at least 31 possible configurations depending on the activation of the bypass diodes. Fig ?? shows two of those possible situations for a given operation voltage.

Considering the aforementioned concepts of the lumping process and inflection points, the following process is proposed for modeling irregular PV arrays: (i) obtaining the inflections points and identifying the operating points in which the bypass diodes become active due to the partial shading conditions; (ii) detect the equivalent circuits adopted by the PV array depending on the status of the bypass diodes; (iii) set an equations system based on the Kirchhoff laws to calculate the current of each possible equivalent circuit to reproduce the I-V and P-V curves of the array.

4.3.1. Computation of inflection points

The values of the short circuit currents associated to each model of the pilot array shown in Fig. 4-5, due to the shading profile, are shown in (4-6). By applying the lumping process, the equivalent currents of the new array shown in 4-6 are given in (4-7).

$$I_{sc} = \begin{bmatrix} 1 & 2 & 4 \\ 4 & 3 & 5 \\ 6 & 6 & 3 \end{bmatrix} \quad (4-6)$$

$$I_{scn} = \begin{bmatrix} 7 & - & - \\ 7 & 5 & - \\ 12 & 3 & - \end{bmatrix} \quad (4-7)$$

By considering the inflection points theory, the following cases can be identified:

- The bypass diode connected to module M_{n1} turns on active at the operating point in which $I_{scn1} < I_{sub1} + I_{sub2}$, that is, when $I_{scn3} = 12A$ and $I_{scn4} = 5A$ (maximum current case) and when $I_{scn2} = 7A$ and $I_{scn5} = 3A$ (minimum current case).
- The bypass diode associated to module M_{n2} becomes active at the operating point in which $I_{scn2} < I_{scn3}$.
- The bypass diode associated to module M_{n5} becomes active at the operation point in which $I_{scn5} < I_{scn4}$.

Since $I_{scn3} > I_{scn2}$ and $I_{scn4} > I_{scn5}$ it is concluded that the bypass diodes associated to the modules M_{n3} and M_{n4} do not become active and the I-V curve of the PV array under study has three inflection points. However, it is important to analyze in which order the bypass diodes become active for modules M_{n1} , M_{n2} and M_{n5} .

It is clear that the maximum current of the PV array is $I_a = 17$ A, which occurs when the voltage is equal to 0 V. Then, by considering a voltage sweep analysis, when the array voltage increases and the array current decreases, at least one module of each sub-array must be active. This confirms that modules M_{n3} and M_{n4} are always active and such modules will.

Module M_{n1} will be active if $I_{sub1} + I_{sub2} < 7A$, which is possible after modules M_{n2} and M_{n5} become active; this because their activation implies that the current flowing through the sub-array 1 is at least $7A$ and the current flowing through sub-string 2 is at least $3A$, which in turns means that $I_{sub1} + I_{sub2}$ is at least $10A$. Therefore, the module M_{n1} is the last module becoming active.

This leads to the task of identifying which module, M_{n2} or M_{n5} , becomes active first in the voltage sweep. Since M_{n3} and M_{n4} are always active. By assuming that the current flowing through sub-array 1 is equal to $7A$, which means that module M_{n2} is inactive, it is possible to determine if module M_{n5} is active or inactive by calculating the current that flows through sub-array 2. Under that assumption, the currents of the array are given by (4-8) and (4-9):

$$I_{sub1} = I_{scn3} + I_{sat,7} \cdot (1 - \exp(B_7 \cdot V_{n3})) + I_{sat,8} \cdot (1 - \exp(B_8 \cdot V_{n3})) \quad (4-8)$$

$$I_{sub2} = I_{scn4} + I_{sat,4} \cdot (1 - \exp(B_4 \cdot V_{n4})) \quad (4-9)$$

The equations system formed by (4-8) and (4-9) must be solved by using a numerical method (i.e. Newton-Raphson), or by using functions already defined in software packages. In this approach the function *fsolve* available in Matlab was used. For simplicity, in this case, parameters I_{sat} and B are considered equal for all the modules. Those parameters are obtained from the manufacturer datasheet of the ERDM85 PV panel, in this case $I_{sat} = 7.5992 \times 10^{-7}$ A and $B = 0.7220$ V⁻¹.

Equations (4-10) allows to calculate V_{n3} and by evaluating such a value in (4-11), I_{sub2} is obtained to define if module M_{n5} is active or inactive.

$$I_{sub1} = I_{scn3} + 2 \cdot I_{sat} \cdot (1 - \exp(B \cdot V_{n3})) \quad (4-10)$$

$$I_{sub2} = I_{scn4} + I_{sat} \cdot (1 - \exp(B \cdot V_{n4})) \quad (4-11)$$

From (4-10) and (4-11), I_{sub2} is equal to 2.5 A which implies that module M_{n5} is active since $I_{scn5} > 2.5$ A. This means that module M_{n5} becomes active before module M_{n2} . To confirm such a conclusion, I_{sub1} is calculated when I_{sub2} is 3A. The obtained current is 8A, which confirms that M_{n2} is inactive because $I_{scn2} < 8A$. Moreover, the inflection point can be described in terms of a couple (V, I) , since that point corresponds to $I_{sub2} = 3A$ and the voltage can be calculated from (4-12). In this way, the inflection point is: (20.48 V, 11 A).

$$V_{inf1} = V_{n4} = \frac{1}{B} \ln \left(1 + \frac{2}{I_{sat}} \right) \quad (4-12)$$

The second inflection point depends is calculated by using (4-13) considering that such point occurs when $I_{sub1} = 7$ A.

$$V_{inf2} = V_{n3} = \frac{1}{B} \ln \left(1 + \frac{5}{2 \cdot I_{sat}} \right) \quad (4-13)$$

The inflection point coordinates (V, I) are obtained by solving the system formed by (4-14) and (4-15) to calculate the current value through sub-array 2. In this case, the second inflection point is (20.78 V, 10 A).

$$I_{n4} = I_{n5} \quad (4-14)$$

$$V_{inf2} = V_{n4} + V_{n5} \quad (4-15)$$

For the analysis of the third inflection point it has to be considered that the current of the array is the same as in module M_{n1} , which in turns is equal to its short-circuit current I_{scn1} . Such a current corresponds to the addition of the currents of sub-arrays 1 and 2, which can be represented as the addition of the current of modules M_{n2} and M_{n4} as is given in (4-16). Taking into account the series connection in each sub-array, equations (4-16) and (4-17) are defined. To complete the analysis, equation (4-18) relates the voltages of the modules. In this way, by solving the system, the voltages can be calculated. The obtained results are: $V_{n2} = 19.46$ V, $V_{n3} = 21.23$ V, $V_{n4} = 21.07$ V and $V_{n5} = 19.62$ V.

The inflection voltage is calculated by adding the modules voltages $V_{n2} + V_{n3}$ and $V_{n4} + V_{n5}$. In this way, the third inflection point is (40,69V, 7A). If the modules have different parameters, an approach similar to the one in (4-10) and (4-11) can be used for solving the inflection voltage. Fig. ?? shows the topologies adopted by the array at each inflection point.

$$I_a = I_{sub1} + I_{sub2} = I_{n2} + I_{n4}I_{n2} = I_{n3} \quad (4-16)$$

$$I_{n4} = I_{n5} \quad (4-17)$$

$$V_{n2} + V_{n3} = V_{n4} + V_{n5} \quad (4-18)$$

4.3.2. Detection of the equivalent circuits and I-V, P-V curves reproduction

Based on the three inflection points computation process, the four regions described in Fig. 4-7 are defined: each one of them corresponding to a particular equivalent circuit adopted by the array due to the activation of the bypass diodes. In this way, by performing a voltage sweep in each equivalent circuit within the corresponding voltage range, the I-V and P-V curves are obtained.

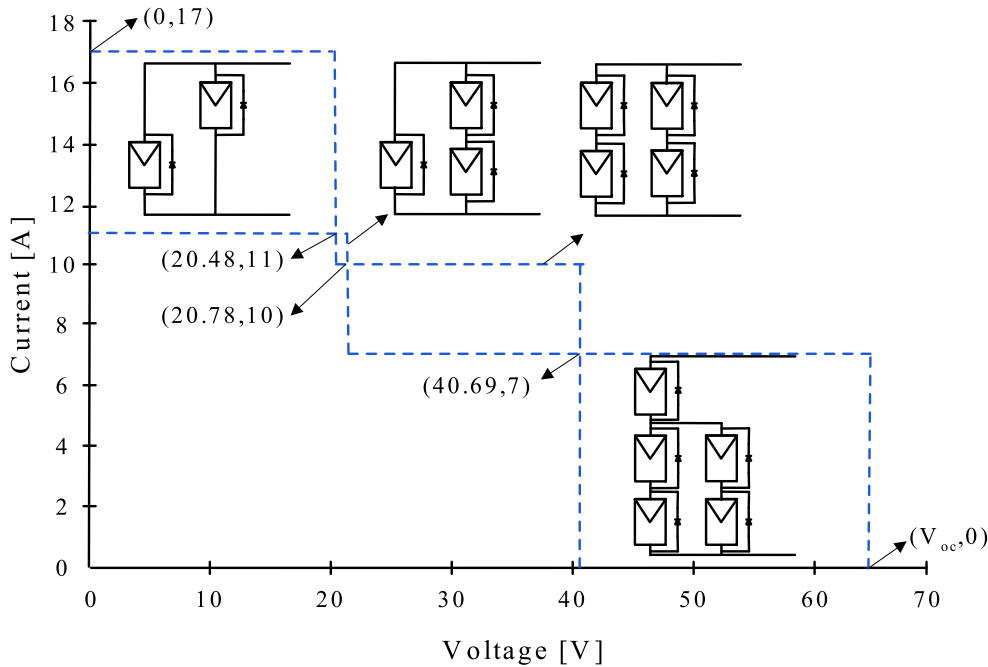


Figure 4-7.: Structures adopted by the array described by regions.

Fig. ?? shows a satisfactory agreement between the I-V and P-V curves obtained with the proposed method and with a circuital simulation performed in Simulink/SimElectronics toolbox using the ideal single diode model. In fact, the proposed solution allows to clearly identify the two inflection points IP1 and IP2 as it is shown in the zoom area of Fig. ?. The simulation result does not show in detail the two inflection points because it requires a smaller step voltage which in turns can increase the execution time. Due to the reduced number of calculations, the proposed approach requires 18% of the execution time used by the circuital simulation and with a mean absolute percentage error (MAPE) [36] in the predicted power of 3.094%; the difference in the curves can be identified in the region near to the first inflection point as is shown in the zoom area of Fig. ?. The MAPE was calculated by applying (4-19), where A_j is the reference value, P_j is the predicted value and k is the number of elements of each vector.

$$MAPE = \left(\frac{1}{k} \sum_{j=1}^k \left| \frac{A_j - P_j}{A_j} \right| \right) \times 100 \quad (4-19)$$

The proposed procedure can be summarized in the following steps:

- Lump the modules connected in parallel and define the new short-circuit current matrix
- Analyze the short-circuit currents to define the operation (activation/deactivation) of the bypass diodes
- Use the inflection points technique to calculate the inflection voltages
- Define the structures adopted by the PV array for the different inflection voltages

Finally, Fig. 4-8 presents the flowchart of the modeling procedure proposed in this section.

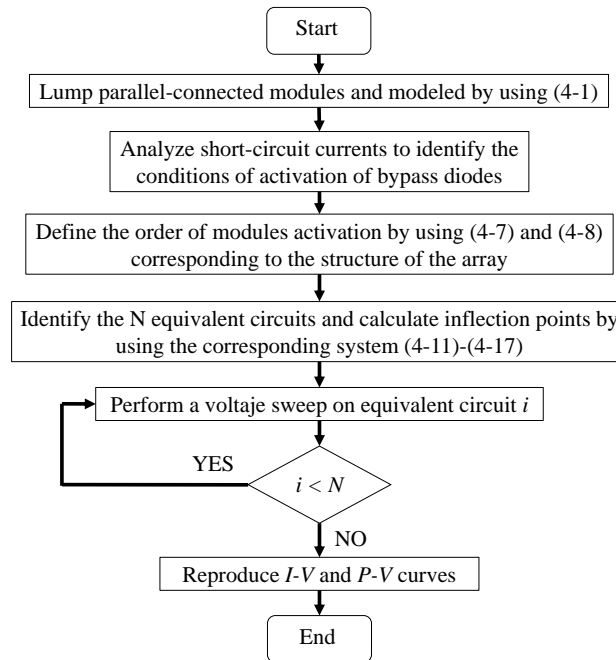


Figure 4-8.: Flowchart of the proposed procedure.

4.3.3. Dynamic simulation

One common application of PV models is the evaluation of MPPT algorithms under partial shading conditions. Therefore, in order to confirm the usefulness of the proposed approach, the model was used to evaluate a classical MPPT algorithm using dynamic simulations. The

example considers a photovoltaic battery charger, implemented in Matlab, and formed by: the irregular PV array previously analyzed, a boost converter and the load (battery) modeled as a voltage source. The MPPT algorithm under test is the *P&O* (Perturb and Observe) approach, which is one of the most widely adopted MPPT techniques for PV systems. Fig. 4-9 presents the application scheme.

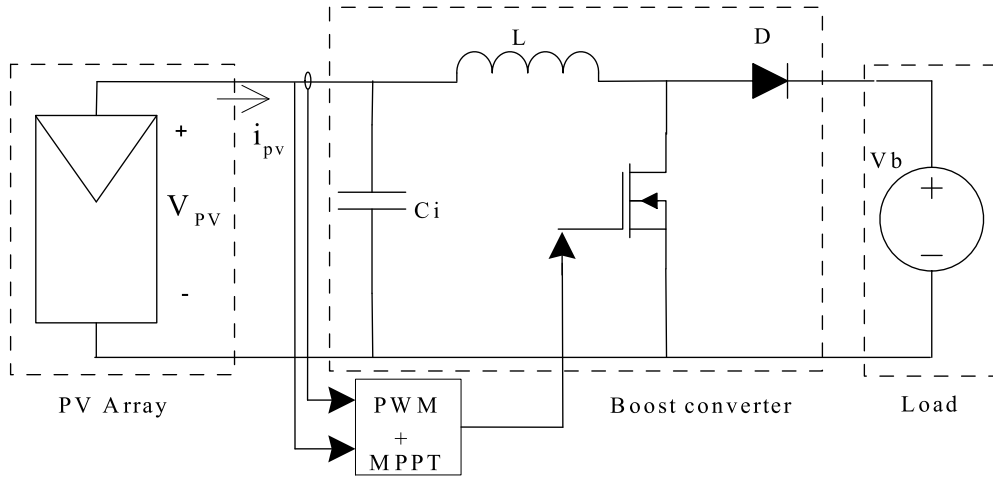


Figure 4-9.: Scheme of the application of a battery charger.

The proposed model based on equivalent circuits was implemented in Matlab code. The PV system is exposed to three different shading patterns represented by three short-circuit current profiles: I_{scP1} , I_{scP2} and I_{scP3} , which are presented in (4-20), (4-21) and (4-22) respectively.

$$I_{scP1} = \begin{bmatrix} 5 & 5 & 4 \\ 4 & 4 & 2 \\ 2 & 1 & 1 \end{bmatrix} \quad (4-20)$$

$$I_{scP2} = \begin{bmatrix} 5 & 2 & 1 \\ 4 & 1 & 3 \\ 2 & 2 & 2 \end{bmatrix} \quad (4-21)$$

$$I_{scP3} = \begin{bmatrix} 3 & 2 & 2 \\ 4 & 2 & 2 \\ 1 & 2 & 4 \end{bmatrix} \quad (4-22)$$

Fig. 4-10 shows the power curves of the PV array under each shading profile. The dynamic simulation starts with the PV array operating under Profile 1, then at $t = 25ms$ the shades change to Profile 2, and at $t = 50ms$ the shades change to Profile 3. To evaluate the *P&O* reliability three simulations were performed. The first simulation consider an initial duty

cycle $D = 0,6$ ($V_{pv} = 48V$), where the $P\&O$ algorithm tracks a local maximum of Profile 1 ($277,8W$); when the profile changes at $t = 25ms$, the MPP of Profile 2 ($312,3W$) is successfully tracked. When the profile changes again, at $t = 50ms$, the $P\&O$ algorithm successfully tracks the MPP of Profile 3 ($265,1W$).

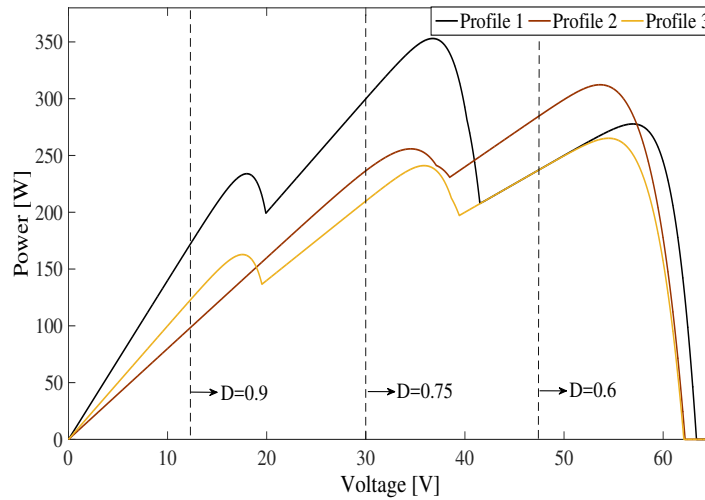


Figure 4-10.: Power profiles for dynamic evaluation.

The second simulation considers an initial duty cycle $D = 0,75$ ($V_{pv} = 30V$), in this case the $P\&O$ algorithm successfully tracks the MPP of Profile 1 ($353W$); but when the profile changes to Profile 2, the $P\&O$ algorithm tracks a local maximum ($255,8W$), and when the profile changes to Profile 3 the $P\&O$ algorithm tracks a local maximum again ($241W$). Finally the third simulation was made with an initial duty cycle $D = 0,9$ ($V_{pv} = 12V$), where again the $P\&O$ tracks local maximum for the three profiles. Fig. 4-11 shows the simulation results.

This example illustrates the usefulness of the proposed model in testing MPPT algorithms: the simulation results show that the classical $P\&O$ algorithm is not reliable under mismatching conditions. Such a conclusion is in agreement with the results given in [114]. The complete single diode model can be considered for a future work, as well as the representation of the bypass diode by means of the Schottky model, which can increase even more the accuracy and provide detailed analysis of the activation of the bypass diodes due to the partial shading conditions.

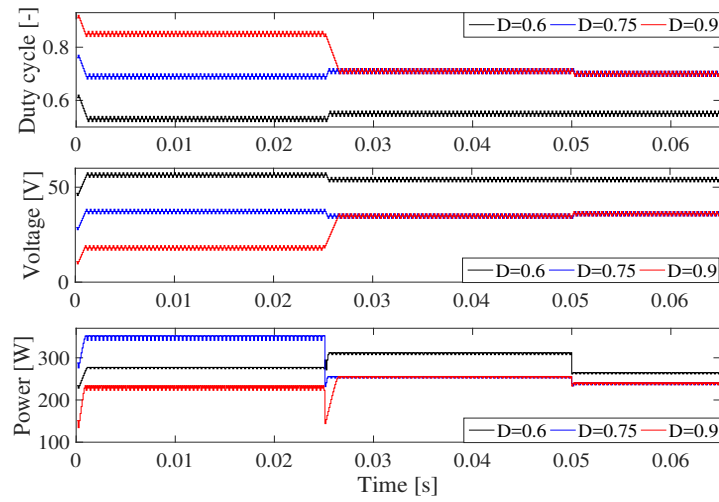


Figure 4-11.: Dynamic simulation results.

4.4. General procedure for modeling PV arrays based on node voltage analysis

The operation of a PV array can be represented through a system of non-linear equations as it was seen in previous chapters. Such a system must be solved in order to calculate the current of the array and then obtaining the power of the array for carrying out different analysis. Usually, the size of the array is defined as $(N \times M)$, where N is the number of rows (modules connected in series) and M the number of columns (strings connected in parallel) of the array. Therefore, for an $(N \times M)$ PV array a system of $(N \times M)$ non-linear equations must be constructed and solved regardless the array configuration. In general, the structure of the non-linear equation system and the Jacobian matrix depends on the array configuration [9], [83], [82], while the details of each equation depend on the PV module representation.

The proposed modeling procedure introduced in this section calculates the array current for a given array voltage. The basic idea of the procedure is to divide the original PV array into smaller PV arrays called sub-arrays, connected in parallel. Thus, instead of solving a $(N \times M)$ system of non-linear equations, the procedure considers multiple systems of non-linear equations that can be solved independently. The concept of sub-array was also used in the previous section, but in the approach presented in this section the concept is redefined further. This procedure can be applied to any PV array: regular or irregular operating under uniform or mismatching conditions.

4.4.1. PV module model

The proposed approach uses the complete single diode model for representing the PV modules of the array. Fig.4-12 shows the typical circuit of the single diode (SD) model including the bypass diode and the node voltages e_a and e_b at the positive and negative terminals of the PV module with respect to the array reference voltage.

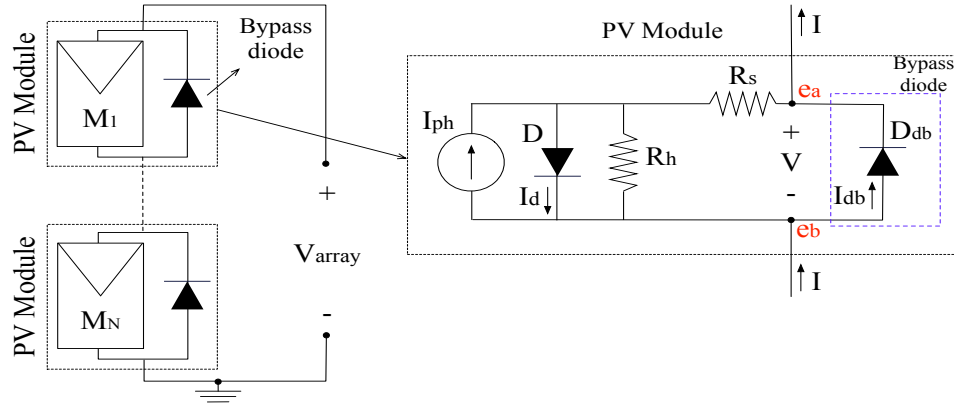


Figure 4-12.: PV module single diode model equivalent circuit including the bypass diode D_{db} .

The relationship between the current (I) and voltage ($V_e = e_a - e_b$) of the PV module can be obtained using the Kirchhoff voltage (KVL) and current (KCL) laws [10], [9]. However, such relationship is not explicit and strongly non-linear; therefore, it is necessary to use the Lambert-W function, denoted by W_o , to express the module current as function of e_a and e_b as shown in (4-23). Moreover, the derivatives of (4-23) with respect to e_a and e_b are presented in (4-24) and (4-25), respectively. In (4-23) to (4-25) N_s is the number of series-connected cells into the module, I_{sat} is the inverse saturation current of the PV module diode, and $V_t = n \cdot k \cdot T / q$ in which n is the ideality factor, k is the Boltzmann constant, q is the electron charge, and T is the module temperature in Kelvin. $I_{sat,db}$ is the inverse saturation current of the bypass diode and $V_{t,db} = n_{db} \cdot k \cdot T / q$ in which n_{db} is the ideality factor of the bypass diode.

$$I = -\frac{N_s \cdot V_t \cdot W_o(\theta)}{R_s} + I_{sat,db} \cdot \left[\exp\left(\frac{-(e_a - e_b)}{V_{t,db}}\right) \right] - I_{sat,db} + \frac{R_h \cdot (I_{ph} + I_{sat}) - (e_a - e_b)}{R_h + R_s} \quad (4-23)$$

$$\theta = \left(\frac{R_h \cdot R_s}{R_h + R_s} \right) \cdot \frac{I_{sat}}{N_s \cdot V_t} \cdot \exp\left[\frac{(R_h + R_s) \cdot (I_{ph} + I_{sat}) + R_h \cdot (e_a - e_b)}{N_s \cdot V_t \cdot (R_h + R_s)} \right]$$

$$\frac{\partial I}{\partial e_a} = \left(\frac{-R_h}{R_s \cdot (R_h + R_s)} \right) \cdot \left(\frac{W_0(\theta)}{1 + W_0(\theta)} \right) - \left(\frac{1}{R_h + R_s} \right) - \left(\frac{I_{sat,db}}{V_{t,db}} \right) \cdot \exp\left(\frac{e_b - e_a}{V_{t,db}}\right) \quad (4-24)$$

$$\frac{\partial I}{\partial e_b} = \left(\frac{R_h}{R_s \cdot (R_h + R_s)} \right) \cdot \left(\frac{W_0(\theta)}{1 + W_0(\theta)} \right) + \left(\frac{1}{R_h + R_s} \right) + \left(\frac{I_{sat,db}}{V_{t,db}} \right) \cdot \exp\left(\frac{e_b - e_a}{V_{t,db}}\right) \quad (4-25)$$

The values of I_{ph} , I_{sat} , n , R_s , R_h , $I_{sat,db}$ and n_{db} can be calculated by means of systematic procedures as the ones introduced in [111], [27], [87], which use the datasheet information of a PV panel and the bypass diode as well as the weather conditions. The parameters n , R_s , R_h , $I_{sat,db}$ and n_{db} can be considered constant while I_{ph} and I_{sat} depend on the irradiance S and temperature T as shown in (4-26) and (4-27).

$$I_{sat} = \frac{I_{sc,STC} + K_{Isc} \cdot (T - T_{STC})}{\exp((V_{oc,STC} + K_{Voc} \cdot (T - T_{STC}))/V_t) - 1} \quad (4-26)$$

$$I_{ph} = (S/S_{STC}) (I_{ph,STC} + K_{Isc} \cdot (T - T_{STC})) \quad (4-27)$$

In (4-26) and (4-27), $I_{sc,STC}$ and $I_{ph,STC}$ are the short-circuit current and photovoltaic current in standard test conditions (STC), respectively, $V_{oc,STC}$ is the open-circuit voltage in STC, K_{Isc} and K_{Voc} are the temperature coefficients of the short-circuit current and open-circuit voltage, respectively, T_{STC} is the module temperature in STC in Kelvin degrees and S_{STC} is the STC irradiance.

4.4.2. Identification of independent sub-arrays and their parameters

The ties between consecutive strings of an $(N \times M)$ array are defined by an $(N - 1) \times (M - 1)$ matrix named connection matrix (M_{conn}), which is filled with ones and zeros to describe the presence or absence of ties, respectively. The column j of M_{conn} describes the connections between the strings j and $j + 1$ of the array. A one/zero in the row i and column j of M_{conn} (i.e. $M_{conn}(i, j)$) indicates a connection/no connection between the negative terminals of the modules (i, j) and $(i, j + 1)$ of the array. In this procedure a sub-array is defined as a string or set of strings that has no ties with other strings to the left and to the right; hence, the sub-arrays can be identified by using M_{conn} . If the column j of M_{conn} is a column of zeros, then there is no connection between strings j and $j + 1$ of the array; therefore, by examining M_{conn} from left to right, each column of zeros indicates the end of a sub-array and the start of the next one. From this analysis it is possible to define the number of sub-arrays in a PV array (N_{sa}) as show in (4-28), where N_z is the number of columns of zeros in M_{conn} .

$$N_{sa} = N_z + 1 \quad (4-28)$$

In the proposed model each sub-array is analyzed independently, hence it is necessary to define the SD model parameters and the connection matrix of each sub-array. Initially the seven parameters required for each PV module (I_{ph} , I_{sat} , V_t , R_s , R_h , $I_{sat,bd}$ and $V_{t,bd}$) are introduced in seven ($N \times M$) matrices: $M_{I_{ph}}$, $M_{I_{sat}}$, M_{V_t} , M_{R_s} , M_{R_h} , $M_{I_{sat,bd}}$, $M_{V_{t,bd}}$. Then, from such matrices it is necessary to extract the parameters matrices for each sub-array. All the sub-arrays have the same number of rows, therefore, to identify the parameters and connection matrices of sub-array i it is only necessary to identify its first ($SA_{fc,i}$) and the last ($SA_{lc,i}$) column. Such an identification uses the vector defined in (4-29), where the first and last elements are 0 and M , respectively, while the rest of the elements correspond to the index of each column of zeros in the connection matrix. Then, $SA_{fc,i}$ and $SA_{lc,i}$ are defined as shown in (4-30).

Finally, the parameters ($M_{I_{ph},i}^{sa}$, $M_{I_{sat},i}^{sa}$, $M_{V_t,i}^{sa}$, $M_{R_s,i}^{sa}$, $M_{R_h,i}^{sa}$, $M_{I_{sat,bd},i}^{sa}$, $M_{V_{t,bd},i}^{sa}$) and connection ($M_{conn,i}^{sa}$) matrices of the sub-array i are introduced in (4-31), and (4-32), respectively. Note that in (4-31) and (4-32) the superscript sa indicates that the matrix corresponds to a sub-array, moreover the dimensions of parameters and connection matrices are ($N \times M_{sa,i}$) and $(N - 1) \times (M_{sa,i} - 1)$, respectively, with $M_{sa,i} = SA_{lc,i} - SA_{fc,i} + 1$. Finally, if a sub-array has only one column the connection matrix is a column of $N - 1$ zeros, because there is not any connection with other strings.

$$C_z = [0 \quad Z_{c,1} \quad \dots \quad Z_{c,i} \quad \dots \quad Z_{c,N_{sa}} \quad M] \quad (4-29)$$

$$SA_{fc,i} = C_z(i) + 1, \quad SA_{lc,i} = C_z(i + 1) \quad (4-30)$$

$$\begin{aligned} M_{I_{ph},i}^{sa} &= M_{I_{ph}}(r, c), \quad M_{I_{sat},i}^{sa} = M_{I_{sat}}(r, c), \quad M_{V_t,i}^{sa} = M_{V_t}(r, c), \\ M_{R_s,i}^{sa} &= M_{R_s}(r, c), \quad M_{R_h,i}^{sa} = M_{R_h}(r, c), \quad M_{I_{sat,bd},i}^{sa} = M_{I_{sat,bd}}(r, c), \\ M_{V_{t,bd},i}^{sa} &= M_{V_{t,bd}}, \quad \forall r \in [1 \dots N], \quad c \in [SA_{fc,i} \dots SA_{lc,i}] \end{aligned} \quad (4-31)$$

$$\begin{aligned} M_{conn,i}^{sa} &= M_{conn}(r_c, c_c), \\ &\forall r_c \in [1 \dots (N - 1)], \quad c_c \in [SA_{fc,i} \dots (SA_{lc,i} - 1)] \end{aligned} \quad (4-32)$$

4.4.3. Calculation of the sub-array current

All the sub-arrays in the ($N \times M$) array are connected in parallel, which implies they are subjected to the same array voltage (V_{array}). This section shows the proposed procedure to calculate the output current of a sub-array i ($I_{sa,i}$) for a given V_{array} . The basic idea is to use nodal analysis to obtain the node voltages in the sub-array, then the sub-array currents of the modules in the first row are calculated, and, in the end, those currents are

added to obtain $I_{sa,i}$. Considering that each sub-array is independent from the others, the sub-array i can be analyzed as an $(N \times M_{sa,i})$ array without internal sub-arrays, where $M_{sa,i} = SA_{lc,i} - SA_{fc,i} + 1$, according to the explanation given in Section 4.4.2. The number of nodes of sub-array i ($N_{n,i}$) is calculated as shown in (4-33), where $N_{t,i}$ is the sum of all the elements of $M_{conn,i}^{sa}$ as described in (4-34). Therefore, in the sub-array i there are $N_{n,i}$ unknown node voltages: $e_{j,i}$ for $j \in [1 \dots N_{n,i}]$, which form the sub-array node voltage vector $V_{n,i}$. The numbering of the node voltages in $V_{n,i}$ is performed from top to bottom and from left to right examining $M_{conn,i}^{sa}$.

$$N_{n,i} = [(N - 1) \cdot M_{sa,i}] - N_{t,i} \quad (4-33)$$

$$N_{t,i} = \sum_{k_2=1}^{M_{sa,i}-1} \sum_{k_1=1}^{N-1} M_{conn,i}^{sa}(k_1, k_2) \quad (4-34)$$

To apply KCL to each node in the sub-array, the current of each module need to be calculated using (4-23). Hence, it is necessary to identify the sub-array node voltage where the positive ($e_a(r, c)$) and negative ($e_b(r, c)$) terminals of the module in row r and column c (i.e. module (r, c)) are connected to. Such an identification is performed using $M_{conn,i}^{sa}$ and knowing that the top and bottom nodes voltages are V_{array} and zero, respectively. To associate each terminal voltage to its corresponding node voltage, the identification is performed through a $(N - 1) \times M_{sa,i}$ matrix ($M_{nv,i}^{sa}$); each column of the $M_{nv,i}^{sa}$ matrix contains the number of the nodes of each column of the sub-array from top to bottom and from left to right. In this way the element $M_{nv,i}^{sa}(r, c)$ contain the number of the node voltage of $e_b(r, c)$, i.e. $M_{nv,i}^{sa}(r, c) = a$ means $e_b(r, c) = V_{n,i}(a) = e_{a,i}$. On the other hand, the element $M_{nv,i}^{sa}(r, c)$ contain the number of the node voltage of $e_a(r + 1, c)$, i.e. $M_{nv,i}^{sa}(r, c) = a$ means $e_a(r + 1, c) = V_{n,i}(a) = e_{a,i}$. The system of $N_{n,i}$ non-linear equations of the sub-array i ($F_i(V_{n,i})$) is obtained by applying KCL to each node of the sub-array, where the unknown variables are the node voltages in $V_{n,i}$ vector. To solve $F_i(V_{n,i})$ by means of the Trust-Region Dogleg or a similar method, it is necessary to define the Jacobian matrix $J_i(V_{n,i})$, which has a dimension $(N_{n,i} \times N_{n,i})$. Both, $F_i(V_{n,i})$ and $J_i(V_{n,i})$, depend on the configuration of the sub-array specified in $M_{conn,i}^{sa}$; therefore, it is not possible to define a general structure for $F_i(V_{n,i})$ and $J_i(V_{n,i})$. Instead, this procedure provides a general procedure for calculating $F_i(V_{n,i})$ and $J_i(V_{n,i})$, which is described in *Algorithm 1*.

In such an algorithm i_f , n_n and j_c are auxiliary variables introduced to simplify the writing of the pseudocode. The *for* loops in lines 2 and 3 go over the nodes of the sub-array from top to bottom and from left to right. Line 4 identifies if a node has been analyzed or not. Then, $SA_{fc,i}$ and $SA_{lc,i}$ for a given node need to be identified. Lines 6 to 10 calculate the current of the module above the analyzed node ($I_{r,c}$), calculating also its partial derivatives ($\partial I_{r,c} / \partial e_a(r, c)$, and $\partial I_{r,c} / \partial e_b(r, c)$) for the module above the analyzed node. The same process is performed for the module bellow the analyzed node in lines 11 to 15. The process

is repeated for the other modules connected to the analyzed node (*for loop* between lines 5 and 16).

Finally, the process described above is repeated for each sub-array node by means of the *for loop* between lines 2 and 20. The node voltages of the sub-array are obtained solving $F_i(V_{n,i})$ with a numerical method that iteratively evaluates $F_i(V_{n,i})$ and $J_i(V_{n,i})$.

Algorithm 1 Calculation of $F_i(V_{n,i})$ and $J_i(V_{n,i})$

INPUT: V_{array} , $V_{n,i}$, $N_{n,i}$, $M_{nv,i}^{sa}$, $M_{conn,i}^{sa}$, sub-array parameters' matrices

OUTPUT: $F_i(V_{n,i})$ and $J_i(V_{n,i})$

```

1: Set  $i_f = 1$ 
2: for node  $j = 1$  to  $M_{sa,i}$  do
3:   for node  $i = 1$  to  $N - 1$  do
4:     if  $j = 1$  OR  $M_{conn,i}^{sa}(i, j - 1) = 0$  then: Identify  $SA_{fc,i}$  and  $SA_{lc,i}$  from  $M_{conn,i}^{sa}$ 
5:     for column  $j_c = SA_{fc,i}$  to  $SA_{lc,i}$  do
6:       Set  $n_n = M_{nv,i}^{sa}(i, j_c)$ ,  $e_b(i, j_c) = V_{n,i}(n_n)$ 
7:       if  $i = 1$  then:  $e_a(i, j_c) = V_{array}$ 
8:       else: Set  $n_n = M_{nv,i}^{sa}(i - 1, j_c)$ , and  $e_a(i, j_c) = V_{n,i}(n_n)$ . Calculate  $\partial I_{i,j_c} / \partial e_a(i, j_c)$ 
       with (4-24). Set  $J_i(i_f, n_n) = J_i(i_f, n_n) + \partial I_{i,j_c} / \partial e_a(i, j_c)$ 
9:     end if


---


10:    Calculate  $\partial I_{i,j_c} / \partial e_b(i, j_c)$  with (4-25),  $I_{i,j_c}$  with (4-23). Set  $n_n = M_{nv,i}^{sa}(i, j_c)$ ,
     $J_i(i_f, n_n) = J_i(i_f, n_n) + \partial I_{i,j_c} / \partial e_b(i, j_c)$ ,  $F_i(i_f) = F_i(i_f) + I_{i,j_c}$ 
11:    Set  $n_n = M_{nv,i}^{sa}(i, j_c)$ ,  $e_a(i + 1, j_c) = V_{n,i}(n_n)$ 
12:    if  $i = N - 1$  then:  $e_b(i + 1, j_c) = 0$  [V]
13:    else: Set  $n_n = M_{nv,i}^{sa}(i + 1, j_c)$ ,  $e_b(i + 1, j_c) = V_{n,i}(n_n)$ . Calculate  $\partial I_{i+1,j_c} / \partial e_b(i + 1, j_c)$ 
    with (4-25). Set  $J_i(i_f, n_n) = J_i(i_f, n_n) - \partial I_{i+1,j_c} / \partial e_b(i + 1, j_c)$ 
14:    end if
15:    Calculate  $\partial I_{i+1,j_c} / \partial e_a(i + 1, j_c)$  with (4-24),  $I_{i+1,j_c}$  with (4-23). Set  $n_n =$ 
     $M_{nv,i}^{sa}(i, j_c)$ ,  $J_i(i_f, n_n) = J_i(i_f, n_n) - \partial I_{i+1,j_c} / \partial e_a(i + 1, j_c)$  and  $F_i(i_f) = F_i(i_f) - I_{i+1,j_c}$ 
16:    end for
17:    Set  $i_f = i_f + 1$ 
18:  end if
19: end for
20: end for
21: Return  $F_i(V_{n,i})$  and  $J_i(V_{n,i})$ 

```

The solution of the systems of non-linear equations obtained with the proposed method

require an algorithm able to guarantee global convergence such as the Line-Search or Trust-Region methods [70]. In this procedure the Trust-Region Dogleg method has been used due to its better convergence rate in comparison with other methods for instance the Trust-Region Reflective or Levenberg-Marquardt methods. The Trust-Region Dogleg method is not presented in this document, since it is deeply described in [70].

Once the node voltages of the sub-array are known, it is simple to calculate the current $I_{sa,i}$ by using (4-35), where $e_a(1, c)$ and $e_b(1, c)$ are the e_a and e_b voltages of the module in the first row of column c in the sub-array.

$$I_{sa,i} = \sum_{c=1}^{M_{sa,i}} I(e_a(1, c), e_b(1, c)) \quad (4-35)$$

4.4.4. Calculation of the array current

The array current (I_{array}) for a given V_{array} is obtained by adding the sub-arrays currents as shown in (4-36), where N_{sa} is the number of sub-arrays defined in (4-28). At this point the model of a PV array with any configuration is complete and it can be used for different applications. For example, it can be used for the reconstruction of the I-V or P-V curves, estimation of the array energy production, dynamic simulations to evaluate MPPT techniques, among others. Finally, the flow chart presented in Fig. 4-13 summarizes the proposed modeling procedure to calculate the array current for a given array voltage.

$$I_{array} = \sum_{i=1}^{N_{sa}} I_{sa,i} \quad (4-36)$$

4.4.5. Application example of the proposed procedure

In this Section the irregular 3×3 PV array, shown in Fig. 4-14, is modeled with the procedure previously described to illustrate the application of the proposed solution. By using this pilot example, with the PV array configuration shown in Fig. 4-14, the general procedure is applied to a practical case. In such an array $N = 3$ and $M = 3$, hence, the seven parameters of the SD model are stored 3×3 matrices and M_{conn} is a 2×2 matrix as shown in (4-37). The array voltage can be settled according to the operating condition to be analyzed. In (4-37) it can be observed that M_{conn} has one column of zeros (column 2); therefore, $N_{sa} = 2$ according to (4-28), and C_z is written as shown in (4-38) according to (4-29). The array in this example has two sub-arrays named SA_1 and SA_2 . The first and last columns of SA_1 and SA_2 are calculated by using (4-30) with: $SA_{fc,1} = 1$, $SA_{lc,1} = 2$

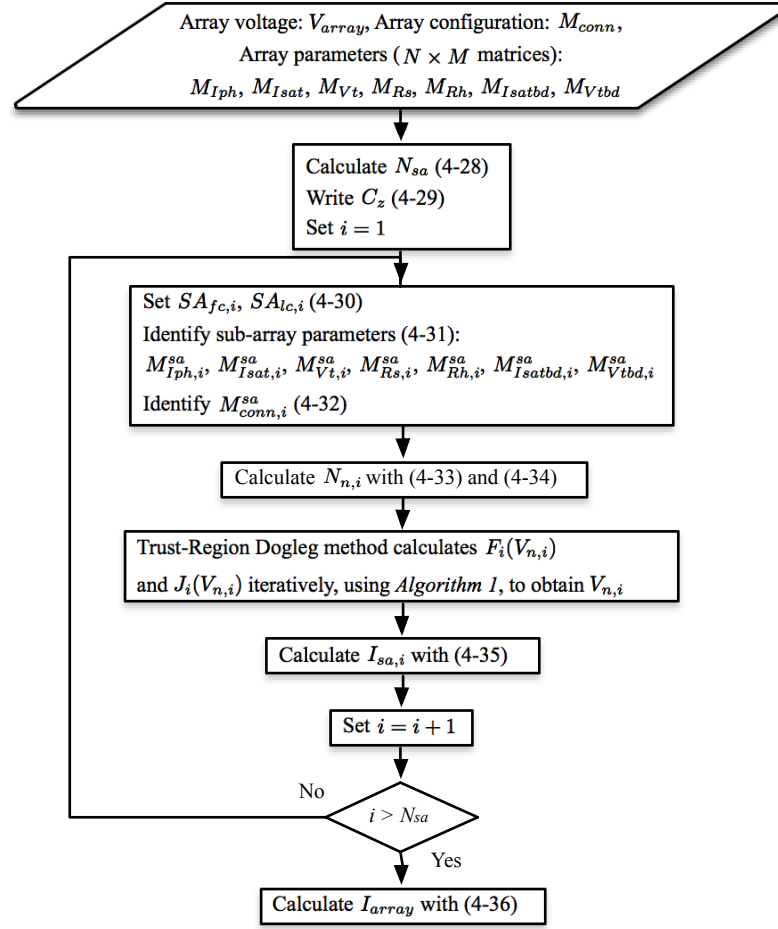


Figure 4-13.: Flow chart of the proposed model.

(4-39) and $SA_{fc,2} = 3$ and $SA_{lc,2} = 3$ (4-40), respectively. Fig. ?? shows each sub-array with their respective nodes voltages, and modules terminal voltages as well as currents.

$$M_{conn} = \underbrace{\begin{bmatrix} 1 & 0 \\ 1 & 0 \end{bmatrix}}_{M_{conn,1}^{sa}} \underbrace{\begin{bmatrix} 0 & 0 \\ 0 & 0 \end{bmatrix}}_{M_{conn,2}^{sa}} \quad (4-37)$$

$$C_z = \begin{bmatrix} 0 & 2 & 3 \end{bmatrix} \quad (4-38)$$

$$SA_{fc,1} = 1 \quad SA_{lc,1} = 2 \quad (4-39)$$

$$SA_{fc,2} = 3 \quad SA_{lc,2} = 3 \quad (4-40)$$

The parameters matrices and connection matrix for each sub-array are obtained using (4-31) and (4-32), respectively. To illustrate this process, expression (4-41) shows M_{Iph} and the underbraces indicate the part of the matrix corresponding to $M_{Iph,1}^{sa}$ and $M_{Iph,2}^{sa}$. Following

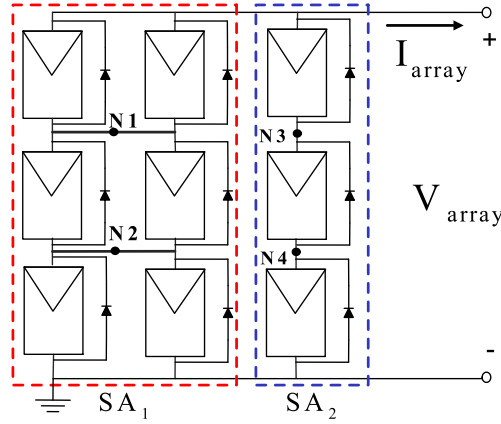


Figure 4-14.: 3×3 PV array used as example.

the same procedure, the rest of parameters matrices can be defined for each sub-array. The matrices $M_{conn,1}^{sa}$ and $M_{conn,2}^{sa}$ are illustrated with underbraces in (4-37). Then, $N_{n,1} = 2$ and $N_{n,2} = 2$ are calculated by applying (4-33) and (4-34) to $M_{conn,1}^{sa}$ and $M_{conn,2}^{sa}$, respectively.

$$M_{I_{ph}} = \begin{bmatrix} I_{ph,1,1} & I_{ph,1,2} & I_{ph,1,3} \\ I_{ph,2,1} & I_{ph,2,2} & I_{ph,2,3} \\ I_{ph,3,1} & I_{ph,3,2} & I_{ph,3,3} \end{bmatrix} \quad (4-41)$$

$\underbrace{\hspace{10em}}_{M_{I_{ph},1}^{sa}} \quad \underbrace{\hspace{10em}}_{M_{I_{ph},2}^{sa}}$

In SA_1 and SA_2 the unknown voltages to solve are $V_{n,1} = [e_{1,1} \ e_{2,1}]$ and $V_{n,2} = [e_{1,2} \ e_{2,2}]$. Before applying the Trust-Region Dogleg method to solve $V_{n,1}$ and $V_{n,2}$ it is necessary to define $M_{nv,1}^{sa}$ and $M_{nv,2}^{sa}$. Following the description introduced in Section 4.4.3 those matrices are obtained and reported in (4-42). At this point, all the data required by *Algorithm 1* to calculate $F_1(V_{n,1})$, $J_1(V_{n,1})$, $F_2(V_{n,2})$, and $J_2(V_{n,2})$ have been constructed.

$$M_{nv,1}^{sa} = \begin{bmatrix} 1 & 1 \\ 2 & 2 \end{bmatrix} \quad M_{nv,2}^{sa} = \begin{bmatrix} 1 \\ 2 \end{bmatrix} \quad (4-42)$$

To illustrate the application of the procedure described in *Algorithm 1*, the structures of $F_1(V_{n,1})$ and $J_1(V_{n,1})$ are presented in (4-43) and (4-44) respectively, while (4-45) and (4-46) present the structures of $F_2(V_{n,2})$, and $J_2(V_{n,2})$.

$$F_1(V_{n,1}) = \begin{bmatrix} I_{1,1}(V_{array}, e_{1,1}) - I_{2,1}(e_{1,1}, e_{2,1}) + I_{1,2}(V_{array}, e_{1,1}) - I_{2,2}(e_{1,1}, e_{2,1}) \\ I_{2,1}(e_{1,1}, e_{2,1}) - I_{3,1}(e_{2,1}, 0) + I_{2,2}(e_{1,1}, e_{2,1}) - I_{3,2}(e_{2,1}, 0) \end{bmatrix} \quad (4-43)$$

$$J_1(V_{n,1}) = \begin{bmatrix} \frac{\partial I_{1,1}}{\partial e_b(1,1)} - \frac{\partial I_{2,1}}{\partial e_a(2,1)} + \frac{\partial I_{1,2}}{\partial e_b(1,2)} - \frac{\partial I_{2,2}}{\partial e_a(2,2)} & -\frac{\partial I_{2,1}}{\partial e_b(2,1)} - \frac{\partial I_{2,2}}{\partial e_b(2,2)} \\ \frac{\partial I_{2,1}}{\partial e_a(2,1)} + \frac{\partial I_{2,2}}{\partial e_a(2,2)} & \frac{\partial I_{2,1}}{\partial e_b(2,1)} - \frac{\partial I_{3,1}}{\partial e_a(3,1)} + \frac{\partial I_{2,2}}{\partial e_b(2,2)} - \frac{\partial I_{3,2}}{\partial e_a(3,2)} \end{bmatrix} \quad (4-44)$$

$$F_2(V_{n,2}) = \begin{bmatrix} I_{1,3}(V_{array}, e_{1,2}) - I_{2,3}(e_{1,2}, e_{2,2}) \\ I_{2,3}(e_{1,2}, e_{2,2}) - I_{3,3}(e_{2,2}, 0) \end{bmatrix} \quad (4-45)$$

$$J_2(V_{n,2}) = \begin{bmatrix} \frac{\partial I_{1,3}}{\partial e_b(1,3)} - \frac{\partial I_{2,3}}{\partial e_a(2,3)} & -\frac{\partial I_{2,3}}{\partial e_b(2,3)} \\ \frac{\partial I_{2,3}}{\partial e_a(2,3)} & \frac{\partial I_{2,3}}{\partial e_b(2,3)} - \frac{\partial I_{3,3}}{\partial e_a(3,3)} \end{bmatrix} \quad (4-46)$$

By applying the Trust-Region Dogleg method to $F_1(V_{n,1})$ and $F_2(V_{n,2})$, the node voltages of each sub-array ($V_{n,1}$ and $V_{n,2}$) are solved, then $I_{sa,1}$ and $I_{sa,2}$ are obtained using (4-35). Finally, I_{array} is calculated from (4-36), which enables to reproduce the electrical behavior of the PV array at the voltage V_{array} .

4.4.6. Validation of the proposed procedure

The modeling procedure was implemented in *C* language using the GNU Scientific Library (GSL) [1] to calculate the Lambert-W function and to perform operations with vectors and matrices. In this procedure the Trust-Region Dogleg method [70] was implemented in *C*. This section presents simulation and experimental results validating the proposed model for SP, TCT and BL arrays formed with PV panels of two modules each, as well as a practical application of the model in reconfiguration.

To evaluate the performance of the proposed procedure, simulations and experimental tests were made with a (3×3) array connected in SP, TCT, and BL configurations. Such configurations were formed using nine JS65 Yingli Solar PV panels, whose main electrical characteristics were obtained from the manufacturer datasheet [102]. The required parameters were calculated using the procedure introduced in [111] and [27] obtaining the following data at STC: $I_{ph} = 3,557 \text{ A}$, $I_{sat} = 25,183 \mu\text{A}$, $V_t = 0,842 \text{ V}$, $R_s = 0,347 \Omega$, $R_h = 202,237 \Omega$. The bypass diode parameters are $I_{sat,bd} = 48,804 \mu\text{A}$ and $V_{t,bd} = 0,141 \text{ V}$. In addition, different irradiance profiles were introduced by modifying the I_{ph} value of each module, this taking advantage that I_{ph} is directly proportional to the irradiance [111],[27].

Each JS65 PV panel has two modules (two bypass diodes), each one with 18 cells connected in series and a bypass diode connected in anti-parallel. Since the PV array connections are made at panel level the TCT and BL configurations are, in fact, irregular configurations in terms of modules. Indeed the connection points between two consecutive modules inside a PV panel are not accessible, so the connection becomes irregular when the consecutive modules in a panel work in mismatched conditions. Instead, the SP configuration can be considered a regular structure at both panel and module levels. The modeled SP, TCT and BL configurations are illustrated in Fig. ??, where the PV panels are represented by dashed rectangles.

In addition, the experimental platform also includes an electronic load BK8510 and a switching matrix as it is shown in Fig. 4-15; the switching matrix enables to change the connection between the PV panels to form the SP, TCT and BL structures.

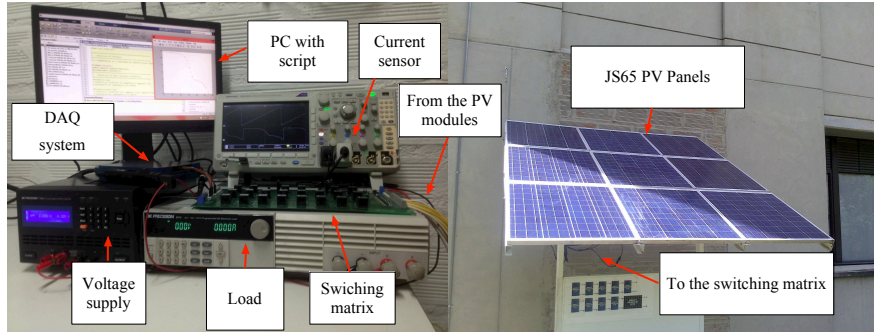


Figure 4-15.: Experimental platform

Two irradiance profiles were considered: one profile to obtain two LMPPs in the P-V curve of SP, TCT, and BL arrays: and another profile to obtain three LMPPs in the P-V curve of SP configuration. The irradiance profiles are described in Table 4-1, where the values represent the percentage of I_{ph} under STC for each module in the array. Fig. ?? and Fig. ?? present the I-V and P-V curves obtained with the proposed model, the experimental platform, and the circuitual implementation of the arrays in Simulink/SimElectronics toolbox, for the two mismatching profiles. The results put into evidence the usefulness and correctness of the proposed model in the reproduction of the I-V and P-V curves of irregular and regular PV array configurations. The appendix A reports the system of equations and Jacobian matrix, evaluated for the SP configuration, to illustrate the calculation of the nodes voltages of a sub-array. Similar systems of equations are obtained for the other configurations (TCT and BL)

Table 4-1.: Percentage values of I_{ph} for experimental tests.

| Mismatching 1 [%] | | | Mismatching 2 [%] | | |
|-------------------|-----|-----|-------------------|-----|-----|
| 100 | 100 | 100 | 100 | 100 | 100 |
| 100 | 100 | 100 | 100 | 100 | 100 |
| 100 | 100 | 100 | 30 | 100 | 100 |
| 100 | 100 | 100 | 30 | 100 | 100 |
| 4.5 | 4.5 | 100 | 55 | 70 | 10 |
| 4.5 | 4.5 | 100 | 55 | 70 | 10 |

The MAPE (4-19) has been evaluated in order to compare the difference in the prediction of the current (E_i), power (E_P) and GMPP (E_{GMPP}) of the proposed model with respect to

the experimental results. Table 4-2 shows E_i , E_P and E_{GMPP} for Mismatching 1 (SP, TCT and BL configurations) and Mismatching 2 (SP configuration), as well as the processing time required to process both the proposed model (t_{mod}) and circuital implementation in Simulink/SimElectronics toolbox (t_{sim}). The simulations were performed on an Intel Core i5 2,7 GHz computer.

Table 4-2.: Mean absolute percentage errors and execution times for experimental tests.

| | Mismatching 1 | | | Mismatching 2 |
|----------------|-----------------------|-----------------------|-----------------------|-----------------------|
| | SP | TCT | BL | SP2 |
| E_i [%] | 1.52 | 1.52 | 1.46 | 1.24 |
| E_P [%] | 1.51 | 1.50 | 1.45 | 1.22 |
| E_{GMPP} [%] | 1.14 | 1.17 | 1.17 | 1.23 |
| t_{mod} [s] | 1.22×10^{-2} | 1.17×10^{-2} | 1.30×10^{-2} | 1.35×10^{-2} |
| t_{sim} [s] | 4.47 | 4.85 | 3.53 | 4.16 |

Those results put into evidence the satisfactory performance of the proposed model in the reproduction of regular and irregular PV arrays operating under mismatching conditions. The results also show a reduction in two orders of magnitude in the processing time with respect to the circuital implementation of a PV array in a commercial software.

4.4.7. Application example: PV array reconfiguration

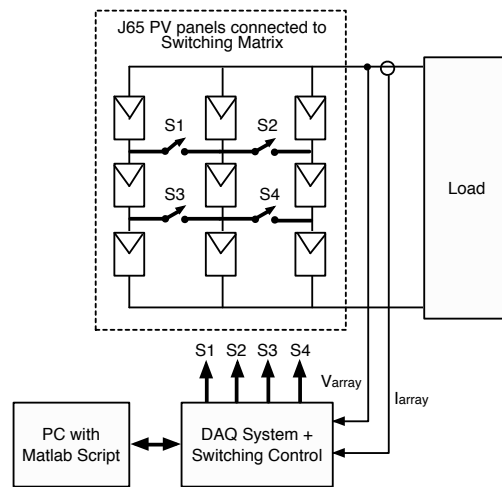
In actual power plants SP and TCT configurations are widely used and under uniform conditions both configurations provide nearly the same power [6], [60]. The authors of [7], [59] show that TCT configurations exhibit better performance under some particular partial shading conditions; however, the authors of [88] and [52] use different shading profiles and array sizes to conclude that HC and BL are better options to mitigate the effects of partial shading on PV arrays. Hence, it is difficult to generalize that a single configuration is better for any shading pattern or array size. A better option is to simulate the particular PV system accounting for different possible configurations and shading profiles to select the most efficient one for that particular case. This subsection uses the proposed mathematical model to compare the performance of SP, TCT and BL configurations (using the PV array of section 4.4.6), under different partial-shading patterns presented in Table 4-3. This confirms the usefulness of the proposed modeling procedure.

The P-V curves of the three configurations (SP, TCT, and BL) for each shading profile (shading profile 1, 2 and 3), obtained with the proposed model, are presented in Fig. ???. For shading profile 1 (Fig. ??) SP configuration provides the highest GMPP power, while for shading profiles 2 (Fig. ??) and 3 (Fig. ??) the highest GMPP power is provided by BL and TCT configurations, respectively. This confirms that there is not a single configuration

Table 4-3.: Mismatching profiles for the evaluation of PV configurations.

| Profile 1 [W/m^2] | | | Profile 2 [W/m^2] | | | Profile 3 [W/m^2] | | |
|-----------------------|-----|-----|-----------------------|-----|-----|-----------------------|-----|-----|
| 500 | 560 | 80 | 620 | 680 | 330 | 60 | 90 | 100 |
| 470 | 830 | 600 | 930 | 60 | 760 | 310 | 8 | 620 |
| 780 | 720 | 640 | 230 | 250 | 660 | 760 | 410 | 120 |
| 220 | 570 | 700 | 660 | 220 | 7 | 680 | 640 | 130 |
| 480 | 240 | 870 | 280 | 650 | 590 | 120 | 700 | 96 |
| 880 | 650 | 960 | 660 | 830 | 380 | 130 | 520 | 140 |

providing the best operation conditions for all the shading patterns. In order to maximize the produced power, SP configuration should be set when shading profile 1 is present, and BL and TCT configurations should be set when shading profiles 2 and 3 appear, respectively. To experimentally test the model predictions, the prototype designed for this particular example enables to settle SP, TCT and BL configurations by means of a switching matrix. It receives a digital signal from a Digital Acquisition system (DAQ) interfacing a processing device (e.g. a PC with Matlab) as presented in Fig. 4-16. The control of the switching matrix is performed in Matlab so that the SP, TCT and BL configuration are selected.

**Figure 4-16.:** Basic structure of the system for evaluating PV configurations.

The experimental results are presented in Fig. 4-17, where the array voltage, current and power are measured at the output of the switching matrix. At the beginning of Fig. 4-17 the shading profile 1 is imposed, therefore, the reconfiguration system sets the best configuration (SP) and the array power (162 W) and voltage (45 V) correspond to the GMPP of the SP configuration shown in Fig. ???. From the time 0,17 s to 0,7 s, shading profile 2 is imposed and the best configuration is BL, hence the array power (132 W) and voltage (35 V) correspond to the GMPP highlighted in Fig. ???. For the last part of the experiment the best configuration

is TCT because the shading profile 3 is imposed, hence the array power (70 W) and voltage (42 V) are in agreement with Fig. ??.

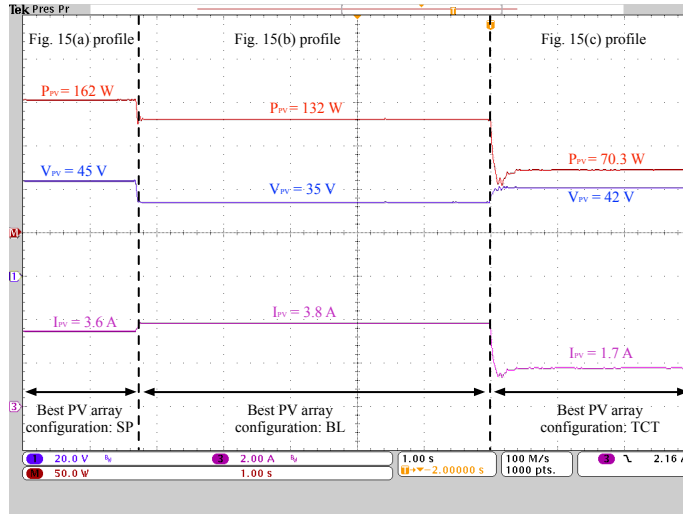


Figure 4-17.: Experimental results of the pre-calculated PV array reconfiguration process.

This experiment confirms the model predictions, hence the best connection depends on the particular operating conditions of the PV array. Moreover, those results put into evidence the applicability of the proposed model for evaluating PV configurations in real-time, so that new reconfiguration algorithms can be designed to reduce the impact of partial-shading.

4.5. General procedure for modeling PV arrays based on mesh currents analysis

In the previous section a modeling procedure for modeling any PV array was introduced. Such a procedure is based on dividing the PV array into sub-arrays, which are defined as a sub-set of the PV array that do not interact with the rest of the array, hence, it can be solved independently. Each sub-array is analyzed by using nodal analysis to create a system of nonlinear equations assuming the array voltage is known, since it is usually defined by the power convert. Such a system of nonlinear equations is solved by using a numerical method to obtain the sub-array current. Finally, all the sub-array currents are added to obtain the array current. Nevertheless, when the number of nodes in the sub-array is higher than the number of meshes, the system of nonlinear equations obtained with nodal analysis is larger than the number of equations obtained with mesh analysis; as consequence, the complexity and the calculation burden required to solve the nonlinear equation system are increased.

This section introduces a modeling procedure for calculating the current of any regular or irregular PV array configuration formed by N rows and M columns of panels ($N \times M$)

operating under uniform or partial shading conditions. The proposed approach divides the array into sub-arrays that can be solved independently but if the number of mesh currents in the sub-array is less than the number of the nodes voltages, then the sub-array is solved by using mesh analysis to calculate the sub-array current, which is the main contribution of the procedure introduced in this section. However, if the number of node voltages is lower than the number of mesh currents, the sub-array is solved by using the procedure presented in the previous section [11]. In this way, it is possible to solve each sub-array with the minimum number of nonlinear equations, which leads to a reduction in the calculation burden and time.

The modeling procedure introduced in this section is explained through a pilot example consisting in a small PV array. For validation purposes, simulation and experimental tests were performed: simulations consider a 10×5 PV array connected in SP and irregular configurations [66] exposed to partial shading conditions. On the other hand, the experimental tests were performed in a 3×3 PV array connected in SP, TCT, BL and irregular configurations operating under partial shading conditions. The following sub-sections describe the details of the proposed modeling approach for complementing the procedure introduced in the previous section [11].

4.5.1. PV module model

As in Section 4.4, the single diode model (SD) is adopted to represent the PV module. Fig. 4-18 shows the equivalent circuit, including the bypass diode, which must be considered when the modules operate under partial shading conditions. In the circuit, the current source I_{ph} represents the photovoltaic current, the diode D models the P-N junction nonlinear behavior, and the resistances R_h and R_s represent the leakage currents and ohmic losses, respectively.

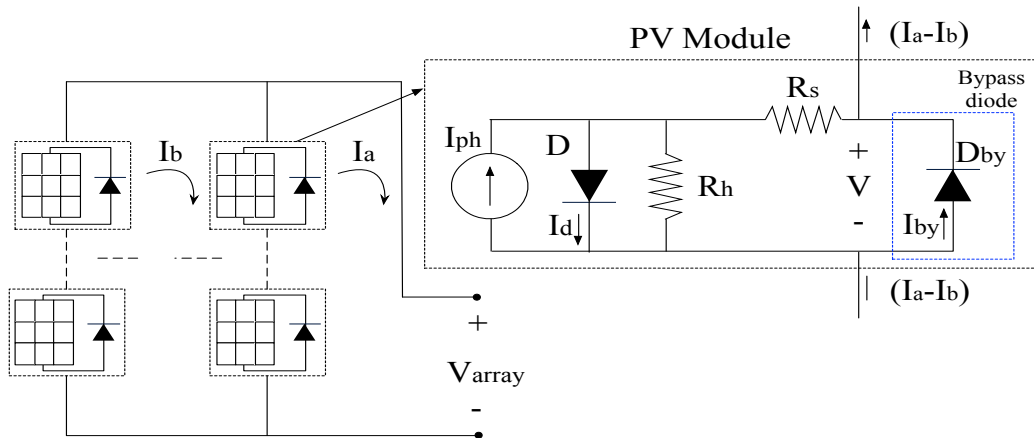


Figure 4-18.: Single diode model equivalent circuit including the bypass diode D_{by} and meshes currents.

When a module is connected into an array it will be shared by two meshes (see Fig. 4-18),

the one at the left and the one at the right of the module. By applying Kirchhoff's voltage (KVL) and current (KCL) laws, it is possible to define the relationship between the module voltage (V) and the mesh currents at the right (I_a) and at the left (I_b) of the PV module, as shown in (4-47), where I_{sat} is the inverse saturation current of the PV module diode, N_s is the number of series-connected cells into the module and $\beta = n \cdot k \cdot T_{pv}/q$, where n is the ideality factor, k is the Boltzmann constant, q is the electron charge, and T_{pv} is the module temperature in Kelvin. Moreover, $I_{sat,by}$ is the inverse saturation current of the bypass diode and $\beta_{by} = n_{by} \cdot k \cdot T_{by}/q$, where n_{by} is the ideality factor of the bypass diode and T_{by} is the bypass diode temperature in Kelvin.

$$(I_a - I_b) = I_{ph} - I_{sat} \cdot \left(\exp \left(\frac{V + (I_a - I_b - I_{by}) \cdot R_s}{N_s \cdot \beta} \right) - 1 \right) - \frac{V + (I_a - I_b - I_{by}) \cdot R_s}{R_h} + I_{sat,by} \cdot \left(\exp \left(\frac{-V}{\beta_{by}} \right) - 1 \right) \quad (4-47)$$

The values of the module parameters (I_{ph} , I_{sat} , n , R_s , R_h , $I_{sat,by}$ and n_{by}) are calculated by means of systematic procedures as the ones proposed in [111] and [27]. Such procedures consider the weather conditions (irradiance (S) and temperature (T)) and the electrical characteristics of the PV module taken from the manufacturer datasheet. Moreover, the works reported in [86, 8, ?]. Finally, the parameters n , R_s , R_h , $I_{sat,by}$ and n_{by} can be considered constant while I_{ph} and I_{sat} depend on S and T for each module [27]. It is worth noting that (4-47) is a not explicit and strongly non-linear function, hence it is not possible to express V as an explicit function of the mesh currents (i.e. I_a and I_b). Then, it is necessary to use a numerical method, like Newton-Raphson, to obtain V from (4-47).

4.5.2. Calculation of the sub-array current

As it was mentioned, this modeling procedure is also based in dividing the original PV array into small arrays named sub-arrays. Such sub-arrays are obtained with the same process described in sub-section 4.4.2 through (4-28) to (4-32). Then, after the sub-arrays and their parameters have been identified, the first step is to calculate the number of meshes in the SA_i ($N_{m,i}$). Analyzing its strings, from left to right, it is possible to identify that there is one mesh between two consecutive strings and each additional tie between two strings creates a new mesh. Moreover, the last string (from left to right) creates a mesh with the array input voltage (V_{array}). Hence, $N_{m,i}$ is calculated by adding the number of columns ($M_{sa,i}$) and the number of ties between the columns of the SA_i ($N_{t,i}$), respectively, where $N_{t,i}$ is obtained by adding the elements of $M_{conn,i}^{sa}$, as shown in (4.5) and (4-34). Therefore, the SA_i has $N_{m,i}$ unknown mesh currents, i.e. $I_{j,i}$ for $j \in [1 \cdots N_{m,i}]$, which form the sub-array mesh currents vector $I_{m,i}$. The numbering of the mesh currents in $I_{m,i}$ is obtained by examining the sub-array from top to bottom and from left to right, while the mesh currents' directions are selected clockwise.

$$N_{m,i} = M_{sa,i} + N_{t,i} \quad (4-48)$$

$$N_{t,i} = \sum_{k_2=1}^{M_{sa,i}-1} \sum_{k_1=1}^{N-1} M_{conn,i}^{sa}(k_1, k_2) \quad (4-49)$$

The second step is to calculate the voltage of each module in the SA_i ; hence, it is necessary to identify its mesh currents (i.e. the elements of $I_{m,i}$) to the left and to the right of each module. The mesh currents to the right and to the left of the module in row r and column c (i.e. module (r, c)) of SA_i are $I_a(r, c)$ and $I_b(r, c)$, respectively. The relation of $I_a(r, c)$ and $I_b(r, c)$ with the elements of $I_{m,i}$ is described by using an $N \times M_{sa,i}$ matrix ($M_{mc,i}^{sa}$), where the element (r, c) of $M_{mc,i}^{sa}$ (i.e. $M_{mc,i}^{sa}(r, c)$) contains the number of the mesh current at the right of the module (r, c) of SA_i . This is, $M_{mc,i}^{sa}(r, c) = a$ means that $I_a(r, c) = I_{m,i}(a) = I_{a,i}$. If $c > 1$, $M_{mc,i}^{sa}(r, c) = a$ also means that the mesh current at the left of the module $(r, c+1)$ is $I_b(r, c+1) = I_{m,i}(a) = I_{a,i}$. Moreover, currents to the left of the first column are zero, i.e. $I_b(r, 1) = 0$ A with $r \in [1 \dots N]$. Once I_a and I_b of each module have been identified, the voltage of each module in SA_i is calculated by solving (4-47).

The vector $F_{mesh,i}$ is obtained by applying KVL to each mesh in the sub-array. The element $F_{mesh,i}(m)$ results from applying the KVL to mesh m and the meshes are numbered from top to bottom and from left to right, in the same way the mesh currents were numbered. The evaluation of $F_{mesh,i}$ for a given set of unknown variables, i.e. a given $I_{m,i}$, can be implemented in a number of ways. The procedure used in this paper is summarized in *Algorithm 2* to simplify its implementation in different programming languages. In such an algorithm n_m is an auxiliary variable used to simplify the construction of the pseudocode. The *for* loops in lines 2 and 3 go over the columns and rows of SA_i , respectively, to identify the meshes currents affecting each module in the sub-array. Then, the current to the right of the module (i, j) ($I_a(i, j)$) is assigned by using $M_{mc,i}^{sa}$. The value of $I_b(i, j)$ is defined as 0 [A] for the first column of the array and it is defined by using $M_{mc,i}^{sa}$ for the other columns. With $I_a(i, j)$ and $I_b(i, j)$ defined, expression (4-23) is solved to obtain $V(i, j)$. Applying KVL in each mesh of SA_i it can be observed that $V(i, j)$ is negative for the mesh to the right of module (i, j) and positive for the mesh to the left of module (i, j) . This is implemented in lines 8, 12 and 13 of *Algorithm 2*. Finally, in the rightmost mesh V_{array} needs to be included with a positive sign.

Algorithm 2 Calculate the sub-array current $I_{sa,i}$

INPUT: V_{array} , $I_{m,i}$, $M_{mc,i}^{sa}$, $N_{m,i}$, $M_{sa,i}$, SA_i parameters matrices

OUTPUT: $F_{mesh,i}$

```

1: Set  $F_{mesh,i}(k) = 0 [V]$  with  $k \in [1, \dots, N_{m,i}]$ 
2: for  $j=1$  to  $M_{sa,i}$  do
3:   for  $i=1$  to  $N$  do
4:     Set  $n_m = M_{mc,i}^{sa}(i, j)$ ,  $I_a(i, j) = I_{m,i}(n_m)$ 
5:     if  $i = 1$  then
6:       Set  $I_b(i, j) = 0 [A]$ 
7:       Solve  $V(i, j)$  from (4-23) with  $I_a(i, j)$  and  $I_b(i, j)$ 
8:       Set  $F_{mesh,i}(n_m) = F_{mesh,i}(n_m) - V(i, j)$ 
9:     else
10:      Set  $n_m = M_{mc,i}^{sa}(i, j - 1)$ ,  $I_b(i, j) = I_{m,i}(n_m)$ 
11:      Solve  $V(i, j)$  from (4-23) with  $I_a(i, j)$  and  $I_b(i, j)$ 
12:      Set  $F_{mesh,i}(n_m) = F_{mesh,i}(n_m) + V(i, j)$ 
13:      Set  $n_m = M_{mc,i}^{sa}(i, j)$  and  $F_{mesh,i}(n_m) = F_{mesh,i}(n_m) - V(i, j)$ 
14:    end if
15:  end for
16: end for
17: Set  $F_{mesh,i}(N_{m,i}) = F_{mesh,i}(N_{m,i}) + V_{array}$ 

```

Once the optimization problem is defined, it is necessary to find the vector $I_{m,i}$ that minimizes $F_{mesh,i}$. In this section, such a vector is obtained by using Trust-Region Dogleg method, which requires the iterative evaluation of $F_{mesh,i}$ [71]. After $I_{m,i}$ has been found, $I_{sa,i}$ is defined as the current of the rightmost mesh in SA_i as shown in (4-50).

$$I_{sa,i} = I_{m,i}(N_{m,i}) \quad (4-50)$$

4.5.3. Calculate the array current

When all the sub-arrays' currents have been calculated for a given array voltage (V_{array}), the array current (I_{array}) is obtained by adding the sub-arrays currents as shown in (4-51), where N_{sa} is the number of sub-arrays. Fig. 4-19 shows the general flowchart of the approach presented in this paper integrated with the procedure introduced in [11].

$$I_{array} = \sum_{i=1}^{N_{sa}} I_{sa,i} \quad (4-51)$$

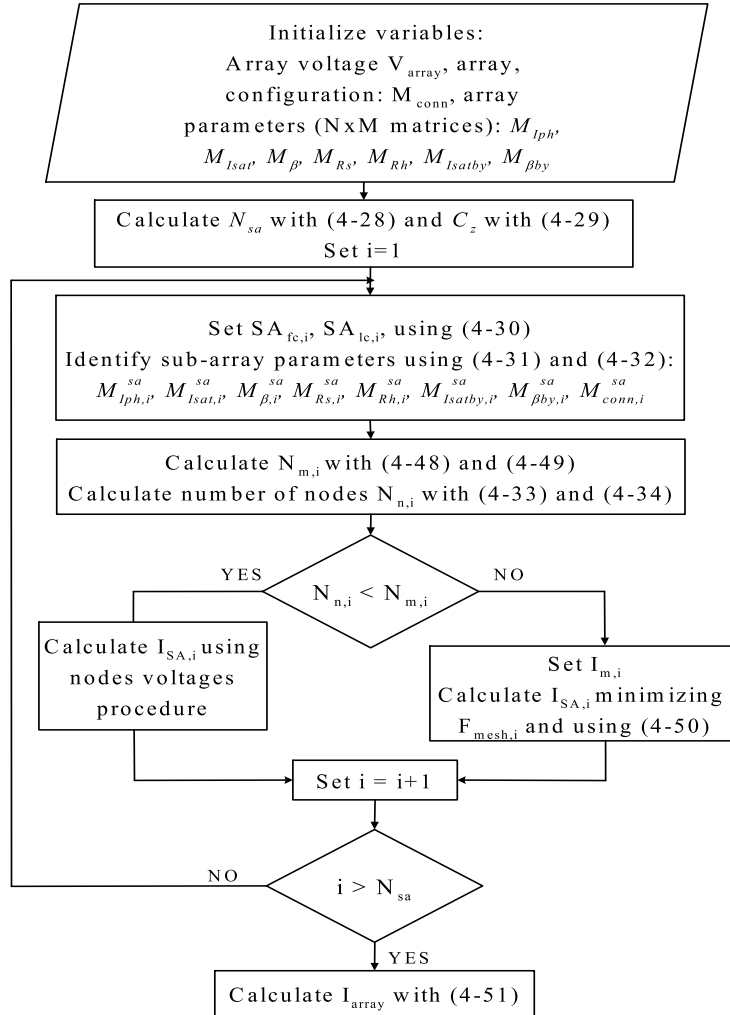


Figure 4-19.: Flowchart of the proposed modeling approach integrated with the nodes voltages procedure given in Section 4.4.

4.5.4. Application of the proposed modeling procedure

The PV array shown in Fig. 4-14 is modeled with the procedure previously described to illustrate the application of the proposed solution. In such an array $N = 3$ and $M = 3$, hence, the seven parameters of the SD model are stored 3×3 matrices and M_{conn} is a 2×2 matrix. Since the pilot example is the same used in sub-section 4.4.5, expressions (4-37) to (4-41) describe the sub-arrays.

The number of meshes ($N_{m,i}$) is calculated by using (4-48) and (4-49); the number of nodes ($N_{n,i}$) is calculated as it is described in sub-section 4.4.3 for each sub-array. For SA_1 , $N_{m,1} = 4$ and $N_{n,1} = 2$, then it is modeled through the nodes analysis [11]. For SA_2 , $N_{m,2} = 1$ and $N_{n,2} = 2$, hence, this sub-array is modeled using the procedure proposed in this section.

Additionally, $N_{m,2} = 1$ which implies that the mesh current vector only contains one element, i.e. $I_{m,2} = [I_{1,1}]$.

Before performing KVL to the mesh it is necessary to calculate the voltage of all the modules. Therefore, it is necessary to solve (4-47) for each module considering that the mesh current to the left of all the modules is zero (i.e. $I_b(i, 1) = 0 [A]$ for $i \in [1 \dots 3]$) and the current to the right of all the modules is the current of mesh 1 ($I_{1,1}$), i.e. $I_a(i, 1) = I_{1,1} = I_{m,2}(1)$ for $i \in [1 \dots 3]$. At this point, all the information required by *Algorithm 2* to evaluate $F_{mesh,2}$ have been defined, thus, it is possible to evaluate $F_{mesh,2}$ for a given V_{array} and a given set of mesh currents ($I_{m,i}$). The structure of $F_{mesh,2}$ is presented in (4-52).

$$F_{mesh,2} = [V_{1,1} + V_{2,1} + V_{3,1} - V_{array}] \quad (4-52)$$

Minimizing $F_{mesh,2}$ for a given value of V_{array} enables to find the vector of mesh currents $I_{m,2}$, which, in this example, only contains $I_{1,1}$. Hence, the current of SA_2 is defined as $I_{sa,2} = I_{m,2}(1)$ by using (4-50). Finally, $I_{array} = I_{sa,1} + I_{sa,2}$ according to (4-36), where $I_{sa,1}$ is obtained by following the procedure proposed in Section 4.4 and $I_{sa,2}$ is obtained by following the procedure proposed in this Section. Such a procedure is applied in the simulation tests, but using a more complex PV array.

4.5.5. Validation of the proposed model

The proposed procedure was validated through simulations and experimental tests. The simulations were performed on Simulink/SimElectronics considering a 10×5 PV array and the experimental tests were made on a 3×3 PV array; in both cases, partial shading conditions were considered. Simulations and experimental results were compared with the ones provided by the proposed solution.

The experimental validation was performed with a 3×3 PV array connected in SP, TCT, BL and the irregular configuration illustrated in Fig. 4-14. Such configurations were formed using nine ERDM10 PV panels as shown in the experimental platform presented in Fig. 4-20. The platform is formed by a current sensor, an oscilloscope a voltage supply, and an electronic device that performs a voltage sweep to obtain the arrays' I-V and P-V curves. In addition, the temperature was measured on the surface of the PV modules using an infrared thermometer. Such a temperature was considered the same for the bypass diodes due to the complexity of taking the measure inside the junction box of each module. In any case, since the bypass diode is placed at the rear of the panel, the temperature of both the bypass diode and panel is very near. From the study presented in [56], it is observed that both module and bypass diode temperatures can be considered similar if the PV array does not

experiment fast irradiance changes. Finally, the experimental measurement of the I-V curves were carried out in a short time in order to avoid sudden changes in the irradiance level.

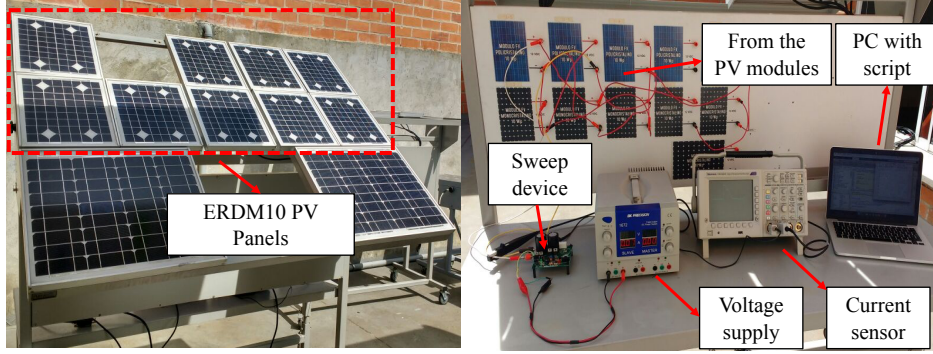


Figure 4-20.: Experimental platform

The electrical characteristics of the panels were obtained from the manufacturer datasheet [101] and the single-diode model parameters were calculated by using the procedures proposed in [111] and [27]. The single-diode model parameters obtained are presented in Table 4-4. The partial shading conditions for the SP, TCT, BL and the irregular configuration are described $M_{I_{ph-SP}}$, $M_{I_{ph-TCT}}$, $M_{I_{ph-BL}}$ and $M_{I_{ph-Irreg}}$ matrices, respectively, as shown in (4-53). Those matrices have different values because the irradiance levels were different for all the tests. Moreover, the same partial shading pattern were considered for all the configurations, i.e. the bottom row of the array was shaded, as can be observed in $M_{I_{ph-SP}}$, $M_{I_{ph-TCT}}$, $M_{I_{ph-BL}}$ and $M_{I_{ph-Irreg}}$. The rest of the single-diode model parameters matrices are defined as 3×3 matrices with the information of Table 4-4. Finally, the connection matrix of the SP and TCT arrays are 2×2 matrices in which all elements are zero and one, respectively; while the connection matrices of BL ($M_{conn-BL}$) and irregular ($M_{conn-Irreg}$) arrays are given in (4-54).

Table 4-4.: Parameters for experimental tests

| Parameter | SP | TCT | BL | Irregular |
|--------------|--------------------------|--------------------------|--------------------------|--------------------------|
| I_{ph} | 0.46 A | 0.57 A | 0.54 A | 0.53 A |
| I_{sat} | 2.27×10^{-10} A | 2.27×10^{-10} A | 4.36×10^{-10} A | 4.36×10^{-10} A |
| n | 1.03 | 1.03 | 1.04 | 1.04 |
| R_s | 2.54 Ω | 2.42 Ω | 2.48 Ω | 2.49 Ω |
| R_h | 504.7 Ω | 637.4 Ω | 602.6 Ω | 591.1 Ω |
| $I_{sat,by}$ | 1×10^{-6} A | 1×10^{-6} A | 1×10^{-6} A | 1×10^{-6} A |
| n_{by} | 0.26 | 0.26 | 0.26 | 0.26 |

$$\begin{aligned}
M_{I_{ph}-SP} &= \begin{bmatrix} 0,46 & 0,46 & 0,46 \\ 0,46 & 0,46 & 0,46 \\ 0,27 & 0,27 & 0,27 \end{bmatrix} [A] & M_{I_{ph}-TCT} &= \begin{bmatrix} 0,57 & 0,57 & 0,57 \\ 0,57 & 0,570 & 0,57 \\ 0,34 & 0,34 & 0,34 \end{bmatrix} [A] & (4-53) \\
M_{I_{ph}-BL} &= \begin{bmatrix} 0,54 & 0,54 & 0,54 \\ 0,54 & 0,54 & 0,54 \\ 0,32 & 0,32 & 0,32 \end{bmatrix} [A] & M_{I_{ph}-Irreg} &= \begin{bmatrix} 0,53 & 0,53 & 0,53 \\ 0,53 & 0,53 & 0,53 \\ 0,31 & 0,31 & 0,31 \end{bmatrix} [A]
\end{aligned}$$

$$M_{conn-BL} = \begin{bmatrix} 1 & 0 \\ 0 & 1 \end{bmatrix} M_{conn-Irreg} = \begin{bmatrix} 1 & 0 \\ 1 & 0 \end{bmatrix} \quad (4-54)$$

Fig. ?? and Fig. ?? present the I-V and P-V curves obtained with the proposed model and with the experimental platform. The results show a satisfactory agreement between the experimental measurements and the behavior predicted by the proposed model. This confirms the usefulness and correctness of the proposed model in the reproduction of the I-V and P-V curves of regular and irregular PV array configurations. In addition, Table 4-5 presents the MAPE in the prediction of the current (E_i), power (E_P) and GMPP (E_{GMPP}) of the proposed model with respect to the experimental results. The values of E_i , E_P and E_{GMPP} are below 0,81 %, 0,78 % and 0,87 %, respectively. Those results demonstrate the satisfactory performance of the proposed modeling procedure in the analysis of both regular and irregular PV arrays operating under partial shading conditions.

Table 4-5.: Mean absolute percentage errors for experimental tests.

| | SP | TCT | BL | Irregular |
|---------------|------|------|------|-----------|
| E_i [%] | 0.15 | 0.78 | 0.71 | 0.81 |
| E_P [%] | 0.15 | 0.78 | 0.75 | 0.71 |
| E_{GMP} [%] | 0.13 | 0.62 | 0.65 | 0.87 |

For simulations, a 10×5 PV array, operating under mismatching conditions, was simulated (in a 2,7 GHz Intel Core i5 processor) to illustrate the performance of the proposed model in medium arrays with respect to the model introduced in [11]. The PV field was connected in SP configuration and an irregular configuration, which were simulated using nodal analysis approach (as described in [11]), mesh analysis approach, and the proposed approach. The results were compared with circuital implementation of the arrays in Matlab/Simulink using the SimElectronics toolbox. The simulated PV arrays considered ERMD85 PV panels [100], which are composed by one module. Moreover, the single-diode model parameters, shown in Table 4-6, were obtained by using the procedures introduced in [111] and [27]. The partial shading profile for both configurations is defined by $M_{I_{ph}}$ matrix, as shown in (4-55); while,

Table 4-6.: Parameters for simulations tests

| Parameter | Value |
|--|-------------------------|
| Photovoltaic current (I_{ph}) | 5.13 A |
| Inverse saturation current (I_{sat}) | 1.18×10^{-9} A |
| Ideality factor (n) | 1.06 |
| Series resistance (R_s) | 0.18 Ω |
| Parallel resistance (R_h) | 261.09 Ω |
| Bypass diode inverse saturation current ($I_{sat,by}$) | 1×10^{-6} A |
| Bypass diode ideality factor (n_{by}) | 0.26 |

the matrices $M_{I_{sat}}$, M_{β} , M_{R_s} , M_{R_h} , $M_{I_{sat,by}}$, and $M_{\beta_{by}}$ are defined as 10×5 matrices with the parameters of Table 4-6.

$$M_{I_{ph}} = \begin{bmatrix} 5,13 & 5,13 & 5,13 & 5,13 & 5,13 \\ 5,13 & 5,13 & 5,13 & 5,13 & 5,13 \\ 5,13 & 5,13 & 5,13 & 5,13 & 5,13 \\ 5,13 & 5,13 & 5,13 & 5,13 & 5,13 \\ 5,13 & 5,13 & 5,13 & 5,13 & 5,13 \\ 5,13 & 5,13 & 3,59 & 3,59 & 3,59 \\ 5,13 & 3,59 & 3,59 & 3,59 & 3,59 \\ 2,56 & 2,56 & 2,56 & 2,56 & 2,56 \\ 2,05 & 2,05 & 2,05 & 2,05 & 2,05 \\ 2,05 & 2,05 & 2,05 & 2,05 & 2,05 \end{bmatrix} \quad (4-55)$$

When the PV field is connected in SP configuration, the connection matrix is a 9×4 matrix of zeros. By applying the procedure described in the flowchart of Fig. 4-19, such an array has five independent sub-arrays ($N_{sa} = 5$), each one with nine nodes and one mesh. According to the proposed model, each sub-array must be solved by using the mesh currents analysis. However, the sub-arrays were solved using node voltage analysis, as proposed in [11], to compare the performance of the two models. Fig. ?? shows the I-V and P-V curves of the SP configuration obtained with the proposed model, the model introduced in [11], and the circuit implementation. Moreover, Table 4-7 presents the simulation time (t_{sim}) of the two models and the MAPE of the reproduction of the current (E_i), power (E_P) and the GMPP (E_{GMPP}) of the two models with respect to the Simulink/SimElectronics results.

Table 4-7.: Simulation time and mean absolute percentage errors for SP simulation test.

| | Proposed Model | Model [11] |
|--------------------|----------------|------------|
| $t_{sim}[min : s]$ | 00:25.3 | 09:18 |
| E_i [%] | 0.86 | 0.86 |
| E_P [%] | 0.86 | 0.86 |
| E_{GMPP} [%] | 0.0012 | 0.0012 |

The values of E_i and E_P are less than 0,9% and E_{GMPP} is about 0,001% for both models, which illustrates the agreement between the models and the circuital implementation. However, the simulation time required by the model proposed in [11] is approximately 22 times greater than the simulation time of the proposed model. This is because the model proposed in [11] needs to solve a system of nine nonlinear equations and nine unknowns for each sub-array; while the proposed model needs to solve one nonlinear equation with one unknown. In general, for an $N \times M$ SP configuration there will be M sub-arrays with $N - 1$ nodes. Then, the model introduced in [11] needs to solve M systems of nonlinear equations, each one with $N - 1$ equations and $N - 1$ unknowns. Instead, the proposed model needs to solve M nonlinear equations with one unknown each, which significantly reduces the calculation burden and the simulation time. The execution time obtained in Simulink/SimElectronics was 13.2 s, which is lower than the times obtained with the proposed procedure and the model reported in [11], both implemented in Matlab. However, the construction of the circuit in the Simulink environment is a time-consuming task when medium or large PV arrays are considered. For example, Fig. 4-21 shows the 10×5 SP array implemented in Simulink, where each module was modeled using the single-diode model.

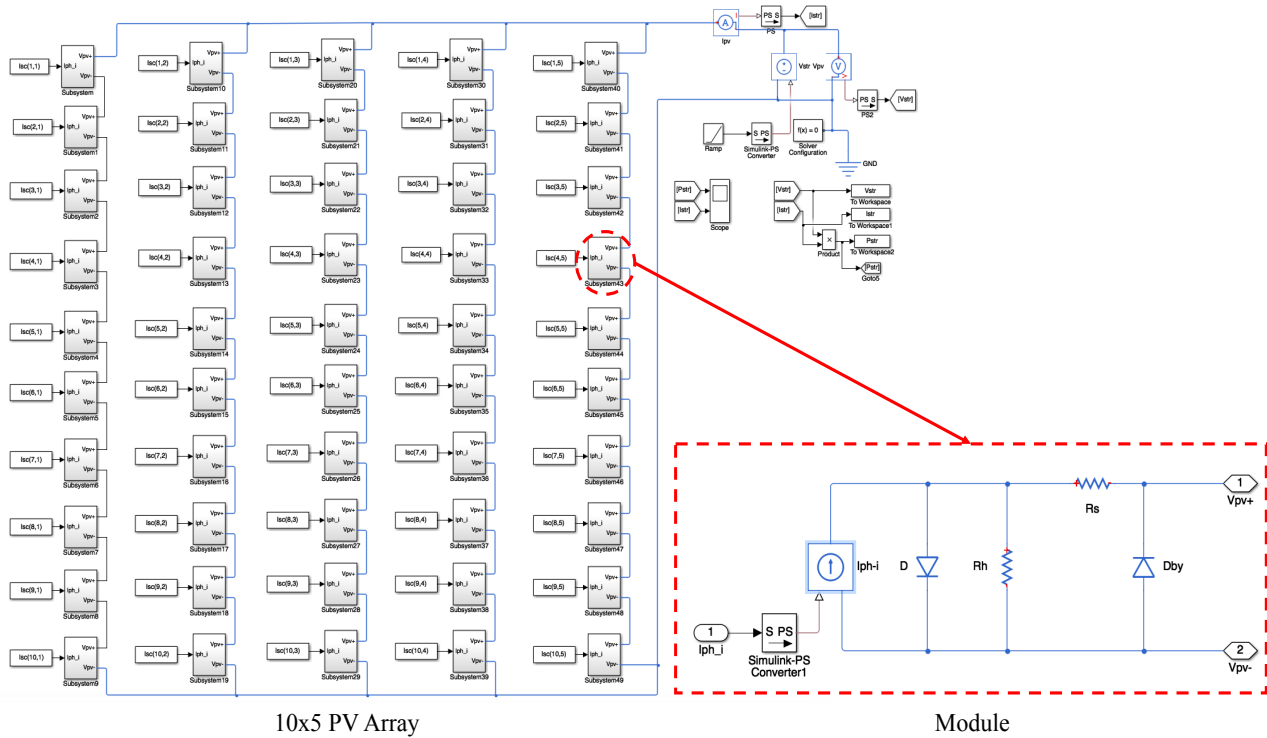


Figure 4-21.: PV array circuit in Simulink/SimElectronics.

It can be seen that the circuit has a considerable size, and any desired change in the value of the parameters or connections (e.g. evaluation of reconfiguration structures) will require the user to modify several elements of the scheme. Instead, the proposed model enables to change the parameters and connections automatically by modifying the corresponding matrices residing in the computer memory. Moreover, the proposed model can be implemented in any programming language, which avoids the use of commercial and costly software such as Simulink/SimElectronics. In addition, implementing this type of models in, for example, $C++$ language will provide much shorter processing times as it was discussed in [11]. In any case, in this work the Simulink/SimElectronics simulation results are taken as a reference to evaluate the accuracy of the proposed procedure due to the extended use of this software in the literature.

The second array configuration used for the simulation tests is shown in Fig. 4-22. The simulated irregular array is formed by three sub-arrays ($N_{sa} = 3$) and its connection matrix is introduced in (4-56). It can be observed that $N_{n,1} = 9$ and $N_{m,1} = 11$ for SA_1 (i.e. nine nodes and eleven meshes), $N_{n,2} = 15$ and $N_{m,2} = 5$ for SA_2 , and $N_{n,3} = 9$ and $N_{m,3} = 1$ for SA_3 . The three sub-arrays were solved by using nodal analysis (as proposed in [11]), meshes analysis, the integration of both methods (as proposed in this paper), and the circuitual implementation. This is to compare the performance of those models and to illustrate the advantages of the proposed model. The I-V and P-V curves obtained with the aforementioned

methods are shown in Fig. ??; additionally, the simulation times and the MAPE of current, power and GMP with respect to the circuital simulation results are presented in Table 4-8.

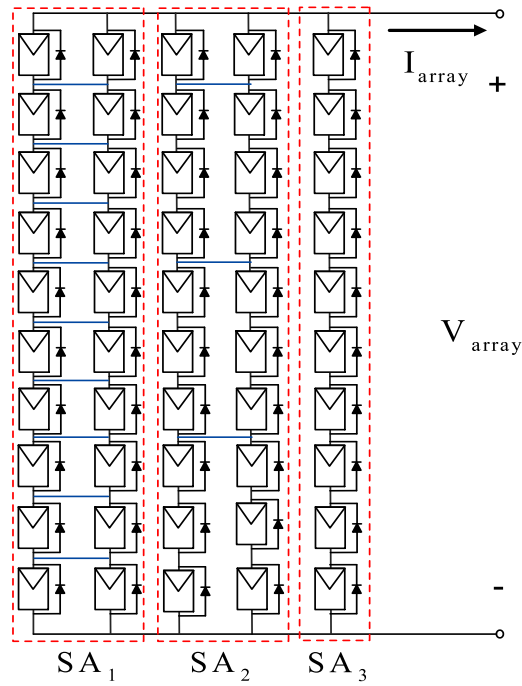


Figure 4-22.: Irregular PV array used in simulations.

$$M_{conn} = \begin{bmatrix} 1 & 0 & 1 & 0 \\ 1 & 0 & 0 & 0 \\ 1 & 0 & 0 & 0 \\ 1 & 0 & 1 & 0 \\ 1 & 0 & 0 & 0 \\ 1 & 0 & 0 & 0 \\ 1 & 0 & 1 & 0 \\ 1 & 0 & 0 & 0 \\ 1 & 0 & 0 & 0 \end{bmatrix} \tag{4-56}$$

Table 4-8.: Simulation time and mean absolute percentage errors for Irregular simulation test.

| | Proposed model (Nodal/Mesh) | Model [11] | Mesh analysis |
|--------------------|--------------------------------|------------|---------------|
| $t_{sim}[min : s]$ | 05:18 | 10:8 | 08:42 |
| E_i [%] | 0.86 | 0.87 | 0.86 |
| E_P [%] | 0.86 | 0.87 | 0.87 |
| E_{GMPP} [%] | 0.0036 | 0.0036 | 0.0037 |

The errors in Table 4-8 show that the three methods are able to reproduce the electrical behavior of an irregular PV array with errors less than 0,9%. However, the simulation time of the proposed model was almost half of the simulation time of the model proposed in [11] and the simulation time with mesh analysis. Therefore, the simulation time integrating mesh currents and nodal voltage analysis, to solve each sub-array with the smaller number of non-linear equations, is less than the simulation time obtained by solving all the sub-arrays with nodal analysis or mesh analysis. The execution time obtained in Simulink/SimElectronics was 11.1 s. As in the previous example, such a time is lower than the ones obtained with the proposed modeling procedure and the procedure presented in [11]. However, as it was discussed in the previous subsection, the simulations results obtained in Simulink/SimElectronics were used as reference for the accuracy of the model.

Finally, the pilot PV array used in section 4.3 shown in Fig. ?? was evaluated using the general model proposed in this section.

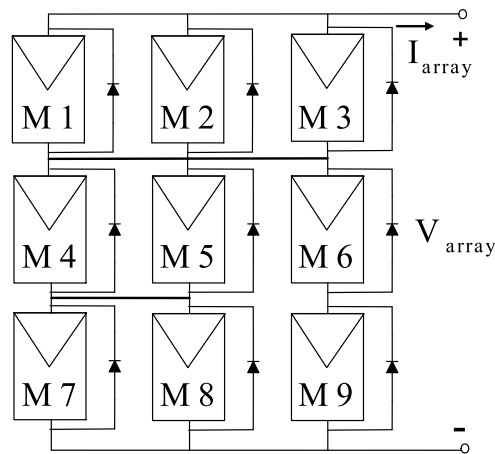


Figure 4-23.: Pilot PV array of section 4.3.

The P-V curves of the array analyzed by the two solutions is presented in Fig. 4-24. It is evident how the P-V curve obtained by the general model has lower values of power this

since such an approach uses the single diode model and the exponential bypass diode model. The MAPE in the power and the *GMPP* is 11.35 % and 0.52 %, respectively. This result put into evidence the improvement achieved by the general model procedure and the usefulness of such an approach to analyze PV arrays under any connection.

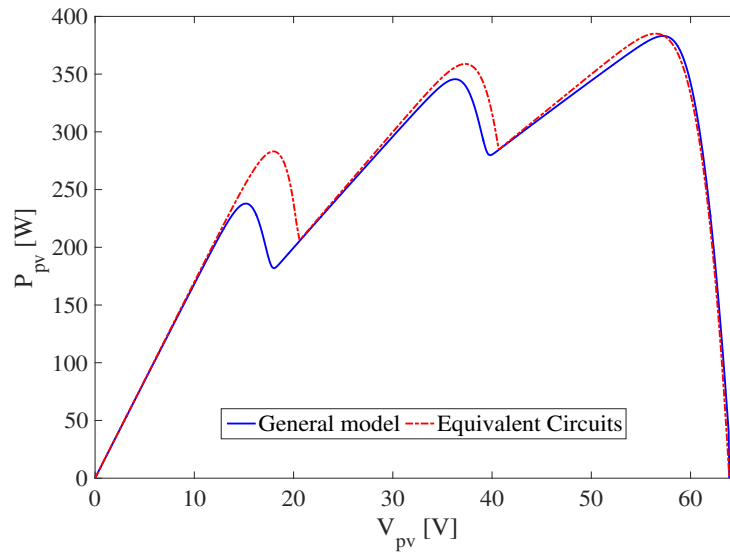


Figure 4-24.: Comparison between the procedure in Section 4.3 and the general model.

4.6. Conclusions

The modeling procedures presented in this chapter are the main contribution of this thesis. In this chapter the concept of irregular array was also introduced; such a concept was a relevant aspect in the process of the implementation of the modeling approaches given in this chapter, since its existence in real applications was justified. In this way, the first approach in this chapter showed a good performance for modeling irregular arrays under uniform or mismatching conditions through the definition of equivalent circuits which correspond to structures that the array can adopt depending on the operating point, in other words, depending on the array voltages in which the bypass diodes of the modules become active. The *sub-array concept* was also introduced in this approach; such a concept is related with sub-structures contained in an array which ease the analysis of the entire array. In this way, by using the aforementioned concepts, the operation range of each equivalent circuit is defined by the inflection points technique given in [82], which are calculated from the analysis of the short circuit currents. Therefore, the proposed modeling technique enables to define a reduced set of electrical equations for each operation interval, it requiring few calculations to obtain the I-V and P-V curves. The validation of the proposed solution was made through simulation tests which demonstrated that the proposed approach achieves a small error of 3.094 % with a large reduction in the simulation time of 18 % in comparison with a classical

solution. On the other hand, the usefulness of the proposed solution was validated through the evaluation of a simple MPPT Perturb and Observe algorithm.

The procedure introduced in Section 4.4 allowed to model PV arrays connected in any configuration and operating under uniform or mismatched conditions. Its operation is based in the classical nodes voltages analysis. The procedure is based on the principle of dividing the original array into small structures named *sub-arrays* as used in the procedure described in Section 4.3. However, some differences can be founded since in this approach the sub-array does not correspond to a simple string; instead it makes reference to small arrays connected in parallel and forming the original array. Each sub-array is analyzed by using nodal analysis to obtain its nodes voltages, which in turn are used to calculate the sub-array current. Finally, the currents of all sub-arrays are added to obtain the array current. The proposed model also introduces an algorithm to evaluate the system of non-linear equations and the Jacobian matrix associated to each sub-array, which are used by the Trust-Region Dogleg method to obtain the node voltages of each sub-array.

The proposed approach has the flexibility to represent a different configuration by only modifying the connection matrix. Hence it makes simple to evaluate different PV array configurations without the need to change the mathematical model. Moreover, the proposed solution eliminates the time consuming task of represent each module by its equivalent circuit as it is required in commercial softwares, e.g. electrical simulators such as Simulink or PSIM. In addition, the proposed procedure is suitable to be implemented in standard programming languages; in this work, the proposed solution was implemented in *C++*, which enables its use through embedded systems. The proposed method has been validated with simulation and experimental tests. The I-V curves of different configurations (SP, TCT and BL configurations) generated with the proposed model were compared with the circuital implementation of those PV arrays in Simulink/SimElectronics toolbox and with experimental measurements obtaining current prediction errors of 1,52 %, 1,52 % and 1,46 % for SP, TCT and BL configurations, respectively. Moreover, the processing times achieved by the proposed model were significantly lower in comparison with the Simulink/SimElectronics toolbox implementation. Those results put into evidence the satisfactory reproduction of I-V and P-V curves of regular and irregular PV arrays under mismatching conditions. Moreover, the errors and processing times are better compared with other reported procedures such as [84] or [83], [82], [9], which in fact are valid only for SP arrays, hence the model proposed in this paper is general. Finally, the applicability of the proposed model was illustrated with a simple example evaluating PV configurations under different shading profiles.

The modeling procedure introduced in Section 4.5 is based on meshes currents analysis. Then, it is a complement to the procedure presented in Section 4.4, which is based on nodes voltages analysis. In this way, the combination of both procedures provides the option to calculate

the sub-arrays currents by solving the least number of operations. For validation purposes, simulations and experimental tests were performed. In both cases, the proposed approach provides a satisfactory performance: the errors in the prediction of current, power and GMPP were below 1% in comparison with circuital simulations made in Simulink/SimElectronics. In addition, the simulation times obtained with the proposed approach were lower than the ones obtained using only the nodes voltages procedure, which confirms the improvement achieved with the integration of both techniques. Similarly, the errors obtained with the proposed modeling procedure for SP, TCT, BL and irregular configurations in the experimental case were below 1%; such results put into evidence the accuracy of the proposed solution. Moreover, the obtained error values are better in comparison with other reported techniques such as [83], [82], [9] or [84], which are procedures applicable only for SP arrays; instead the procedure introduced in this paper can be used for any PV array configuration. In this way, the proposed modeling procedure can be use for PV systems reconfiguration analysis, validation of MPPT strategies and, in general, for design and planning of PV systems.

Unlike the procedure described in Section 4.4, the integration of the nodes voltages method and the meshes currents method presented in Section 4.5 was implemented in a Matlab script, but it is also suitable to be implemented in other programming languages such *C* or *C++* because it is based on well known programming structures and mathematic functions, which are commonly included in standard libraries. The proposed solution requires the PV array has the same number of modules in each columns (i.e. symmetric structure), this can be considered a main limitation. However, symmetric structures are usually adopted in commercial PV arrays [88].

5. Conclusions and Future Works

This thesis presents a general background on modeling PV arrays operating under uniform and mismatched conditions with different connection structures. The literature review, given in Chapter 2, showed that the single diode is the most used model in literature since it provides a good tradeoff between accuracy and complexity; such a model has been used to represent both PV cells and PV modules. However, if PV cells operate at low irradiance levels, the single diode model loses accuracy and it becomes suitable to consider the two-diode model. A main drawback is that the two-diode model requires more parameters than the single diode model; this increasing the complexity of the mathematical procedures. On the other hand, when PV cells operate under partial shading conditions, some cells may operate in the second quadrant and the single diode model, or the two-diode model, do not represent the operation of the cells accurately. The Bishop model has been used to represent the operation of the cells in that second quadrant; such a model requires some parameters which represent the avalanche breakdown effect, but at present in literature there is not a clear procedure to calculate those parameters. Then, it is necessary to develop procedures to facilitate the use of the two-diode model and the Bishop model to improve the accuracy of the modeling techniques; this will allow to achieve deeper analysis for some relevant topics as hot spots, PV panels degradation, among others.

Another aspect associated to the modeling of PV modules is the bypass diode representation. Such diodes are a key factor when PV arrays operate under partial shading conditions. The exponential model (Schottky model), the linear model or the piecewise model are widely used in literature. However, a lack of detail concerning the calculation of the model parameters was detected in the literature review presented in Chapter 2. Therefore, procedures to address this issue are required. In the same way, further studies could consider strategies based on new configurations to connect the cells to the bypass diodes in order to mitigate the partial shading effects.

PV cell models have been scaled up to represent modules and arrays with different configurations such as SP, TCT, BL and HC, where the SP configuration has been, by far, the most widely studied structure. PV arrays can be analyzed with different purposes: reproduction of the characteristic I-V and P-V curves, power and energy prediction and shading effects. In this context, in Chapter 3 some modeling techniques for SP arrays were introduced. Such techniques were implemented at module level using different combinations of module and

bypass diode models, which allowed to achieve different accuracy levels and simulation times. The technique introduced in Section 3.2 (SQ approach) is an improved version of a procedure known as Fast approach. In such an approach, the PV module is represented through the ideal single diode model in which the series and parallel resistances are neglected and the bypass diode is modeled as an ideal switch. Then, if the bypass diode associated to a module is active, the module becomes short-circuited and the losses caused by its operation in the second quadrant are not considered. Instead, in the SQ approach the bypass diode is represented by a linear model. Then, the approach allowed to include the operation in the second quadrant but maintaining low execution times. The SQ approach is mainly oriented to power prediction, but due to the improvement in the representation of the bypass diode, it also could be useful for reproduction of the I-V and P-V curves and evaluation of MPPT strategies. A further improvement for the SQ approach could be the use of the Bishop model.

The Lambert-W approach is a modeling technique based on the single diode model and the exponential form of the bypass diode. It requires the Lambert-W function to obtain explicit relationships between the voltages and the currents of the modules; the use of such a function increase the complexity of the mathematical expressions and the computation speed. On the other hand, the Fast approach is a simplified solution based on the ideal models of the module and the bypass diode. The modeling approach presented in Section 3.3.1 is a tradeoff between the Lambert-W approach and the Fast approach, where the module is represented using the single diode model but the bypass diode is considered through a linear model. In this way, the losses due to the operation in the second quadrant are included. The technique proposes a set of equations which allow to eliminate the use of the Lambert-W function without reducing the accuracy. Instead, a reduction in the computation time is achieved. The simulations results show the good balance between accuracy and complexity introduced by the solution. Finally, the modeling procedure is mainly oriented to power prediction, but the characteristic curves can also be obtained.

The main target of the reproduction of the curves is to understand the behavior of the MPP for a given operating condition. In this way, Section 3.3.2 presented a procedure in which only some points in the neighborhood of the LMPP's are calculated for a particular irradiance condition, which allows to reduce the execution times for calculating the MPP. Moreover, taking advantage of the auxiliary expressions introduced in Section 3.3.1, the Lambert-W function was avoided, this improving the computation time. According to the literature review, the modeling techniques for reproducing the PV array curves are commonly implemented at cell level. However, the approach presented in Section 3.3.2 provided good accuracy and acceptable calculation speed in comparison with the classical procedure. Finally, the approach presented in Section 3.3.3 consisted of a model to introduce the shadow profile that affect each individual module in a PV array. In this way, the dynamic behavior of the shadow is considered; such a behavior is a key factor in the prediction of the power

and energy produced by a PV system for long periods. The model is based on a simple architecture that requires data from irradiance forecast and measurements of the short-circuit current in each module, which is not a complex task. In fact, electronic devices similar to reconfiguration matrixes can be used for this measurement. The approach considered the ideal single diode model and the ideal bypass diode model, but it can be extended to other module and bypass diode representations.

The techniques introduced in Chapter 3 were developed at module level, which provides an acceptable prediction of the PV power. According to the review presented in Chapter 2, such a granularity level is suitable for the modeling techniques oriented to power predictions. However, it can be useful to implement, at least, one of the proposed procedures at cell level to perform comparisons in accuracy and calculation times. On the other hand, all the modeling procedures introduced in Chapter 3 were implemented in Matlab scripts, using widely known programming structures and mathematical functions, so it could be useful to migrate those codes to languages like *C* or *C++*. In this way, the procedures may be used in other computational platforms, such as embedded systems, for other purposes like monitoring or diagnosis.

In this thesis, the concept of irregular array was introduced as an option to mitigate the negative effects caused by partial shading conditions. An irregular array does not follow any connection pattern as the classical structures do: SP, TCT, BL or HC. There is a lack of study in this kind of structures, only some hybrid structures based on the combination of conventional configurations have been reported. Such hybrid structures conserve square or rectangular forms which allows to describe them by the number of rows and columns of PV panels. The modeling approach introduced in Section 4.3 gives some basic tools for analyzing the behavior of irregular structures. The approach introduced the sub-array concept, which is defined as a smaller part of the array that can be modeled independently; this considering also a lumping process to group modules in parallel connection. The division of the PV array facilitates the analysis since the equation systems are simpler. In addition, based on the inflection points concept, the procedure allowed to define the configuration adopted by the array for different voltages intervals, which also enables to reduce the calculation burden to obtain the I-V and P-V curves of the whole array. This procedure was implemented at module level using the ideal single diode model while the bypass diode was considered as an ideal switch. Further approaches may adopt the single diode model, the Bishop or the two-diode model with the exponential form to represent the bypass diode. In the same way, by defining the configurations adopted by the array from zero to its open circuit voltage, this modeling technique is suitable to be implemented using parallel computing tools.

TCT, BL and HC configurations have not been deeply studied, in fact, the reported modeling procedures consider individual solutions, i.e. independent mathematical procedures for

modeling only one of such structures. This makes the evaluation of more than one configuration for a given operating condition a complex task. The modeling procedures introduced in Section 4.4 and Section 4.5 overcome this issue; the procedures allow to analyze PV arrays with any configuration under both uniform or mismatching conditions. The parameters of the array are introduced in matrices which avoids the time consuming task of representing each module by its equivalent circuit. Similarly, the configuration of the array is introduced in a matrix, then by doing simple modifications on such a matrix it is possible to change the configuration under study. The procedures were validated through simulation and experimental tests on regular arrays (SP, TCT, and BL), and irregular configurations. The results confirm the good performance of the proposed solutions. The proposed general modeling procedure can be applied in reconfiguration analysis, MPPT strategies evaluation, planning and design of PV systems. However, since the procedure was implemented at module level, further improvement consists in implementing it at cell level and sub-cell level. Moreover, the use of the Bishop model and the two-diode model could expand the features of the approach; for instance, detailed analysis of the cells operation at low irradiance levels, or in the second quadrant, could be performed. In addition, since the general procedure is based on dividing the PV array into smaller parts (sub-arrays), each one of them can be solved independently using parallel computing to achieve shorter processing times.

The study of irregular configurations can be considered as a new research area. A future work derived from this thesis is to analyze in detail the effect of the ties between strings in a PV array. In particular, the mitigation of the negative effects of partial shading conditions is of particular interest, which in turns can be used to propose new reconfiguration strategies. All the modeling procedures introduced in this thesis were oriented to arrays that can be represented by a number of rows and a number of columns; such arrays can be considered as symmetric arrays. Then, another further development consists in extending the general modeling technique to asymmetric irregular arrays. In the same way, the techniques introduced in Sections 4.3 and 4.5 can be implemented in languages as *C* or *C++* to improve their versatility and expand their use to embedded systems.

In general, this thesis has presented modeling techniques for PV arrays, at module level, using different module and bypass diode representations. The thesis provided the fundamental background to develop tools for the reproduction of the characteristic I-V and P-V curves, but also for performing power and energy predictions. It is expected that the contributions of this work support future projects to strengthen the development of PV systems and microgrids.

Finally, Table 5-1 reports the most important issues afforded in this thesis with the relative link to the corresponding sections and publications which support the contribution.

Table 5-1.: Main issues afforded in this thesis

| Issue | Section | Publication |
|---|----------------|--|
| A literature review on modeling techniques for PV systems oriented to different applications | Section 2.4 | Techniques for modeling photovoltaic systems under partial shading |
| Approach for modeling SP arrays considering the second quadrant | Section 3.2 | Modeling of PV systems based on inflections points technique considering reverse mode |
| Procedures for power estimation in SP arrays | Section 3.3 | Energy prediction in urban photovoltaic systems, Estimating the produced power by photovoltaic installations in shaded environments and Fast calculation of the maximum power point of photovoltaic generators under partial shading |
| Analysis of irregular configurations | Section 4.3 | Equivalent circuits for simulating irregular PV arrays under partial shading conditions |
| General procedure based on nodes voltages analysis for modeling PV arrays of any configuration | Section 4.4 | General modeling procedure for photovoltaic arrays |
| A meshes currents analysis based procedure for modeling PV arrays and its integration with the model of section 4.4 | Section 4.5 | A procedure for modeling photovoltaic arrays under any configuration and shading conditions |

A. System of equations and Jacobian matrix used in simulations

This appendix presents the numerical matrices used to calculate the nodes voltages of one of the sub-arrays of the SP array simulated in subsection 4.4.6; those matrices were parameterized with the values given in subsection 4.4.6. The SP array has three independent sub-arrays calculated by using (4-28), and each sub-array has five nodes as it is obtained by using (4-33). The unknowns of the first sub-array SA_1 (first string from left to right of array shown in Fig.??) are the nodes voltages $V_{n,1} = [e_{(1,1)}, e_{(2,1)}, e_{(3,1)}, e_{(4,1)}, e_{(5,1)}]$, which are defined in terms of the terminal voltages given in (A-1) to (A-7). In this way, by applying (4-23) to (4-25) and (4-29) to (4-32), the elements of the functions matrix $[F_1]_{5,1}$, constructed using the Algorithm 1, are shown in (A-8) to (A-12). Similarly, elements of matrix $[J_1]_{5,5}$, also constructed using the Algorithm 1, are shown in (A-13) to (A-25), where elements $J_{1(1,3)}$, $J_{1(1,4)}$, $J_{1(1,5)}$, $J_{1(2,4)}$, $J_{1(2,5)}$, $J_{1(3,1)}$, $J_{1(3,5)}$, $J_{1(4,1)}$, $J_{1(4,2)}$, $J_{1(5,1)}$, $J_{1(5,2)}$, $J_{1(5,3)}$ are equal to zero. Finally, an initial guess solution based on the open-circuit voltage is defined, and the system is solved by applying the Trust-Region Dogleg method described in [70] to obtain the current $I_{sa,1}$. The process is repeated for SA_2 and SA_3 (second and third strings from left to right of array shown in Fig.??, respectively) to calculate $I_{sa,2}$ and $I_{sa,3}$, respectively, and (4-36) is used to calculate I_{array} . In this way, different values of V_{array} are evaluated through the same process going from zero to 65 V to obtain the array I-V and P-V curves.

$$e_{(1,1)} = e_{b(1,1)} = e_{a(2,1)} \tag{A-1}$$

$$e_{(2,1)} = e_{b(2,1)} = e_{a(3,1)} \tag{A-2}$$

$$e_{(3,1)} = e_{b(3,1)} = e_{a(4,1)} \tag{A-3}$$

$$e_{(4,1)} = e_{b(4,1)} = e_{a(5,1)} \tag{A-4}$$

$$e_{(5,1)} = e_{b(5,1)} = e_{a(6,1)} \tag{A-5}$$

$$V_{array} = e_{a(1,1)} \tag{A-6}$$

$$e_{b(6,1)} = 0 \tag{A-7}$$

$$F_{N1} = -43.7W_0(\theta_{1,1}) + (48,8 \times 10^{-6}) \exp\left(\frac{-V_{e1}}{0.141}\right) - (48,8 \times 10^{-6}) \quad (\text{A-8})$$

$$+ (3.55 - 5 \times 10^{-3}V_{e1}) + 43.7W_0(\theta_{2,1}) - (48,8 \times 10^{-6}) \exp\left(\frac{-V_{e2}}{0.141}\right) \\ + (48,8 \times 10^{-6}) - (3.55 - 5 \times 10^{-3}V_{e2})$$

$$F_{N2} = -43.7W_0(\theta_{2,1}) + (48,8 \times 10^{-6}) \exp\left(\frac{-V_{e2}}{0.141}\right) - (48,8 \times 10^{-6}) \quad (\text{A-9})$$

$$+ (3.55 - 5 \times 10^{-3}V_{e2}) + 43.7W_0(\theta_{3,1}) - (48,8 \times 10^{-6}) \exp\left(\frac{-V_{e3}}{0.141}\right) \\ + (48,8 \times 10^{-6}) - (3.55 - 5 \times 10^{-3}V_{e3})$$

$$F_{N3} = -43.7W_0(\theta_{3,1}) + (48,8 \times 10^{-6}) \exp\left(\frac{-V_{e3}}{0.141}\right) - (48,8 \times 10^{-6}) \quad (\text{A-10})$$

$$+ (3.55 - 5 \times 10^{-3}V_{e3}) + 43.7W_0(\theta_{4,1}) - (48,8 \times 10^{-6}) \exp\left(\frac{-V_{e4}}{0.141}\right) \\ + (48,8 \times 10^{-6}) - (3.55 - 5 \times 10^{-3}V_{e4})$$

$$F_{N4} = -43.7W_0(\theta_{4,1}) + (48,8 \times 10^{-6}) \exp\left(\frac{-V_{e4}}{0.141}\right) - (48,8 \times 10^{-6}) \quad (\text{A-11})$$

$$+ (3.55 - 5 \times 10^{-3}V_{e4}) + 43.7W_0(\theta_{5,1}) - (48,8 \times 10^{-6}) \exp\left(\frac{-V_{e5}}{0.141}\right) \\ + (48,8 \times 10^{-6}) - (3.55 - 5 \times 10^{-3}V_{e5})$$

$$F_{N5} = -43.7W_0(\theta_{5,1}) + (48,8 \times 10^{-6}) \exp\left(\frac{-V_{e5}}{0.141}\right) - (48,8 \times 10^{-6}) \quad (\text{A-12})$$

$$+ (3.55 - 5 \times 10^{-3}V_{e5}) + 43.7W_0(\theta_{6,1}) - (48,8 \times 10^{-6}) \exp\left(\frac{-V_{e6}}{0.141}\right) \\ + (48,8 \times 10^{-6}) - (3.55 - 5 \times 10^{-3}V_{e6})$$

$$J_{1,1}=2.88 \left(\frac{W_0(\theta_{1,1})}{1+W_0(\theta_{1,1})} \right) + 2.88 \left(\frac{W_0(\theta_{2,1})}{1+W_0(\theta_{2,1})} \right) \quad (\text{A-13})$$

$$+ 3.46 \times 10^{-4} \exp\left(\frac{-V_{e1}}{0.141}\right) + 3.46 \times 10^{-4} \exp\left(\frac{-V_{e2}}{0.141}\right) + 9,8 \times 10^{-3}$$

$$J_{1,2}=-2.88 \left(\frac{W_0(\theta_{2,1})}{1+W_0(\theta_{2,1})} \right) - 4.9 \times 10^{-3} - 3.46 \times 10^{-4} \exp\left(\frac{-V_{e2}}{0.141}\right) \quad (\text{A-14})$$

$$J_{2,1}=-2.88 \left(\frac{W_0(\theta_{2,1})}{1+W_0(\theta_{2,1})} \right) - 4.9 \times 10^{-3} - 3.46 \times 10^{-4} \exp\left(\frac{-V_{e2}}{0.141}\right) \quad (\text{A-15})$$

$$J_{2,2}=2.88 \left(\frac{W_0(\theta_{2,1})}{1+W_0(\theta_{2,1})} \right) + 2.88 \left(\frac{W_0(\theta_{3,1})}{1+W_0(\theta_{3,1})} \right) \quad (\text{A-16})$$

$$- 3.46 \times 10^{-4} \exp\left(\frac{-V_{e2}}{0.141}\right) + 3.46 \times 10^{-4} \exp\left(\frac{-V_{e3}}{0.141}\right) + 9,8 \times 10^{-3}$$

$$J_{2,3}=-2.88 \left(\frac{W_0(\theta_{3,1})}{1+W_0(\theta_{3,1})} \right) - 4.9 \times 10^{-3} - 3.46 \times 10^{-4} \exp\left(\frac{-V_{e3}}{0.141}\right) \quad (\text{A-17})$$

$$J_{3,2}=-2.88 \left(\frac{W_0(\theta_{3,1})}{1+W_0(\theta_{3,1})} \right) - 4.9 \times 10^{-3} - 3.46 \times 10^{-4} \exp\left(\frac{-V_{e3}}{0.141}\right) \quad (\text{A-18})$$

$$J_{3,3}=2.88 \left(\frac{W_0(\theta_{3,1})}{1+W_0(\theta_{3,1})} \right) + 2.88 \left(\frac{W_0(\theta_{4,1})}{1+W_0(\theta_{4,1})} \right) \quad (\text{A-19})$$

$$- 3.46 \times 10^{-4} \exp\left(\frac{-V_{e3}}{0.141}\right) + 3.46 \times 10^{-4} \exp\left(\frac{-V_{e4}}{0.141}\right) + 9,8 \times 10^{-3}$$

$$J_{3,4}=-2.88 \left(\frac{W_0(\theta_{4,1})}{1+W_0(\theta_{4,1})} \right) - 4.9 \times 10^{-3} - 3.46 \times 10^{-4} \exp\left(\frac{-V_{e4}}{0.141}\right) \quad (\text{A-20})$$

$$J_{4,3}=-2.88 \left(\frac{W_0(\theta_{4,1})}{1+W_0(\theta_{4,1})} \right) - 4.9 \times 10^{-3} - 3.46 \times 10^{-4} \exp\left(\frac{-V_{e4}}{0.141}\right) \quad (\text{A-21})$$

$$J_{4,4}=2.88 \left(\frac{W_0(\theta_{4,1})}{1+W_0(\theta_{4,1})} \right) + 2.88 \left(\frac{W_0(\theta_{5,1})}{1+W_0(\theta_{5,1})} \right) \quad (\text{A-22})$$

$$- 3.46 \times 10^{-4} \exp\left(\frac{-V_{e4}}{0.141}\right) + 3.46 \times 10^{-4} \exp\left(\frac{-V_{e5}}{0.141}\right) + 9,8 \times 10^{-3}$$

$$J_{4,5}=-2.88 \left(\frac{W_0(\theta_{5,1})}{1+W_0(\theta_{5,1})} \right) - 4.9 \times 10^{-3} - 3.46 \times 10^{-4} \exp\left(\frac{-V_{e5}}{0.141}\right) \quad (\text{A-23})$$

$$J_{5,4}=-2.88 \left(\frac{W_0(\theta_{5,1})}{1+W_0(\theta_{5,1})} \right) - 4.9 \times 10^{-3} - 3.46 \times 10^{-4} \exp\left(\frac{-V_{e5}}{0.141}\right) \quad (\text{A-24})$$

$$J_{5,5}=2.88 \left(\frac{W_0(\theta_{5,1})}{1+W_0(\theta_{5,1})} \right) + 2.88 \left(\frac{W_0(\theta_{6,1})}{1+W_0(\theta_{6,1})} \right) \quad (\text{A-25})$$

$$- 3.46 \times 10^{-4} \exp\left(\frac{-V_{e5}}{0.141}\right) + 3.46 \times 10^{-4} \exp\left(\frac{-V_{e6}}{0.141}\right) + 9,8 \times 10^{-3}$$

Where:

$$\begin{aligned}
 \theta_{1,1} &= (5.8 \times 10^{-7}) \exp(0.23 + 0.07V_{e1}) \\
 \theta_{2,1} &= (5.8 \times 10^{-7}) \exp(0.23 + 0.07V_{e2}) \\
 \theta_{3,1} &= (5.8 \times 10^{-7}) \exp(0.23 + 0.07V_{e3}) \\
 \theta_{4,1} &= (5.8 \times 10^{-7}) \exp(0.23 + 0.07V_{e4}) \\
 \theta_{5,1} &= (5.8 \times 10^{-7}) \exp(0.23 + 0.07V_{e5}) \\
 \theta_{6,1} &= (5.8 \times 10^{-7}) \exp(0.23 + 0.07V_{e6})
 \end{aligned} \tag{A-26}$$

$$\begin{aligned}
 V_{e1} &= V_{array} - e_{b(1,1)} \\
 V_{e2} &= e_{a(2,1)} - e_{b(2,1)} \\
 V_{e3} &= e_{a(3,1)} - e_{b(3,1)} \\
 V_{e4} &= e_{a(4,1)} - e_{b(4,1)} \\
 V_{e5} &= e_{a(5,1)} - e_{b(5,1)} \\
 V_{e6} &= e_{a(6,1)}
 \end{aligned} \tag{A-27}$$

B. Publications

The main results of this doctoral research have been intended to be published in journal papers and conference proceedings. The following papers are published and they contribute to the divulgation of the results achieved in this work.

Restrepo, B., Trejos, A., Ramos-Paja, C. A. Modeling of PV systems based on inflections points technique considering reverse mode. *Tecnológicas Edición especial* (2013), p. 237-248. This journal was indexed B by Publindex at the moment of publication.

Ramos-Paja, C.A., Trejos, A., Restrepo, B. Energy prediction in urban photovoltaics systems. *Revista Tecnológicas Edición Especial* (2013), p. 81-93. This journal was indexed B by Publindex at the moment of publication.

Ramos-Paja, C. A., Saavedra-Montes, A.J., Trejos, A. Estimating the produced power by photovoltaic installations in shaded environments. *Dyna* 82 (2015), Nr. 192, p. 37-43. This journal was indexed A1 by Publindex and Q2 by Scopus at the moment of publication.

Trejos, A., Ramos-Paja, C. A., Saavedra-Montes, A. J. Equivalent circuits for simulating irregular PV arrays under partial shading conditions. *Revista Tecnológicas* 18 (2015), Nr. 35, p. 57-69. This journal was indexed A2 by Publindex at the moment of publication.

Trejos, A., Ramos-Paja, C.A., Saavedra-Montes, A.J. Techniques for modeling photovoltaic systems under partial shading. *Revista Tecnura* 20 (2016), Nr. 48, p. 171-183. This journal was indexed A2 by Publindex at the moment of publication.

Ramos-Paja, C. A., Trejos, A., Herrera-Murcia, J. Fast calculation of the maximum power point of photovoltaic generators under partial shading. *Ingeniería e Investigación* 36 (2016), Nr. 3, p. 58-65. This journal was indexed A1 by Publindex and Q3 by Scopus at the moment of publication.

Bastidas-Rodriguez, Juan D., Trejos-Grisales, Luz A., Gonzalez- Montoya, Daniel, Ramos-Paja, Carlos A., Petrone, Giovanni, Spagnuolo, Giovanni. General modeling procedure for photovoltaic arrays. *Electric Power Systems Research* 155 (2018), p. 67-79. This journal was indexed A1 by Publindex and Q1 by Scopus at the moment of publication.

The following publications were supported by partial results of this thesis:

Trejos A., Goez, M. Ramos-Paja, C. A., Arango, E. Digital controllers design analysis for DC/DC converters in PV applications. 4th IEEE International Symposium on Power Electronics for Distributed Generation Systems (PEDG) (2013), p. 1-6.

Saavedra Montes, Andrés Julian, Ramos Paja, Carlos Andrés, Trejos Grisales, Luz Adriana. Adaptive maximum power point tracking algorithm for multi-variable applications in photovoltaic arrays. Revista EIA 10 (2013), Nr. 20, p. 193-206. This journal was indexed A2 by Publindex at the moment of publication.

Bastidas-Rodriguez, Juan D., Ramos-Paja, Carlos A., Trejos-Grisales Adriana. Mathematical model of bridge-linked photovoltaic arrays operating under irregular conditions. Revista Tecnológicas Edición Especial (2013), p. 223-235. This journal was indexed B by Publindex at the moment of publication.

Ortiz-Valencia Paula A., Trejos-Grisales Adriana, Ramos-Paja, Carlos A. Photovoltaic system regulation based on a PID fuzzy controller to ensure a fixed settling time. Revista Tecnológicas Edición Especial (2013), p. 605-616. This journal was indexed B by Publindex at the moment of publication.

Ortiz-Valencia Paula A., Trejos-Grisales Adriana, Ramos-Paja, Carlos A. Maximum power point tracking in PV systems based on adaptive control and sliding mode control. Revista Facultad de Ingeniería Universidad de Antioquia (2015), Nr. 75, p. 67-79. This journal was indexed A1 by Publindex and Q4 by Scopus at the moment of publication.

References

- [1] *GNU Scientific Library*. November 2016
- [2] ADAMO, F. ; ATTIVISSIMO, F. ; DI NISIO, A. ; SPADAVECCHIA, M.: Characterization and testing of a tool for photovoltaic panel modeling. En: *IEEE Transactions on Instrumentation Measurement* 60 (2011), p. 1613–1622
- [3] ADITYAN, P. R. ; VIJAYAKUMAR, K. ; FERNANDEZ, G.: Design of a MPPT controller along with a reconfiguration technique for a PV system under partially shaded condition. En: *International Journal of Control Theory and Applications* 9 (2016), Nr. 37, p. 791–802
- [4] ALONSO-GARCIA, M.C. ; RUIZ, J.M. ; HERRMANN, W.: Computer simulation of shading effects in photovoltaic arrays. En: *Renewable Energy* 31 (2006), p. 1986–1993
- [5] AZAB, M.: Improved circuit model of photovoltaic array. En: *International Journal of Power and Energy Systems and Engineering* 3 (2009), Nr. 2, p. 185–188
- [6] BALATO, M. ; COSTANZO, L. ; VITELLI, M.: Series–Parallel PV array re-configuration: Maximization of the extraction of energy and much more. En: *Applied Energy* 159 (2015), December, Nr. 2015, p. 145–160
- [7] BANA, S. ; SAINI, R. P.: Experimental investigation on power output of different photovoltaic array configurations under uniform and partial shading scenarios. En: *Energy* 127 (2017), p. 438–453
- [8] BASSAM, A. ; MAY TZUC, O. ; ESCALANTE SOBERANIS, M. ; RICALDE, L. J. ; CRUZ, B.: Temperature Estimation for Photovoltaic Array Using an Adaptive Neuro Fuzzy Inference System. En: *Sustainability* 9 (2017), Nr. 8, p. 1–16
- [9] BASTIDAS, J D. ; FRANCO, E ; PETRONE, G ; RAMOS-PAJA, C A. ; SPAGNUOLO, G: A model of photovoltaic fields in mismatching conditions featuring an improved calculation speed. En: *Electric Power Systems Research* 96 (2013), p. 81–90. – ISSN 0378–7796
- [10] BASTIDAS-RODRIGUEZ, J.D. ; FRANCO, E ; PETRONE, G ; SPAGNUOLO, G: Model Based Indicators To Quantify Photovoltaic Module Degradation. En: *11th Interna-*

- tional Conference on Modeling and Simulation of Electric Machines, Converters and Systems (ELECTRIMACS 2014)*, 2014, p. 49–54
- [11] BASTIDAS-RODRIGUEZ, Juan D. ; TREJOS-GRISALES, Luz A. ; GONZALEZ-MONTOYA, Daniel ; RAMOS-PAJA, Carlos A. ; PETRONE, Giovanni ; SPAGNUOLO, Giovanni: General modeling procedure for photovoltaic arrays. En: *Electric Power Systems Research* 155 (2018), p. 67–79
- [12] BATZELIS, E.I. ; ROUTSOLIAS, I.A. ; PAPATHANASSIOU, S.A.: An explicit pv string model based on the Lambert W function and simplified mpp expression for operation under partial shading. En: *IEEE Transactions on Sustainable Energy* 5 (2014), Nr. 1, p. 301–312
- [13] BISHOP, J.W.: Computer simulation of the effects of electrical mismatches in photovoltaic cell interconnection circuits. En: *Solar Cells* 25 (1988), Oktober, Nr. 1, p. 73–89. – ISSN 03796787
- [14] BOYLESTAD, R. L. ; NASHELSKY, L.: *Electronic Devices and Circuit Theory*. 10. Prentice Hall, 2009
- [15] BRESSAN, M. ; BASRI, Y. E. ; GALEANO, A. G. ; ALONSO, C.: A shadow fault detection method based on the standard error analysis of I-V curves. En: *Renewable Energy* 99 (2016), p. 1181–1190
- [16] BUILDING ; AUTHORITY, Construction: *Handbook for Photovoltaic (PV) Systems*. Building and Construction Authority
- [17] CARRASCO, J. M. ; FRANQUELO, L. G. ; BIALASIEWICZ, J. T. ; GALVAN, E. ; GUI-SADO, R. C. P. ; PRATS, Ma. A. M. ; LEON, J. I. ; MORENO-ALFONSO, N.: Power-Electronic Systems for the Grid Integration of Renewable Energy Sources: A Survey. En: *IEEE Transactions on Industrial Electronics* 53 (2006), Nr. 4, p. 1002–1016
- [18] CELIK, A.N. ; ACIKGOZ, N.: Modelling and experimental verification of the operating current of mono-crystalline photovoltaic modules using four and five parameter models. En: *Applied Energy* 84 (2007), p. 1–15
- [19] CHAN, D. ; PHANG, J.: Analytical methods for the extraction of solar-cell single and double diode model parameters from I-V characteristics. En: *IEEE Transaction on Electronic Devices* 34 (1987), Nr. 2, p. 286–293
- [20] CHENNI, R. ; MAKHLOUF, M. ; KERBACHE, T. ; BOUZID, A.: A detailed modeling method for photovoltaic cells. En: *Energy* 32 (2007), p. 1724–1730

- [21] CHIN, V.J. ; SALAM, Z. ; ISHAQUE, K.: An accurate modelling of the two-diode model of PV module using a hybrid solution based on differential evolution. En: *Energy Conversion and Management* (2016), Nr. 124, p. 42–50
- [22] CIULLA, G. ; LO BRANO, V. ; DI DIO, V. ; CIPRIANI, G.: A comparison of different one-diode models for the representation of I–V characteristic of a PV cell. En: *Renewable and Sustainable Energy Reviews* 32 (2014), p. 684–696
- [23] DE MINAS Y ENERGIA REPUBLICA DE COLOMBIA, Ministerio. *Resolución 18-919*. 2010
- [24] DE MINAS Y ENERGIA REPUBLICA DE COLOMBIA, Ministerio. *Ley 1715 de 2014*. 2014
- [25] DAVIS, A. *Diode models*. Electronic. September 2009
- [26] DE BLAS, M.A. ; TORESS, J.L. ; PRIETO, E. ; GARCIA, A.: A. Selecting a suitable model for Selecting a suitable model for characterizing photovoltaic devices. En: *Renewable Energy* 25 (2002), p. 371–380
- [27] DE SOTO, W. ; KLEIN, S.a. ; BECKMAN, W.a.: Improvement and validation of a model for photovoltaic array performance. En: *Solar Energy* 80 (2006), Januar, Nr. 1, p. 78–88. – ISSN 0038092X
- [28] DELINE, C. ; DOBOS, A. ; JANZOU, S. ; MEYDBRAY, J. ; DONOVAN, M.: A simplified model of uniform shading in large photovoltaic arrays. En: *Solar Energy* 96 (2013), p. 274–282
- [29] DIQING, Z. ; WU, Ch. ; LI, Z.: Modeling and Simulation of Partial Shaded PV Modules. En: *System Simulation and Scientific Computing Communications in Computer and Information Science* 2012 (2012), p. 124–134
- [30] DRIF, M. ; MELLIT, A. ; AGUILERA, J. ; PEREZ, P.J.: A comprehensive method for estimating energy losses due to shading of GC-BIPV systems using monitoring data. En: *Solar Energy* 86 (2012), p. 2397–2404
- [31] DUFFIE, J.A. ; BECKMAN, W.A.: *Solar engineering of thermal processes*. 3. John Wiley & Sons, 2006
- [32] EICKER, U.: *Solar Technologies for Buildings*. John Wiley & Sons, 2003
- [33] ELBASET, A. ; ALI, H. ; EL SATTAR, M.A.: New seven parameters model for amorphous silicon and thin film PV modules based on solar irradiance. En: *Solar Energy* 138 (2016), p. 26–35

-
- [34] ESRAM, T. ; CHAPMAN, P. L.: Comparison of Photovoltaic Array Maximum Power Point Tracking Techniques. En: *IEEE Transactions on Energy Conversion* 22 (2007), Nr. 2, p. 439–449
- [35] FUENTES, M. ; NOFUENTES, G. ; AGUILERA, J. ; TALAVERA, D. L. ; CASTRO, M.: Application and validation of algebraic methods to predict the behaviour of crystalline silicon PV modules in Mediterranean climates. En: *Solar Energy* 81 (2007), Nr. 11, p. 1396–1408
- [36] GAROUDJA, Elyes ; HARROU, Fouzi ; SUN, Ying ; KARA, Kamel ; CHOUDER, Aissa ; SILVESTRE, Santiago: Statistical fault detection in photovoltaic systems. En: *Solar Energy* 150 (2017), p. 485–499
- [37] GARRIDO-ALZAR, C.: Algorithm for extraction of solar cell parameters from I–V curve using double exponential model. En: *Renewable Energy* 10 (1997), p. 125–128
- [38] GHANBARI, Teymoor: Permanent partial shading detection for protection of photovoltaic panels against hot spotting. En: *IET Renewable Power Generation* 11 (2016), Nr. 1, p. 123–131
- [39] GREEN, M.A. ; EMERY, K. ; HISHIKAWA, Y. ; WARTA, W. ; DUNLOP, E. ; LEVI, D. ; HO-BAILLIE, A.W.Y.: Solar cell efficiency tables (Version 49). En: *Progress in Photovoltaics* (2016), November, Nr. 25, p. 3–13
- [40] HADJ ARAB, A. ; CHENLO, F. ; BENGHANEM, M.: Loss-of-load probability water pumping systems. En: *Solar Energy* 76 (2004), p. 713–723
- [41] HAOUARI-MERBAH, M. ; BELHAMEL, M. ; TOBIAS, I. ; RUIZ, J.: Extraction and analysis of Extraction and analysis of solar cell parameters from the illuminated current–voltage curve. En: *Solar Energy Material and Solar Cells* 87 (2005), p. 225–233
- [42] HEJRI, M. ; MOKHTARI, H.: On the comprehensive parametrization of the photovoltaic (PV) cells and modules. En: *IEEE Journal of Photovoltaics* 7 (2017), Nr. 1, p. 250–258
- [43] HUMADA, A.M. ; HOJABRI, M. ; MEKHILEF, S. ; HAMADA, H.: Solar cell parameters extraction based on single and double-diode models: A review. En: *Renewable and Sustainable Energy Reviews* 56 (2016), Nr. 494–509
- [44] INTERNATIONAL ENERGY AGENCY, IEA. *Trends 2016 in Photovoltaics Applications*. 2016
- [45] ISHAQUE, K. ; SALAM, Z. ; SYAFARUDDIN: A comprehensive MATLAB Simulink PV system simulator with partial shading capability based on two-diode model. En: *Solar Energy* 85 (2011), p. 2217–2227

- [46] ISHAQUE, K. ; SALAM, Z. ; TAHERI, H. ; SYAFARUDDIN: Modeling and simulation of photovoltaic system during partial shading based on a two diode model. En: *Simulation Modelling Practice and Theory* 19 (2011), p. 1613–1626
- [47] JACKSON, F.: *Planning and Installing Photovoltaic Systems*. London : Earthscan, 2007
- [48] JACOBS, D. ; MARZOLF, N. ; PAREDES, J. R. ; RICKERSON, W. ; FLYNN, H. ; BECKER-BIRCK, C. ; SOLAZO-PERALTA, M.: Analysis of renewable energy incentives in the Latin America and Caribbean region: The feed-in tariff case. En: *Energy Policy* 60 (2013), p. 601–610
- [49] JUNG, T.H. ; WOO KO, J. ; KANG, G. ; AHN, H: Output characteristics of PV module considering partially reverse biased conditions. En: *Solar Energy* 92 (2013), p. 214–220
- [50] KADRI, R. ; ANDREI, H. ; J.P., Gaubert. ; IVANOVICI, T. ; CHAMPENOIS, G. ; ANDREI, P.: Modeling of the photovoltaic cell circuit parameters for optimum connection model and real-time emulator with partial shadow conditions. En: *Energy* 42 (2012), p. 57–67
- [51] KARATEPE, E. ; BOZTEPE, M. ; COLAK, M.: Development of a suitable model for characterizing photovoltaic arrays with shaded solar cells. En: *Solar Energy* 81 (2007), p. 977–992
- [52] KAUSHIKA, Narendra D. ; GAUTAM, Nalin K.: Energy yield simulations of interconnected solar PV arrays. En: *IEEE Transactions on Energy Conversion* 18 (2003), März, Nr. 1, p. 127–134. – ISSN 0885–8969
- [53] KESRAOUI, M. ; LAZIZI, A. ; CHAIB, A.: Grid Connected solar PV system: modeling, simulation and experimental tests. En: *International Scientific Conference “Environmental and Climate Technologies”, CONECT 2015*, 2015, p. 181–188
- [54] KHANNA, V. ; DAS, B. ; BISHT, D. ; SINGH, P.: A three diode model for industrial solar cells and estimation of solar cell parameters using PSO algorithm. En: *Renewable Energy* 78 (2015), p. 105–113
- [55] KING, D. L.: Sandia’s PV module electrical performance model / Sandia National Laboratories. 2000. – Informe de Investigación
- [56] KO, S. W. ; JU, Y. C. ; HWANG, H. M. ; SO, J. H. ; JUNG, Y. S. ; SONG, H. ; KIM, S. ; KANG, G. H.: Electric and thermal characteristics of photovoltaic modules under partial shading and with a damaged bypass diode. En: *Energy* 128 (2017), p. 233 – 243
- [57] KOURO, S. ; LEON, J. ; VINNIKOV, D. ; FRANQUELO, L. G.: Grid-Connected Photovoltaic Systems An Overview of Recent Research and Emerging PV Converter Technology. En: *IEEE Industrial Electronics Magazine* 9 (2015), March, Nr. 1, p. 47–61

- [58] KRITHIGA, S. ; GOUNDEN, N. Gounder A.: Power electronic configuration for the operation of PV system in combined grid-connected and stand-alone modes. En: *IET Power Electronics* 7 (2013), Nr. 3, p. 640–647
- [59] KUMAR, A. ; KUMAR-PACHAURI, R. ; CHAUHAN, Y. K.: Experimental analysis of SP-TCT PV array configurations under partial shading conditions. En: IEEE (Ed.): *1st IEEE International Conference on Power Electronics, Intelligent COntrol and Energy Systems (ICPEICES-2016)*, 2016, p. 1–6
- [60] LA MANNA, Damiano ; LI VIGNI, Vincenzo ; RIVA SANSEVERINO, Eleonora ; DI DIO, Vincenzo ; ROMANO, Pietro: Reconfigurable electrical interconnection strategies for photovoltaic arrays: A review. En: *Renewable and Sustainable Energy Reviews* 33 (2014), Mai, p. 412–426. – ISSN 13640321
- [61] LALWANI, M. ; KOTHARI, D.P. ; SINGH, M.: Investigation of solar photovoltaic simulation softwares. En: *International Journal of Applied Engineering Research* 1 (2010), p. 585–601
- [62] LI, Y. ; DING, D. ; LIU, C. ; WANG, C.: A pixel-based approach to estimation of solar energy potential on building roofs. En: *Energy and Buildings* 129 (2016), p. 563 – 573
- [63] LIU, G. ; NGUANG, S.K. ; PARTRIDGE, A.: A general modeling method for I-V characteristics of geometrically and electrically configured photovoltaic arrays. En: *Energy Conversion and Management* 52 (2011), p. 3439–3445
- [64] MAKI, A. ; VALKEALAHTI, S.: Power Losses in Long String and Parallel-Connected Short Strings of Series-Connected Silicon-Based Photovoltaic Modules Due to Partial Shading Conditions. En: *IEEE Transactions on Energy Conversion* 27 (2012), p. 173–183
- [65] MARTINEZ-MORENO, F. ; MUNOZ, J. ; LORENZO, E.: Experimental model to estimate shading losses on PV arrays. En: *Solar Energy Materials and Solar Cells* 94 (2010), p. 2298–2303
- [66] MISHRA, N. ; YADAV, A. ; PACHAURI, R. ; CHAUHAN, Y. ; YADAV, V.: Performance enhancement of PV system using proposed array topologies under various shadow patterns. En: *Solar Energy* 157 (2017), p. 641–656
- [67] MOBALLEGH, S. ; JIANG, J.: Modeling, Prediction, and Experimental Validations of Power Peaks of PV Arrays Under Partial Shading Conditions. En: *IEEE Transactions on Sustainable Energy* 5 (2014), Nr. 1, p. 293–300
- [68] MUNOZ-GARCÍA, M.A. ; MARIN, O. ; M.C., Alonso-García ; CHENLO, F.: Characterization of thin film PV modules under standard test conditions: Results of indoor and

- outdoor measurements and the effects of sunlight exposure. En: *Solar Energy* (2012), August, Nr. 86, p. 3049–3056
- [69] NISHIOKA, K. ; SAKITANI, N. ; URAOKA, Y. ; FUYUKI, T.: Analysis of multicrystalline silicon solar cells by modified 3-diode equivalent circuit model taking leakage current through periphery into consideration. En: *Solar Energy Material and Solar Cells* 91 (2007), p. 1222–1227
- [70] NOCEDAL, J ; WRIGHT, S J.: *Numerical Optimization*. 1999. – 164–75 p.. – ISBN 0387987932
- [71] NOCEDAL, J. ; WRIGHT, S. J. ; SPRINGER (Ed.): *Numerical Optimization*. 2. 2006. – ISBN 0387987932
- [72] OLALLA, C. ; CLEMENT, D. ; MAKSIMOVIC, D. ; DELINE, C.: A cell-level photovoltaic model for high-granularity simulations. En: IEEE (Ed.): *Power Electronics and Applications (EPE), 2013 15th European Conference on*, 2013, p. 1–10
- [73] OLIVA, D. ; CUEVAS, E. ; PAJARES, G.: Parameter identification of solar cells using artificial bee colony optimization. En: *Energy* 72 (2014), p. 93–102
- [74] ORIOLI, A. ; DI GANGI, A.: A procedure to calculate the five-parameter model of crystalline silicon photovoltaic modules on the basis of the tabular performance data. En: *Applied Energy* 102 (2013), p. 1160–1177
- [75] ORIOLI, A. ; GANGI, A. D.: Review of the energy and economic parameters involved in the effectiveness of grid-connected PV systems installed in multi-storey buildings. En: *Applied Energy* 113 (2014), p. 955–969
- [76] OROZCO-GUTIERREZ, M.L. ; RAMIREZ-SCARPETTA, J.M. ; SPAGNUOLO, G. ; RAMOS-PAJA, C.A.: A technique for mismatched PV array simulation. En: *Renewable Energy* 51 (2013), p. 417–427
- [77] OROZCO-GUTIERREZ, M.L. ; RAMIREZ-SCARPETTA, J.M. ; SPAGNUOLO, G. ; RAMOS-PAJA, C.A.: A method for simulating large PV arrays that include reverse biased cells. En: *Applied Energy* 123 (2014), p. 157–167
- [78] PARASKEVADAKI, V. ; PAPATHANASSIOU, A.: Evaluation of MPP voltage and power of mc-Si PV modules in partial shading conditions. En: *IEEE Transactions On Energy Conversion* 3 (2011), Nr. 26, p. 923–932
- [79] PATEL, H. ; AGARWAL, V.: MATLAB-Based Modeling to Study the Effects of Partial Shading on PV Array Characteristics. En: *IEEE Transactions on Energy Conversion* 23 (2008), Nr. 1, p. 302–310

- [80] PENG, L. ; SUN, Y. ; MENG, Z.: An improved model and parameters extraction for photovoltaic cells using only three state points at standard test condition. En: *Journal of Power Sources* 248 (2014), p. 621–631
- [81] PETRONE, G. ; RAMOS-PAJA, C. A. ; SPAGNUOLO, G. ; PRESS, IEEE (Ed.): *Photovoltaic sources modeling*. 1st. Wiley, 2017
- [82] PETRONE, G. ; RAMOS-PAJA, C.A.: Modeling of photovoltaic fields in mismatched conditions for energy yield evaluations. En: *Electric Power Systems Research* 81 (2011), Nr. 4, p. 1003–1013. – ISSN 03787796
- [83] PETRONE, G. ; SPAGNUOLO, G. ; VITELLI, M.: Analytical model of mismatched photovoltaic fields by means of Lambert W-function. En: *Sol. Energy Mater. and Sol. Cells* 91 (2007), November, Nr. 18, p. 1652–1657. – ISSN 09270248
- [84] PICAULT, D. ; RAISON, B. ; BACHA, S. ; DE LA CASA, J. ; AGUILERA, J.: Forecasting photovoltaic array power production subject to mismatch losses. En: *Solar Energy* 84 (2010), Juli, Nr. 7, p. 1301–1309. – ISSN 0038092X
- [85] PVEDUCATION. *Mismatch effects*
- [86] RABINOVICI, R. ; DAGAN, T.: Assessment of Solar Irradiance in Large-Scale Photovoltaic Fields by Means of Video Processing. En: IEEE (Ed.): *2012 IEEE 27th Convention of Electrical and Electronics Engineers in Israel*, 2012, p. 1–5
- [87] RAMABADRAN, Ramaprabha: Matlab based modelling and performance study of series connected SPVA under partial shaded conditions. En: *Journal of Sustainable Development* 2 (2009), Nr. 3, p. 85–94
- [88] RAMAPRABHA, R. ; MATHUR, B. L.: A Comprehensive Review and Analysis of Solar Photovoltaic Array Configurations under Partial Shaded Conditions. En: *International Journal of Photoenergy* 2012 (2012), p. 1–16. – ISSN 1110–662X
- [89] RAMOS-PAJA, C. A. ; SAAVEDRA-MONTES, A.J. ; TREJOS, A.: Estimating the produced power by photovoltaic installations in shaded environments. En: *Dyna* 82 (2015), Nr. 192, p. 37–43
- [90] RAMOS-PAJA, C.A. ; TREJOS, A. ; RESTREPO, B.: Energy prediction in urban photovoltaics systems. En: *Tecnologicas Edicion Especial* (2013), p. 81–93
- [91] RATHEE, R. ; KHANNA, V. ; DAS, B.K.: Spice based modelling and simulation to study the effects of partial shading on PV array characteristics. En: *International Journal of Engineering Science Invention* 2 (2013), Nr. 5, p. 68–73

- [92] RESTREPO, B. ; TREJOS, A. ; RAMOS-PAJA, C. A.: Modeling of PV systems based on inflections points technique considering reverse mode. En: *Tecnologicas Edicion especial* (2013), p. 237–248
- [93] REZAAE JORDEHI, A.: Parameter estimation of solar photovoltaic (PV) cells: A review. En: *Renewable and Sustainable Energy Reviews* 61 (2016), p. 354–371
- [94] RODRIGO, P. ; FERNANDEZ, E. ; ALMONACID, F. ; PEREZ-HIGUERAS, P.J.: A simple accurate model for the calculation of shading power losses in photovoltaic generators. En: *Solar Energy* 93 (2013), p. 322–333
- [95] SAAVEDRA-MONTES, A. J. ; RAMIREZ-SCARPETTA, J. M. ; C.A., Ramos-Paja ; MALIK, O.P.: Identification of excitation systems with the generator online. En: *Electric Power Systems Research* 87 (2007), p. 1–9
- [96] SAAVEDRA-MONTES, A.J. ; RAMIREZ-SCARPETTA, J.M. ; MALIK, O.P.: Methodology to estimate parameters of an excitation system based on experimental conditions. En: *Electric Power Systems Research* 81 (2011), Nr. 1, p. 170– 176
- [97] SAMI, M. ; HAZEM, K. ; ABDALLAH, A.: PV solar system feasibility study. En: *Energy Conversion and Management* 65 (2013), p. 777–782
- [98] SILVESTRE, S. ; BORONAT, a. ; CHOUDER, a.: Study of bypass diodes configuration on PV modules. En: *Applied Energy* 86 (2009), Nr. 9, p. 1632–1640. – ISSN 03062619
- [99] SILVESTRE, S. ; CHOUDER, A.: Effects of shadowing on photovoltaic module performance. En: *Progress in Photovoltaics* 16 (2007), Nr. 2, p. 141–149
- [100] SOLAR, ERDM. *Datasheet ERDM SOLAR 75SM 80SM5 85SM*. 2016
- [101] SOLAR, ERDM. *Datasheet ERDM 10 W Monocrystalline panel*. 2017
- [102] SOLAR, Yingli. *Datasheet Yingli Solar JS70 Series*. 2016
- [103] SOON, J. ; LOW, K. ; GOH, Sh.: Multi-dimension diode photovoltaic (PV) model for different PV cell technologies. En: IEEE (Ed.): *2014 IEEE 23rd International Symposium on Industrial Electronics (ISIE)*, 2014, p. 2496–2501
- [104] STUTENBAEUMER, U. ; MESFIN, B.: Equivalent model of monocrystalline, polycrystalline and amorphous silicon solar cells. En: *Renewable Energy* 18 (1999), p. 501–512
- [105] SUN, L. ; LU, L. ; YANG, H.: Optimum design of shading-type building-integrated photovoltaic claddings with different surface azimuth angles. En: *Applied Energy* 90 (2012), p. 233–240

- [106] SUNANDA, S. ; CHANDEL, S.: Review of software tools for hybrid renewable energy systems. En: *Renewable Energy and Sustainable Energy Reviews* 32 (2014), p. 192–205
- [107] SUSKIS, P. ; GALKIN, I.: Enhanced Photovoltaic Panel Model Enhanced photovoltaic panel model for MATLAB-Simulink Environment Considering Solar Cell Junction Capacitance. En: IEEE (Ed.): *39th Annual Conference of the IEEE Industrial Electronics Society, IECON 2013*, 2013, p. 1613–1618
- [108] SYAFARUDDIN ; KARATEPE, Engin ; HIYAMA, Takashi: Development of Real-Time Simulator based on Intelligent Techniques for Maximum Power Point Controller of PV. En: *The International Journal of Innovative Computing, Information and Control* 6 (2010), Nr. 4, p. 1623–1642
- [109] TREJOS, A. ; RAMOS-PAJA, C. A. ; SAAVEDRA-MONTES, A. J.: Equivalent circuits for simulating irregular PV arrays under partial shading conditions. En: *Tecnologicas* 18 (2015), Nr. 35, p. 57–69. – ISSN 0123–7799
- [110] TREJOS, A. ; RAMOS-PAJA, C.A. ; SAAVEDRA-MONTES, A.J.: Techniques for modeling photovoltaic systems under partial shading. En: *Tecnura* 20 (2016), Nr. 48, p. 171–183
- [111] VILLALVA, M.G. ; GAZOLI, J.R. ; FILHO, E.R.: Comprehensive Approach to Modeling and Simulation of Photovoltaic Arrays. En: *IEEE Trans. Power Electron.* 24 (2009), Mai, Nr. 5, p. 1198–1208. – ISSN 0885–8993
- [112] WANG, Y. ; HSU, P.: Analytical modelling of partial shading and different orientation of photovoltaic modules. En: *IET Renewable Power Generation* 4 (2009), p. 272–282
- [113] WANG, Y-W. ; HSU, P-Ch.: Analysis of partially shaded PV modules using Piecewise Linear Parallel Branches Model. En: *World Academy of Science, Engineering and Technology* 60 (2009), p. 783–789
- [114] WANG, Yaw-Juen ; HSU, Po-Chun: An investigation on partial shading of PV modules with different connection configurations of PV cells. En: *Energy* 36 (2011), Nr. 5, p. 3069–3078. – ISSN 0360–5442
- [115] ZEGAOU, A. ; PETIT, P.: Experimental validation of photovoltaic direct and reverse mode model influence of partial shading. En: *Energy Procedia* 18 (2012), p. 1247–1253
- [116] ZEGAOU, A. ; PETIT, P. ; AILLERIE, M. ; SAWICKI, J.P. ; BELARBI, A.W. ; KRACHAI, M.D. ; CHARLES, J.P.: Photovoltaic cell panel array characterizations and modeling considering both reverse and direct modes. En: *Energy Procedia* 6 (2011), p. 695–703